# Malaria pre-erythrocytic stage vaccines: targeting antigen combinations

Thesis submitted for the degree of Doctor of Philosophy

Trinity Term 2012

**Karolis Bauza**
Hertford College

Word count: ~47,000 (excl. Bibliography, Appendix, Tables and Diagrams)

# Malaria pre-erythrocytic stage vaccines: targeting antigen combinations

Karolis Bauza, Hertford College, University of Oxford
Thesis submitted for the degree of Doctor of Philosophy, Trinity Term 2012

## Abstract

Consistent efficacy in human clinical trials has been achieved by two leading malaria vaccine candidates encoding either the *P. falciparum* circumsporozoite (CSP) or thrombospondin-related adhesion (TRAP) proteins. However, protection in humans relies on high antibody (Ab) titers or potent T cells, respectively, when these antigens are used individually. Therefore, a concurrent induction of both anti-CSP antibodies and TRAP-specific T cells may further improve the protective efficacy associated with these immunogens.

This thesis investigates the protective potential associated with CSP and TRAP combination vaccines by employing a pre-clinical *Plasmodium berghei* (*P. berghei*) mouse malaria challenge model. Depletion of $CD4^+$ and $CD8^+$ T cells indicated that protection by the CSP antigen relied solely on antibodies while TRAP protected through $CD8^+$ T cell responses. Moreover, the administration of relatively small amount of anti-CSP monoclonal antibodies (mAb) substantially enhanced the sub-optimal protection elicited by TRAP. A way to maximize both, anti-CSP antibodies by adenovirus/protein (Ad-P) prime-boost vaccinations and anti-TRAP T cell responses using adenovirus/modified vaccinia strain Ankara (Ad-M), was explored. Combination of the two approaches stimulated optimal humoral and cellular responses that afforded sterile protection in the C57BL/6 animal model. Additional analyses of the effector functions of Abs indicated that the efficacy of this vaccine relied on a two-stage attack against the parasite: anti-CS antibodies reduced the number of sporozoites reaching the liver, thus decreasing the number of infected hepatocytes required to be eliminated by the dual action of natural killer (NK) cells and $CD8^+$ T cells. These proof-of-concept studies using a wild-type (wt) *P. berghei* challenge model allowed progression towards the development of human malaria *Plasmodium vivax* (*P. vivax*) vaccines using PvCSP and PvTRAP antigens. The immunogenicity of PvCSP and PvTRAP-based vaccine candidates was assessed in multiple mouse strains. Additionally, transgenic (tg) *P. berghei* parasites expressing *P. vivax* genes were generated and used to demonstrate the protective efficacy of Ad-P PvCSP and Ad-M PvTRAP vaccines.

# Acknowledgements

First of all I would like to thank my supervisors Professor Adrian Hill and Dr. Arturo Reyes-Sandoval for their scientific input throughout this project.

A special thank you goes to Dr. Simon Draper for an always-honest opinion and never-ending support.

I would also like to thank all the other members of the Jenner Institute past and present for their help, in particular: Simone de Cassan, Mathew Dicks, Alexander Douglas, Leanne Marsay, Katharine Collins, Alex Spencer, Teresa Lambe, Matt Cottingham, and Andrew Williams. A big thank you also to Julie Furze, Andrew Worth, all members of the Vector Core Team, the Adjuvant Bank manager Anita Milicic, Gary Strickland, Viv Clark, Carol Williams and the staff at the FgF. Thank you for your scientific support and technical assistance.

I would also like to thank my collaborators Dr. Oliver Billker from Wellcome Trust Sanger Institute, Hinxton, England, and Dr. Chris Janse from Leiden University Medical Center, the Netherlands, for their experimental input and for the provision of reagents.

Another special thanks goes to my friends, especially on Oxford University Men's Basketball team, keeping me sane throughout the duration of this thesis.

Finally, a huge thank you goes out to my family, without which all of this would be impossible: Mum, Dad, Egle and my grandparents. Thank you for all your support and countless food packages that kept me comforting during the worst time of thesis write up.

# Table of Contents

**Abstract** ..... 1

**Acknowledgements** ..... 2

**Table of Contents** ..... 3

**Table of Figures** ..... 7

**Table of Tables** ..... 10

**Abbreviations** ..... 11

**1 Introduction** ..... 15

**1.1 The need for a malaria vaccine** ..... 15

**1.2 Malaria life cycle** ..... 19

**1.3 The pathogenesis of malaria infection** ..... 22

1.3.1 Host-parasite interactions ..... 22

1.3.2 Immunopathology ..... 23

**1.4 Natural immunity** ..... 24

1.4.1 Antibody-mediated factors in natural protection ..... 25

1.4.2 Cellular immunity in naturally-acquired protection ..... 27

**1.5 The most studied malaria vaccine antigens** ..... 28

1.5.1 Pre-erythrocytic stage antigens ..... 29

1.5.1.1 Circumsporozoite protein (CSP) ..... 29

1.5.1.2 Thrombospondin-related adhesive protein (TRAP) ..... 30

1.5.1.3 Cell-traversal protein for ookinetes and sporozoites (TOS) ..... 33

1.5.2 Blood-stage antigens ..... 33

1.5.2.1 Malaria surface protein 1 (MSP-1) ..... 34

1.5.2.2 Apical membrane antigen 1 (AMA-1) ..... 35

1.5.2.3 Reticulocyte-binding protein homologue 5 (RH-5) ..... 35

1.5.2.4 Duffy-binding protein ..... 36

1.5.3 Transmission-blocking antigens ..... 37

1.5.3.1 Pfs25/Pvs25, Pfs230, and Pfs48/45 ..... 37

**1.6 A vaccine for malaria: how close are we?** ..... 38

1.6.1 Whole-parasite vaccination strategies ..... 39

1.6.2 The leading pre-erythrocytic stage subunit vaccines ..... 41

**1.7 Viral vector vaccine platforms** ..... 43

1.7.1 Poxvirus-based vaccine vectors ..... 43

1.7.2 Adenovirus-based vaccine vectors ..... 44

1.7.3 Heterologous prime-boost regimens ..... 46

1.7.4 Adjuvants ..... 48

**1.8 Small-animal models of malaria** ..... 50

1.8.1 Rodent malaria species ..... 50

1.8.2 Tg *P. berghei* malaria parasites ..... 51

**1.9 Thesis aims** ..... 56

**1.10 Overview of thesis chapters** ..... 56

**Materials and Methods** ..... 59

**2 Materials and Methods** ..... 60

**2.1 Materials ..... 60**
2.1.1 Reagents ..... 60
2.1.2 Solutions ..... 65
**2.2 Methods – Molecular Biology ..... 66**
2.2.1 Agarose gels ..... 66
2.2.2 Restriction digest ..... 67
2.2.3 Ligation reactions ..... 67
2.2.4 Bacterial transformations ..... 68
2.2.5 Polymerase chain reaction (PCR) ..... 68
2.2.6 Plasmid DNA preparation ..... 68
2.2.7 Antigen insert ..... 69
2.2.8 Restriction cloning into ChAd63 vector ..... 71
2.2.9 Restriction cloning into MVA shuttle vector ..... 71
2.2.10 Recombinant protein synthesis ..... 73
2.2.11 SDS-PAGE ..... 73
**2.3 Methods – Molecular Virology ..... 74**
2.3.1 Adenovirus Transfection and Purification ..... 74
2.3.2 MVA Transfection and Purification ..... 75
**2.4 Methods – Molecular Parasitology ..... 75**
2.4.1 Generation of DNA construct targeting allelic exchange of *P. berghei* TRAP ..... 75
2.4.2 Generation of DNA constructs targeting allelic exchange of *P. berghei* CSP ..... 81
2.4.3 Generation of double-tg *P. berghei* parasites ..... 84
2.5.4 Parasite electroporations and clone selection ..... 84
2.5.5 Bacterial electroporations for recombineering ..... 86
2.5.6 Genomic parasite DNA isolation from infected RBCs ..... 86
**2.5 Methods – Immunology ..... 87**
2.5.1 Animals ..... 87
2.5.2 Viral vector vaccines ..... 87
2.5.3 Protein vaccines ..... 88
2.5.4 Whole IgG Enzyme-linked immunosorbent assay (ELISA) ..... 88
2.5.5 Peptides ..... 89
2.5.6 Splenocyte preparation ..... 89
2.5.7 *Ex-vivo* IFN-γ ELISPOT assay ..... 90
2.5.8 Intracellular cytokine staining (ICS) ..... 91
2.5.9 *In vivo* $CD8^+$ and $CD4^+$ T-cell depletions ..... 91
2.5.10 *In vivo* Kupffer and natural killer (NK) cell depletions ..... 92
2.5.11 Whole IgG passive transfer ..... 92
2.5.12 3D11 monoclonal antibody (mAb) ..... 93
2.5.13 3D11 mAb fragmentation ..... 94
2.5.14 Spz neutralization assay (SNA) ..... 96
2.5.15 Isolation of liver resident lymphocytes ..... 96
**2.6 Parasitology ..... 97**
2.6.1 Tg *P. berghei* expressing firefly luciferase ..... 97
2.6.2 Parasite preparation ..... 97
2.6.3 Preparing Thin-blood Smears ..... 97
2.6.4 Immunofluorescence assay (IFA) ..... 98
2.6.5 Statistical model for parasitaemia prediction ..... 98
2.6.6 *In vivo* imaging system (IVIS) ..... 99

**2.7 Statistics** ..... **99**

**3 Quantification of *Plasmodium berghei* malaria parasite density** ..... **102**
**3.1 Introduction** ..... **102**
**3.2 Results** ..... **104**
*3.2.1 In vivo* quantification of *P. berghei* parasite load using live animal imaging ..... 104
3.2.2 Quantification of blood-stage *P. berghei* infection using conventional Giemsa stained blood films ..... 108
3.2.3 Extrapolating *P. berghei* liver-to-blood parasite load and time to 1% blood-stage infection from blood films ..... 112
3.2.4 Validation of *in vivo* imaging and linear regression model using a vaccine against pre-erythrocytic stage malaria ..... 116
**3.3 Discussion** ..... **120**

**4 Investigation of *Plasmodium berghei* malaria pre-erythrocytic stage vaccine efficacy: targeting antigen combinations** ..... **125**
**4.1 Introduction** ..... **125**
**4.2 Results** ..... **129**
4.2.1 The assessment of protective efficacy elicited by different combinations of leading malaria pre-erythrocytic stage vaccine candidates in C57BL/6 strain of mice ..... 129
4.2.2 T cell and Ab responses in combination vaccines are susceptible to antigenic interference ..... 133
4.2.3 The protective efficacy elicited by different malaria pre-erythrocytic stage vaccine candidates in ICR (CD1) outbred strain of mice ..... 137
**4.3 Discussion** ..... **141**

**5 Tailoring a PbCSP and PbTRAP combination vaccine** ..... **148**
**5.1 Introduction** ..... **148**
**5.2 Results** ..... **151**
5.2.1 Immunogenicity and protective efficacy of PbCSP and PbTRAP combination vaccine ..... 151
5.2.2 Mediators of protection following Ad-M CS and Ad-M TR vaccinations ..... 156
5.2.3 Extremely high anti-PbCSP Ab requirement for the protection against *P. berghei* challenge in C57BL/6 mice ..... 160
5.2.4 The synergistic effect of 3D11 and Ad-M TR combination vaccine ..... 163
5.2.5 The synergistic effect of Ad-P CS and Ad-M TR combination vaccine ..... 166
5.2.6 Pre-challenge cellular and humoral immune responses in different PbCSP and/or PbTRAP antigen-based vaccine formulations ..... 173
5.2.7 Depletion of Natural killer, but not Kupffer cells abolishes the protection in Ad-M TR + 3D11 combination vaccine ..... 177
5.2.8 The increased activation of NK and $CD8^+$ T cells in the ChAd63-PbTRAP vaccinated animals as a response to *P. berghei* spz challenge ..... 183
**5.3 Discussion** ..... **187**

**6 *Plasmodium vivax* vaccines** ..... **196**
**6.1 *P. vivax* TRAP vaccine** ..... **196**
6.1.1 Introduction ..... 196
6.1.2 Results ..... 198
6.1.2.1 Generation of maker-free *P. berghei* expressing *P. vivax* TRAP ..... 198
6.1.2.2 Assessment of the tg parasite's biological fitness ..... 201

6.1.2.3 Immunogenicity of ChAd63-PvTRAP prime – MVA-PvTRAP boost regime ..... 204
6.1.2.4 Mapping the immunodominant T cell epitopes in mice ..... 207
6.1.2.5 ChAd63-MVA expressing PvTRAP protects against tg *P. berghei* spz challenge ..... 210
6.1.2.6 Both Ab and T cells are important for the protection against tg challenge ..... 212
6.1.3 Discussion ..... 214
**6.2 *P. vivax* CSP-based vaccines and vaccine combinations ..... 219**
6.2.1 Introduction ..... 219
6.2.2 Results ..... 223
6.2.2.1 The immunogenicity of recombinant ChAd63-PvCSP VK210 viral vector ..... 223
6.2.2.2 Immunogenicity of PvCSP-based vaccine constructs in heterologous prime-boost regimen ..... 226
6.2.2.3 Generation of tg *P. berghei* expressing either VK210 or VK247 variants of PvCSP and the assessment of their phenotype ..... 230
6.2.2.4 Protective efficacy of PvCSP-based vaccine constructs against tg *P. berghei* challenge ..... 235
6.2.2.5 Immunogenicity of PvCSP and PvTRAP combination vaccine administered in heterologous prime-boost regimen ..... 238
6.2.2.6 Generation and assessment of tg *P. berghei* expressing both PvCSP VK210 and PvTRAP genes ..... 242
6.2.2.7 Protection conferred by the PvCSP and PvTRAP combination vaccine against a double-tg *P. berghei* spz challenge ..... 245
6.2.3 Discussion ..... 248
**7 Discussion and Future Directions ..... 254**
**7.1 Overview ..... 254**
**7.2 Conclusions and future directions ..... 258**
7.2.1 Comparative assessment of pre-erythrocytic stage antigens ..... 258
7.2.2 Killing intrahepatic forms of malaria parasite ..... 260
7.2.3 Tg *P. berghei* technology ..... 262
7.2.4 Evaluation of *P. vivax* vaccines ..... 264
**7.3 Final Remarks ..... 267**
**References ..... 271**
**Appendix One ..... 299**

# Table of Figures

Figure 1: The estimated global spatial limits of Plasmodium vivax transmission in 2009. ..... 17

Figure 2: The estimated cumulative probability of death from malaria in 2010. ..... 18

Figure 3: The life-cycle of *Plasmodium* parasite. ..... 21

Figure 4: The make-up of two major pre-erythrocytic stage malaria antigens. ..... 32

Figure 5: Cloning steps involved in generation of DNA constructs required for viral vector manufacture. ..... 72

Figure 6: Generation of DNA constructs targeting allelic exchange of PbTRAP gene. ..... 79

Figure 7: Generation of DNA constructs necessary for the making of tg *P. berghei* expressing PvCSP either VK210 or VK247 allele. ..... 83

Figure 8: Non-reducing SDS-PAGE assay was employed to confirm the successful 3D11 fragmentation. ..... 95

Figure 9: *In vivo* imaging of whole animals. ..... 107

Figure 10: Quantification of blood-stage infection using Giemsa stained blood films. ..... 111

Figure 11: The use of linear regression modeling to predict liver-to-blood parasite density and Tto1. ..... 114

Figure 12: The quantitative assessment of four methods quantifying *P. berghei* malaria parasite densities. ..... 115

Figure 13: Validation of IVIS and Tto1 malaria infection quantification methods in the vaccine setting. ..... 118

Figure 14: The correlation matrix comparing all four methods of quantifying *P. berghei* parasite burden. ..... 119

Figure 15: The protective efficacy of different antigen combination vaccines in C57BL/6 strain of mice. ..... 132

Figure 16: Humoral and cellular post-boost immune responses following Ad-M vaccinations encoding different pre-erythrocytic stage antigens and antigen combinations. ..... 136

Figure 17: The protective efficacy of Ad-P CS and Ad-P TOS combination vaccine. ..... 140

Figure 18: Protective efficacy of PbCSP and PbTRAP combination vaccine administered in heterologous ChAd63-prime, MVA-boost regimen. ..... 154

Figure 19: Kinetic humoral and cellular immune responses. ..... 155

Figure 20: Depletions of either $CD4^+$ or $CD8^+$ T cells in animals immunized with Ad-M PbCSP or Ad-M PbTRAP vaccines. ..... 159

Figure 21: High concentrations of anti-PbCSP mAb are required to protect against *P. berghei* malaria in C57BL/6 strain of mice. ..... 162

Figure 22: The synergistic effect of 3D11 mAb and Ad-M PbTRAP combination vaccine. ..... 165

Figure 23: The synergistic effect of PbCSP and PbTRAP combination vaccine administered as heterologous prime-boost regimen employing viral vector and protein modalities. ..... 172

Figure 24: The post-boost ICS and humoral responses. ..... 176

Figure 25: Immunological mechanisms of 3D11 and Ad-M PbTRAP combination vaccine. ..... 182

Figure 26: The ICS analysis of liver-resident lymphocytes. ..... 186

Figure 27: Generation of marker-free tg *P. berghei* parasites expressing *P. vivax* TRAP. ..... 200

Figure 28: The assessment of tg parasite's development in *A. stephensi* mosquitoes, IFAT analysis, and the infectivity of vertebrate host. ..... 203

Figure 29: The kinetics of the humoral and cellular immune responses following Ad-M PvTRAP vaccination. ..... 205

Figure 30: Polychromatic $CD8^+$ T cell responses. ..... 206

Figure 31: Immunodominant peptide mapping. ..... 208

Figure 32: The phenotype of the immunodominant epitopes. ..... 209

Figure 33: The protective efficacy conferred by Ad-M PvTRAP vaccination against tg *P.berghei* parasite. ..... 211

Figure 34: Both PvTRAP-specific T cells and Abs mediate protection against tg *P. berghei* challenge. ..... 213

Figure 35: Alignment of PvCSP variants VK210 and VK247. ..... 222

Figure 36: Interstrain comparison of ChAd63-PvCSP VK210 vaccine immunogenicity. ..... 225

Figure 37: Immunogenicity of PvCSP-based vaccines..... 229

Figure 38: The making of tg *P. berghei* expressing either VK210 or VK247 variants of PvCSP. ..... 234

Figure 39: Protective efficacy of PvCSP-based vaccines against tg *P. berghei* sporozoite challenge. ..... 237

Figure 40: Immunogenicity of PvCSP and PvTRAP combination vaccine. ..... 241

Figure 41: Genotyping analysis and assessment of infectivity phenotype of tg *P. berghei* expressing both PvCSP VK210 and PvTRAP genes. ..... 244

Figure 42: Pre-erythrocytic stage efficacy of PvCSP and PvTRAP combination vaccine. ..... 247

# Table of Tables

Table 1: Selected list of published tg *P. berghei* parasites relevant for vaccine studies. . 55

Table 2: Reagents used throughout this thesis. ..... 64

Table 3: Outline of all of the malarial antigens used throughout this thesis..... 70

Table 4: Primers used for the generation of DNA constructs targeting allelic exchange of PbTRAP and PbCSP with homologous *P. vivax* genes. ..... 80

Table 5: The comparative assessment of malaria pre-erythrocytic stage antigens and antigen combinations in C57BL/6 strain of mice. ..... 131

Table 6 The screening of the pre-erythrocytic stage antigen combinations in ICR (CD1) outbred strain of mice. ..... 139

Table 7: Ad-M TR and Ad-P vaccination groups (Experiment 1)..... 170

Table 8: Ad-M TR and Ad-P CS vaccination groups (Experiment 2)..... 171

Table 9: The table listing the different Ad-P PvCSP variant vaccinations. ..... 228

Table 10: The table listing the immunization groups for PvCSP and PvTRAP combination vaccine. ..... 240

# Abbreviations

| | |
|---|---|
| αα | Amino acid |
| Ab | Antibody |
| ACK | Ammonium chloride potassium |
| Ad | Adenovirus |
| ADCC | Antibody-dependent cellular cytotoxicity |
| HAdV-5 | Human adenovirus serotype 5 |
| ADRB | Antibody-dependent respiratory burst |
| Ad-M | Adenoviral prime, MVA boost regime (8 week interval) |
| AMA-1 | Apical Membrane Antigen 1 |
| Ad-P | Adenoviral prime, protein boost regime (8 week interval) |
| APC | Antigen presenting cells |
| AS | Adjuvant System |
| BCG | Bacillus Calmette-Guérin |
| BLS | Bioluminescence signal |
| bp | Base pairs |
| CD | Cluster of differentiation |
| CEF | Chicken embryonic fibroblasts |
| CI | Confidence interval |
| ChAd63 | Simian adenovirus Ch63 |
| CMV | Cytomegalovirus |
| CR-1 | Complement-receptor 1 |
| CRIR-1 | Cysteine-rich interdomain region 1 |
| CSA | Chondroitin sulfate A |
| CSP | Circumsporozoite surface protein |
| CTL | Cytotoxic T lymphocytes |
| DARC | Duffy antigen receptor complex |
| DBP | Duffy Binding Antigen |
| DC | Dendritic cells |
| DMSO | Dimethyl Sulfoxide |
| ds | Double-stranded |
| EBA | Erythrocyte binding antigen |
| EDTA | Ethylenediaminetetraacetic acid |
| ELISA | Enzyme-linked immunosorbant assay |
| ELISpot | Enzyme-linked immunosorbent spot assay |
| EMP-1 | Erythrocyte membrane protein 1 |
| Fab | Fragment antigen-binding |
| FabB/F | Enzyme of the type II fatty acid biosynthesis (FAS II) |
| FC | Fluorocytosine |
| FcR | Fc Receptor |
| FP9 | Fowlpox strain virus FP9 |
| g | The acceleration due to gravity |
| GAP | Genetically-attenuated parasites |
| GFP | Green fluorescent protein |

| | |
|---|---|
| GIA | Growth Inhibitory Activity |
| GPI | Glycosylphosphatidylinositol |
| GSK | GlaxoSmithKline |
| h | Hour |
| HBsAg | Hepatitis B surface antigen |
| HBV | Hepatitis B virus |
| *hDHFR* | Human dihydrofolate reductase |
| HIV | Human immunodeficiency virus |
| HPV | Human papilloma virus |
| HSPG | Highly sulfated heparan sulfate proteoglycan |
| HZ | Haemozoin |
| i.m. | Intra-muscular |
| i.p. | Intra-peritoneal |
| i.v. | Intra-venous |
| IVIS | *In vivo* imaging system |
| IC | Immune complex |
| ICAM-1 | Intracellular adhesion molecule 1 |
| ICS | Intracellular cytokine staining |
| IE | Infected erythrocyte |
| IFA | Immunoflourescence assay |
| IFN | Interferon |
| Ig | Immunoglobulin |
| IL | Interleukin |
| iu | Infectious units |
| kDa | Kilodalton |
| KO | Knock-out |
| LB | Luria broth |
| mAb | Monoclonal antibody |
| ME | Multi epitope string |
| MEM | Minimum essentials medium |
| MHC | Major histocompatibility complex |
| min | Minute |
| MSP | Merozoite surface protein |
| MVA | Modified vaccinia virus Ankara |
| NF-kB | Nuclear Factor-kappa B |
| NK | Natural killer |
| NYVAC | New York vaccinia virus |
| NO | Nitric oxide |
| O/W | Oil-in-water |
| OD | Optical density |
| ODN | Oligodeoxynucleotide |
| OVA | Ovalbumin |
| Pat50 | Parasitaemia at 50 hours after challenge |
| *P.* | *Plasmodium* |
| PBMC | Peripheral blood mononuclear cells |
| PBS | Phosphate buffered saline |

| | |
|---|---|
| PBS/T | 0.05% Tween 20 in phosphate buffered saline |
| PCR | Polymerase chain reaction |
| pfu | Plaque forming units |
| PHZ | Phenylhydrazine |
| pRBC | Parasitized red blood cell |
| RAP | Rhoptry-associated protein |
| RAS | Radiation-attenuated sporozoites |
| RBC | Red blood cell |
| RESA | Ring-infected erythrocyte surface antigen |
| Rh5 | Reticulocyte binding protein 5 |
| RIFIN | Repetitive interspersed family |
| RNA | Ribonucleic acid |
| RPM | Revolutions per minute |
| RT | Room temperature |
| RT-PCR | Reverse transcriptase – polymerase chain reaction |
| RTS,S | CSP based malaria vaccine based on a HB**s**Ag fusion polypeptide from GSK |
| SAP1 | Sporozoite asparagine-rich protein 1 |
| s.c. | Subcutaneous |
| SFU | Spot forming unit |
| SNA | Sporozoite neutralization assay |
| Spz | Sporozoite |
| ss | Single-stranded |
| STEVOR | Subtelomeric variable open reading frame |
| SUB-1 | Subtilin-like serine protease |
| SURFIN | Surface-associated interspersed gene family |
| TB | Tuberculosis |
| TCR | T-cell Receptor |
| Tg | Transgenic |
| TLR | Toll-like receptor |
| TM | Transmembrane |
| TNF | Tumour necrosis factor |
| TOS | Cell-traversal protein for ookinetes and sporozoites |
| tPA | Tissue plasminogen activator |
| TRAP | Thrombospondin-related adhesion protein |
| TSR | Thrombospondin type-1 repeat superfamily |
| Tto1 | Time to 1% blood-stage infection |
| UIS | Upregulated in infectious sporozoites |
| WHO | World Health Organization |
| WT | Wild type |

# Chapter 1

# Introduction

# 1 Introduction

## 1.1 The need for a malaria vaccine

Malaria is a parasitic disease of humans and other vertebrates, including birds, reptiles, monkeys, chimpanzees and rodents (1). It is transmitted through the bite of infected mosquito vectors. The causative agent of malaria is the protozoan of the genus *Plasmodium* of which five species can infect humans, including *P. falciparum*, *P. vivax*, *P. ovale*, *P. malariae*, and the zoonotic *P. knowlesi* (2).

The two most commonly occurring species of human malaria are *P. falciparum* and *P. vivax*. Nearly 98 percent of malaria infections in sub-Saharan Africa are caused by *P. falciparum*, whereas, according to recent estimates, *P. vivax* is the most prevalent form of malaria outside Africa accounting for 25-40% of global malaria burden, especially with high frequency of incidence in Asia and South America (Figure 1) (3-5).

According to the recent World Health Organization (WHO) report, in 2010 malaria caused an estimated 216 million cases and 655 000 deaths of whom around 86 percent were children under the age of five (Figure 2). Approximately 3.3 billion people are at risk of malaria infection across an estimate of 106 countries (4).

In addition to being a significant health risk, malaria also contributes to the loss of productivity and economic prosperity in endemic nations. It is approximated that in Africa alone financial losses due to malaria amount to $12bn per year (6) and there is a strong negative correlation between country's long-term economic growth prospects and

the disease burden (7).

Despite malaria's huge health and socioeconomic burden there are some indications that the disease incidence in the endemic regions is decreasing. This is thought mainly to be due to the recent increase in access to anti-malaria interventions, such as artemisinin-based combination drugs, long-lasting insecticide-treated bed nets and indoor residual spraying (8). However, the deployment of efficacious vaccine(s) would probably have the greatest impact on the disease burden (9, 10), and therefore, the malaria vaccine field remains an active area of biomedical research.

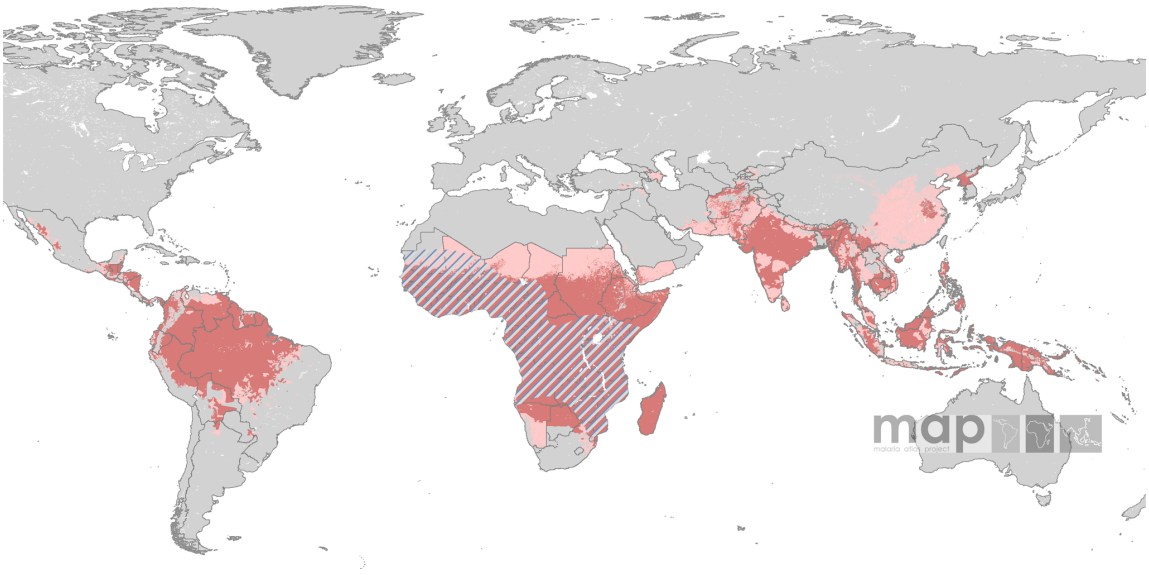

**Figure 1: The estimated global spatial limits of *Plasmodium vivax* transmission in 2009.**

Adapted from (5). Temperature and aridity exclusion layers were applied onto the demographic data estimating *P. vivax* annual parasite incidence (API). Furthermore, the medical intelligence and predicted Duffy negativity layers (hatched) were overlaid on the modified *P. vivax* API data, indicating where the presence of this genetic trait modulates the estimates of population at risk (PAR) most significantly. Red and pink areas indicate stable (defined as *Pv*API≥0.1 per 1,000 people per annum) and unstable (*Pv*API<0.1 per 1,000 per annum) regions of transmission, whereas no risk areas are shown in grey.

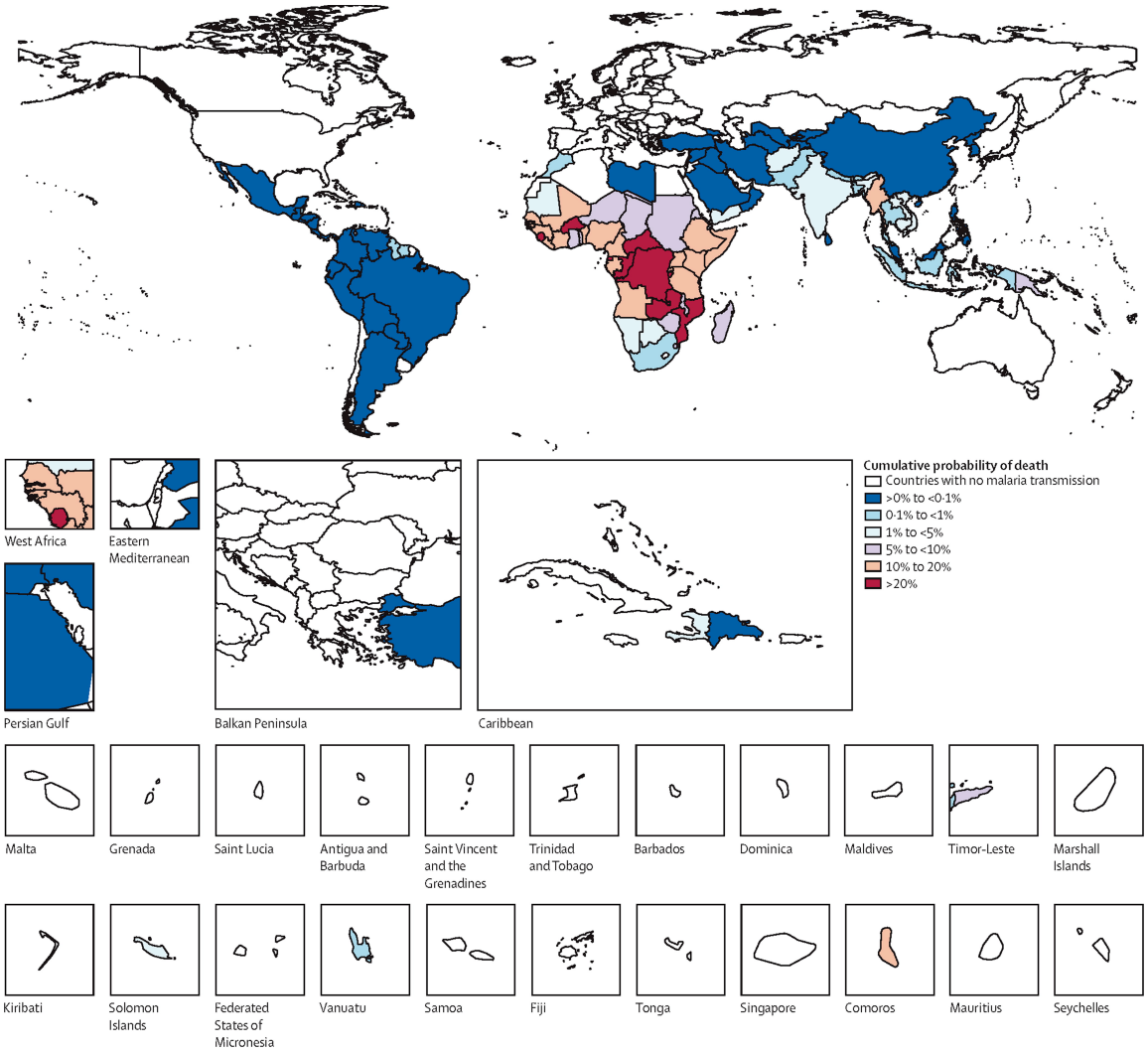


**Figure 2: The estimated cumulative probability of death from malaria in 2010.**

Adapted from (8). Overall probability of dying from malaria in the absence of all other causes from birth to age 80 years in 2010.

## 1.2 Malaria life cycle

The complex life cycle of the malaria parasite (Figure 3) has to be appreciated in order to identify the key host - pathogen interactions most vulnerable to attack by an effective vaccine. The malaria infection in humans commences with the so-called **pre-erythrocytic stage** when an infected female *Anopheles* mosquito bites for a blood meal consequently also depositing sporozoites either into the surrounding tissue or directly into the circulatory system. Within minutes sporozoites journey to the liver and establish an intrahepatic infection. Inside hepatocytes parasites develop within a parasitophorous vacuole where asexual multiplication leads to the generation of 20,000 – 40,000 merozoites (11). The liver stage development for most human malaria species lasts for 5-9 days, whereas a much shorter period of 2-3 days is enough for rodent malaria species, including *P. berghei*, *P. yoelii*, *P. chabaudi*, and *P. vinckei*. It is at this stage that some *P. vivax* parasites are able to establish the dormant hypnozoite forms responsible for relapses of infection a few months or even years later (12). The asymptomatic liver stage concludes upon egress of merosomes containing 100-300 mature merozoites into the circulation initiating the blood-stage infection (13) (11, 14).

During the **blood-stage,** merozoites invade red-blood cells (RBCs). Once inside erythrocytes malaria parasites progress from immature or early trophozoite ring-stage parasites to late mature trophozoites and then schizonts. The intra-erythrocytic maturation concludes with the eventual rupture of the RBC and the release of 8-32 mature merozoites into the circulation that instantly infect new RBCs. Each cycle of the parasite's intra-erythrocytic development lasts 36-48 hours in the case of *P. falciparum*, *P.*

*vivax*, or *P. ovale*, and 22-24 hours in the case of rodent malaria species. Malaria-associated symptoms in humans become apparent during blood-stages. If blood-stage malaria infection progresses unchecked, illness associated with complicated malaria or even death may ensue.

Some of maturing merozoites differentiate into male and female gametocytes that if ingested by feeding mosquito would fuse to form a zygote in the mosquito gut, initiating the **sexual-stage** development. Diploid zygotes in the mosquito mid-gut develop into ookinetes, which subsequently penetrate the gut lining and implant as an oocyst within the gut wall. Sporozoites produced within developing oocysts by meiotic division are eventually released and deposited into the hemocoel. From there sporozoites migrate to mosquito salivary glands, invade them, and once inside, complete their development. The release of these sporozoites during the mosquito's next feed would start the developmental cycle all over again.

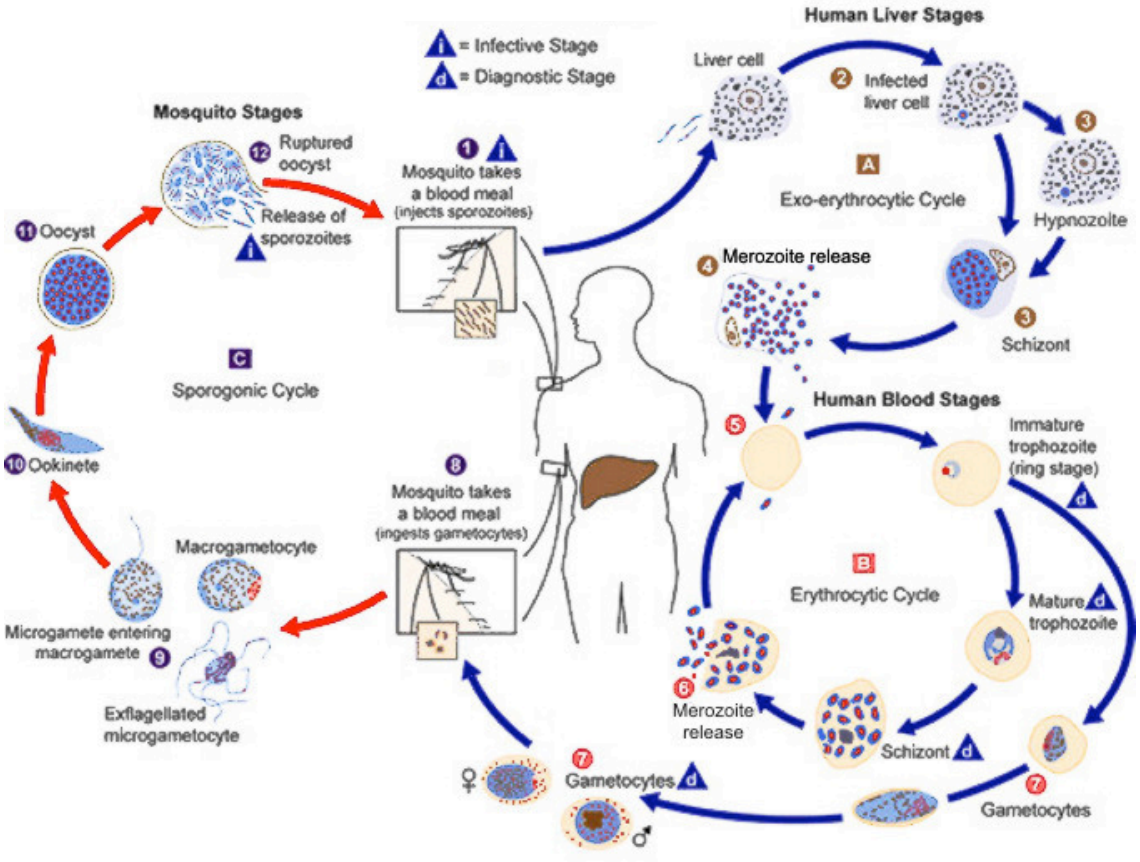


**Figure 3: The life-cycle of *Plasmodium* parasite.**

Adapted from (8). The malaria infection in humans commences with (A) pre-erythrocytic- (or exo-erythrocytic cycle) and concludes with the (B) blood-stage (erythrocytic cycle) development. (C) The ingestion of male and female gametocytes by mosquito vector results in the (C) sexual development stage (sporogonic cycle). Also, during the exo-erythrocytic cycle *P. vivax* parasites may form dormant hypnozoite forms able to persist inside hepatocytes for many months and even years and subsequently cause relapse infections.

## 1.3 The pathogenesis of malaria infection

As mentioned above, the symptoms associated with malaria rapidly develop during the blood stage and usually manifest themselves in febrile-like illness including bouts of fever, nausea, headache, arthralgia that coincide with the rupture of infected erythrocytes. Some infections with *P. falciparum* and to a lesser extent *P. vivax* may progress to severe, life-threatening conditions, whereas *P. malariae* and *P. ovale* are an infrequent cause of mild-moderate clinical malaria. However, *P. falciparum* causes by far the most fatalities and three distinct but overlapping syndromes, including severe malarial anemia, cerebral malaria, and respiratory distress (a sign of underlying metabolic acidosis) are responsible for the majority of deaths. The pathogenic basis of these classical clinical ailments of severe malaria is complex and both immunopathology as well as direct host-parasite interactions are thought to be contributors.

### 1.3.1 Host-parasite interactions

The attachment of infected erythrocytes (IEs) to the endothelial wall of microvasculature plays a pivotal role in the severe malaria pathogenesis. The IE cytoadhesion is mediated by the host cell receptors and parasite proteins expressed on the surface of infected RBCs, such as *P. falciparum* erythrocyte membrane protein 1 (PfEMP1) (15). The PfEMP1 gene is coded by the *var* multigene family that contains ~60 different variants that are divided into three families A, B and C, based on their conserved upstream regions. Each variant displays clonal antigenic switching in response to immune pressure and some of them are implicated as major virulence factors (16) (17, 18). For example, group B and C variants can bind to the protein receptor CD36 (also a co-receptor for toll-like receptor 2)

expressed on the endothelial cells of microvasculature leading to IE sequestration, and activate $CD4^+$ T cells (19) and/or modulate the development of dendritic cells (DCs) (20). On the other hand, group A variants do not bind CD36, and have been implicated in mediating RBC rosetting (21, 22) (23), a process whereby IEs adhere to the complement-receptor 1 (CR1) located on the surface of uninfected erythrocytes causing RBC clustering (24). Also, parasites causing placental malaria, the form of severe malaria in pregnant women, uniformly express a particular PfEMP1 protein (VAR2CSA) that mediates binding to chondroitin sulfate A (CSA) in the intervillous space (25). Furthermore, histological studies performed on patients who died from cerebral malaria have shown that IEs and intercellular adhesion molecule-1 (ICAM-1) colocalise on microvascular endothelial cells (26) (27), suggesting that cytoadhesion through ICAM-1 may contribute to the IE sequestration in severe malaria.

### 1.3.2 Immunopathology

It is thought that equally important to the pathogenesis of severe malaria are pro-inflammatory immune responses, leading to sepsis-like symptoms in the patients with severe malaria (28). The initial trigger for the production of pro-inflammatory cytokines by the innate immune system is, probably, provided by the pattern-recognition receptors, such as toll-like receptors (TLRs). It has been suggested that glycosylphosphatidylinositol (GPI) moiety, anchoring some of malaria proteins onto the surface membrane, can activate macrophages through the recognition of TLR2/TLR1 receptor complex (29). Similarly, it has been found that the product of parasite-mediated intraerythrocytic digestion of hemoglobin, haemozoin (HZ), through the contaminating

plasmodial DNA can activate TLR9 (30, 31). However, the development of cerebral malaria in the absence of individual TLR receptors has been observed in mice (32), suggesting that it is unclear which (if any) of these TLRs are on the severe malaria causal pathway.

Various inflammatory cytokines have also been linked with severe malaria. Ten times greater levels of circulating tumour necrosis factor-alpha (TNF-a) have been observed in patients with cerebral malaria as opposed to the individuals with uncomplicated malaria (33). It has been suggested that TNF-a upregulates ICAM-1 molecule levels in the cerebral malaria patients leading to enhanced IE sequestration (34). Similarly, severe malaria anemia has been associated with significantly lower interleukin 10 (IL-10) responses (35), whereas relatively high levels of IL-10 and TNF-a have been observed in patients with malaria-induced respiratory distress (36). Experimental animal models indicate that TNF-a induces enhanced erythrophagocytosis and dyserythropoiesis (37), processes that, coupled with enhanced bone-marrow suppression, (38) could be responsible for exacerbating severe malaria anemia. However, the consistent link between these or other inflammatory mediators and severe malaria is lacking and thus more studies may be needed to confidently determine the mechanistic basis of immunopathology.

## 1.4 Natural immunity

A body of epidemiological data exists demonstrating that individuals living in malaria endemic areas do not develop severe malaria despite chronic parasitaemia in their blood. This state of protection against malaria is referred to as naturally-acquired immunity and

the existing evidence suggests that this type of protection is obtained relatively rapidly against the homologous strain of the parasite. Although less substantial, there is also evidence of early acquisition of heterologous immunity as demonstrated by less-severe episodes of malaria-associated clinical symptoms (39). Also, perhaps most interestingly, it has been shown that a single exposure to malaria is sufficient to protect individual against death due to malaria infection (40). Despite the importance to the malaria vaccine field, the major correlates responsible for the naturally-acquired immunity against malaria remain to be defined.

Malaria parasites can be targeted by the immune system at any point during their developmental cycle in mammalian host. However, it is thought that naturally-acquired immunity contributes little at the pre-erythrocytic stage (the whole-parasite vaccination strategies relying on liver-stage $CD8^+$ T cell responses are discussed later) (41). The direct injection of blood-stage parasites into naturally-immune individuals bypassing the pre-erythrocytic stage, have showed that these adults were able to control parasite multiplication rates in the blood and avoid the disease symptoms (42).

During blood stage, intraerythrocytic and free merozoite forms of parasite can be targeted by the immune system and both humoral and cellular immune responses have been implicated in the acquisition of natural immunity.

### 1.4.1 Antibody-mediated factors in natural protection

The ability of anti-AMA1 (apical membrane antigen 1), anti-MSP1 (merozoite surface protein 1) and anti-RAP1 (rhoptry-associate protein 1) Abs to bind to free merozoites and

block the erythrocyte invasion is well documented (43). Also, their age- and exposure dependent acquisition has been demonstrated (44) (45) (46). However, much less is known about what role these Abs play in opsonization and complement-mediated lysis of free merozoites.

The predominance of different immunoglobulin G (IgG) isotopes has been linked to protection or susceptibility to malaria infection. It has been shown that the dominance of immunoglobulin IgG1 and IgG3, two cytophilic isotypes, correlated strongly with protection, whereas the non-cytophilic IgG2 predominated in nonprotected subjects (47). Also, the acquisition of IgG1 and IgG3 was associated with age and exposure and high levels of AMA-1-specific IgG3 and $MSP1_{19}$-specific IgG1 were strongly predictive of a reduced risk of symptomatic malaria in a longitudinal cohort of children in Papua New Guinea (48). Interestingly, high levels of IgG2 specific against RESA (ring-infected erythrocyte surface antigen) and MSP2 epitopes correlated strongly with the reduced, whereas IgG4 with the enhanced risk of malaria infection (49).

As mentioned above, sequestration of *P. falciparum* infected erythrocytes is mediated by the interaction of host microvasculature receptors and the parasite-derived proteins that translocate onto the surface of infected RBCs. The anti-sequestration agents interrupt the attachment of those parasitized erythrocytes to the endothelia, thus preventing the onset and development of the vast majority of severe malaria cases. Multiple parasite-derived surface antigens are present on the infected erythrocytes that may be targets of protective anti-sequestration Ab response, including *P. falciparum* erythrocyte membrane protein 1 (PfEMP1) (15), repetitive interspersed family (RIFIN) proteins (50), subtelomeric

variable open reading frame (STEVOR) proteins (51), and surface-associated interspersed gene family (SURFIN) proteins (52). These antigens expressed on the surface of infected erythrocytes are relatively polymorphic and the protection associated with them seems to be strain-specific (53) (54). Nonetheless, recently it has been suggested that the anti-PfEMP1 Ab response is the key determinant of the infection outcome in the naturally immune individuals (55). The cysteine-rich interdomain region 1 (CRIR1), one of the PfEMP1 cytoadhesion modules, interacts with CD36 receptor and participates in the adhesion of infected erythrocytes to the endothelial microvascular cells. CRIR1 is highly conserved and can induce Abs that prevent cytoadhesion of infected erythrocytes (56). The vaccination of Aotus monkeys with recombinant CRIR1 alpha did not protect monkeys, however, significant reduction in the severe anemia was observed (57).

In conclusion, the mechanisms which are involved in the Ab-mediated natural protection include binding of the merozoites and the prevention of RBC invasion, antibody-dependent cellular cytotoxicity (ADCC) mediated by cytophilic Abs, and binding of antibodies to the parasite-specific molecules translocated to the surface of IEs that way preventing parasitized RBC sequestration and, possibly, leading to greater clearance of infected RBCs.

### 1.4.2 Cellular immunity in naturally-acquired protection

The protective importance of T cells against blood-stage infection in murine models have been clearly demonstrated (58-60). Also, it has been shown that $CD4^+$ and $CD8^+$ T cells from non-exposed individuals are able to inhibit *P. falciparum* growth *in vitro* (61).

However, it is less clear what contribution cellular immune responses provide to the naturally immune individuals.

In one study, the *in vitro* lymphocyte proliferation and interferon-gamma (IFN-γ) production in a response to MSP1 antigen increased with age and strongly correlated (together with Ab responses) with the resistance to episodes of malaria-associated fever in partially immune children in West Africa (43). Also, strong association between the number of malaria episodes and the frequency of anti-MSP1 T cell responses in the exposed donors following *in vitro* stimulation was observed in Brazil (62), suggesting that the induction of blood-stage cellular immunity may heavily rely on the number of malaria episodes. Interestingly, repeated exposure of malaria naïve volunteers to subclinical blood-stage *P. falciparum* infections that were cured early with drugs induced sterile protection on a subsequent challenge. The immunity was independent of enzyme-linked immunosorbent assay (ELISA) Ab titres and was associated with $CD4^+$ and $CD8^+$ T cells secreting IFN-γ (63). Furthermore, it has been shown that the cellular immune responses against parasitized RBCs remain undiminished for up to 14 months even after a single episode of malaria and that many cell types including alpha beta T cells, gamma delta T cells and natural killer (NK) cells contributed to the increased IFN-γ response (64).

## 1.5 The most studied malaria vaccine antigens

Many of the malaria surface proteins essential for the parasite's motility, attachment and/or infectivity have been targets of ongoing efforts to develop efficacious vaccine. Unfortunately, most of the leading vaccine targets are species- and even stage-specific.

### 1.5.1 Pre-erythrocytic stage antigens

#### 1.5.1.1 Circumsporozoite protein (CSP)

Malaria CS protein ranges in size from 36 to 45 kDa (kilo-Dalton) depending on parasite species, and is abundantly expressed on the surface of mosquito midgut and salivary gland sporozoites (65). CSP is comprised of an N-terminal region, a highly conserved protease cleavage site termed region I, a repeat region, a short conserved sequence termed region III, and a C-terminal domain with sequence homology to the thrombospondin type-1 repeat superfamily (TSR) (Figure 4A). The C terminus of the CSP also contains an attachment site for a GPI anchor, which is responsible for the association of CSP with the sporozoite plasma membrane (66). The CS protein is involved in the parasite's motility (67) and is essential for sporozoite release from the oocysts (68), attachment and invasion of mosquito salivary glands (69, 70) and the liver of the vertebrate host (67). It has been suggested that the CS ligands are highly sulfated heparan sulfate proteoglycans (HSPGs), which are ubiquitous in liver sinusoidal areas (71). CSP attachment to HSPGs is mediated by the TSR region of the protein providing the signal for sporozoites to arrest in the liver and initiate the invasion cascade (71-73). Some studies even suggest that the CS protein is a key player in promoting the parasite's

liver-stage development. CS is able to translocate from parasitophorous vacuole into the infected hapatocyte's cytoplasm where it competes with NF-κB transcription factor (nuclear factor *kappa*-light-chain-enhancer of activated *B* cells) for binding to importin-α3, a molecule that regulates protein import into the nucleus (74, 75). Thus, it is possible that CSP down-regulates host pro-inflammatory responses, necessary to inhibit parasite's liver-stage development, by preventing NF-κB molecules from reaching the cell nucleus.

More recently, it has been suggested that the CS protein undergoes remarkable conformational changes as the parasite journeys from the mosquito midgut to vertebrate liver (76). Coppi *et al*. showed that CSP has two conformational states, an adhesive conformation, in which the C-terminal cell-adhesive domain is exposed, and a nonadhesive conformation, in which the N terminus hides the adhesive domain. As the parasites migrate from mosquito to vertebrate liver, a nonadhesive conformation is maintained to protect TSR region from antibody recognition. However, in the vertebrate host, proteolytic cleavage of CSP regulates the switch to an adhesive conformation, necessary for subsequent traversal and invasion of hepatocytes (76).

#### 1.5.1.2 Thrombospondin-related adhesive protein (TRAP)

Another highly studied and well-characterized pre-erythrocytic stage malaria antigen is thrombospondin-related adhesive protein (TRAP) (Figure 4B). TRAP is an approximately 65-kDa micronemal protein essential for attachment and invasion of mosquito salivary glands (77) and vertebrate liver (78, 79). TRAP also plays a key role in gliding motility, the parasite's way of locomotion (79, 80), as it is linked with an actomyosin motor via TRAP-aldolase interactions (81). TRAP's ectodomain has

sequence homologies to von Willebrand factor like A domain and TSR and a repeat region. The TSR has high affinity for heparin (82).

Transcriptomics data indicate that TRAP messenger RNA is expressed early in the intrahepatic development, thus this protein may be a target of T cell-based vaccines. Moreover, cultured memory T cell responses against TRAP were associated with a significantly reduced incidence of malaria (83). Also, children with high levels of IgG antibodies to CSP and TRAP had a decreased risk of clinical malaria (84), although TRAP-specific Abs alone did not seem to inhibit sporozoite infectivity *in vivo* (85), suggesting that naturally acquired TRAP-specific IgG may be the evidence of exposure rather than protection.

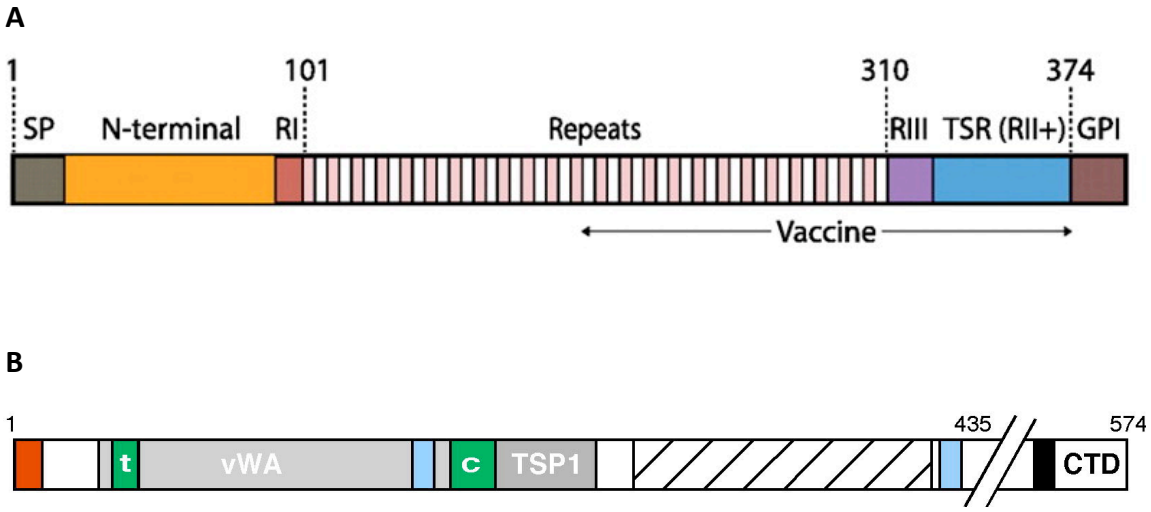


**Figure 4: The make-up of two major pre-erythrocytic stage malaria antigens.**

(A) Adapted from (72). *P. falciparum* CSP is shown with its major gene structures, including signal peptide (SP), N-terminus, highly conserved protease site (RI), central repeat region, another conserved region RIII, thrombospondin type-1 repeat superfamily domain (TSR), and the GPI-anchor. The portion of CSP fused to hepatitis B surface antigen in the RTS,S vaccine is indicated by "vaccine."

(B) Adapted from (86). *P. falciparum* TRAP contains a von Willerbrand factor domain A (boxed in light grey), a thrombospondin type 1 motif (boxed in grey), a degenerate repeat region (hatched box) and a cytoplasmic tail domain (CTD), which contains highly conserved signature residues of the TRAP family transmembrane proteins.

#### 1.5.1.3 Cell-traversal protein for ookinetes and sporozoites (TOS)

The protein important for malaria parasite's cell traversal at the ookinete and the sporozoite stages (TOS) is emerging as another promising pre-erythrocytic stage malaria vaccine candidate. TOS is localized to micronemes, and the gene's deletion in *P. berghei* reduced the parasite's ability to infect mosquito salivary glands and mammalian liver, as well as significantly reducing its cell traversal ability (87). Immunizations with *P. falciparum* TOS recombinant protein vaccine protected multiple strains of mice against challenge with heterologous *P. berghei* sporozoites (88) and the protection was both antigen (Ag)-specific and Ab- and T cell-dependent (89). Also, malaria immune people following vaccination with radiation-attenuated sporozoites (RAS) demonstrated stronger cellular immune responses against PfTOS than those seen against PfCSP peptides (90).

### 1.5.2 Blood-stage antigens

As mentioned above, most adults living in malaria-endemic areas over time develop 'natural immunity' to the parasite (91). In this state, naturally-immune individuals do not suffer from malaria-associated clinical symptoms, despite maintaining low-density blood-stage parasitaemia. It has been suggested that both humoral (92, 93) and cellular (94) immune responses play a role in naturally protected adults. Thus, using different vaccination regimes, most of blood-stage vaccine efforts have focused in trying to re-create those antibody or T cell responses seen in naturally-immune individuals. Targeting antigens that are expressed on the surface of merozoites is particularly attractive option as they could both inhibit RBC invasion (95, 96) and affect growth and development of intra-erythrocytic parasite forms (97, 98).

### 1.5.2.1 Malaria surface protein 1 (MSP-1)

Malaria surface protein 1 (MSP-1) is one of the most extensively studied erythrocytic stage vaccine candidates (99) and is essential for parasite liver egress and RBC invasion (100). MSP-1 orthologues are present in most *Plasmodium* species (101). The protein is expressed as a ~190-kDa precursor and is attached to the merozoite surface membrane via a GPI-anchor (102). During egress and prior to RBC invasion MSP-1 is proteolytically processed by two subtilisin-like serine proteases called PfSUB-1 (103) (104) and PfSUB-2 (105) (106). Protease-mediated processing of MSP-1 at the invasive blood stage occurs in two stages. The first one is mediated by PfSUB-1 and takes place during merozoite maturation (107). It results in four fragments of 83, 28-30, 38-45 and 42-kDa size that remain noncovalently associated together on the parasite's surface. The second stage of proteolytic processing is mediated by PfSUB-2 and occurs immediately before the invasion of a new erythrocyte. The 42-kDa MSP-1 fragment ($MSP\text{-}1_{42}$) is cleaved by the PfSUB-2 protease into 33 kDa and ~10 kDa fragments termed $MSP\text{-}1_{33}$ and $MSP\text{-}1_{19}$. Only $MSP\text{-}1_{19}$ remains attached to the merozoite surface at the carboxy-terminal end via a GPI moiety resulting in the shedding of MSP-1 and the associated protein complex (105).

Exposure to malaria appears to induce antibodies against $MSP\text{-}1_{19}$ (108) and several studies have demonstrated the relationship between the presence of such antibodies and protection from *P. falciparum* malaria in children from the Gambia (43) and Papua New Guinea (109). Experimental evidence using mice (110) and *Aotus* monkey (111) models further suggest that high antibody titres against $MSP\text{-}1_{19}$ can protect, but the protection is

strain-specific (112). The use of MSP-1 in human clinical trials has been met with limited success and a phase 2b study using MSP-$1_{42}$ adjuvanted with AS02 (adjuvant system 02) did not protect vaccinated children in Western Kenya despite inducing high levels of antibody (113).

#### 1.5.2.2 Apical membrane antigen 1 (AMA-1)

Another leading erythrocytic stage vaccine candidate is apical membrane antigen 1 (AMA-1). AMA-1 is essential for mammalian host cell invasion and is expressed by both pre-erythrocytic (114) and blood-stage (115) forms of parasite. Just like MSP-1, AMA-1 undergoes extensive proteolytic processing. The protein is expressed as an 83-kDa precursor and is rapidly processed by cleavage of an N-terminal peptide to a 66-kDa molecule, which localizes to the micronemal membrane within the merozoite apex (116). Around the time of schizont rupture and merozoite release the processed 66-kDa form becomes associated with the merozoite surface. Prior to invasion AMA-1 undergoes another cleavage mediated by membrane-bound 'sheddase' protease PfSUB-2 resulting in 42-kDa component being shed (117).

AMA-1-based vaccine studies have demonstrated that the protection is achieved in animals upon the induction of high-antibody titres (118), however, high level of antigenic polymorphism renders protection strain-specific (119).

#### 1.5.2.3 Reticulocyte-binding protein homologue 5 (RH-5)

One way to circumvent the difficulties associated with blood-stage antigen diversity could be to employ minimally polymorphic genes as vaccine immunogens (91). *P.*

*falciparum* reticulocyte-binding protein homologue 5 (PfRH5) has 3.3-fold lower polymorphism density (10 out of 526 amino acids) (120) than the aforementioned MSP-$1_{19}$ (6 out of 96 amino acids) (121), and is emerging as promising blood-stage vaccine candidate offering protection against multiple parasite strains as measured by *in vitro* growth-inhibition assay (GIA) (120). Interestingly, despite being highly susceptible to antibody-mediated neutralization, PfRH5 probably demonstrates minimal susceptibility to immune selection pressure, and relatively low levels of anti-PfRH5 IgG antibodies were recorded in malaria-exposed Kenyans (120).

#### 1.5.2.4 Duffy-binding protein

While *P. falciparum* uses a myriad of complex receptor-mediated erythrocyte invasion pathways (122-125), it is understood that *P. vivax* and *P. knowlesi* invasion is dependent on Duffy antigen/receptor for chemokines (DARC) present on red-blood cells (126, 127). The Duffy binding protein (DBP) translocates from micronemes onto the surface of *P. vivax* and *P. knowlesi* merozoites and serves as the ligand (128-130) for DARC (131) in erythrocyte-invasion complex. Thus, inhibition of this DARC-DBP interaction is an attractive option for *P. vivax* blood-stage vaccine developers. DBP is a 140-kDa transmembrane protein consisting of two cysteine-rich regions (II and IV) (130). Most of the vaccine studies using this antigen have focused on DBP region II (DBPII), since it contains residues necessary for receptor recognition (128, 132). It was demonstrated that antibodies raised against *P. knowlesi* DBPα (orthologous to PvDBPII) could inhibit invasion of both human and rhesus erythrocytes *in vitro* (133). Moreover, the incubation of *P. vivax* merozoites with anti-PvDBPII antibodies, generated either in rabbits or

humans, more than 50% inhibited the invasion of human red-blood cells in short term *in vitro* cultures (134).

### 1.5.3 Transmission-blocking antigens

Some malaria antigens expressed on the surface of gametes or ookinete stage parasites are the targets of ongoing efforts to develop transmission-blocking vaccines. This type of vaccine intervenes with the parasite's sexual stage development aiming to reduce number of oocysts, potentially resulting in the interrupted transmission of malaria. Therefore, transmission-blocking vaccines would protect only at the population level, as they do not directly benefit the vaccinees, potentially raising some ethical issues.

#### 1.5.3.1 Pfs25/Pvs25, Pfs230, and Pfs48/45

Probably the leading candidate antigens for malaria transmission blocking vaccines are *P. falciparum* and *P. vivax* ookinete surface proteins Pfs25 and Pvs25, respectively. The Phase I clinical trial using these antigens as recombinant proteins formulated with Montanide ISA-51 demonstrated that uniformly high levels of Abs against these Ag could be induced in malaria-naïve volunteers, and these Abs correlated strongly with the transmission blocking activity (135). Although, the further clinical development of this vaccine had to be terminated due to unexpected level of reactogenicity owing to the vaccine formulation, it clearly demonstrated the feasibility of inducing transmission-blocking immunity in humans.

Some other transmission-blocking vaccine candidates have focused on Pfs230 and Pfs48/45 gamete surface proteins. A significant reduction in infectivity of *P. falciparum*

parasites to mosquitoes was observed with antisera raised in mice after vaccinating with recombinant Pfs230 fused to maltose-binding protein (136). Also, a plant-synthesized Pfs230 immunization of rabbits induced high Ag-specific Ab titres capable of reducing oocyst counts by 99% as determined by membrane feeding assay (137). Similarly, the immunizations of nonhuman primates with *E. coli*-synthesized Pfs48/45 recombinant protein formulated with Montanide ISA-51 adjuvant induced 93% and nearly 100% of transmission blocking activity after single and double vaccinations, respectively (138).

## 1.6 A vaccine for malaria: how close are we?

It is now more than 130 years since the French physician Charles Louis Alphonse Laveran first observed malaria parasites under the microscope (139), and more than 110 years since Ronald Ross identified the vector of malaria transmission (140); observations that were later awarded the Nobel Prize. Despite the relatively aged discovery of the causative agent of malaria, a licensed vaccine against this protozoan parasite is still lacking. Malaria vaccine efforts have been impeded not only by an incredibly sophisticated parasite life cycle, but also by the parasite's preferential development inside host cells, thus reducing the potential antigenic targets. Approximately 5300 genes make up the *P. falciparum* genome (141) and different antigens are expressed during different developmental stages, further complicating the search for protective immunogens. Other immune evasion strategies that malaria parasites have evolved include highly polymorphic surface proteins, clonal antigenic switching in a response to immune pressure, and masking of protective epitopes (142) (143) (144), called crypticity. These factors have all contributed to the challenge of designing an efficacious vaccine.

### 1.6.1 Whole-parasite vaccination strategies

Despite all the hurdles, it has been known for more than 40 years that radiation-attenuated whole-sporozoite (RAS) vaccinations administered by mosquito bite confer high degree of sterile protection in various animal models and humans that lasts for up to 42 weeks (145, 146). The RAS vaccinations work through priming the immune system against many different pre-erythrocytic stage antigens as, due to radiation-induced DNA damage, the parasite's liver-stage development is arrested shortly after hepatocyte invasion (147). Furthermore, experimental animal models have demonstrated that the protection after RAS immunization is mediated by parasite-specific $CD8^+$ and $CD4^+$ T cells and Ab responses (148-150). However, the difficulties associated with this type of vaccination, including the need for ~1000 mosquito bites (the number necessary for high-level efficacy) and irradiation of infected mosquitoes under highly controlled conditions, have prevented this regimen from becoming a viable vaccine against malaria.

In an alternative strategy, genetically-attenuated parasites (GAP) have been developed that, similarly to RAS, are unable to complete liver-stage development. GAPs have been generated by deleting genes such as UIS-3 and UIS-4 (upregulated in infectious sporozoites-gene 3 or 4) (151), P36p (152), SAP-1 (encoding sporozoite asparagine-rich protein 1) (153), and FabB/F (enzyme of the type II fatty acid biosynthesis (FAS II)) (154). GAPs, unlike RAS, not only abolish the need for irradiation, but also, owing to their more defined, genetically identical parasite population arrest uniformly at the same stage. Moreover, SAP-1 and especially FabB/F knockout parasites confer a superior protection when compared to RAS because FabB/F parasites are able to invade

hepatocytes and exponentially increase in parasite biomass exposing more antigens for immune system's targeting (155). In contrast, in RAS and early-arresting SAP-1 knockout parasites, development is limited to very early liver stages. The enhanced immunity observed with late-arresting as opposed to early-arresting whole-parasite vaccines highlight the importance of prolonged liver stage parasite development.

More recently, it has been found that exceptionally high levels of long-lasting protection in humans can be achieved through infection with low-dose of live sporozoites administered under prophylactic drug coverage (94). Using this strategy, parasites are able to fully complete their liver-stage development. This potentially exposes even more antigens for immune attack as compared to RAS or GAP vaccination approaches. It has been demonstrated that $CD4^+$ and $CD8^+$ T cell mediate the protection (156), although small quantities of blood-stage merozoites are also present to the immune system, thus, it remains to be determined what contribution immunity against blood-stage parasite forms provides to the overall protection in this regimen.

Whilst more recently developed whole-parasite vaccination strategies abolish the need for irradiation, the difficulties associated with manufacture, and cryopreservation of later generation whole-parasite vaccines, along with their lack of efficacy in humans using needle immunization, still pose major obstacles for large-scale field immunizations. Nonetheless, the success achieved using whole-parasites vaccine approaches have encourage the malaria field to employ the alternative vaccine strategies that are not only feasible to deploy, but also provide comparable levels of sterile efficacy.

### 1.6.2 The leading pre-erythrocytic stage subunit vaccines

Some early studies suggested that the protection elicited by RAS vaccination in mice was dependent on anti-CSP immune responses (157) (158). Therefore, it comes as no surprise that a great deal of effort has been invested in creating a pre-erythrocytic stage malaria vaccine based on CSP. The first demonstration of the ability of anti-CSP antibody to protect against malaria sporozoite challenge was performed in rodent malaria parasite *P. berghei* (159). It paved the way for the development of the most successful, thus far, pre-erythrocytic stage vaccine termed RTS,S (160), which is manufactured by GlaxoSmithKline (GSK) and administered as a protein-in-adjuvant formulation. 19 tetrapeptide CS repeats and the sequence of the TSR region at its carboxy terminal end fused to the hepatitis B virus surface antigen (HBsAg) comprise the RTS (repeat/TSR/HBsAg) portion (Figure 1.4A). The same yeast cells also co-express a HBsAg particle, named S, giving the final product its name RTS,S. RTS,S with GSK's adjuvant system 01 (AS01) currently is undergoing Phase III clinical trials and the initial results indicated that 35% of infants and under 1-year olds receiving three vaccine doses were protected against severe malaria for at least 11 months after immunization (161). It has been suggested that the protective immunity induced by the RTS,S correlates with the strong antibody response to NANP repeats (162).

The T cell depletion experiments performed in rodent models following the aforementioned RAS vaccinations suggested that sufficiently high levels of $CD8^+$ T cells against liver stage antigens may be able to sterilely protect against malaria (163) (164). Therefore, in contrast to Ab-inducing RTS,S vaccination, the alternative approach aims at

stimulating high levels of $CD8^+$ T cells specific for the PfTRAP antigen. Priming with chimpanzee adenoviral vector (ChAd63) and boosting the immune responses with modified vaccinia strain Ankara (MVA) encoding PfTRAP fused to a multi-epitope string encompassing other malarial and non-malarial antigenic T cell determinants (ME.TRAP) have demonstrated exceptionally high levels of sterile protection in pre-clinical studies using rodents (165). Moreover, the protection depended on antigen-specific $CD8^+$ T cells. Similarly, ChAd63/MVA prime-boost regimen encoding ME.TRAP in Phase Ia clinical trial demonstrated protective efficacy in approximately 58% of vaccinees (21% sterile protection) (Ewer *et al.* submitted).

In summary, the whole-parasite vaccination approaches have clearly demonstrated that a vaccine against malaria is a realistic aim. However, efforts to match the protection induced by whole-parasite vaccination strategies using subunit vaccines have been met with various levels of success. To date, consistent efficacy in clinical trials has been achieved by two leading malaria vaccine candidates –RTS, S and viral vectors expressing ME.TRAP- that target the CS and TRAP proteins, respectively. However, individually both of these approaches provide only sub-optimal levels of protection, and efficacy with RTS,S is higher than with ME.TRAP. Part of this thesis assesses the protective potential of TRAP- and CSP-based combination vaccine using viral vector and protein immunization strategies.

## 1.7 Viral vector vaccine platforms

### 1.7.1 Poxvirus-based vaccine vectors

In 1796 Edward Jenner deliberately inoculated 23 individuals with cowpox virus to demonstrate that the infection also conferred immunity against variola virus, the causative agent of smallpox (166). Both of these poxviruses belong to the genus orthopox and their cross-protection was indicative of their close antigenic relatedness. As a result of Jenner's success, vaccinia, another orthopox virus closely related to smallpox, was employed by the World Health Organization (WHO) for their Smallpox Eradication Program in 1966-1980, which succeeded in the global eradication of variola (167). To this day, smallpox eradication remains as one of the greatest achievements of medicine.

Although relatively rare, adverse side-effects associated with the use of wild-type (wt) vaccinia, especially in immunocompromised individuals, have led to the development of attenuated forms of vaccinia, such as modified vaccinia strain Ankara (MVA) and New York vaccinia (NYVAC). MVA was developed from the end of the 1950s in Germany, by passaging wt form for ~570 times in chick embryo fibroblasts (CEFs). As a result of its attenuation MVA has lost around 15% of its genome and together with it the ability to replicate within most of mammalian cells, including human cells. Beginning in 1968, its improved safety profile was confirmed by vaccinating >100,000 people in Germany (168). Also, the relatively large MVA double-stranded DNA (dsDNA) genome (~180kb) is capable of stable incorporation of large pieces of foreign DNA (~25kb) making it an excellent vaccine and gene delivery vector.

To date, MVA has been used as a viral vaccine vector for numerous diseases including malaria (169) (170), HIV (171), tuberculosis (172) and even cancer (173) (174). MVA expressing *Mycobacterium tuberculosis* (*M. tuberculosis*) antigen 85A, designated MVA85A, was successfully used to enhance T cell immunogenicity and protective efficacy in small and large animal models initially primed with BCG vaccination (175, 176) (177, 178). Also, MVA85A safety and immunogenicity has been evaluated in Phase I/II human clinical trials in the United Kingdom and Africa (179) (180) (181). In these studies MVA85A vaccination not only demonstrated an excellent safety profile, but also was able to boost BCG-specific $CD8^+$ and especially $CD4^+$ T cell responses.

MVA encoding pre-erythrocytic stage malaria antigens either ME.TRAP or CSP have also been successfully employed as part of the prime-boost (discussed below) vaccination strategy in clinical testing (182). Interestingly, the immunization of malaria naïve individuals with multivalent NYVAC recombinant virus expressing 7 different *P. falciparum* antigens (183) was safe, sterilely protected 1 out of 35 volunteers and significantly enhanced the prepatent period in the parasitaemic vaccinees (184). More recently, MVA encoding influenza nucleoprotein and matrix protein 1 was demonstrated to be safe and remarkably immunogenic against both inserts in a phase I clinical trial conducted in healthy adults (185).

### 1.7.2 Adenovirus-based vaccine vectors

Recombinant adenoviruses are another widely used vaccine delivery vehicle. Although initially used for gene therapy applications (186), their ability to induce strong and sustained insert-specific immune responses has been instrumental in the development of

adenoviruses as vaccine agents (187). Adenoviruses belong to the family *Adenoviridae* and are medium-sized (60-90 nm), non-enveloped, icosahedral particles, with a protein capsid (240 hexons and 12 pentons) encapsulating dsDNA (~34-43kbp). To date, 57 different virus serotypes have been described based on their cross-neutralizing Ab responses against the outer capsid proteins.

However, probably the most commonly used serotype is human adenovirus type 5 (HAdV-5). Its genome has been well characterized and through the deletion of the E1 transcriptional unit HAdV-5 is rendered replication-incompetent minimizing the possible pathogenic side effects. Further, the removal of the E3 region, which codes for some of adenoviruses' immunomodulatory factors, allows incorporation of ~8kbp inserts without affecting the growth of the virus in permissive cell lines (188).

The recombinant HAdV-5 viral vector as a vaccine candidate has been safely used to target multiple infectious agents including malaria (189) (190), influenza (191), HIV (192) (193), and dengue virus (194) and has demonstrated the ability to induce robust humoral, and particularly potent cellular immune responses against the transgene in several model systems. Also, it has been demonstrated that generally a single administration of HAdV-5 induces stronger responses and elicits a higher degree of protection than poxviruses coding the same antigen (195). A single dose of recombinant HAdV-5 encoding *P. yoelii* CS antigen induced a high frequency of CS-specific $CD8^+$ and $CD4^+$ T cells and sterilely protected a large proportion of mice (196). However, neutralizing Abs induced during a wt adenoviral infection can affect the subsequent use of recombinant HAdV-5 as anti-vector immunity may dampen the viral vector's

immunogenicity. Since the seroprevalence of neutralizing antibodies against HAdV-2 or HAdV-5 serotypes is high within human populations, the attention has shifted towards the use of adenoviruses from other species.

Chimpanzee adenoviruses are emerging as a powerful substitute for the human adenoviruses in clinical vaccine applications (197). Moreover, the immune responses induced by chimp adenoviruses are comparable to the ones seen by human adenoviruses. Two chimpanzee adenoviruses, ChAd63 and ChAd3, have been tried in human clinical trials and potent T cell and Ab responses have been observed (198). ChAd63 vectors have been extensively used in human clinical trials encoding different malaria vaccine antigens, and demonstrated an excellent safety profile and strong immunogenicity (199). Also, to further improve the options available for vaccine delivery a new viral vector, ChAdOX1 based on a different chimpanzee adenovirus backbone, Y25, has been generated at the Jenner Institute and is now being assessed in human clinical trials (200).

### 1.7.3 Heterologous prime-boost regimens

The development of different viral vectored vaccine platforms has provided tools for the induction of powerful cellular immune responses. However, despite these advances, limited protection has been observed against sophisticated pathogens when single vaccinations or multiple immunizations using the same viral vector have been employed (201). The induction of potent transgene-specific immune responses by sequential immunization with the same viral vector has been unsuccessful due to anti-vector immunity generated after the first vaccination. Therefore, attention has been shifted

towards heterologous prime-boost vaccine strategies based on using one vaccine agent for the prime and a different one expressing the same insert for the boost.

In the initial heterologous prime-boost vaccinations, DNA plasmids were employed as the priming agent, while modified poxviruses expressing the same antigen were used at the boost. Regimens included DNA-NYVAC (202) and DNA-MVA (203). Later these regimens also encompassed fowlpox virus (FPV)-MVA (204), influenza-MVA (205), heterologous HAdV26-HAdV5 (206) and even DNA-protein (207) prime-boost strategies targeting various diseases, including malaria (208, 209), tuberculosis (176), HIV (206), and cancer (210). Interestingly, these studies found that MVA was an optimal vector for boosting, whereas adenovirus (Ad) was better for priming both cellular and humoral immune responses, leading to the development of the Ad/MVA prime-boost vaccine strategy. Additionally, the prime-boost interval seemed to be critical and using mice (211, 212) and human (Ewer *et al.* submitted) studies was optimized to 8 weeks.

At the Jenner Institute, heterologous prime-boost regimens have been extensively evaluated with liver- and blood-stage malaria antigens and consistently induced strong immune responses in murine (191, 212), rabbit (213), rhesus monkey (214) and human models (199, 208, 209). In Phase IIa human clinical trials, the sequential immunization with 2 doses of DNA followed by single dose of MVA expressing malaria pre-erythrocytic stage vaccine candidate ME.TRAP elicited sterile protection in 1 out of 8 vaccinees, and the overall protective efficacy strongly correlated with the peak cellular immune responses against the insert (182). Furthermore, an excellent safety profile coupled with powerful $CD8^+$ T cell responses and 58% (21% sterile protection)

protective efficacy was observed after administering ME.TRAP in an ChAd63/MVA prime-boost regimen (199) (Ewer *et al.* submitted). Additionally, the blood-stage antigens, such as MSP-1 and AMA-1, each administered in the identical ChAd63/MVA prime-boost manner in Phase Ia clinical trials induced exceptional levels of antigen-specific $CD4^+$ and $CD8^+$ T cells as well as substantial IgG Ab responses, which, in the case of AMA-1, were also able to demonstrate growth inhibitory activity *in vitro* (208, 209).

Recently it was also shown that a adenovirus prime -- protein-in-adjuvant boost strategy (Ad-P) enhances humoral immune responses when compared to each regimen alone (214-217). Moreover, the use of Ad for priming in Ad-P regimen allowed one to overcome the differential induction of Ab response associated with recombinant protein-in-adjuvant vaccines, and thus comparable immunogenicity was observed regardless of the adjuvant employed (217). Further, the sequential immunizations with Ad-M and protein-in-adjuvant modalities achieved a concurrent T cell and Ab induction, suggesting that it may be possible to tailor subunit vaccines towards even more complete immune responses encompassing powerful humoral and cellular immune factors simultaneously (215).

### 1.7.4 Adjuvants

To enhance the immunogenicity, chemical or molecular compounds, called adjuvants, may be incorporated into the vaccine formulation. One of the most studied, and the only licensed adjuvant for the use in the US is alum, which predominantly enhances Ab responses (218). Alum's mode of action is not known precisely, however, it is thought

that the adjuvant facilitates cell apoptosis, which, in turn, leads to the increased recruitment of dendritic cells (DC) to the sites of injection and augmented presentation of Ag to the helper $CD4^+$ T cells (219).

To date, in addition to alum, five other adjuvants have been licensed for clinical use, including aluminum-phosphate, the oil-in-water emulsion MF59 (licensed by Novartis), virosomes and GSK's AS03 and AS04 adjuvant systems. In fact, GSK's adjuvants are being used with the most-advanced malaria vaccine. It has been shown that the protective efficacy of RTS,S has been improved from 30% to 53% against clinical malaria in children when more immunogenic AS01E, rather than AS02A adjuvant was employed (220). Although this difference was not statistically significant it suggested a possible benefit of the AS01 adjuvant.

Unfortunately, most of currently licensed adjuvant systems, similarly to alum, have only been shown to potentiate the induction of protective antibodies, not T cell responses. However, in many infections like HIV, malaria and tuberculosis as well as cancers, durable and protective T cell immunity is also necessary, therefore there is an immense need for development of adjuvants capable of enhancing T cell responses as well. One approach has been to use oligomerization domains fused to the antigen in order to facilitate with antigen's structural stability (221). The consistent increase in $CD4^+$ and $CD8^+$ T cell responses was observed in mice and non-human primate models when major *M. tuberculosis* antigen 85A was fused to IMX313 oligomerization domain and administered as MVA vaccine (222). Nonetheless, the further development of different

adjuvant systems that increase cellular as well as humoral immune responses is needed in order to target the most complex diseases, including malaria.

## 1.8 Small-animal models of malaria

### 1.8.1 Rodent malaria species

One of the major limitations in the malaria vaccine field is the fact that *P. falciparum* and *P. vivax* do not infect rodents. This eliminates the most commonly used animal models from straightforward assessment of human malaria vaccine candidates. Although, four different malaria species exist that infect mice and have been employed for vaccine studies they differ substantially from human parasites. Moreover, it has been suggested that immune-effector functions of $CD8^+$ T cells against liver stage antigens may be Plasmodium species specific. Butler *et al.* demonstrated that $CD8^+$ T cell-mediated protection against both most widely used murine malaria parasite species *P. berghei* and *P. yoelii*, in part depended on IFN-γ, whereas other effector molecules, such as perforin, were also critical in protection against *P. yoelii* (223). This is in agreement with other studies suggesting that generally it is more difficult to sterilely protect mice against *P. yoelii* rather than *P. berghei* sporozoite challenge (155, 224). On the other hand, normally blood-stage infection is lethal with *P. berghei* parasites, whereas some strains of *P. yoelii* result in chronic infection that over time resolve themselves, and thus those strains are preferred by blood-stage malaria vaccine developers. Despite their intrinsic differences rodent malaria parasites have provided invaluable insights into malaria vaccine design and continue to be the major *in vivo* proof-of-concept models.

Another option for evaluating and optimizing human malaria vaccine candidates has been the use of transgenic (tg) rodent malaria parasites, whereby a gene from *P. falciparum* or *P. vivax* is expressed by one of murine malaria species. Due to historical reasons, mostly *P. berghei* parasites are employed for genetic modification, although some tg based on *P. yoelii* model also exist (225).

### 1.8.2 Tg *P. berghei* malaria parasites

The development of tg murine malaria *P. berghei* technology (226) has revolutionized the field of malaria research with major benefits for drug and vaccine research. Many different tgs have been generated since the first stable integration of exogenous DNA within the *P. berghei* genome (227), ranging from mutants designed to answer parasite fundamental biology questions (228) (229) (230), to tgs that possess human malaria parasite genes, and thus provide an attractive option for *in vivo* evaluation of human malaria vaccines.

In fact, tg *P. berghei* parasites containing genes from human malaria are emerging as a useful tool to assess functional immunogenicity of clinical vaccine constructs *in vivo* and *in vitro* (231). Assays measuring ag specific antibodies or T cell numbers are important, because they demonstrate the level of vaccine's immunogenicity in mice. However, due to the lack of correlates of protection immunogenicity alone does not predict the vaccine's efficacy in the clinic. Tg *P. berghei* models facilitate the optimization of vaccine's clinical constructs providing a robust tool for the assessment of human malaria vaccine's efficacy in murine models.

The tg parasite technology is based on either allelic replacement of the endogenous *P. berghei* gene with the homolog from human malaria (232), or integration of human malaria gene into dispensable loci (233) (234) within *P. berghei* genome by double-homologous crossover recombination. Currently, allelic replacement is by far the preferred method for generating tg relevant for vaccine studies. The table below lists majority of the *P. berghei* tg with the potential use for vaccine studies (Table 1).

Numerous *P. berghei* tg have been reported where endogenous PbCSP gene has been replaced with either full-length *P. falciparum* CSP (67) or a hybrid CSP gene encompassing different regions from both PfCSP and PbCSP genes (235). Biologically both types of *P. berghei* CSP tgs had a significantly reduced ability to infect mosquito salivary glands and vertebrate liver. It has been suggested that the reduced infectivity may be due to gene incompatibility, whereby the PfCSP substitute does not completely overtake PbCSP gene's functions. Also, more recently it has been demonstrated that a mere inclusion of a selection marker downstream of PbCSP gene to an otherwise wt *P. berghei*, significantly reduced parasites' ability to invade hepatocytes *in vivo* (236).

Despite PfCSP tg parasite's decreased infectivity they have been successfully used in vaccine studies. By employing CS(Pf) tg Persson *et al.* (235) demonstrated a sterile protection in immunized C57BL/6 mice and a substantial degree of protection was achieved in animals immunized by passive transfer of PfCSP-specific immunoglobulin. The same tg parasites were also used to develop *in vitro* serum neutralization assay termed a tg sporozoite neutralization assay (237). It allows the quantification of CS(Pf) infectivity of HepG2 cells by real-time PCR, following incubation with human serum.

Thus, tg *P. berghei* expressing chimeric PfCSP can be used in *in vivo* and *in vitro* situations to study functional neutralization of sporozoites in actively immunized animals or by incubating with immune serum and assaying the level of HepG2 cell infectivity.

Tg *P. berghei* expressing PfTRAP has also been generated (232). Wengelnik *et al.* demonstrated that an allelic replacement of PbTRAP with the full-length PfTRAP did not affect parasite's biological properties, including motility, invasion of mosquito salivary glands, and infection of vertebrate host. PfTRAP tg has been an invaluable tool deciphering protein's fundamental biological functions (232). However, currently there are no reports of vaccine studies making use of this mutant.

Tg *P. berghei* parasites expressing some blood-stage antigens from human malaria species have also been generated. As mentioned above, antibodies against PfMSP-$1_{19}$ are associated with protection against blood-stage malaria infection (238) (239) (240). In order to examine the *in vivo* functional activity of PfMSP$1_{19}$-specific antibodies, tg *P. berghei* was generated by allelic replacement of PbMSP-1 with a chimeric gene where the endogenous C-terminal portion of the gene has been substituted with the corresponding *P. falciparum* gene PfMSP-$1_{19}$ (241). Using this *P. berghei* transgenic mutant (Pb-PfM19) de Koning-Ward *et al.* demonstrated that sera from mice immunized with Pb-PfM19 protected RBCs from *P. falciparum* infection in GIA assay (241). Moreover, mice that were vaccinated by passive transfer with the same immune serum were also protected against subsequent Pb-PfM19 challenge (241).

In order to investigate the promoter's role on antigen's subcellular localization, heterologous PfAMA-1 was integrated into *P. berghei* genome leaving the endogenous PbAMA-1 gene unaltered (234). This transgenic parasite, generated by employing the method of allelic integration, successfully expressed the trans-species AMA-1, and the protein also attained correct functional confirmation. Moreover, the temporal expression and subcellular localization of the protein was heavily dependent on the promoter region and high titre antibodies against PfAMA-1 were induced after mice were immunized with this mutant parasite (234).

There have also been a few successful attempts to generate tg *P. berghei* parasites based on transmission-blocking antigen P25 from both *P. falciparum* (TrPfs25Pb) (242) and *P. vivax* (Pv25DR and Pv25DR3) (243) species. Moreover, a greater than 90% reduction in tg TrPfs25Pb oocyst number was observed in female *Anopheles stephensi* mosquitoes after they were fed on the blood of mice that received anti-Pfs25 immune sera from non-human primates by passive transfer. Also, mice immunized with a Pfs25 DNA vaccine demonstrated reduced transmission of TrPfs25Pb mutant when compared to mice immunized with a control plasmid.

To conclude, the availability of tg *P. berghei* mutants expressing human malaria antigens corresponding to each of three parasite's life cycles provide a useful tool for *in vivo* evaluation of functional immunogenicity. The use of these tg parasites facilitates the optimization of putative vaccine candidates, potentially paving the way for more protective regimes in humans. In this thesis the development of further tg *P. berghei* parasites is described, and their usefulness in the vaccine study evaluated.

| Abbreviated name | Transgene | Method of insertion | Reference |
|---|---|---|---|
| **Transgenics based on human pre-erythrocytic stage antigens** | | | |
| CSP-9 | Full-length PfCSP | ARDChr | (67) |
| CS(Pf) | Chimeric PfCSP | ARSChr | (235) |
| 87-11 | Full-length PfTRAP | ARDChr | (232) |
| **Transgenics based on blood-stage antigens** | | | |
| PF83/AMA-1 | Full-length PfAMA1 | AIDChr | (234) |
| Pb-PfM19 | Chimeric PfMSP1 | ARDChr | (241) |
| **Transgenics based on transmission-blocking antigens** | | | |
| TrPfs25Pb | Full-length Pfs25 | ARDChr | (242) |
| Pv25DR and Pv25DR3 | Full-length Pvs25 | ARDChr | (243) |

**Table 1: Selected list of published tg *P. berghei* parasites relevant for vaccine studies.**

The abbreviated name, transgene, the integration method and the references are provided. ARDChr = allelic replacement by double crossover homologous recombination, AIDChr = allelic insertion by double crossover homologous recombination, ARSChr = allelic replacement by single crossover homologous recombination.

## 1.9 Thesis aims

- To compare the immunogenicity and protective efficacy associated with different pre-erythrocytic stage malaria antigen combinations using *P. berghei* challenge system.
- To tailor the most promising pre-erythrocytic antigen combination vaccine towards the maximization of protective efficacy in highly susceptible to malaria infection C57BL/6 mice strain.
- To investigate the immune factors mediating the pre-erythrocytic stage protection.
- To generate *P. berghei* tg parasites enabling the assessment of *P. vivax* vaccine candidates.
- To assess the immunogenicity and protective efficacy of Ad-M prime-boost strategy encoding *P. vivax* TRAP.
- To assess the immunogenicity and protective efficacy of Ad-P prime-boost regimen encoding different *P. vivax* CSP constructs.
- To quantify the protective efficacy of PvCSP and PvTRAP combination vaccine using double-tg *P. berghei* mutant.

## 1.10 Overview of thesis chapters

The work described in this thesis reports the use of *P. berghei* mouse malaria model for a proof-of-concept evaluation of different pre-erythrocytic stage malaria antigen combinations. Further, the observations obtained using *P. berghei* challenge system are applied for the development and optimization of novel *P. vivax* vaccines based on the heterologous prime-boost strategy employing different viral vector and protein-in-adjuvant formulations.

**Chapter 2** outlines the materials and methods employed throughout this thesis. Also, the generation of DNA constructs necessary for the making of tg *P. berghei* parasites and recombinant protein synthesis is described.

**Chapter 3** describes the comparative evaluation of two methods for the quantification of vaccine efficacy in mice, namely *in vivo* imaging of whole animals and linear regression modeling based on blood-stage parasitaemia.

**Chapter 4** investigates the protection against *P. berghei* sporozoite challenge associated with different pre-erythrocytic stage antigen combinations in C57BL/6 and CD1 strains of mice administered in heterologous prime-boost regimen employing ChAd63 and MVA viral vectors, respectively. Also, immunogenicity of each antigen is investigated.

**Chapter 5** describes the further optimization of the most protective pre-erythrocytic antigen combination identified in chapter 4. The immunogenicity associated with different vaccination regimens is shown. Also, mechanistic experiments delineating the factors mediating the protection are investigated.

**Chapter 6** applies the observations made using *P. berghei* challenge model to the development and optimization of *P. vivax* CSP- and TRAP-based vaccines. The immunogenicity and protective efficacy of PvCSP and PvTRAP vaccines is individually evaluated using *P. berghei* tg parasites expressing either PvCSP or PvTRAP transgenes. Finally, a PvCSP and PvTRAP combination vaccine is evaluated using the double-tg *P. berghei* parasites.

**Chapter 7** summarizes the results described in this thesis and indicates the future directions of this project.

# Chapter 2

# Materials and Methods

# 2 Materials and Methods

## 2.1 Materials

### 2.1.1 Reagents

Table 2 details major commercially available reagents used in this study.

| Material | Supplier | Catalogue Number |
|---|---|---|
| 0.1mm electroporation cuvettes | Bio-Rad | 165-2083 |
| 0.2μm syringe filter | Sartorius | 16534 |
| 15mL centrifuge tubes | Fisher, Inc. | FB55950 |
| 2-β Mercaptoethanol [50μm] | Gibco | 31350-010 |
| 5-Fluorocytosine | Invivogen | 2022-85-7 |
| 50mL centrifuge tubes | Greiner | 227261 |
| 60mm petri dishes | Corning | 430166 |
| 6-well tissue culture plates | Fisher, Inc. | TKT-520-030T |
| Agarose | Sigma Aldrich | A9539 |
| Ampicillin | Sigma Aldrich | A5354 |
| Antarctic Phosphatase | New England Biolabs (NEB) | M0289L |
| Anti-asialo GM1 (Rabbit) for 1ml | Alpha laboratories | 986-10001 |
| Anti-mouse CD3ε AlexFluor700 | R&D Systems | FAB100N |
| Anti-mouse CD4 PE clone RM4-4 | eBioscience | 12-0043 |
| Anti-mouse CD4 eFluor650 | eBioscience | 95-0041-42 |
| Anti-mouse CD8α PerCP-Cy5.5 | Becton Dickinson Ltd. | 551162 |
| Anti-mouse CD8α eFluor450 | eBioscience | 48-0081-80 |

| | | |
|---|---|---|
| Anti-mouse IFN-γ APC | eBioscience | 17-7311-82 |
| Anti-mouse interleukin-2 (IL-2) PE-Cy7 | eBioscience | 25-7021-80 |
| Anti-mouse TNFα eFluor450 | eBioscience | 48-7321-80 |
| Anti-mouse CD107a PE | eBioscience | 12-1071-83 |
| Anti-mouse NK1.1 FITC | eBioscience | 11-5941-81 |
| Anti-mouse CD69 PE-Cy7 | BioLegend | 104511 |
| CD1d Tetramer PE | Proimmune | N/A |
| CD16/32 (Fc block) | eBioscience | 14-0161-82 |
| CF11 cellulose powder | Whatman | 4021-500 |
| Cell strainers | BD Biosciences | 352350 |
| Cytofix/Cytoperm™ fixation/permeabilization solution kit | Becton Dickinson Ltd. | 555028 |
| DH5α sub-cloning efficiency cells | Invitrogen | 18265-017 |
| Diethanolamine buffer | Pierce | 34064 |
| Dimethyl sulphoxide (DMSO) | Sigma Aldrich | D2650 |
| D-Luciferin potassium salt 1.0g | Caliper Lifesciences | 122796 |
| Domitor™ | Oxford University Veterinary Services | N/A |
| Dried skimmed milk powder | Waitrose | N/A |
| Dulbecco's PBS | Sigma Aldrich | D8537 |
| Dulbecco's Modified Eagle's Medium | Sigma Aldrich | D6546 |
| Ethylenediaminetetraacetic acid (EDTA) | Sigma Aldrich | E7889 |
| ELIspot colour development kit | BioRad | 170-6432 |
| Endotoxin Free water | Sigma Aldrich | W3500 |
| Ethanol | Sigma Aldrich | 32221 |

| | | |
|---|---|---|
| Mouse IgG1 Fab and F(ab')2 Preparation Kits | Pierce | 44980 |
| Fetal Calf Serum (FCS) | Sigma Aldrich | F-2442 |
| Ultra-low IgG Fetal Bovine Serum (FBS) | Invitrogen | 16250-086 |
| Gateway® LR Clonase® II enzyme mix | Invitrogen | 11791-020 |
| Giemsa | Sigma Aldrich | GS1L |
| Glycerol | Sigma Aldrich | G5516-1L |
| Goat anti-mouse whole IgG alkaline phosphatase conjugate | Sigma Aldrich | A-3562 |
| GolgiPlug | Becton Dickinson Ltd. | 555028 |
| Heparin | Sigma Aldrich | H3149 |
| Hydrochloric Acid (HCl) [1M] | Sigma Aldrich | S-7653 |
| Immersion Oil | Sigma-Aldrich | 10890 |
| Isofluorane | Oxford University Veterinary Services | N/A |
| Kanamycin | Sigma Aldrich | K0254 |
| Ketaset™ | Oxford University Veterinary Services | N/A |
| $KHCO_3$ [1mM] | Sigma Aldrich | P-9144 |
| Klenow DNA Polymerase | Fermentas | EP0421 |
| L-glutamine [4mM] | Sigma Aldrich | G-7513 |
| Lipofectamine™ | Invitrogen | 11668-019 |
| Low phosphate PBS | Gibco | 10010-031 |
| MAIP ELIspot Plates | Millipore | MAIPS4510 |
| MEM α-modification | Sigma Aldrich | M-4526 |
| Methanol | Sigma Aldrich | 32213 |
| Micro-fine Insulin Syringe with needle 1mL 29g x 12.7mm | Nu-care products | M4891 |

| | | |
|---|---|---|
| Microlance needle 26g x 5/8 inch | Nu-care products | M4300 |
| Microvette tubes | Sarstedt | CB300K2E |
| MinElute gel extraction kit | QIAgen | 28606 |
| Mouse IFN-γ ELISPOT kit (ALP) | Mabtech | 3321-2A |
| $CaNa_2EDTA$ | Sigma Aldrich | ED2SC |
| $Na_2EDTA$ | Sigma Aldrich | ED2SS |
| Neomycin sulfate | Invitrogen | 21810-031 |
| Neutral buffered formalin | Sigma-Aldrich | HT501128 |
| $NH_4Cl$ [0.15M] | Sigma Aldrich | A-4514 |
| NUNC Maxisorp 96-well plates | Fischer, Inc. | DIS-971-030J |
| Nycodenz | Lucron Bioproducts | 1002424 |
| One-shot PIR1 competent *E.coli* | Invitrogen | C1010-10 |
| Ovalbumin (Grade VII) | Sigma Aldrich | A7641 |
| Phire® Hot Start DNA Polymerase | Thermo Scientific | F-120S |
| Phosphate Buffered Saline (PBS) | Sigma Aldrich | D-8537 |
| Phusion® High-Fidelity DNA Polymerase | NEB | M0530L |
| PBS/Tween Sachets | Sigma Aldrich | P3563 |
| p-Chlorophenylalanine | Sigma Aldrich | C8655 |
| Pen/strep [100U penicillin 100μg strep] | Sigma Aldrich | P-0781 |
| Percoll | Sigma Aldrich | P1644 |
| Pyrimethamine | Sigma Aldrich | P-7771 |
| Plastipak syringe 1mL Luer slip | Nu-care products | M0013 |
| pNPP (20mg tablets) | Sigma Aldrich | N-2765 |
| Proteinase K | Qiagen | 1017738 |

| | | |
|---|---|---|
| Purified Mouse IgG1 | Sigma Aldrich | |
| Purified Rat IgG | Sigma Aldrich | I4131 |
| Qiagen plasmid midi kit | Qiagen | 12143 |
| QIAprep spin miniprep kit | Qiagen | 27106 |
| QIAamp DNA mini kit | Qiagen | 51304 |
| Restriction and Ligation Enzymes | NEB | Various |
| RPMI-1640 | Sigma Aldrich | R0883 |
| SimplyBlue™ SafeStain | Invitrogen | LC6065 |
| Sodium dodecyl sulfate (SDS) | Sigma Aldrich | L4390 |
| S.O.C. medium | Invitrogen | 15544-034 |
| Smart Ladder DNA marker | EurogenTec | MW-1700-02 |
| Sodium Azide | Sigma Aldrich | S2002 |
| SYBR Safe in DMSO | Invitrogen | S33102 |
| Terrific Broth | Sigma Aldrich | T0918 |
| Tetracycline hydrochloride | Sigma Aldrich | T7660-5G |
| Trizma® HCL buffer solution (Ph8) | Sigma Aldrich | T2694 |
| Tris-acetate-EDTA | Fischer, Inc. | BP1332-1 |
| Trisodium citrate | Sigma Aldrich | S1804 |
| U bottom plates, with lid, 96-well | Jencons | 734-0027 |
| V bottom plates, 96-well | Fischer, Inc. | DIS-210-150L |
| Zeocin | Invivogen | ant-zn-1 |

**Table 2: Reagents used throughout this thesis.**

The reagent name, supplier and catalog number are shown.

### 2.1.2 Solutions

**ACK Lysis Buffer**: 8.29g $NH_4Cl$ (0.15M), 1g $KHCO_3$ (1mM), 37.2mg $Na_2EDTA$ in 800mL $dH_2O$. pH adjusted to 7.2-7.4 with HCl (1M) before making a final solution up to 1L with $dH_2O$.

**Buffered medium for Nycodenz**: 5 mM Tris/HCl, 3 mM KCl, 0.3 mM CaNa2EDTA; pH adjusted to 7.5 before making a final solution up to 500ml with $dH_2O$.

**Coating Buffer**: 15mM sodium carbonate and 35mM sodium bicarbonate capsules were dissolved in $dH_2O$ and autoclaved.

**Complete Medium (D10)**: Minimal Essential Media (MEM) α-modification was supplemented with 5mL L-glutamine (2mM), 5mL pen/strep (100U penicillin, 100μg streptomycin), 500μl 2-Mercaptoethanol (50μm) and 50mL of heat inactivated foetal calf serum (FCS) (10%).

**Diethanolamine Buffer**: A 5x stock was purchased and diluted with $dH_2O$ before use.

**FACS buffer:** 2.5g (0.5%) Bovine Serum Albumin (BSA) was added to 500mL PBS.

**Giemsa:** 5% Giemsa (10mL Giemsa plus 190mL Milli-Q water).

**Loading Dye:** 0.4% orange G, 15% Ficoll® 400, 10mM Tris-HCl (pH 8.0), 50mM EDTA (pH 8.0) made up with $dH_2O$.

**Nycodenz density-gradient stock solution:** 138 g Nycodenz powder was dissolved in 500 ml Buffered Medium (density of 1.15 g/ml at 20ºC) and sterilized by autoclaving for 20 min at 120ºC.

**Phosphate buffered saline (PBS)** 0.01M: NaCl 0.138M, KCl 0.0027M, pH 7.4: made by dissolving tablets in $dH_2O$.

**PBS Formalin 1%:** 15mL of 4% formaldehyde was added to 45mL PBS.

**PBS/Tween (PBS/T):** 0.01M NaCl, 0.138M, KCl 0.0027M, pH 7.4 Tween-20 0.05%. Sachets are dissolved in $dH_2O$.

**Pyrimethamine solution:** Pyrimethamine powder dissolved in 10mL of DMSO shaking bottle vigorously. 3mL of the solution transferred to 1L of tap water with an adjusted pH of 3.5-5.0 (with 1M HCl).

**Tris-acetate-EDTA** (TAE) buffer: Made up from 50x concentrate with $dH_2O$.

**Terrific broth**: 12g bacto-tryptone, 24g bacto-yeast extract, 4mL glycerol made up to 900mL with distilled water and autoclaved. 100mL sterile solution of 0.17M $KH_2PO_4$, 0.72M $K_2HPO_4$ added before use.

**Tris buffer:** a stock solution of 1M Tris was diluted in $dH_2O$ to a working concentration of 20mM. The pH was adjusted to 7.5 with HCl (1M) and the solution was filter sterilized for use *in vivo*.

## 2.2 Methods – Molecular Biology

### 2.2.1 Agarose gels

DNA restriction digest or PCR products were separated by 1% agarose gel electrophoresis (100V, 40-60min) in 1x Tris-acetate-EDTA (TAE) buffer stained using SYBR Safe. A relevant amount of 6x loading dye was added to each sample immediately before loading of DNA onto the gel. Visualization of the DNA was accomplished by the

use of transilluminator. The size of bands was estimated by comparison to the DNA marker smart ladder.

### 2.2.2 Restriction digest

DNA was digested in either 20 or 50µL reaction mixtures as outlined below. Most of the digestions were incubated for 2-3h at 37ºC, unless the suggested incubation temperature for enzymes differed. Digestions generating complementary 'sticky ends' were treated with Antarctic Phosphatase (AP) for 30 min at 37ºC to minimize the vector religation.

| 20 µL reaction | 50 µL reaction | |
|---|---|---|
| 2 µL | 5 µL | Total NEB Restriction Enzyme(s) (10,000U/mL)* |
| 2 µL | 5 µL | NEB restriction buffer (10x) |
| 2 µL | 5 µL | BSA (10x) |
| x µL (0.5-1µg) | x µL (5-10 µg) | Plasmid DNA |
| →20 µL | →50 µL | Sterile distilled $H_2O$ |

*If double-digest performed using two enzymes, the volume of each enzyme was halved.

### 2.2.3 Ligation reactions

Digested DNA fragments were excised from agarose gels, purified using QIAgen MinElute gel extraction kit eluting the contents into 10µL of $dH_2O$. Ligation was then performed overnight at 16ºC using the reactions and controls outlined below and in Jenner Protocol (J) 98 (all relevant Jenner Protocols can be found in Appendix One). Once completed 1-2µL of ligation reaction was used for bacterial transformations.

| Reagent | Uncut control | No Insert control | No ligase control | Ligation Reaction |
|---|---|---|---|---|
| $dH_2O$ | 6 µL | 6 µL | 4 µL | 5 µL |
| 10x ligation buffer | 2 µL | 2 µL | 2 µL | 2 µL |
| Plasmid DNA | 1 µL uncut | 1 µL | 1 µL | 1 µL |
| Insert DNA | - | - | 3 µL | 1 µL |
| T4 DNA ligase | 1 µL | 1 µL | - | 1 µL |

### 2.2.4 Bacterial transformations

Chemically competent sub-cloning efficiency DH5-alpha *E. coli* cells were used for the transformation reactions (NEB). The bacteria were thawed on ice and 50µL of cells transferred into a new 1.5mL tube. 10-15ng of DNA plasmid or 1µL of ligation reaction was then gently mixed with the cells and left on ice for 30 minutes. The reaction mixture was inserted into the 42ºC water bath for 45 s. Following the heating *E. coli* and DNA mixture was placed on ice for 2-5 min before adding 250µL of SOC media. The whole mixture was then placed into 37ºC shaking incubator for 60 min before seeding the cells onto the agar plates containing the relevant antibiotic.

### 2.2.5 Polymerase chain reaction (PCR)

To modify the relevant DNA constructs or perform diagnostic analysis of obtained DNA or parasite clones PCR was employed. For the modification of DNA sequences high-fidelity Phusion PCR was used (NEB), whereas diagnostic PCR was performed using Phire Hot Start II polymerase (NEB) following manufacturer's recommended conditions.

### 2.2.6 Plasmid DNA preparation

Individual colonies from LB Agar plates supplemented with relevant antibiotic were selected and cultured overnight in 3mL LB broth plus the same antibiotic. Next day

plasmid constructs were purified by Qiagen QIAprep spin miniprep kits. The identity of DNA was confirmed using diagnostic restriction enzyme digests carried out as described in section 2.2.2. Bacteria containing a correct version of each construct were amplified by incubation overnight in 200mL LB medium plus selection antibiotics. Following incubation a 1mL aliquot was removed. This was mixed with 1mL 50% glycerol in complete media to form a bacterial stock, which was stored at -80ºC for long-term use. DNA from the remaining 200mL culture was purified using Qiagen plasmid midi kits and stored at -20ºC. DNA concentrations were measured using NanoDrop spectrophotometer.

### 2.2.7 Antigen insert

DNA plasmids encoding either full-length or modified malaria antigens, codon-optimized for expression in mammalian system, were synthesized by Geneart (Regensburg, Germany) (Table 2). The antigen modifications included: tPA (human plasminogen activator) (GenBank Accession no. K03021) leader sequence was inserted in the upstream region of the gene replacing the native endogenous leader sequence as it has been suggested that this adjustment facilitates with antigen expression within the host cells (244). In addition, the transmembrane (TM) domain or GPI-anchor was removed from TRAP or PvCSP genes, respectively, by introducing two stop codons in order to maximize protein secretion from any virus-transduced cell (213).

| Antigen | NCBI accession no. | Antigen length (in bp) | Modifications |
|---|---|---|---|
| *P. berghei* TRAP | AAB63302.1 | 1821 | +tPA/-TM |
| *P. berghei* CSP | PB001026.00.0 | 1023 | none |
| *P. berghei* CelTOS | XP_676794.1 | 558 | none |
| *P. vivax* TRAP (Salvador I) | XP_001614147.1 | 1671 | +tPA/-TM |
| *P. vivax* CSP VK210 (Belem) | P08677 | 861 | +tPA/-GPI |
| *P. vivax* CSP VK247 (PNG) | M69059 | 864 | +tPA/-GPI |
| *P. vivax* CSP VK210/247 | N/A | 1131 | +tPA/-GPI |
| *P. vivax* NC control | N/A | 594 | +tPA/-GPI |

**Table 3: Outline of all of the malarial antigens used throughout this thesis.**

The malarial antigens with their NCBI unique identifier, gene length and relevant modifications are shown. +tPA identifies the replacement of endogenous leader sequence with that of human plasminogen activator, whereas –TM/-GPI indicates that for some genes either transmembrane or GPI-anchor domains were also removed where relevant.

### 2.2.8 Restriction cloning into ChAd63 vector

All of DNA constructs required for ChAd63 virally vectored vaccine manufacture were generated using the same methods and cloning strategies (Figures 5A). In the first step of cloning, unique predesigned Acc65I and NotI sites were used to insert the synthetic transgenes into the adenovirus entry plasmid. The transgene was placed upstream of BGH poly(A) transcription termination sequence and under the control of long cytomegalovirus (CMV) promoter (encodes regulatory element, enhancer, and intron A). The entry plasmid also contained attachment L (attL) sequences, which were required for site-specific recombination with attachment R (attR) sites located on the destination vector.

In the second step of cloning, *in vitro* Gateway reaction was performed mediated by LR Clonase II system (Invitrogen), whereby entry vector containing transgene together with its transcription and translation regulation elements was integrated into the destination plasmid by site-specific recombinase through attL-attR interaction. The diagnostic PCR was performed to confirm the desired integration before continuing with recombinant ChAd63 production.

### 2.2.9 Restriction cloning into MVA shuttle vector

Similarly, all of the malarial antigens were inserted into the MVA shuttle vector using identical cloning strategy (Figure 5B). Unique predesigned Acc65I and XhoI sites were used for integration and the transgenes were inserted under the control of endogenous P7.5 promoter. Diagnostic PCR and restriction digests were used to verify the correct insertion before linearization of the MVA-GFP2 plasmid as outlined in section 2.3.2.

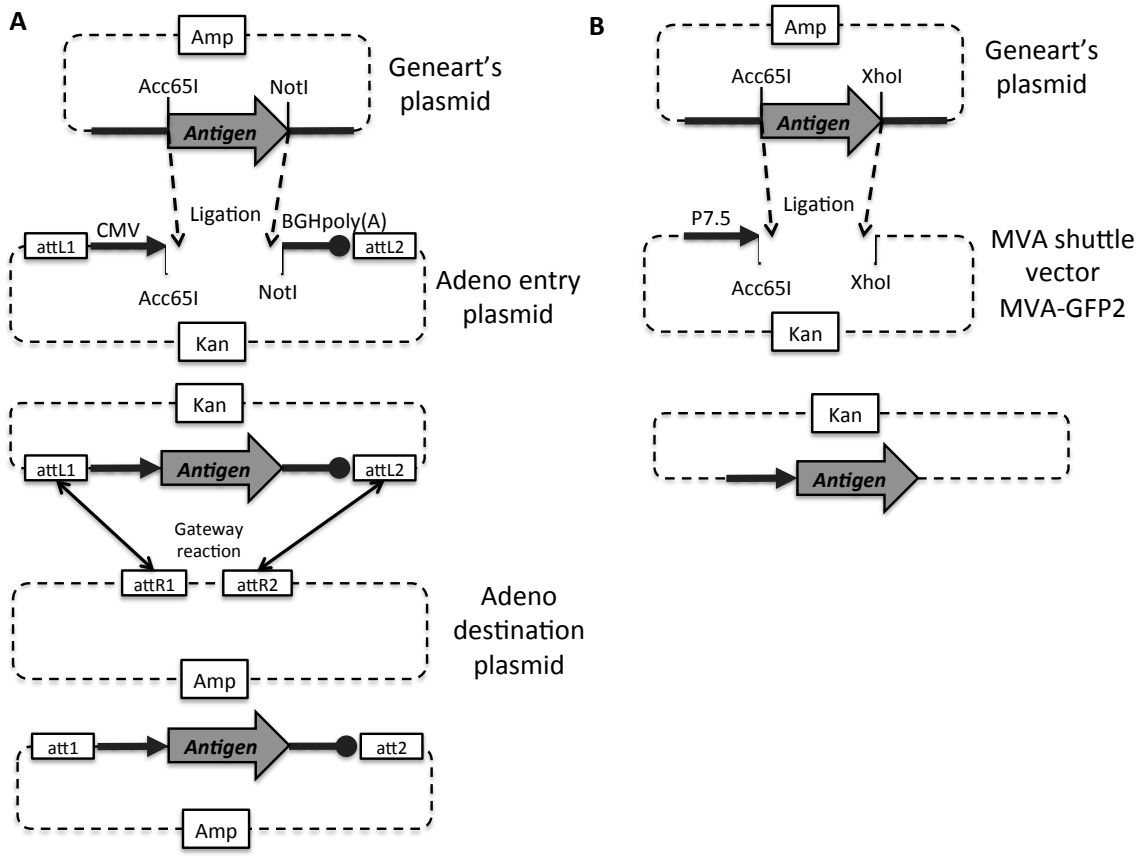


**Figure 5: Cloning steps involved in generation of DNA constructs required for viral vector manufacture.**

Malarial antigens were synthesized by Geneart and cloned into plasmids at the pre-designed unique restriction sites. (A) Acc65I and NotI sites located at the 5' and 3' ends of the transgene, respectively, were used for inserting synthetic malarial antigen into the adenovirus entry plasmid between CMV promoter and BGH poly(A) regions. In the second step of cloning, site-specific recombination between attL and attR sequences was performed resulting in transgene incorporation into the adenovirus destination vector. (B) The same Geneart construct containing synthetic malarial antigen was digested at the unique Acc65I and XhoI sites. The released antigen was then ligated in a single step into the MVA shuttle vector, termed MVA-GFP2, which was subsequently used for the production of recombinant MVA.

### 2.2.10 Recombinant protein synthesis

All of the recombinant proteins used throughout this thesis were synthesized by Dr. T. Malinauskas from the Division of Structural Biology (STRUBI) at the University of Oxford, using previously described method (245). In brief, the codon optimized *P. berghei* CSP, TRAP, TOS and *P. vivax* TRAP, VK210, VK247, and N- and C-terminal ends of PvCSP genes were cloned into the pHLsec plasmid between AgeI and KpnI restriction sites in frame with the His-tag at the 3'end and placed under the control of CMV enhancer and chick beta-actin promoter. The constructs were bulked-up in 2L of *E. coli* cultures and purified using Endotoxin-free Plasmid Mega Kit (Qiagen). 2 mg of resulting DNA was used for subsequent transient transfection into HEK-293T cells utilizing polyethylenimine (PEI) as a transfection reagent. This resulted in the secreted protein with N-terminal ETG and C-terminal GTK($His_6$) tags. Protein was purified from dialyzed (against PBS buffer) conditioned medium by immobilized $Co^{2+}$-affinity chromatography followed by size-exclusion chromatography in 20 mM Tris-HCl pH 8.0, 300 mM NaCl. The protein size was verified by Western blotting using the PentaHis monoclonal primary antibody (1:1000 dilution, Qiagen) and goat anti-mouse IgG peroxidase-conjugated secondary antibody (1:2000, Sigma).

### 2.2.11 SDS-PAGE

Sodium dodecyl sulfate polyacrylamide electrophoresis (SDS-PAGE) was performed as described in J119. In brief, the electrophoresis tank was filled with Tris-HEPES-SDS running buffer. Pierce pre-cast gel was placed in the gel holder and the central reservoir was filled with the same Tris-HEPES-SDS running buffer. Samples were loaded and run

under reducing conditions at 70V for 25 min. Then the voltage was increased to 100V and the samples were run for another 35-45 min. The gel was stained with SimplyBlue SafeStain Coomassie stain (Invitrogen, USA) overnight and de-stained in $dH_2O$.

## 2.3 Methods – Molecular Virology

### 2.3.1 Adenovirus Transfection and Purification

Adenovirus vector preparation and transfection was carried out as indicated in J004a and J004b, respectively. Briefly, to expose the left and right viral ITRs to allow proper viral replication and packaging plasmid encoding adenovirus was linearized with PmeI restriction enzyme. Linearized DNA was mixed with Lipofectamine 2000 transfection reagent. 600µL of these DNA/lipid complexes were loaded onto the 293TREx cells and incubated for 4 h after which the transfection reagent was replaced with 5mL of antibiotic-free media. The 293TREx cells are permissive for the synthesis of replication-incompetent adenoviruses as the cell line provides E1 transcripts *in trans*. Cells were placed at 37ºC, 5% CO2 and starting at 48 h post-transfection their viability and cytophilic effect was monitored using microscope. Cells showing cytophilic effect were detached from the flask by gentle tapping. Recombinant adenovirus was purified using caesium chloride (CsCl) gradient as described in J005. Virus titre was quantified using plaque forming unit assay (pfu) as suggested in J006 and immunostaining of infected cell monolayers as described in J259.

### 2.3.2 MVA Transfection and Purification

The linearization of MVA shuttle vector was performed by digesting the plasmid at the restriction site(s) located outside TKR and TKL regions as outlined in protocol J017. Chick embryo fibroblasts (CEF) used for production of MVA prior to transfections were maintained as described in protocol J013. When CEFs reached approximately 90% confluency, cells were infected with MVA expressing red fluorescent protein (RFP) as described in J176. At the same time the transfection mix containing linearized MVA shuttle vector was also added to the CEFs containing MVA-RFP. This allowed the exchange of RFP with the shuttle vector cassette encoding both antigen and GFP by the recombination event that took place at the TL locus of MVA genome. After 2-day incubation with virus, CEFs were prepared for MoFlo cell sorting (performed by D. Worth at the Jenner Flow Sorting Facility) as indicated in protocol J131. CEFs containing MVAs expressing GFP rather than original RFP gene were selected and their cell lysates after cell sorting used to infect another batch of CEFs as in J016. Repeated rounds of plaque picking were then used to select successful recombinant MVAs containing GFP as outlined in J018. Purified MVAs were bulked-up as in J019 and PCR verifying the identity and determining the purity of virus was performed as detailed in J079. The recombinant MVA viral titre in plaque forming units (PFU) was then quantified as outlined in J111.

## 2.4 Methods – Molecular Parasitology

### 2.4.1 Generation of DNA construct targeting allelic exchange of *P. berghei* TRAP

The constructs targeting the allelic exchange of *P. berghei* TRAP by *P. vivax* TRAP were made as previously published with minor modifications (246). First, to facilitate the translation of the exogenous protein, a *P. vivax* TRAP gene from the Salvador I strain was codon optimized for expression in *P. berghei*. Additionally, the PvTRAP gene at the 5'end was flanked with 50 bp and at the 3'end with 600 bp sequences corresponding to 5' and 3'UTR PbTRAP regions, respectively. The whole 2.3 kbp construct termed pMA-PvTR-trans was ordered from Geneart.

Different pJAZZ clones and original DNA plasmids used for recombineering, including pSC101gbaA-tet (247), pR6K-ZEO (248), and pR6K-3xHA (249) were kindly provided by Dr. Oliver Billker (Wellcome Trust Sanger Institute). The plasmids were further modified as follows: the *zeo-pheS* cassette was amplified from pR6K-Zeo plasmid using the following forward 5'-GTA TTT ACT ATT TCC AAA AGA ATT ATG GAT AAA ACA AAA AAG TGA TAA TAA AGG CGC ATA ACG ATA CCA C and reverse 5'-ATC GCT GCA TTA ATG ATT TGC CTA TTT TTT TAC CAA TTC ATT TTA TTA TGC CGC CTA CTG CGA CTA TAG A primers (the primers used for the making of tg parasite are listed in table 4). The resulting 2kb PCR fragment containing *zeo-pheS* cassette flanked by Gateway *attR1-attR2* sites and 50 bp homology regions was used in the first stage of recombineering (Figure 6A).

For the second cloning stage, the plasmid pR6K-3xHA was modified as follows. Firstly, to remove the 3'UTR *Pb*DHFR upstream of the *hDHFR-yfcu* cassette, the plasmid was double-digested with PspOMI and FseI, ends were blunted using Klenow DNA Polymerase. The resulting construct was self-ligated back together. The newly modified

plasmid was termed pR6K-3xHA-noRR. Secondly, a 500 bp fragment homologous to the 3'UTR *Pb*TRAP was cloned into unique Acc65I site within pR6K-3xHA-noRR downstream of *hDHFR-yfcu* cassette. The 500 bp insert from the 3'UTR PbTRAP region present immediately downstream of the PbTRAP gene provided a site for a homologous recombination event that took place in the *P. berghei* parasites during negative selection step as outlined in chapter 6. The 500 bp fragment was generated by amplifying the pMA-PvTR-trans plasmid as a template using the following forward 5'- TAG TAG GGT ACC TTT TAA TAA ACA TAT ATA TCT AGA TGA TTA TTC and reverse 5'- TAG TAG GGT ACC GCG GCC GCG TAT TAT CAC TTT TTT GTT TTA TCC ATA ATT C primers. The resulting new construct was named pR6K-3xHA-noRR500.

Next, *E. coli* was co-transformed with both pMA-PvTR-trans and pSC101gbaA-tet plasmids and propagated at $30^0$C in LB Broth containing both Ampicillin and Tetracycline. pSC101gbaA-tet plasmid, encoding the bacteriophage *λ red* operon and *E. coli recA*, allows plasmid modification by the method of recombineering (247). Next, using homologous recombination in *E. coli*, an intermediate vector was generated, in which the *zeo-PheS* PCR fragment was inserted into the pMA-PvTR-trans plasmid 500 bp downstream of PvTRAP gene. The *zeo-PheS* construct confers resistance to zeocin through the bleomycin resistance gene (Sh ble) from *Streptoalloteichus hindustanus* and susceptibility to p-chlorophenylalanine through mutant allele of a phenylalanine tRNA synthase (pheS). The resulting recombineering construct pMA-PvTR-trans-ZEO was then released by double digestion with PacI and SacI restriction endonucleases. The linear construct was then used for integration into the pJAZZ clone (250) containing 8 kb

fragment of the wt *P. berghei* gDNA representing TRAP loci by double cross-over homologous recombination event. In the second stage of cloning *in vitro* Gateway LR reaction was used to exchange the bacterial marker by site-specific recombination for a much larger *hdhfr-yFCU* cassette allowing positive and negative selection in *P. berghei* (249). The desired recombination products were obtained after negative selection on yeast extract glucose medium containing p-chlorophenylalanine (YEG-Cl). The diagnostic PCR was used throughout the cloning procedure to verify the correct integration of DNA constructs (Figure 6B). Finally, to generate the linear target construct for electroporation into schizont stage *P. berghei* parasites, pJAZZ vector containing 2.9kb of 5'UTR PbTRAP region, codon-optimized *P. vivax* TRAP gene, and 500bp of 3'UTR PbTRAP with a *hdhfr-yFCU* cassette downstream of it was digested with NotI enzyme.

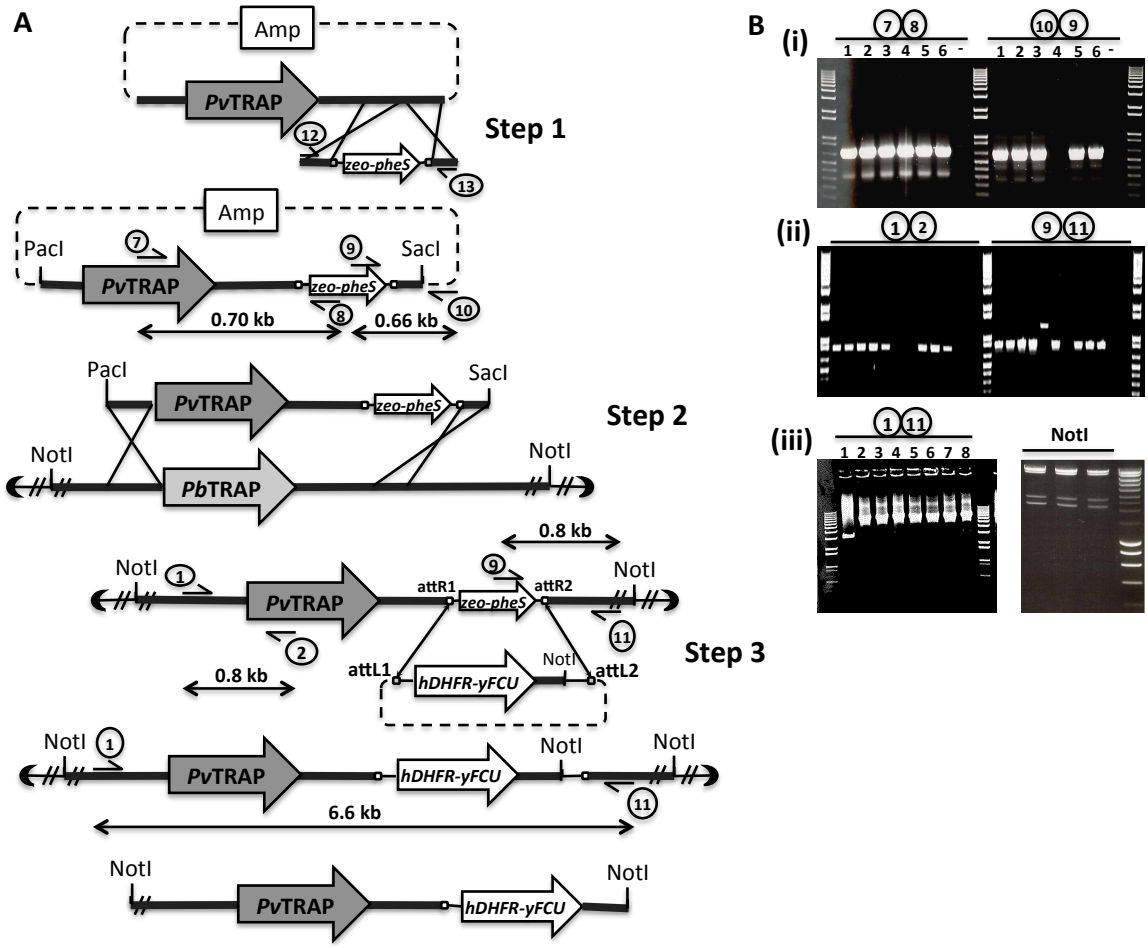


**Figure 6: Generation of DNA constructs targeting allelic exchange of PbTRAP gene.**

(A) During the initial stage of cloning (Step 1) *zeo-pheS* cassette was incorporated at the designated location downstream of PvTRAP gene by recombineering. Next, the resulting plasmid pMA-PvTR-trans-ZEO was digested at PacI and SacI sites and incorporated by double homologous crossover recombination into the pJAZZ clone replacing PbTRAP gene during the second stage of recombineering (Step 2). Finally, *zeo-pheS* was exchanged for *hDHFR-yFCU* cassette by site-specific recombinase reaction in the third step of cloning (Step 3). The final construct was digested at NotI sites releasing integration cassette containing PvTRAP gene, which on both sides was flanked by long homology arms corresponding to 5' and 3' UTR PbTRAP. (B) The correct integration of DNA constructs was confirmed by diagnostic PCR following (i) step 1, (ii) step 2, and (iii) step 3. The circled numbers indicate the primers used for genotyping and can be found in table 4.

| No. | Name | Primer sequence (5’ -> 3’) |
|---|---|---|
| **Generation of transgenic *P. berghei* PvTRAP** | | |
| 1 | oISA00573 | 5'-CATTTAATTTCCTCAGACGTTATTGAAG |
| 2 | PvTRAP-trans(R) | 5'-CAATTAGGTTCTCTTGGTCTACATCCTGCTATTA |
| 3 | PvTRAP-trans(F3) | 5'-AGGTGCAGATGGAAATCCAGTAGAAG |
| 4 | KB3 | 5'-TAAATGACTCCAGACATAATAACACAGATA |
| 5 | 1F_yfcu | 5'-GTTGGGTGACTTTGGTGACAGATACTAC |
| 6 | PbTRAP-trans(1R) | 5'-GTGGTGAATAATTATTTTGAAGTTGTGC |
| 7 | PvTRAP_trans(F4) | 5'-GCCTTTAAATAATAAACTCATAAACTCGT |
| 8 | ZEO_R1 | 5'-GAACGGCACTGGTCAACTTG |
| 9 | ZEO_F1 | 5'-TCATTCTTCGAAAACGATCT |
| 10 | PbTRAP_trans(R1) | 5'-GGGATGTGCTGCAAGGCGATTA |
| 11 | oISA00574 | 5'-GCAACTACAAATAACGAAGAAAATGAAAG |
| 12 | oISA00571 F | 5'-GTATTTACTATTTCCAAAAGAATTATGGATAAAACAAAAAAGTGATAATAAAGGCGCATAACGATACCAC |
| 13 | oISA00572 R | 5'-ATCGCTGCATTAATGATTTGCCTATTTTTTTACCAATTCATTTTATTATGCCGCCTACTGCGACTATAGA |
| 14 | TRAPtrans-3'U(F) | 5’-TAGTAGGGTACCTTTTAATAAACATATATATCTAGATGATTATTC |
| 15 | TRAPtrans-3’U(R) | 5’-TAGTAGGGTACCGCGGCCGCGTATTATCACTTTTTTGTTTTATCCATAATTC |
| 16 | Forward | 5’-TAGTAGaccggtGACGAGAAGGTGGTGGACGAAG |
| 17 | Reverse | 5’-TAGTAGggtaccCTTGTAGCCGTTGTTGCTGGAC |
| **Generation of transgenic *P. berghei* PvCSP expressing either VK210 or VK247 alleles** | | |
| 18 | CSrec1(F) | 5'-AAAAAACATTAACAAAAAACAAAATCTATATATACACGCATATATTTAAAAAGGCGCATAACGATACCAC |
| 19 | CSrec1(R) | 5'-AATATTTATATAATATATAAATATTTATAATCATGCGTAATGTTTATTTACCGCCTACTGCGACTATAGA |

**Table 4: Primers used for the generation of DNA constructs targeting allelic exchange of PbTRAP and PbCSP with homologous *P. vivax* genes.**

The table includes the designated number, name and the sequence of primers used for the generation of DNA constructs relevant for the making of tg *P. berghei* parasites.

### 2.4.2 Generation of DNA constructs targeting allelic exchange of *P. berghei* CSP

The allelic replacement of *P. berghei* CSP with different alleles of *P. vivax* CSP gene was performed using published "Gene-in/Marker-out (GIMO)" technique with minor modifications (251). The DNA constructs mediating the insertion of PvCSP variants into the *P. berghei* genome were generated as follows:

Initially, *zeo-pheS* cassette was amplified from pR6K-Zeo plasmid using the following forward 5'-AAA AAA CAT TAA CAA AAA ACA AAA TCT ATA TAT ACA CGC ATA TAT TTA AAA AGG CGC ATA ACG ATA CCA C and reverse 5'-AAT ATT TAT ATA ATA TAT AAA TAT TTA TAA TCA TGC GTA ATG TTT ATT TAC CGC CTA CTG CGA CTA TAG A primers. The resulting 2kb PCR fragment containing *zeo-pheS* cassette flanked by newly added 50bp homology regions was then incorporated into the PbG01-2400h06 pJAZZ clone by the recombineering technique (Figure 7A). The correct integration of the selection marker was confirmed by diagnostic restriction digest.

In the second round of cloning *in vitro* Gateway LR reaction was performed to exchange the *zeo-pheS* cassette by site-specific recombination for a much larger *hdhfr-yFCU* cassette. Just as before, the desired recombination products were obtained after negative selection on YEG-Cl plates. To generate the linear target construct suitable for electroporation into schizont stage *P. berghei* parasites, PbG01-2400h06 vector containing *hdhfr-yFCU* cassette instead of PbCSP gene was digested with NotI enzyme. After electroporation, the parasite clones that incorporated the *hdhfr-yFCU* cassette were selected by treating mice with pyrimethamine in drinking water as described in section 2.5.4. The final DNA construct was verified by diagnostic restriction digest (Figure 7B).

Upon the identification of *P. berghei* mutants that successfully integrated *hdhfr-yFCU* cassette another round of electroporations were performed, whereby either VK210 or VK247 variants of *P. vivax* CSP gene were inserted instead of selection marker by double crossover homologous recombination event as indicated in chapter 6. The DNA plasmids targeting the allelic exchange of *hdhfr-yFCU* with PvCSP variants were synthesized by Geneart and prior to electroporations were digested with SacI and PacI restriction enzymes. The exchange of *hdhfr-yFCU* with either VK210 or VK247 alleles was facilitated by negative selection of unwanted clones with 5-fluorocytosine (5-FC) prodrug. Correct integration of the DNA constructs within the final *P. berghei* clones was determined by PCR and/or Southern blot analysis of digested genomic DNA or chromosomes separated by pulse-field gel (PFG) electrophoresis performed by Dr. Chris Janse. Blots were hybridized with the 3′UTR *dhfr/ts* of *P. berghei ANKA* probe.

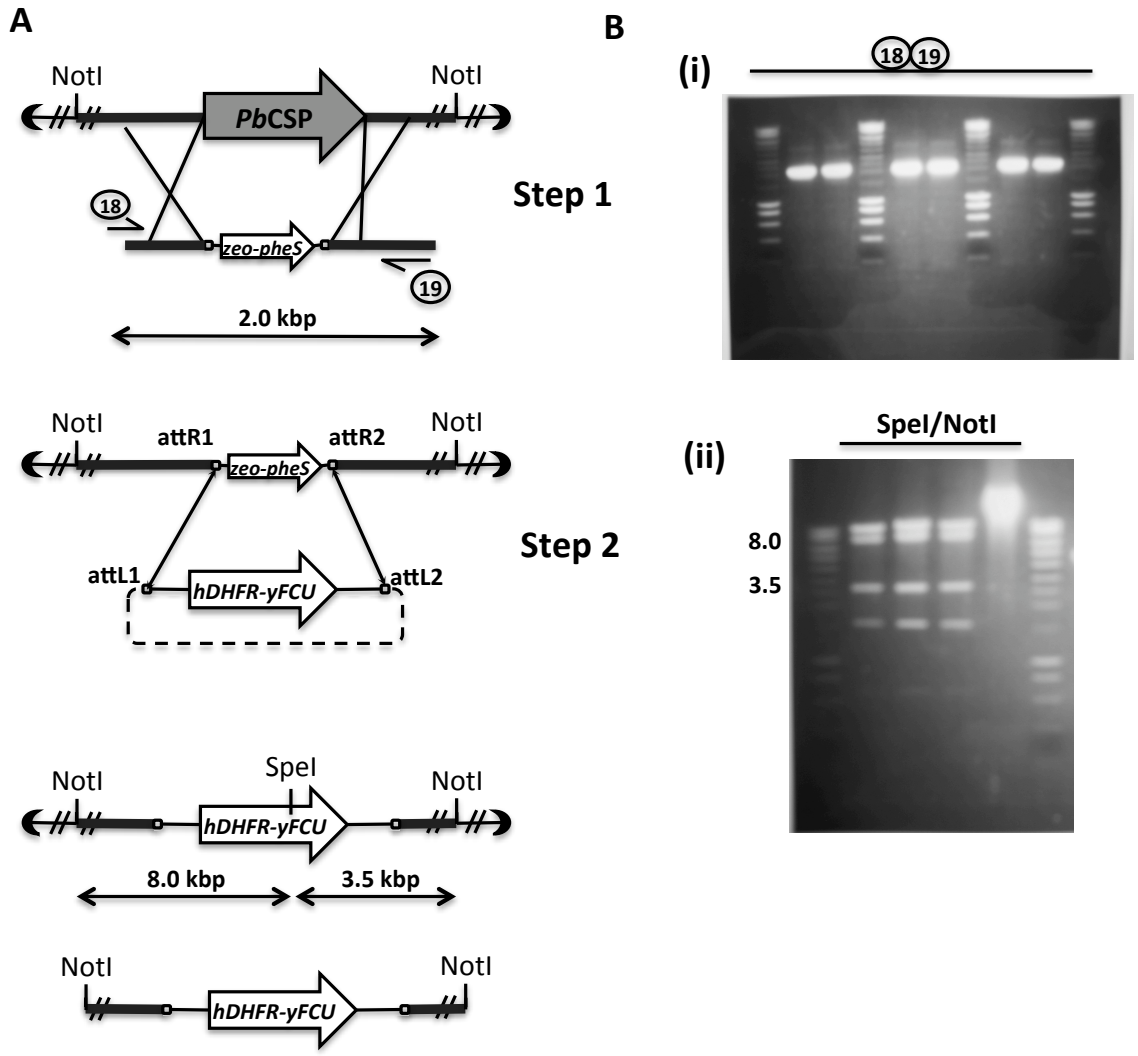


**Figure 7: Generation of DNA constructs necessary for the making of tg *P. berghei* expressing PvCSP either VK210 or VK247 allele.**

(A) During the first step of recombineering *zeo-pheS* cassette was used to knockout PbCSP gene within the PbG01-2400h06 pJAZZ clone. Next, the *zeo-pheS* sequence was replaced with much larger *hDHFR-yFCU* cassette at the second step of recombineering. The resulting construct was digested at the NotI sites and used to replace PbCSP gene *in vivo* as described in the results chapter 6. (B) Both (i) the expected size of *zeo-pheS* PCR product and (ii) the correct integration of *hDHFR-yFCU* cassette was confirmed by running the samples on the agarose gel. The circled numbers indicate the primers used (the primer sequences are shown in table 4).

### 2.4.3 Generation of double-tg *P. berghei* parasites

The double-tg *P. berghei* parasites containing both PvCSP VK210 and PvTRAP genes were generated on the VK210 tg *P. berghei* background, replacing endogenous PbTRAP with exogenous PvTRAP gene. The same materials and procedures were employed as in making of single-tg *P. berghei* PvTRAP as outlined in sections 2.4.1 and 2.5.3.

### 2.5.4 Parasite electroporations and clone selection

Schizont-stage *P. berghei* electroporations and mutant selections were carried out as described elsewhere with minor modifications (252). Also, during the making of tg *P. berghei* expressing PvCSP all the necessary electroporations were performed by Dr. Chris Janse at the Leiden University Medical Center. Briefly, around 1mL of blood from infected TO mouse was obtained by cardiac puncture. 500µL of the blood was mixed with 50mL of complete media supplemented with 20% of FBS. The flask containing culture was then flushed with gas mixture of 5% CO2, 5% O2, 90% N2 before being closed tightly and incubated overnight at $37^0$C in the shaking incubator. Next morning the level of erythrocyte infection was determined and schizonts were purified using Nycodenz gradient. Electroporations of freshly purified schizonts were carried out using 10µL of insert DNA at a concentration of 1 µg/µL, which was further diluted in the required volume of commercially available Amaxa buffer prior to electroporations. Immediately after the electroporations the reaction mixture was resuspended into 200µL of fresh blood obtained from phenylhydrazine (PHZ) treated mice and incubated for 30 min at $37^0$C with a slight shaking to allow erythrocyte reinfection. The freshly infected erythrocytes were, then, injected into PHZ treated mice intraperitoneally (IP). Next day

the mice were started on pyrimethamine treatment in drinking water. Once the mutant parasites emerged in the blood (determined by Giemsa stained blood smears), blood was collected by cardiac puncture and 100µL of it was injected back into uninfected mice to commence one more round of pyrimethamine selection. The remaining blood was used for genotyping analysis. Once the parasitaemias reached approximately 1% during the second round of pyrimethamine treatment, a drop of blood was used to clone the parasites by limited dilution technique. 10 naive mice were injected with 1-2 infected erythrocytes intravenously and monitored for blood-stage infection. The animals that became parasitaemic on days 8-9 after the injection of parasitized RBCs were started on 5-FC prodrug treatment administered in drinking water for 4-5 consecutive days. Normally, soon after the introduction of 5-FC prodrug blood-stage parasitaemia diminished reflecting the killing of parasites that failed to excise the selection marker (PvTRAP transgenics) or to incorporate the incoming DNA construct (PvCSP transgenics). Once the blood-stage infection could be detected again by Giemsa stained blood films, indicating the emergence of resistant clones, blood was collected once more, and 100µL of it injected into naïve animal IP for the second round of 5-FC selection. The remainder of the blood was used for the genotyping analysis. The infected naive mice were immediately started on 5-FC prodrug treatment. Once the parasitaemia reached 1% a dilutional cloning was performed once again to obtain a homogenous marker-free *P. berghei* mutants expressing *Pv*TRAP.

### 2.5.5 Bacterial electroporations for recombineering

The bacterial electroporations necessary for recombineering were carried out using a BioRad XCell electroporator and 0.1mm electroporation cuvette (BioRad). *E. coli* containing the desired target plasmids were maintained for two days at 32ºC in the shaking incubator refreshing the media containing the relevant antibiotics after the first 24 h. At the end of 48-h maintenance period, the optical density (OD) of the bacterial culture was measured, adjusted to 0.1 $OD_{600}$ and once again placed in the shaking incubator set to 32ºC for additional 2.5 h. At the end of incubation, 60µL of L-arabinose added to 3mL of bacterial culture to induce recombination enzymes (coded by pSC101gbaA-tet plasmid) and the colony transferred to 37ºC for 45-50 min. Then, 1mL of the bacterial culture transferred into fresh 1.5mL tube and spun for 5 min at 5000g. The pelleted bacteria were washed twice with 1mL of ice-cold $dH_2O$ and transferred into electroporation cuvette. Chilled 0.75-1µg of insert DNA contained in 5µL of $dH_2O$ added to 45µL bacterial culture and the whole content immediately electroporated with the following settings: 10 µF, 600 Ohms, and 1800 Volts. Following electroporations 950µL of SOC media added and the bacteria recovered for 1 h at 37ºC. After recovery bacteria were seeded onto the agar plates containing relevant antibiotic.

### 2.5.6 Genomic parasite DNA isolation from infected RBCs

Cardiac puncture was performed on anesthetized animals infected with the desired *P. berghei* mutant to obtain 1mL of blood. Whole-blood peripheral blood mononuclear cells (PBMCs) were removed by running the blood diluted in 6mL of chilled PBS over the 10mL syringe barrel packed with CF11 cellulose powder. The column was subsequently

washed with 7mL of ice-cold PBS and the efflux containing the enriched fraction of parasitized RBCs (pRBCs) was collected in the 50 mL tube. pRBCs were pelleted by spinning at 3000g for 5 min and subsequently treated with ice-cold ACK buffer for 5 min, which resulted in the lysis of pRBCs releasing *P. berghei* parasites. The parasites were then washed once with PBS, resuspended in 200µg of fresh PBS and their genomic DNA isolated using QIAamp DNA Mini Kit following manufacturer's recommendations.

## 2.5 Methods – Immunology

### 2.5.1 Animals

Age-matched 6 weeks-old female inbred BALB/c (H-$2^d$), C57BL/6 (H-$2^b$), C3H (H-$2^k$), and outbred CD1 (ICR) strains of mice used throughout this study were purchased from Harlan (USA). All animals and procedures were used in accordance with the terms of the UK Home Office Animals Act Project License. Procedures were approved by the University of Oxford Animal Care and Ethical Review Committee.

### 2.5.2 Viral vector vaccines

Prior to immunization animals were anaesthetized using inhalation chamber containing mixture of gases comprised of isofluorane (2–3.5%) and oxygen (1–2 L/min). Mice were primed with simian adenoviral vector 63 (ChAd63) encoding different transgenes at a dose of $1x10^8$ infectious units (IU) and 8 weeks later boosted with vaccinia-modified virus strain Ankara (MVA) encoding the relevant transgene at a concentration of $1x10^7$ plaque forming unit (pfu) per mL, unless stated otherwise. All viral vector vaccines were administered intramuscularly in endotoxin-free PBS. Vaccinations with two different

transgenes in co-administration groups were carried out either each vaccine injecting into separate left or right thigh muscle, or the mixture of two vaccines administering in a single muscle as indicated in the results section. Different viral vectors encoding either ME.TRAP or OVA antigens were kindly provided by Dr. A. Reyes-Sandoval and Dr. S. de Cassan, respectively. All recombinant ChAd63 and MVA viral vectors used throughout this study were generated at the Jenner Institute's vector core facility.

### 2.5.3 Protein vaccines

All recombinant protein vaccinations were administered intramuscularly as a 50µL dose containing sterile PBS and 15µg of protein formulated with 5µL of Abisco 100 adjuvant (provided by Jenner Institute adjuvant bank). For the viral vector and protein mixture group, 50µL vaccine dose comprised PBS, MVA expressing relevant transgene, and 15µg of relevant recombinant protein formulated with 5µL of Abisco 100 adjuvant.

### 2.5.4 Whole IgG Enzyme-linked immunosorbent assay (ELISA)

ELISAs measuring total IgG were carried out as described previously (212). In brief, blood was collected from tail vein bleeds and stored overnight at $4^0$C. On the following day the tubes were spun at 13.000 RPM for 4 min, the serum collected and stored in the fridge until the assay. The Nunc Immuno Maxisorp Plates were coated at a concentration of 1µg/ml with protein diluted in PBS overnight at room temperature. Plates were washed with PBS/0.05% Tween 20 (PBS/T) and blocked with 10% skimmed milk powder in PBS/T. Sera were diluted typically at a starting concentration of 1:100, added in duplicate wells, and serially diluted 3-fold down the plate. Plates were incubated for 2 h at room temperature and then washed as before. Goat anti-mouse whole IgG conjugated to

alkaline phosphatase was added for 1 h at room temperature. Following a final wash *p*-nitrophenylphosphate at 1 mg/mL in diethanolamine buffer was used as a developing substrate. OD was read at 405 nm using a Model 550 Microplate Reader. Serum antibody endpoint titers were taken as the x-axis intercept of the dilution curve at an absorbance value three standard deviations greater than the OD405 for serum from a naïve mouse. A standard positive serum sample and naïve serum sample were added as controls for each assay. Naïve mouse serum was negative for antigen-specific responses against all of the recombinant proteins used.

### 2.5.5 Peptides

Crude 20-mer peptides overlapping by 10 amino acids and representing full-lengths of *P. vivax* TRAP, VK210, and VK247 as well as *P. berghei* CSP, TRAP, and TOS proteins were synthesized by Mimotopes. Peptides were re-constituted in DMSO at a concentration of 50 mg/mL. Part of the peptides were combined into a single pool or three different sub-pools for their use in ICS and *ex-vivo* IFN-γ ELISPOT assays, respectively, at a final individual peptide concentration of 5 μg/mL. For the immunodominant peptide screen individual peptides were loaded onto 96-well plates in triplicates and used in the *ex-vivo* IFN-γ ELISPOT assay at a final concentration of 10 μg/mL.

### 2.5.6 Splenocyte preparation

Naïve mice were culled by cervical dislocation technique and spleens isolated by dissection. Spleens were homogenized in PBS, passed through 70μm cell strainer and cells pelleted by spinning at 500g for 5 min. The cell pellet was then treated with ACK

lysis buffer for 5 min before being washed with 25 mL of PBS. Splenocytes were then immediately spun at 500g for 5 min and the resulting pellet resuspended in 10mL of complete medium (D10) per spleen. Total number of splenocytes was determined by CASY counter and adjusted to $1x10^7$ cells per ml of complete medium for the use in *ex-vivo* IFN-γ ELISPOT assay.

### 2.5.7 *Ex-vivo* IFN-γ ELISPOT assay

*Ex* vivo IFN-gamma (IFN-γ) ELISPOTs were carried out using PBMCs isolated from the blood as previously described (253). In brief, nitrocellulose bottomed 96-well Multiscreen HA filtration plates were coated with anti-mouse-IFN-γ mAb overnight at 4°C. PBMCs were isolated from peripheral blood collected from tail vein bleeds into 200µL 10mM EDTA/PBS. Erythrocytes were lysed using ACK lysis buffer and PBMCs harvested through centrifugation. Cells were washed, re-suspended in complete medium, counted using CASY counter and 50µL of culture plated into duplicate wells. 50µL of each of peptide sub-pools diluted in medium plus 250,000 naïve splenocytes were added to test wells. Medium and naïve splenocytes were also plated onto the negative control wells. Plates were incubated at 37°C, 5% CO2 for approximately 18 h. Plates were then washed and incubated with biotinylated anti-mouse-IFN-γ mAb, followed by an incubation with a streptavidin alkaline phosphatase polymer. Spots were developed by addition of color development buffer, and counted using ELISPOT reader and accompanying software. Results are expressed as spot forming units (SFU) per million of PBMCs. Background responses in media-only wells were subtracted from those measured in wells stimulated by one of three peptide sub-pools.

### 2.5.8 Intracellular cytokine staining (ICS)

For intracellular cytokine staining (ICS), ACK lysis buffer treated whole-blood PBMCs were incubated for 5.5-6 h in the presence of peptide pool representing the antigen of interest at individual peptide concentrations of 5 μg/mL. 1 μl/mL Golgi-Plug and anti-CD107a PE (clone eBio/D4B) at a final dilution of 1:200 were also included. Phenotypic analysis of $CD8^+$ and $CD4^+$ T cells was performed by staining PBMCs using the following antibody clones: anti-CD8 PerCP-Cy5.5 (clone 53-6.7), and eFluor650 coupled anti-CD4 (GK1.5), anti-IFN-γ APC (XMG1.2), anti-TNF-a eFluor 450 (MP6-XT22), anti-IL-2 PE-Cy 7 (JES6-5H4). Also, the surface staining of liver-resident lymphocytes was performed using the following antibodies: anti-NK1.1 FITC, anti-CD3 AlexaFluor 700, anti-CD69 PE-Cy7, anti-CD8 eFluor 450. The liver-resident iNKT cells were stained with CD1d tetramer conjugated to PE. Non-specific binding of antibodies was prevented by incubating with anti-CD16/CD32 Fcγ III/II receptor prior to staining. Flow cytometric analyses were performed using an LSRII instrument. Data were analyzed with either FACSDiva or FlowJo software. Analysis of multifunctional $CD8^+$ T cell responses was performed using a Boolean analysis in FlowJo software, Pestle and SPICE 4.0 kindly provided by M. Roederer (NIH, Bethesda).

### 2.5.9 *In vivo* $CD8^+$ and $CD4^+$ T-cell depletions

The T cell depletions were performed as described previously (254). Briefly, in vivo-depleting monoclonal antibodies (mAbs) were purified by protein G affinity chromatography columns from hybridoma culture supernatants. Anti-CD4 GK1.5 (rat IgG2a) and anti-CD8 2.43 (rat IgG2a) were sterile filtered and diluted in sterile PBS.

Normal rat IgG (nRatIgG) was purchased from Sigma and purified by the same method. For depletion of $CD4^+$ or $CD8^+$ T cells, mice were injected intraperitoneally (IP) with 200 μg of the relevant mAb on days −2 and −1 before and on the day of challenge. *In vivo* T cell depletion was confirmed by flow cytometry of surface-stained PBMCs from depleted and control mice a day after challenge. The level of depletion for both $CD4^+$ and $CD8^+$ T cells was confirmed by surface staining of PBMCs one day after the challenge.

### 2.5.10 *In vivo* Kupffer and natural killer (NK) cell depletions

The *in vivo* depletion of liver-resident Kupffer cells was accomplished by intravenous administration of liposome formulated clodronate 48 h prior to challenge at a concentration of 10μL of suspension per 1 g of mouse (255). The control liposomes containing PBS were also included.

To deplete NK cells, mice received a single dose of 200 μL of anti-asialo GM1 antiserum diluted 1:8 in 0.5× PBS on days −2, 0, and +2 relative to challenge as described previously (150). Naïve rabbit serum was also used as a control (kindly provided by Dr. A. Douglas).

### 2.5.11 Whole IgG passive transfer

Outbred CD1 mice, vaccinated with heterologous ChAd63/MVA prime-boost regimen encoding relevant antigen, were anaesthetized in the isofluorane chamber as described above. Blood from unconscious animals was obtained by cardiac puncture into the syringe containing 25μL of heparin. The collected blood was transferred into 1.5mL tubes and stored overnight in the fridge. On the following day tubes were spun at 13,000

rpm for 4 min and the serum collected. Whole IgG was combined within vaccine group, purified using pierce columns pre-packed with 2mL of protein G resin abiding to manufacturer's instructions. 2mg of purified whole IgG obtained from immunized animals was injected into each naïve CD1 mouse. The whole IgG purified from the serum of animals vaccinated with empty viral vectors was also included. Animals received the passive whole IgG vaccination in the morning and were subsequently challenged 6 h later.

### 2.5.12 3D11 monoclonal antibody (mAb)

A hybridoma cell line expressing 3D11 mAb was obtained from Malaria Research and Reference Reagent Resource Center (MR4). A total of $2.5x10^7$ hybridoma cells were seeded and propagated in 15 mL of DMEM medium supplemented with 100units of penicillin/ml, 100µg streptomycin/ml and 2mM L-glutamine and 20% of ultra-low IgG FBS in a two-chamber CELLINE bioreactor incubated at 37°C, 5% CO2. Every 3-4 days the hybridoma cells were passaged as follows. The cell suspension was removed from the chamber, counted and $2.5 \times 10^7$ cells were re-suspended in a total of 15mL complete medium and placed back into the same chamber. The remaining cells were pelleted at 600g for 5 min and the supernatant was stored at -20°C.

3D11 mAb was purified from culture supernatants using Pierce Protein G column according to manufacturer's recommendations. Eluted 3D11 mAb was immediately buffer exchanged into the PBS using 30.000 MWCO centrifugal filter unit from Millipore.

### 2.5.13 3D11 mAb fragmentation

Fab fragments of 3D11 mAb were generated by incubation with immobilized Ficin in the presence of 25 mM cysteine according to the manufacturer's instructions. Fab fragments were purified from intact antibody and Fc fragments by passing twice over a Protein A column. Purity of Fab fragments was verified by non-reducing SDS-PAGE (Figure 8).

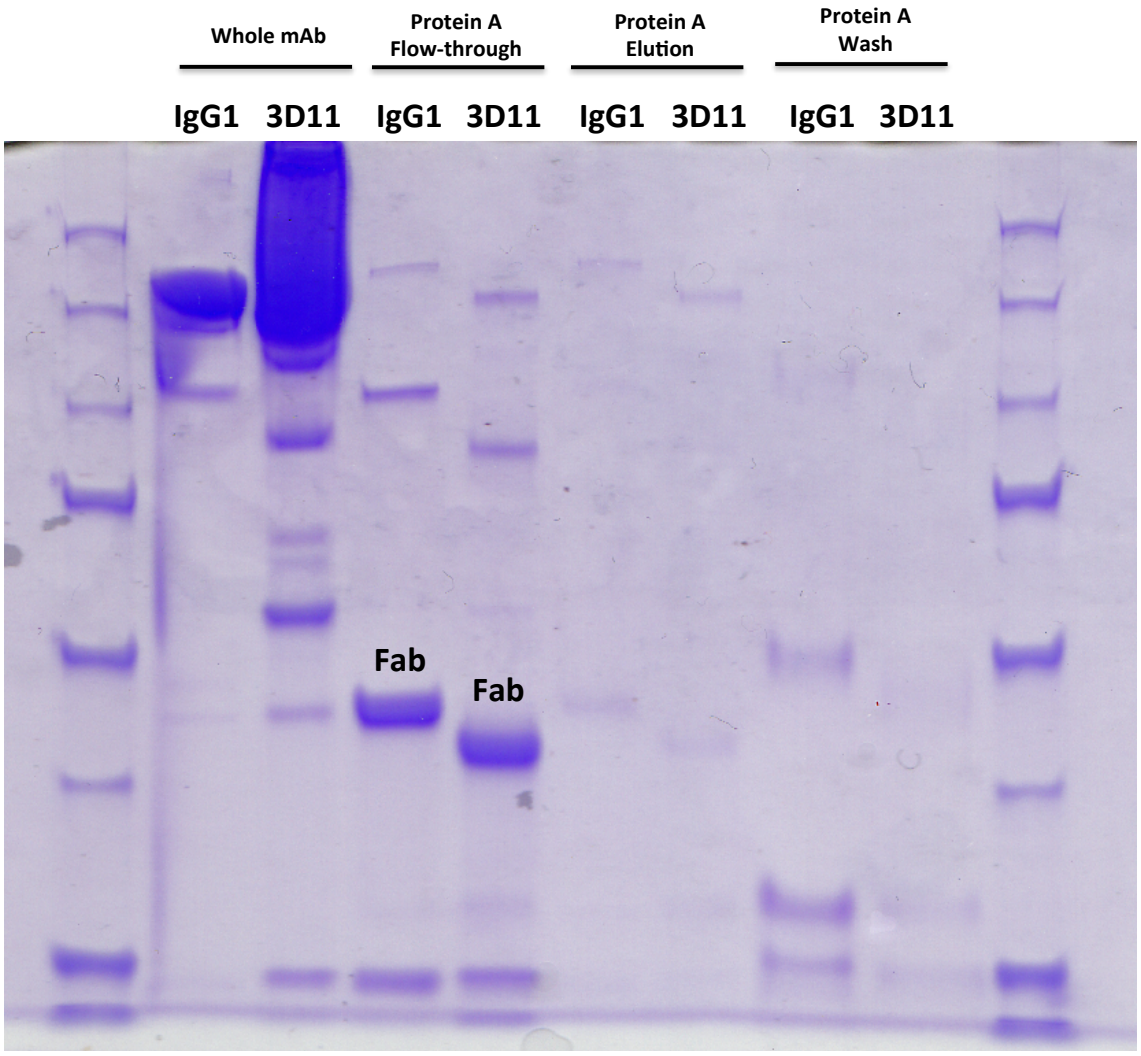


**Figure 8: Non-reducing SDS-PAGE assay was employed to confirm the successful 3D11 fragmentation.**

Between 0.15-2µg of sample protein was loaded and run as indicated in the materials and methods section 2.2.11. Commercially available mouse IgG1 isotype control was included.

### 2.5.14 Spz neutralization assay (SNA)

Sporozoite neutralization assay was performed as described previously (159). Briefly, salivary gland wt *P. berghei* sporozoites were isolated into RPMI-1640 media and counted using hemocytometer. 50,000 sporozoites were incubated for 30 min at room temperature with the required amount of either whole intact 3D11 or Fab in total of 0.5mL of RPMI-1640. Following the incubation 500μL of ice-cold RPMI-1640 was added and all sample tubes were placed on ice. Immediately thereafter 100μL of culture containing 5000 sporozoites was injected intravenously (IV) into each animal.

### 2.5.15 Isolation of liver resident lymphocytes

Mice were sacrificed by cervical dislocation and liver exposed by dissection. Portal vein was used to perfuse liver by injection of sterile PBS. Following the perfusion livers were dissected out and, after the removal of gall bladder, placed into a tube containing PBS and put on ice. Then, each liver was mashed through single 100μm cell strainer into 50 mL falcon tube. Filter was washed with PBS before spinning down the tube containing hepatocytes at 1350rpm for 7 min. The pellet was re-suspended in 15 ml of 33% isotonic Percoll reagent. The mixture of hepatocytes and Percoll solution was then spun at 693g for 12 min without the brake. After centrifugation, the hepatocyte debris was removed with transfer pipette and Percoll solution poured off. The pellet was re-suspended in 2mL of ACK and RBCs lysed for 5 min. Immediately after that, 25 mL of PBS was added and the mixture was spun-down at 1500 rpm for 5 min. Lymphocytes were washed once with complete medium before being re-suspended in 500μL of complete medium. The total

number of lymphocytes was determined using CASY counter and for surface staining cells were transferred onto 96-well plate.

## 2.6 Parasitology

### 2.6.1 Tg *P. berghei* expressing firefly luciferase

The tg *P. berghei* parasites (PbGFP-Luc$_{con}$) used in these studies expressed fusion GFP (mutant 3) and firefly luciferase (LucIAV) gene under the control of constitutive EF1a promoter (252). The parasites were generated by a stable double-crossover homologous integration of the transgene into P230p locus in the reference line of *P. berghei* ANKA clone cl15cy1. The tg parasite was kindly provided by Dr. Oliver Billker from Wellcome Trust Sanger Institute, Hinxton, UK.

### 2.6.2 Parasite preparation

Female *A. stephensi* mosquitoes were fed onto PHZ treated female TO mice infected with wt or tg *P. berghei* parasites. 21 days after the feed mosquitoes were dissected, salivary glands isolated and salivary gland sporozoites extracted and diluted in RPMI-1640. Total number of sporozoites was determined using hemocytometer and varying quantities of them injected into mice IV.

### 2.6.3 Preparing Thin-blood Smears

Thin-blood smears were prepared on glass slides from a drop of blood obtained from the tail clip. The blood smear was allowed to air-dry, before fixation with methanol, and staining for at least 1 h with 5% Giemsa diluted in $dH_2O$. Slides were then removed and allowed to air-dry at room temperature.

### 2.6.4 Immunofluorescence assay (IFA)

Sporozoites isolated from mosquito salivary glands were loaded onto the glass slides and allowed to air-dry overnight at room temperature. The following day sporozoites were fixed in 4% paraformaldehyde and quenched with 0.01% sodium borohydride. Slides were then blocked for 1 h with 10% goat serum, 1% BSA in PBS before the addition of either 3D11 mAb specific to repeat region of PbCSP, or anti-PbTRAP and anti-PvTRAP specific sera. Bound IgG was detected with goat anti-mouse IgG-Alexa 488 conjugate. Nuclear DNA was counterstained with 4,6-diamidino-2-phenylindole. Slides were viewed under a Leica DMI3000 microscope.

### 2.6.5 Statistical model for parasitaemia prediction

To extrapolate liver-to-blood parasite load or predict time to 1% blood-stage infection a linear regression modeling was used as described previously (165). Briefly, blood parasite counts were obtained for 3-5 consecutive days, twice a day, starting on day 4 after challenge. Blood smears were stained with Giemsa, and percentages of parasitaemia calculated in all animals. The logarithm to base 10 of the calculated percentage of parasitaemia was plotted against the time after challenge and Prism 5 for Mac OS X (GraphPad software) statistical analysis package used for generating linear regression model on the linear part of the blood-stage growth curve. Potential influence of vaccine on blood stage growth was assessed visually. As expected for vaccines containing only pre-erythrocytic stage ags, all infected mice exhibited similar exponential blood stage growth regardless of treatment group. A survival analysis to assess vaccine efficacy was employed, using time to 1% parasitaemia (although any other level of parasitaemia could

also be used with equivalent results) as an outcome. This approach has been previously used; because time to blood-stage parasitaemia reflects number of parasites erupting from the liver, provided there is no blood stage immunity (256).

### 2.6.6 *In vivo* imaging system (IVIS)

Bioluminescent luciferase signal (BLS) was detected through imaging whole animals using *in vivo* IVIS 200 imaging system as described before (230). Briefly, after the intravenous injection of tg *P. berghei* sporozoites, animals were anaesthetized at a different time points depending on the experiment using isofluorane chamber. Prior to imaging 100µL of D-luciferin substrate, dissolved in sterile PBS at a concentration of 50 mg/kg, was injected into the neck region of mice subcutaneously (SC). Animals were imaged for 60-180 seconds at binning value of 8 and FVO of 12.8 cm, 8 min after the injection of the substrate. Mice were kept anaesthetized throughout the whole procedure.

Quantification of BLS was performed using Living Image 4.2 image analysis software. Regions of interest were designed around the liver area of mouse body and kept constant for all of the animals. The measurements were expressed on a log scale as total flux of photons emitted from animals adjusted per second of exposure time.

## 2.7 Statistics

For all statistic analysis, GraphPad Prism version 5.0 for Max OS was used unless indicated otherwise. Prior to statistical analysis to compare two or more populations, the Kolmogorov-Smirnov test for normality was used to determine whether the values followed a Gaussian distribution. An unpaired t-test was employed to compare two

normally distributed groups, whereas Mann-Whitney rank test was used for comparing two non-parametric groups. If more than two groups were present non-parametric data was compared using Kruskal-Wallis test with Dunn's multiple comparison post-test, whereas normally distributed data were analyzed by one-way ANOVA with Bonferroni's multiple comparison post-test (except for chapter 1 where t-test and Mann-Whitney tests were employed despite multiple groups). The effect of two variables was explored using two-way ANOVA with Bonferroni's multiple comparison post-test. Correlation strength was tested using either Pearson's or Spearman's tests as indicated in the results chapters. Kaplan-Meier survival curves were used to represent protective efficacy to a challenge with any *P. berghei* parasite lines. When required, protection was also assessed using IVIS *in vivo* imaging and data $\log_{10}$ transformed prior to analysis. All ELISA titres were also $\log_{10}$ transformed before analysis. The value of $p<0.05$ was considered statistically significant (*$p<0.05$, **$p<0.01$, **$p<0.001$, and ***$p<0.001$).

# Chapter 3

# Quantification of *Plasmodium berghei* malaria parasite density

# 3 Quantification of *Plasmodium berghei* malaria parasite density

## 3.1 Introduction

Despite malaria's global burden a good vaccine against this protozoan parasite is still lacking. Vaccine efforts have focused on all three stages of the parasite's development, including pre-erythrocytic-, blood-stage and transmission blocking vaccines and the greatest level of success to date has been achieved using various pre-erythrocytic stage antigens as vaccine immunogens such as the circumsporozoite (CS) and thrombospondin-related adhesive (TRAP) proteins.

The recombinant protein-in-adjuvant vaccine termed RTS,S/AS01 that contains part of the most ubiquitous sporozoite surface protein PfCS as well as an adenoviral prime - MVA boost regimen using the antigen ME.TRAP (based on multi-epitope (ME) string fused to PfTRAP) have provided significant levels of protection in human clinical trials (161) (Ewer *et al.* submitted). Nevertheless, neither RTS,S/AS01, nor viral vector based PfTRAP alone at their present formulations confer the required 80% protective efficacy that lasts for more than four years against episodes of clinical malaria envisaged by the malaria vaccine community (Malaria Vaccine Technology Roadmap Final Report). Thus, malaria vaccines based on novel pre-erythrocytic stage antigens (89) (257) or antigen combinations are being developed (258) (259) in order to improve protective efficacy.

In human clinical trials both pre-erythrocytic and blood-stage malaria vaccine efficacy is assessed by measuring blood-stage parasite densities. This is accomplished using either conventional blood-film analysis or measuring parasite DNA copy numbers by PCR (260). The PCR-based quantification is more sensitive allowing detection of as few as 20 parasites per mL of blood (L.A., N.E., R.F.A., D.W., S.D., M.W., P.B., A. Hunt-Cooke, G. Bergson, F. Sanderson, A.V.S.H., and S.C.G., unpublished data). Also, the PCR data collected over a few time points can be used to extrapolate parasite liver-to-blood inoculum, which is related to the vaccine's efficacy during malaria parasite's development at the pre-erythrocytic stage (256).

Frequently, pre-clinical human malaria vaccine development involves the rodent *P. berghei* malaria model, which is used for *in vivo* proof-of-concept studies. Also, *P. berghei* homologous genes to those from human malaria species can be employed to study the pre-erythrocytic or blood-stage vaccine efficacy. However, despite their importance for the human malaria vaccine field, *P. berghei* parasites also differ substantially from their human counterparts. First, the blood-stage infection of mice with *P. berghei* does not resemble the cyclical patterns corresponding to red-blood cell (RBC) lysis observed with human malaria species. Also, *P. berghei* liver stage development lasts for about 48 hours (h) as opposed to 7-9 day period required for most human *Plasmodia* species. Also, unlike with *P. falciparum* infections in humans, pre-clinical studies using rodent *P. berghei* permit RT-PCR analysis of malaria-infected livers to quantify pre-erythrocytic vaccine efficacy (261) (262). On the other hand, conventional Giemsa stained blood-films have been the method-of-choice for measuring blood-stage vaccine

efficacy in *P. berghei* as well, as it is cheap and relatively easy. Also, recently a novel way of quantifying pre-erythrocytic stage vaccine efficacy by employing linear regression modeling on blood-stage parasitaemias gathered over three consecutive days has been reported (165). Another novel method of measuring vaccine efficacy *in vivo* uses transgenic (tg) *P. berghei* parasites expressing the luciferase gene (263). Bioluminescence (BLS) emitted from infected animals is closely related to the parasite load and can be used to directly quantify both exo-erythrocytic and blood stage parasitaemias in the same animals, which was not possible with previous methods.

In this chapter, two novel methods capable of quantifying malaria parasite density, including *in* vivo imaging of animals infected with the tg *P. berghei* expressing luciferase and a mathematical model predicting the time needed to reach a certain percentage of parasitaemia, are comparatively assessed for the use in vaccine studies.

## 3.2 Results

### *3.2.1 In vivo* quantification of *P. berghei* parasite load using live animal imaging

BALB/c mice were injected with increasing numbers of *P. berghei* sporozoites (spz) expressing a fusion of a green fluorescent protein gene and a luciferase gene (GFP/Luc) intravenously (IV). At various time points after the challenge parasite densities were measured using an *in vivo* imaging system (IVIS), whereby the BLS produced by tg parasites and emitted from infected mice was quantified using specialized equipment and accompanying software. The BLS measured over the course of 12-116 h after the challenge followed a dose-response curve where the amount of emitted light increased

proportionally with the increase in parasite densities. Also, the time points of 44 and 116 h post-challenge had the strongest BLS emitted by infected animals corresponding to either liver or blood stages of infection, respectively (Figure 9A, B).

Next, the optimal time point for quantifying mice *P. berghei* infection using IVIS was delineated by correlating the BLS detected with the number of spz injected. Correlations between BLS and spz numbers were obtained for the time points representing pre-erythrocytic (44 h post-challenge) and blood-stage infections (68, 92, and 116 h). The results revealed that the time corresponding to 44 h after the challenge gave the strongest correlation coefficient ($p=0.0004$, $R^2=0.7655$ by Spearman's test) between the amount of luciferase signal and number of spz injected (Figure 9C). Statistically significant correlations were also observed between BLS and challenge dose of spz for the relevant time points representing blood-stage infection, although the correlation coefficients were lower than those seen at 44-h time point post-challenge ($p=0.0028/R^2=0.6935$, $R^2=0.6655$, $R^2=0.6105$ for 68, 92, and 116-h time points post-challenge by Spearman's test, respectively).

The ability of the IVIS method to distinguish between groups of mice receiving different doses of sporozoites was investigated next (Figure 9D). The time point of 44 h post-challenge was chosen because the initial data yielded the strongest correlation between BLS and spz dose at this particular time point. Since the data points were normally distributed (by Kolmogorov-Smirnov test) a series of student's t-tests were performed comparing all of the adjacent groups in pairs, then all the groups that were 4-folds apart and so on (Figure 9D). For example, the BLS emitted by animals that received 500 spz

was compared first against 1000 spz group, then 2000, then 4000 and so on. 1000 spz group was initially compared against 2000, then 4000 spz groups and so on. This type of analysis was carried out for all of the experimental groups and the number of pairs that were statistically significantly different ($p<0.05$ by student's t-test) was recorded. The direct comparison of all the possible pairs showed that 14 pairs in total were statistically significantly different, suggesting that IVIS imaging is a relatively sensitive method for distinguishing between different numbers of malaria parasites.

Taken together, these data indicated that IVIS imaging of the whole animals provided a robust and reproducible way of quantifying infection by *P. berghei* at the pre-erythrocytic and the blood stages of parasite development. Results showed that a more accurate measurement could be made when BLS was quantified at a 44 h time point after challenge, indicating that this could be a useful tool for evaluating malaria interventions, such as vaccines, targeting pre-erythrocytic stage of parasite development.

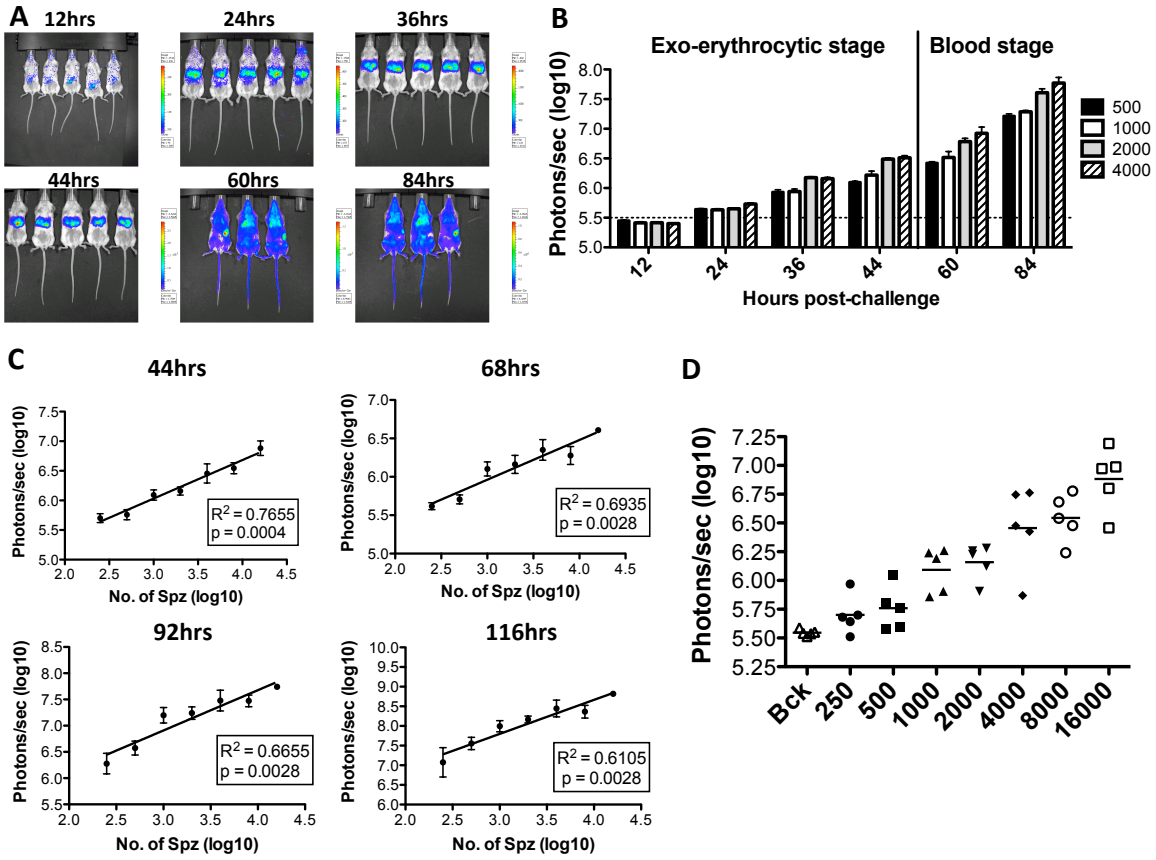


**Figure 9: *In vivo* imaging of whole animals.**

BALB/c mice (n=5/group) were injected varying numbers of *P. berghei* spz expressing luciferase gene. (A) Animals were imaged at different times points as indicated above the image (group that received 4000 spz dose is presented) and (B) total flux of luciferase signal emitted by each animal was quantified using Living Image 4.2 software (the spz challenge dose is indicated on the right side of the graph). Mean with SEM are shown. (C) The correlations between spz challenging dose (x-axis) and BLS (y-axis) were generated for several time-points (shown above the graph) and the correlation strengths recorded (calculated using Spearman's test). Also, a best-fit line generated and the deviation from the prediction indicated by $R^2$ value. (D) A series of student's t-tests were performed on 44 h post-challenge time-point values to test the ability of IVIS to distinguish between different sporozoite doses (please, refer to the results section for more details).

### 3.2.2 Quantification of blood-stage *P. berghei* infection using conventional Giemsa stained blood films

One of the most common and simple ways of quantifying blood-stage parasitaemia is accomplished by counting red-blood cells (RBCs) infected with malaria parasites. That way the percentage of infected RBCs could be determined over several time points and used to quantify blood-stage vaccine efficacy. Interestingly, the level of blood-stage parasitaemia has also been used to infer about efficacy of pre-erythrocytic stage vaccine, as it has been demonstrated that liver-to-blood parasite inoculum reflects the number of spz surviving to exit the liver (256).

To assess *P. berghei* parasite blood-stage development following the challenge with various doses of spz, Giemsa stained blood films were obtained starting with a 96 h time point post-challenge and percentage of RBC infection recorded. In line with the expected *P. berghei* blood-stage development in the absence of efficacious vaccine, an almost linear increase in $\log_{10}$ transformed parasite densities (proportion of infected RBCs) was observed at early phase of blood-stage infection corresponding to 96-144 h time gap after challenge (Figure 10A). As expected parasitaemias plateaued towards the last time points when measurements were taken, corresponding to 156 and 168 h post-challenge. Also, the parasitaemia plateau was observed earlier in the mice that were challenged with the highest dose of spz (8000 and 16000).

Next, the correlations between the level of blood-stage parasitaemia and the spz challenge dose were generated for 3 time points that were located within the linear part (120, 132, and 144 h post-challenge) and 1 time point that was on the plateau part (156 h)

of the growth curve (Figure 10B). The correlation coefficient's obtained confirmed that substantially stronger associations between the spz challenge dose and the resulting parasitaemias were present for time points representing earlier phase of parasite blood-stage development ($p=0.0004$, $R^2=0.6490$ for 120 h versus $p=0.0067$, $R^2=0.5217$ for 144h, and $p=0.0028$, $R^2=0.3935$ for 156 h time points post-challenge by Spearman's test).

Historically, comparing the level of blood-stage infection between naïve and immunized mice at the specific day post-challenge has been the model method for representing either pre-erythrocytic or blood-stage vaccine efficacy. The blood-stage parasitaemia values ($\log_{10}$ transformed) of different experimental groups were plotted for days 5, 6, and 7 post-challenge (Figure 10C). A series of Mann-Whitney (for data that were not distributed normally by Kolmogorov-Smirnov test) and student's t-tests (for normally distributed data) were performed comparing all the experimental groups in pairs as was previously done with IVIS results (500 spz versus 1000 spz, then 2000 spz, and so on). The day 5 parasitaemia values were used for the analysis as this time point represented the linear part of the growth curve. The results demonstrated that much less distinguishing power was provided by this method when compared to IVIS. Only 10 pairs were statistically significantly different by this method.

This set of data confirmed that the sporozoite dose at the time of challenge generally correlated strongly with the ensuing blood-stage infection. However, the strongest associations between spz challenge dose and the level of blood-stage infection were generated when values representing early phase of asexual-stage parasite development were employed for quantification. Also, the use of day 5 post-challenge parasitaemia

readout values demonstrated that plotting blood-stage infection is a less sensitive method for distinguishing between different experimental groups as compared to IVIS.

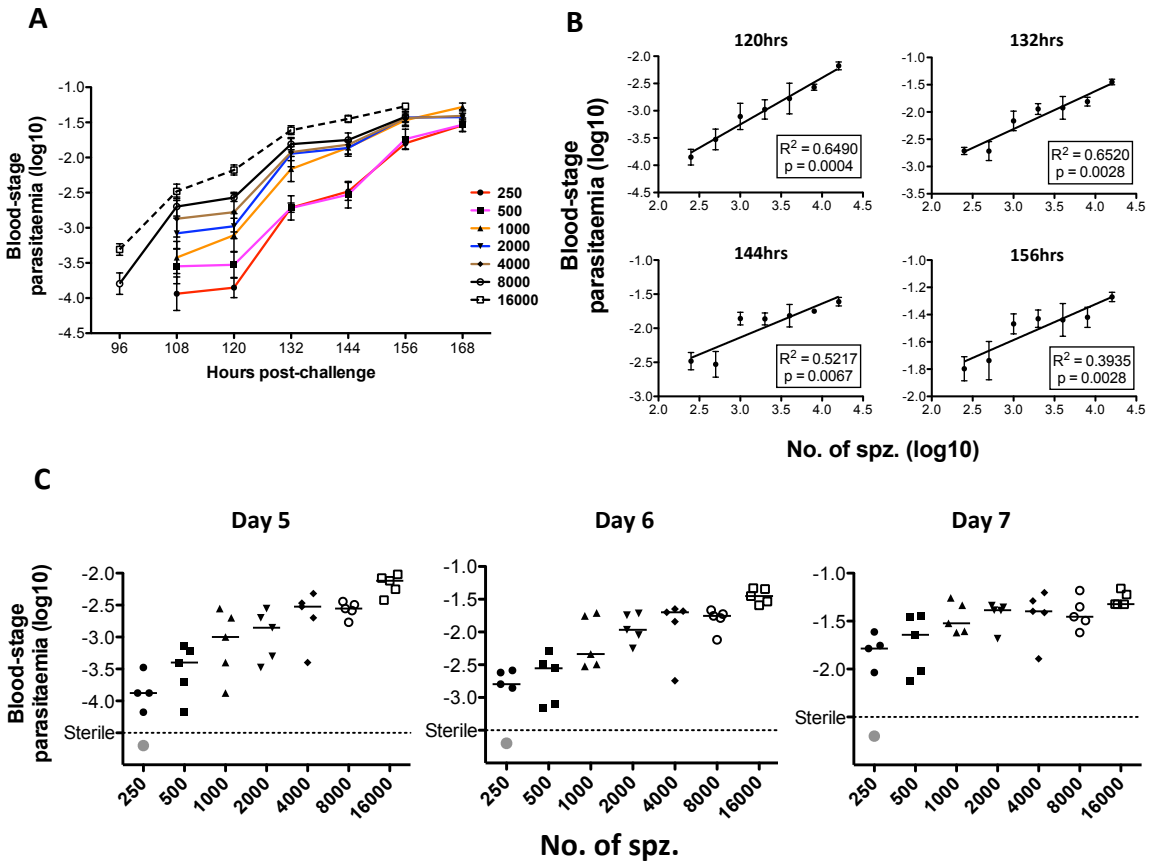


**Figure 10: Quantification of blood-stage infection using Giemsa stained blood films.**

BALB/c mice (n=5/group) were injected varying numbers of *P. berghei* GFP/Luc spz. Blood-stage parasitaemia was monitored by Giemsa stained blood-film analysis and (A) growth curves representing each group generated. Y-axis indicates the proportion of RBCs infected transformed by logarithmic to the base 10. (B) The correlations representing proportion of RBCs infected (y-axis) over the number of spz injected (x-axis) were calculated (Spearman's test) for different time-points (indicated above the graphs). The correlation strengths diminished with the increasing blood-stage parasite densities. (C) Proportion of infected RBCs presented for individual days. Day 5 values were used for the analysis of methods ability to distinguish between different groups with statistical significance using a series of Mann-Whitney and student's t-tests. The grey dots correspond to sterilely protected animals (absence of blood-stage infection on day 15 after challenge).

### 3.2.3 Extrapolating *P. berghei* liver-to-blood parasite load and time to 1% blood-stage infection from blood-films

*In vivo* imaging of live animals using IVIS is becoming a useful tool for the monitoring of malaria pre-erythrocytic stage infection. As opposed to the other commonly used method for measuring the level of *P. berghei* liver infection, which is based on reverse transcriptase polymerase chain reaction (RT-PCR), IVIS allows the quantification of liver-resident parasite numbers quickly and robustly without sacrificing the mice. However, despite its advantages, IVIS has some major limitations as it requires expensive equipment and user expertise.

Having obtained curves representing the *P. berghei* blood-stage parasitaemia, a linear regression model (Figure 11A) predicting time to 1% blood-stage infection (Tto1) and values representing liver-to-blood parasite load (parasitaemia at 50 hours post-challenge) was generated (Pat50) (165). A 50 h time point post-challenge was chosen as this is the point in the *P. berghei* development cycle when merozoites erupt from the liver, however, other earlier or later time points could have been selected, as the merozoite eruption starts and finishes some hours before and after 50 h post-infection, respectively (11). To verify that the values generated by the prediction method correlated with a spz challenge inoculum, associations between prediction and the spz dose were generated. The high correlation coefficients confirmed that there were strong associations between Tto1 values and number of spz injected ($p=0.0028$, $R^2=0.6616$ by Spearman's test) (Figure 11B(i)). Also, comparably strong correlations ($p<0.0001$, $R^2=0.8224$ by Spearman's test) were obtained between Tto1 and IVIS readouts (Figure 11B(ii)), indicating that the level

of blood-stage parasitaemia is closely related to the sporozoite challenging dose, and subsequently, *in vivo* imaging analysis when used.

The examination of correlations between data representing Pat50 post-challenge and either spz challenge dose ($p=0.0341$, $R^2=0.4248$ by Spearman's test) (Figure 11C(i)) or IVIS ($p<0.0001$, $R^2=0.5207$ by Spearman's test) (Figure 11C(ii)) also revealed relatively strong associations for both, indicating that linear regression analysis could robustly predict not only Tto1, but also Pat50.

As previously, a series of Mann-Whitney and Student's t-tests were carried out to compare all possible experimental groups in pairs for both Pat50 (Figure 12A) and Tto1 (Figure 12B) prediction values. The results showed that only 8 pairs of experiment groups were statistically significantly different within Pat50 method, whereas the values generated using Tto1 extrapolation could be statistically significantly distinguished in 13 pairs (Figure 12C).

All these data together demonstrated the power of the linear regression model to be used as a valid method of inferring the pre-erythrocytic stage parasite burden. Between the two prediction values used, the extrapolation generating Tto1 correlated more strongly with the actual spz challenge dose and also offered more distinguishing power as measured by series of Mann-Whitney and Student's t-test than the one predicting Pat50.

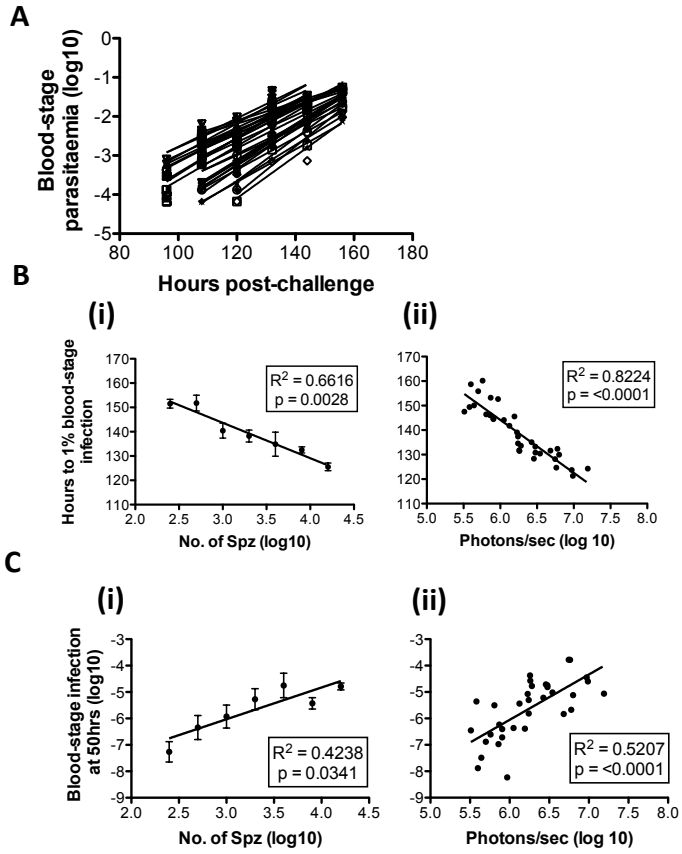


**Figure 11: The use of linear regression modeling to predict liver-to-blood parasite density and Tto1.**

Linear regression modeling was applied to blood-stage parasitaemia values. (A) The lines representing proportion of infected RBCs for each animal were generated and slopes compared visually. (B) Correlations testing the strength of association (by Spearman's test) between the Tto1 prediction versus either (i) sporozoite dose or (ii) BLS were generated. (C) Alternatively, the correlations between extrapolation of blood-to-liver parasitaemia (assumed to be 50 h time-point after the challenge (Pat50)) versus (i) sporozoite dose or (ii) BLS were also compared.

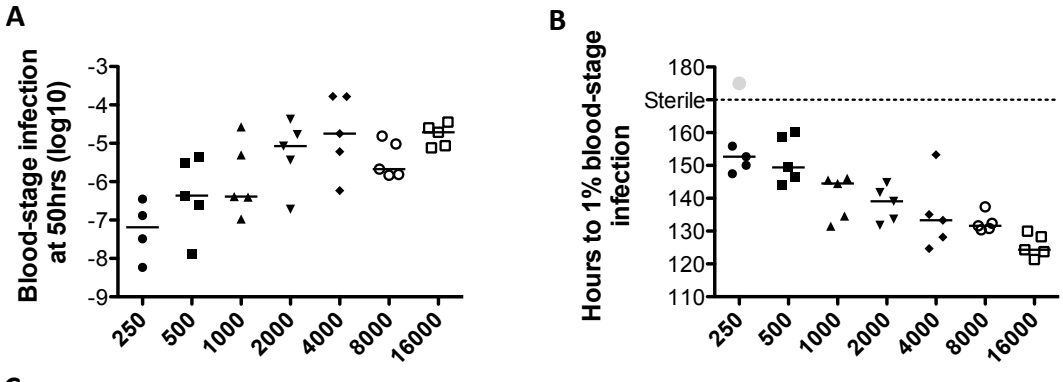


C

| *In vivo* imaging 44hrs | Blood-stage P on day 5 | Linear regression Time to 1% | Linear regression P at 50hrs |
|---|---|---|---|
| 250 vs 1000 (**) [St.] | 250 vs 1000 (*) [M-W] | 250 vs 1000 (**) [M-W] | 250 vs 2000 (*) [M-W] |
| 500 vs 1000 (*) [St.] | 500 vs 4000 (*) [St.] | 500 vs 1000 (*) [St.] | 500 vs 4000 (*) [St.] |
| 1000 vs 8000 (**) [St.] | 1000 vs 16000 (**) [St.] | 1000 vs 8000 (*) [St.] | 1000 vs 16000 (*) [St.] |
| 2000 vs 8000 (*) [St.] | 2000 vs 16000 (**) [St.] | 2000 vs 16000 (**) [St.] | |
| **14** | **10** | **13** | **8** |

**Figure 12: The quantitative assessment of four methods quantifying *P. berghei* malaria parasite densities.**

Linear regression model was used on blood-stage parasitaemia data for each animal. Prediction values were obtained either for (A) 50 h time-point, corresponding to liver-to-blood parasite load, or (B) time (in hours) taken for the blood-stage parasitaemia to reach 1% of RBC infection for each animal. (C) A series of Mann-Whitney or Student's t-tests were carried out initially comparing all groups adjacent to each other in pairs (250 vs 500, 500 vs 1000, etc.) then all groups that were 4 folds apart (250 vs 1000, 500 vs 2000, etc.), then all groups that were 8 folds apart (250 vs 2000, 500 vs 4000, etc.) and so on. In total 21 different pairs were possible. Each pair that was statistically different ($p=<0.05$) was given a score of 1. That way all four different methods of measuring *P. berghei* malaria infection, including *in vivo* imaging at 44 h (first data column), conventional blood-stage parasitaemia (2nd column), linear regression analysis predicting Tto1 (3rd column), and Pat50 (parasitaemia at 50 h post-challenge) (4th column) were analyzed and total number of statistically significantly different pairs obtained (recoded in the last row). IVIS and linear regression predicting Tto1 were the methods with the highest combined score, indicating that they possibly possess the highest between-groups distinguishing power.

### 3.2.4 Validation of *in vivo* imaging and linear regression model using a vaccine against pre-erythrocytic stage malaria

To validate the methods of IVIS imaging and linear regression analysis for assessing vaccine efficacy, BALB/c mice were immunized with one of the following regimes conferring varying levels of protection: ChAd63-ME.TRAP (10^8 infectious units (iu)), MVA-ME.TRAP (10^7 plaque forming units (pfu)), or the most protective ChAd63-MVA (Ad-M) ME.TRAP in a heterologous prime-boost regimen (the amount of each recombinant virus was the same as in single vaccinations) (165). The protective efficacy following vaccination with ME.TRAP construct in BALB/c mice is mediated by $CD8^+$ T cells targeting immunodominant Pb9 epitope located within PbCS protein (264). Animals immunized with empty ChAd63 and MVA viral vectors in a prime-boost regimen were also included as controls. Two weeks after vaccination mice were challenged with either 1000 or 16000 luciferase-expressing *P. berghei* spz administered intravenously. As previously, 44 h post-challenge BLS emitted by infected animals was quantified using IVIS (Figure 13A). Also, starting at day 4 post-challenge twice a day the same animals were monitored for blood stage infection using Giemsa stained blood films. Values obtained after microscopic examination of blood films were used to generate a linear regression model predicting Tto1 (Figure 13B). The IVIS and Tto1 readouts were chosen because they showed the highest level of sensitivity regarding the discrimination between different spz challenge dose in previous experiments.

Both IVIS and Tto1 methods of quantifying pre-erythrocytic stage vaccine efficacy indicated that, as expected, Ad-M ME.TRAP regime conferred the highest degree of

protection against both 1000 and 16000 spz challenge (165). A direct comparison of ChAd63-ME.TRAP versus MVA-ME.TRAP single vaccination groups (regimes that are suboptimal for complete sterile protection) revealed that significantly higher vaccine efficacy was observed for both lower (1000) and higher (16000) spz challenge doses when measured using IVIS ($p<0.05$ for both challenge doses when by Mann-Whitney test) (Figure 13A). Linear regression modeling predicting Tto1 indicated that statistically significant difference between single ChAd63-ME.TRAP and MVA-ME.TRAP vaccination groups was observed only for the higher 16000 spz challenge dose ($p<0.01$ by Mann-Whitney test) (Figure 13B).

The results in this chapter strongly suggest that *P. berghei* parasite burden quantification methods investigated herein, including IVIS, Giemsa-stained blood film analyses and the associated extrapolations employing linear regression model, all have relatively strong correlations with the challenging dose of spz or with each other (Figure 14). Also, vaccination-induced pre-erythrocytic stage protection against malaria can adequately be assessed by using either IVIS or Tto1 methods for quantifying parasite density. While small differences seemed to be better resolved using the former, the latter was just as powerful in the vaccine setting, when the challenge inoculum was increased.

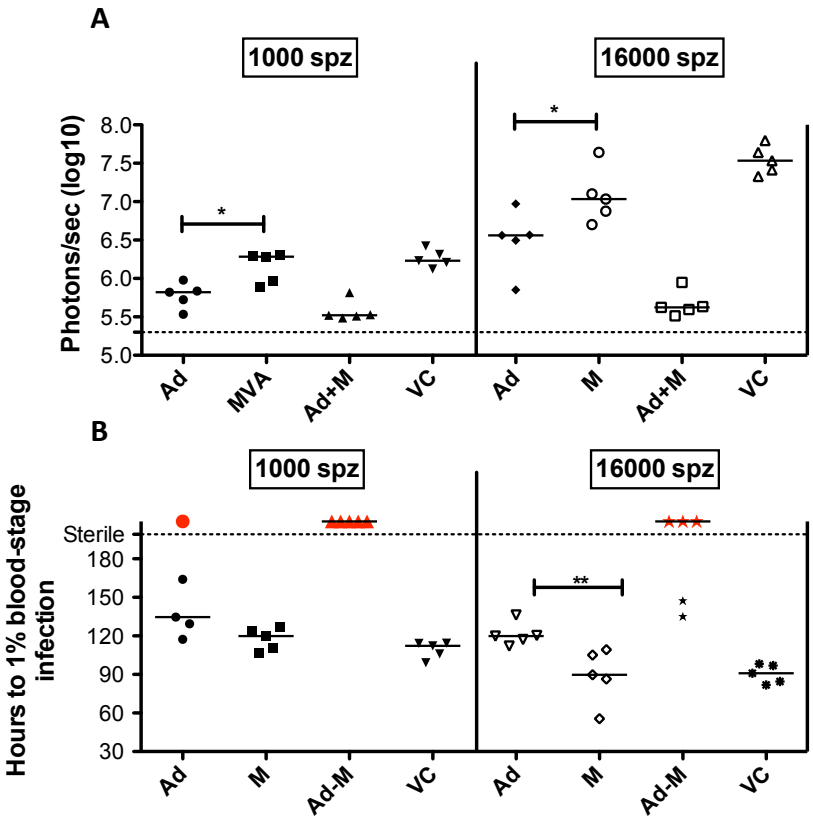


**Figure 13: Validation of IVIS and Tto1 malaria infection quantification methods in the vaccine setting.**

BALB/c mice (n=5/group) received a single vaccination of recombinant ChAd63 (Ad) or MVA (M) viral vectors expressing ME.TRAP antigen containing immunodominant $CD8^+$ T cell epitope. Another group of mice were vaccinated with the heterologous prime-boost regimen employing both ChAd63 and MVA vectors expressing the same ME.TRAP transgene (Ad-M). The control animals received empty ChAd63 and MVA in the identical prime-boost manner (VC). Two weeks after single prime (for Ad and M alone immunizations) or prime-boost (for Ad-M) vaccination mice were challenged with either the lower 1000 or the higher 16000 spz dose. (A) 44 h post-challenge vaccinations' efficacy was measured by IVIS. (B) The same animals were also monitored for blood-stage infection and linear regression analysis performed predicting Tto1. Data points in red represent sterilely protected animals. Individual dot points are shown with the line indicating the median. *$p<0.05$, **$p<0.01$ by Mann-Whitney test.

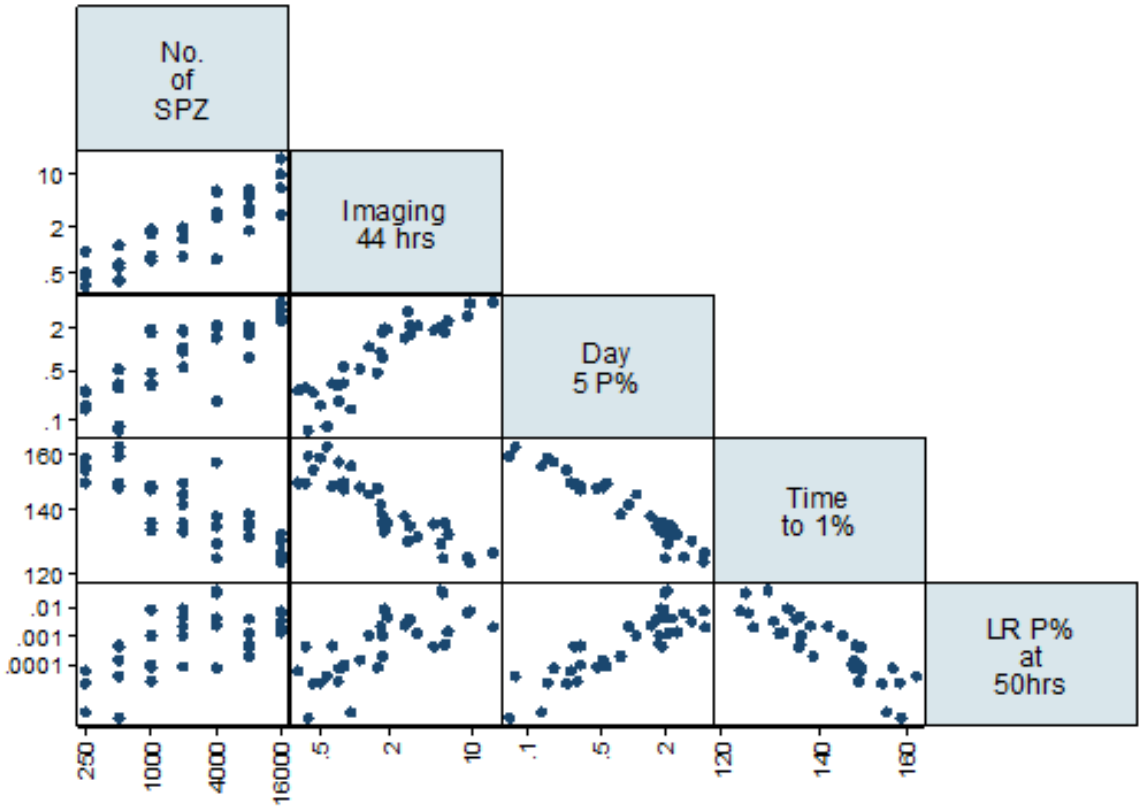


**Figure 14: The correlation matrix comparing all four methods of quantifying *P. berghei* parasite burden.**

Data analysis and statistical software (STATA) package was used to obtain the correlation matrix containing all four methods of measuring *P. berghei* parasite burden. The high degree of linear association between all of the variables indicate that all four methods could be employed to quantify *P. berghei* parasite densities, however, the most accurate results would most likely be generated by IVIS and linear regression analysis predicting Tto1. Spz challenge inoculum (No of Spz.), raw percentage parasitaemia on day 5 (Day 5%), time to 1% blood-stage infection (Time to 1%), and parasitaemia at 50 h post-challenge (LR P% at 50hrs) are shown.

## 3.3 Discussion

The exo-erythrocytic stage of malaria is considered a bottleneck in the parasite's development. A malaria-infected mosquito normally deposits a few hundred infectious sporozoites in the vertebrate host of which a small proportion succeeds in establishing an intrahepatic infection (265) (266). Once inside the hepatocyte, parasites start to multiply at an exceedingly high rate. The liver stage development, which in the case of *P. berghei* infection lasts a little longer than 48 h, concludes when merosomes containing around 100-200 mature merozoites fuse away from the liver releasing parasites into the blood stream (11), where they start another cycle of continuous infection and re-infection of RBCs. It is during the blood-stage development that peak parasite numbers are reached in vertebrate hosts. Consistent with the parasite's life cycle, a BLS emitted from infected mice at 12- and 24-h time-points post-challenge was indistinguishable from the background, suggesting that parasite numbers were too low to be quantified using IVIS. At the later time points much stronger BLS was observed corresponding with the sharp increase in parasite densities initially at the intrahepatic and later at the blood stages.

It has been demonstrated that the BLS emitted by tg *P. berghei* carrying luciferase gene correlated tightly with the RT-PCR values during liver infection (230). Also, the same tg parasite's usefulness for the evaluation of immune responses at the pre-erythrocytic stage and during the *in vitro* neutralization assay has been tested (263). Similarly, it has been suggested that liver-to-blood inoculum is directly related to the pre-erythrocytic stage vaccine efficacy (256). Thus, in order to quantify protection afforded by specifically pre-erythrocytic stage antigen, it is possible to image parasites during late-liver or early blood

stages, provided that the vaccine does not have any non-specific blood stage effect. The results in this chapter showed that a 44 h time-point post-challenge gave the strongest correlations between number of sporozoites injected and BLS, although the same correlations for later time points were also relatively strong. It is quite possible that the correlation strength at the later time points of blood-stage infection is diminished due to increased parasitized RBC sequestration in the vasculature and spleen (267).

In addition, the results obtained by IVIS were consistent with blood-stage infection recorded over 3-5 consecutive days using Giemsa stained blood-films. A steady drop in the correlation strengths was observed when the blood-stage parasitaemias from later time points were plotted against spz dose. Some factors, such as the immune system's response to ongoing infection and inaccuracies associated with scoring highly infected RBCs might have contributed to that. Also, by day 7 post-challenge many animals start developing anemia, thus the blood film counting becomes less precise. It was progressively more difficult to calculate infected RBCs due to the increasing level of blood-stage parasitaemia, therefore less fields of view were calculated, which might have also contributed to the diminished correlation strengths. The series of statistical tests comparing two separate groups showed that the method of simply plotting proportion of infected RBCs for the specific day was not as sensitive as IVIS, because substantially fewer groups could be distinguished with the required certainty.

A linear regression model was developed after scoring blood-stage parasitaemias. Results confirmed that the slopes representing parasite growth rate in the blood of individual animals were not different. The model allowed extrapolation of parasitaemia values for

individual animals for both Pat50 time point (assumed to be the time when merozoites erupt from the liver) and Tto1. The extrapolation to predict liver-to-blood parasite densities is especially relevant for human malaria pre-erythrocytic stage vaccine evaluation in clinical trials when the parasite liver eruption loads are needed to see if there is a pre-erythrocytic stage vaccine effect on parasites making it out of the liver, and which can be calculated from blood-stage infection (256). Extrapolating liver-to-blood parasite load (Pat50) was not as accurate as predicting Tto1 as evidenced by decreased correlation strength. The explanation for that could be the fact that, in the case of the former, estimations are made further into the past, thus the deviation from the actual slope is bigger than when predicting Tto1. In the analysis for the generation of lines representing blood-stage infection first 3-4 from a total of 5-6 time points were used; however, the outcome did not change when all of the points were included in the generation of the linear regression model (data not shown). It is possible that more accurate predictions could be obtained by employing PCR analysis of blood-stage infection rather than blood-films. However, as the method is not that relevant in pre-clinical mice models the hypothesis was not tested in this system. Moreover, using linear regression modeling on IVIS values for 68-, 92-, and 116-h time-points, similar results were obtained (data not shown).

The usage of IVIS imaging and Tto1 methods in vaccine studies provides a robust way of quantifying both pre-erythrocytic and blood-stage vaccine efficacy. As observed with the injection of varying doses of sporozoites into naive animals, IVIS imaging technology

allowed slightly more accurate quantification of vaccine efficacy at the lower and thus, more physiologically relevant, dose of sporozoite challenge.

Overall, the data indicate that all of the *P. berghei* parasite burden quantification methods investigated herein, including *in vivo* imaging or Giemsa-stained blood film analyses and the associated extrapolations employing a linear regression model, have strong correlations with the challenging dose of sporozoites and with each other. However, the linear regression modeling predicting Tto1 is an accurate and possibly the least expensive way to quantify the pre-erythrocytic vaccine effect. Imaging, while offering a slightly better resolution between groups, is expensive to perform and requires special equipment. On the other hand, the linear regression model would not be possible if the antigen has both liver- and blood-stage effect. Also, it is possible that if a vaccine induces sterilizing protection at the later phase of liver stage development parasites can be detected by IVIS even if there is no ensuing blood-stage infection. In these circumstances IVIS may provide the only way to assess both liver- and blood-stage effects separately in the same animals. Thus, the *in vivo* imaging of whole animals and linear regression modeling predicting Tto1 using parasitaemias over multiple days both offer powerful tools for testing malaria vaccine efficacy and thus they will be employed throughout the remainder of this thesis.

# Chapter 4

# Investigation of *Plasmodium berghei* malaria pre-erythrocytic stage vaccine efficacy: targeting antigen combinations

# 4 Investigation of *Plasmodium berghei* malaria pre-erythrocytic stage vaccine efficacy: targeting antigen combinations

## 4.1 Introduction

Despite the ongoing efforts to develop a single antigen subunit vaccine against malaria, many speculate that the first highly efficacious subunit vaccine against this protozoan parasite will incorporate multiple antigens, targeting a single and/or multiple stages of parasite development. The basis for such beliefs stems from the fact that whole parasite-based vaccination approaches, including radiation- or genetically-attenuated parasites, or parasites administered under prophylactic drug coverage, have consistently demonstrated exceptionally high levels of protection in mouse (156) (155) studies. Bites of mosquites with irradiated sporozoites and infection plus treatment protocols also show efficacy in humans (94, 145). Attenuated whole parasites are capable of establishing intrahepatic stage infection, however, their development beyond liver-stages is arrested. It is thought that the long-lasting immunity elicited by radiation-attenuated parasites (RAS) in humans or, more recently, genetically-attenuated parasites (GAPs) in pre-clinical models, is mediated mostly by anti-parasite specific $CD8^+$ T cells that target multiple pre-erythrocytic stage antigens (90). Furthermore, Butler *et al.* comparing early-arresting versus late-arresting GAPs showed that the significantly higher degree of protective efficacy was associated with the latter type of GAPs, demonstrating the importance of

diversifying antigenic targets (155). However, the difficulties associated with the production and deployment of whole-parasite malaria vaccines to the endemic regions, as well as their current lack of any efficacy when delivered by needle and syringe in humans (268), make this vaccination strategy of no interest to most malaria funders today. Nonetheless, great interest in trying to mimic the degree of protection observed with whole-parasite vaccinations delivered by mosquito bite using single- or multiple-antigen vaccines administered by needle and syringe has been ignited.

The attempts to combine multiple antigens using subunit vaccines have encountered varying levels of success. The vaccination of monkeys with DNA and poxvirus vectors encoding four *P. knowlesi* antigens, including circumsporozoite (CS), thrombospondin-related adhesive protein (TRAP), merozoite surface protein 1 ($MSP\text{-}1_{42}$), and apical membrane antigen 1 (AMA-1) resulted in significantly better control of blood-stage parasitaemia compared to PkCSP vaccination alone (259). In addition, Limbach *et al.* reported that the protection elicited by a combination of *P. yoelii* upregulated in infectious sporozoites 3 (UIS-3) and falstatin antigens in the DNA followed by MVA vaccination regimen exceeded the sum of the protection elicited by the single antigen vaccines against the *P. yoelii* sporozoite challenge, indicating a potential synergistic interaction (257). Similarly, the combined administration of PyMSP-1 and PyCSP vectored vaccines elicited higher level of protection than the same vaccines administered alone (269). Additional impetus towards the manufacture of multi-antigen vaccine regimens is the fact that single antigen vaccinations may not induce broad enough responses able to protect heterogeneous populations of people. Therefore, by

incorporating two or more antigens in the vaccination regimen, broader immunity can be elicited. For example, the concurrent injection of DNA plasmids encoding PyHEP17 and PyCSP antigens enhanced level of protection in various strains of mice as compared to the same single antigen vaccinations against pre-erythrocytic challenge (258).

On the other hand, vaccinating with multiple-antigen vaccines may not always have a beneficial effect. The administration of either MSP-$1_{42}$ or RTS,S together with AMA-1 protein vaccines to rhesus macaques significantly reduced AMA-1-specific antibody responses and parasite growth inhibitory activity when compared to AMA-1 alone vaccination as measured by enzyme-linked immunosorbent (ELISA) and *in vitro* growth inhibition assays (GIA), respectively (270). Also, the attempts to administer a mixture of DNA containing nine *P. falciparum* malaria antigens have been thwarted by antigenic interference, whereby immunogenicity against each individual antigen in the mixture administration was significantly lower than if those antigens were administered individually (271).

In this chapter three malaria pre-erythrocytic stage candidate antigens including circumsporozoite (CS) and thrombospondin-related adhesive proteins (TRAP), and cell-traversal protein for ookinetes and sporozoites (TOS) were comparatively assessed alone or in different combinations with each other in heterologous Ad-M regimen using the *P. berghei* rodent malaria sporozoite challenge model. CSP and TRAP were selected because different vaccine formulation based on these antigens have been extensively explored and have consistently elicited some level of protective efficacy in pre-clinical (264)(Hafalla *et al.* submitted) and clinical studies (161, 170, 182). Similarly, pre-clinical

studies in mice have demonstrated that when PfTOS was administered as a recombinant protein emulsified with Montanide ISA-720 a relatively high degree of protection against heterologous *P. berghei* challenge (88) (89) was induced.

## 4.2 Results

### 4.2.1 The assessment of protective efficacy elicited by different combinations of leading malaria pre-erythrocytic stage vaccine candidates in C57BL/6 strain of mice

To delineate, which of the aforementioned pre-erythrocytic stage antigens or antigen combinations elicit the highest degree of protection, C57BL/6 mice were vaccinated with heterologous prime-boost regimes employing Chimpanzee adenovirus 63 (Ad) and modified vaccinia strain Ankara (M) recombinant viruses expressing a single malaria antigen 8 weeks apart (Ad-M) (Table 5). To minimize the immune interference present when two antigens are co-administered into the same animal, the Ad-M combination vaccines were injected bilaterally into thigh muscles (269).

The results obtained after challenging mice with 2000 *P. berghei* sporozoites showed that among individually administered antigens the highest degree of protection was elicited by vaccine encoding PbTRAP (Ad-M TR) as measured by time to 1% blood-stage infection (Tto1) (described in chapter 3) (mean Tto1 for the group 6.4) ($p<0.001$ by one-way ANOVA with Bonferroni's post-test) (Figure 15). The Ad-M regimen expressing PbCSP (CS) was the second best (mean Tto1 5.6) ($p<0.05$ by one-way ANOVA with Bonferroni's post-test), whereas PbTOS transgene administered in an identical Ad-M manner did not induce a statistically significantly higher level of protection when compared to the animals that were immunized with empty Ad-M vector control vaccines (Ad-M VC).

Further, the protective potential of combination vaccines was evaluated. The highest degree of protective efficacy was elicited by Ad-M CS and Ad-M TR combination vaccine (Ad-M CS+TR) (mean Tto1 6.7) ($p<0.001$ by one-way ANOVA with Bonferroni's post-test) (Figure 15). On the other hand, combination vaccines containing Ad-M TOS, including Ad-M TR+TOS (mean Tto1 5.8) and Ad-M CS+TOS (mean Tto1 5.9) resulted in even lower level of protective efficacy when compared to the individual Ad-M TR and Ad-M CS vaccines, respectively.

The results obtained using Ad-M TR, CS, and TOS vaccines administered individually or as all the possible combinations of two, showed that in the C57BL/6 strain of mice the most potent regimens were Ad-M TR administered alone or together with Ad-M CS. Unfortunately, no significant enhancement of protection was obtained with the Ad-M CS+TR or other combination vaccines when compared to the most protective single Ad-M TR immunization.

| Group | Priming agent (Dose)(Route) | Boosting agent (Dose)(Route) | Time to 1% blood-stage infection (days) (mean (95% CI)) |
|---|---|---|---|
| **Ad-M TR** | ChAd63-PbTRAP (1X10^8 iu) (IM) | MVA-PbTRAP (1X10^7 pfu) (IM) | **6.416 (5.777, 7.055)** |
| **Ad-M CS** | ChAd63-PbCSP (1X10^8 iu) (IM) | MVA-PbCSP (1X10^7 pfu) (IM) | **5.648 (5.281, 6.014)** |
| **Ad-M TOS** | ChAd63-PbCelTOS (1X10^8 iu) (IM) | MVA-PbCelTOS (1X10^6 pfu) (IM) | **5.036 (4.710, 5.363)** |
| **Ad-M CS+TR** | ChAd63-PbCSP (1X10^8 iu) (IM) | MVA-PbCSP (1X10^7 pfu) (IM) | **6.660 (6.176, 7.145)** |
| | ChAd63-PbTRAP (1X10^8 iu) (IM) | MVA-PbTRAP (1X10^7 pfu) (IM) | |
| **Ad-M CS+TOS** | ChAd63-PbCSP (1X10^8 iu) (IM) | MVA-PbCSP (1X10^7 pfu) (IM) | **5.875 (5.118, 6.632)** |
| | ChAd63-PbCelTOS (1X10^8 iu) (IM) | MVA-PbCelTOS (1X10^6 pfu) (IM) | |
| **Ad-M TR+TOS** | ChAd63-PbTRAP (1X10^8 iu) (IM) | MVA-PbTRAP (1X10^7 pfu) (IM) | **5.836 (5.271, 6.401)** |
| | ChAd63-PbCelTOS (1X10^8 iu) (IM) | MVA-PbCelTOS (1X10^6 pfu) (IM) | |
| **Ad-M VC** | ChAd63-EMPTY (1X10^8 iu) (IM) | MVA-GFP-OVA (1X10^7 pfu) (IM) | **4.693 (4.476, 4.910)** |

**Table 5: The comparative assessment of malaria pre-erythrocytic stage antigens and antigen combinations in C57BL/6 strain of mice.**

C57BL/6 mice (n=6/group) were immunized IM as outlined above. The name of the vaccination group, priming and boosting agents, and the protective efficacy against 2000 *P. berghei* spz challenge of the specified regimen are shown. Where two antigens are employed for vaccination, each antigen was administered into a separate thigh muscle. The protective efficacy was measured by employing linear regression model on blood-stage parasitaemia to predict Tto1 (time in days until 1% of circulating red-blood cells become infected).

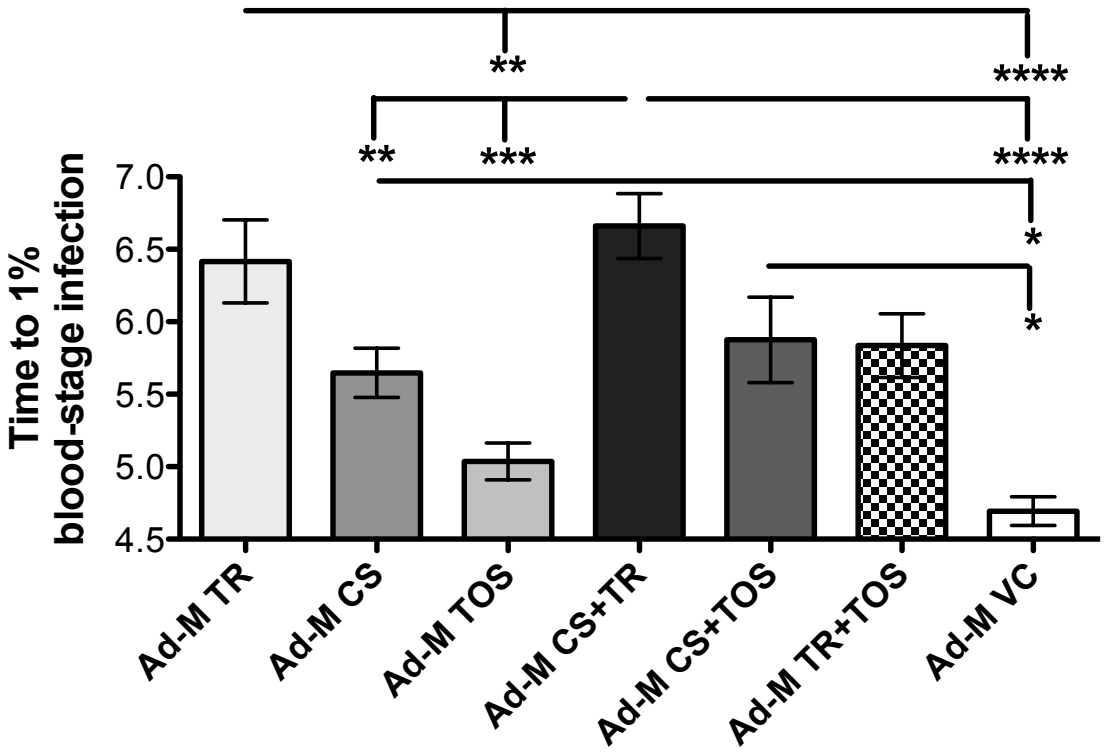


**Figure 15: The protective efficacy of different antigen combination vaccines in C57BL/6 strain of mice.**

The C57BL/6 mice (n=6/group) were vaccinated as outlined in table 1. Two weeks after the boost animals were challenged by IV injection of 2000 *P. berghei* sporozoites. Blood-stage parasitaemia was monitored starting with day 4 post-challenge, and Tto1 calculated using linear regression modeling (for this and every subsequent diagram the time is expressed in days). *p<0.05, **p<0.01, ***p<0.001, ****p<0.0001 by one-way ANOVA with Bonferroni's multiple comparison post-test.

### 4.2.2 T cell and antibody responses in combination vaccines are susceptible to antigenic interference

To quantify immune responses induced against each antigen, two weeks after booster immunization ELISA and intracellular cytokine staining assays (ICS) were employed.

The end-point ELISA indicated that high whole IgG antibody (Ab) titres with the mean responses of 4.87 ELISA units (EU), 4.96 EU, and 4.25 EU against PbCSP, PbTRAP, and PbTOS recombinant proteins, respectively, were measured in the individual vaccination groups (Figure 16A). However, significantly lower anti-CS IgG titres were observed in the Ad-M CS+TR combination group when compared to the Ad-M CS alone vaccination ($p<0.05$ by one-way ANOVA with Bonferroni's post-test) (Figure 16A(i)). Also, there was a non-significant trend towards diminished Ab responses when PbTRAP and PbTOS were co-administered with other antigens (Figures 16A(ii) and (iii), respectively), although the individual differences were not statistically significant.

The ICS analysis revealed that high frequencies of $CD8^+IFN\text{-}\gamma^+$ T cells were stimulated by Ad-M CS (mean frequency was ~4.5%) (Figure 16B(i)) and Ad-M TR (mean frequency ~45%) (Figure 16B(ii)) vaccinations, whereas Ad-M TOS (Figure 16B(iii)) construct was relatively un-immunogenic for inducing $CD8^+$ T cell responses. Despite the separate-site administration of combination vaccines, statistically significantly lower proportions of anti-CS $CD8^+IFN\text{-}\gamma^+$ T cells were quantified in the Ad-M CS+TR (mean frequency ~1.5%), and Ad-M CS+TOS (mean frequency ~1.25%) co-administration groups, when compared to Ad-M CS alone vaccination ($p<0.001$ by one-way ANOVA with Bonferroni's post-test). The same trend was also observed for anti-TRAP $CD8^+$ T

cell responses. The Ad-M TOS+TR combination vaccine, when compared to the individual Ad-M TR vaccination, had statistically significantly lower frequencies of $CD8^+IFN\text{-}\gamma^+$ T cell subset ($p<0.01$ by one-way ANOVA with Bonferroni's post-test). Relatively low frequencies of $CD4^+IFN\text{-}\gamma^+$ T cells were observed against all three antigens (Figure 16C).

The investigation of humoral and cellular immune responses demonstrated that all three malaria pre-erythrocytic antigens were highly immunogenic for Ab induction, however, only PbCSP and PbTRAP induced $CD8^+$ T cell responses above background. Also, a trend towards diminished humoral and cellular immune responses was observed when antigen combinations were employed for immunization, indicating that despite separate-site administration of antigens in the co-administration regimen, immune interference could not be overcome.

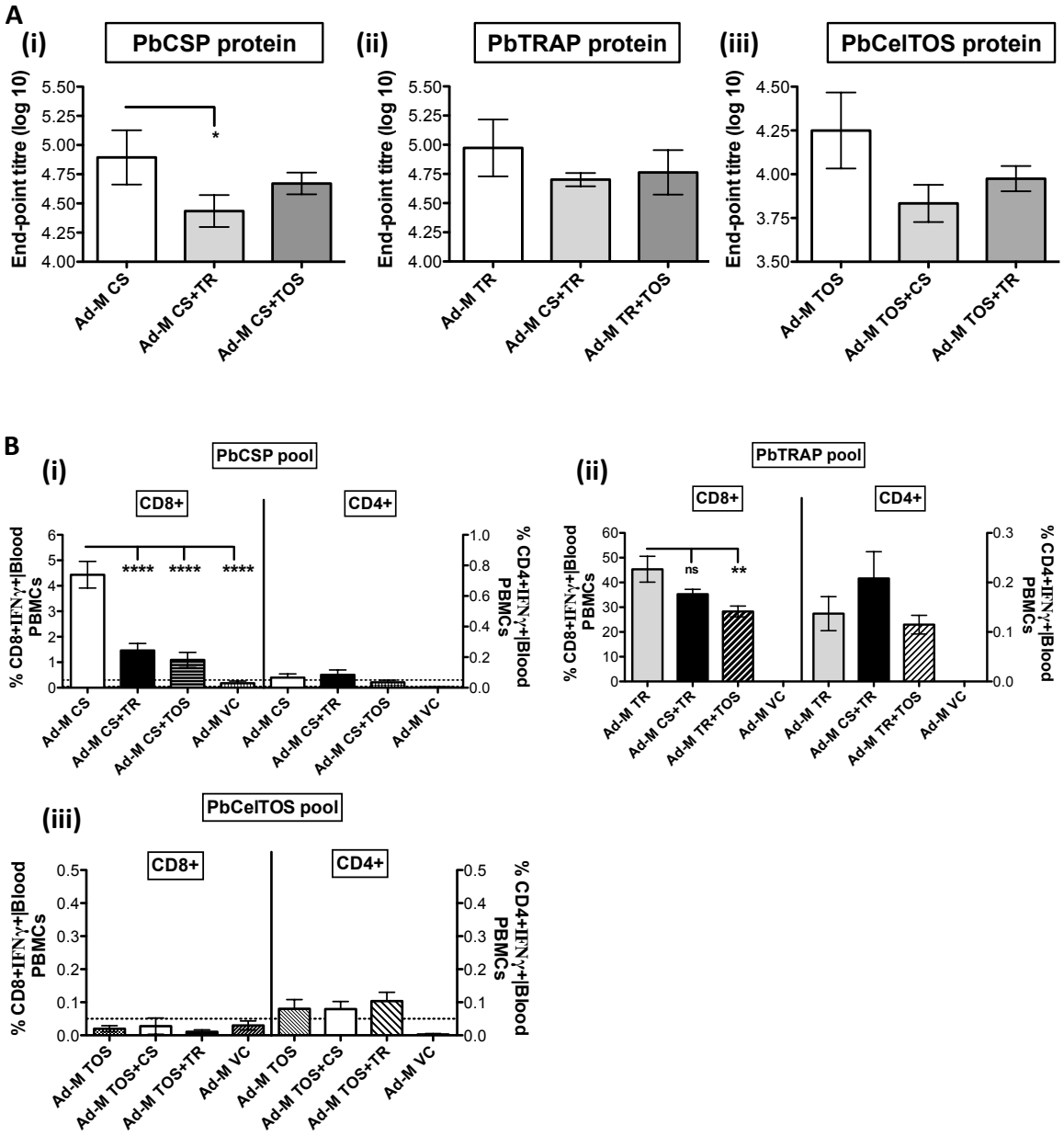
A
(i)
PbCSP protein
(ii)
PbTRAP protein
(iii)
PbCelTOS protein
End-point titre (log 10)
Ad-M CS
Ad-M CS+TR
Ad-M CS+TOS
Ad-M TR
Ad-M CS+TR
Ad-M TR+TOS
Ad-M TOS
Ad-M TOS+CS
Ad-M TOS+TR
B
(i)
PbCSP pool
CD8+
CD4+
% CD8+IFNγ+|Blood PBMCs
% CD4+IFNγ+|Blood PBMCs
****
Ad-M CS
Ad-M CS+TR
Ad-M CS+TOS
Ad-M VC
(ii)
PbTRAP pool
ns
**
Ad-M TR
Ad-M CS+TR
Ad-M TR+TOS
Ad-M VC
(iii)
PbCelTOS pool
Ad-M TOS
Ad-M TOS+CS
Ad-M TOS+TR
Ad-M VC

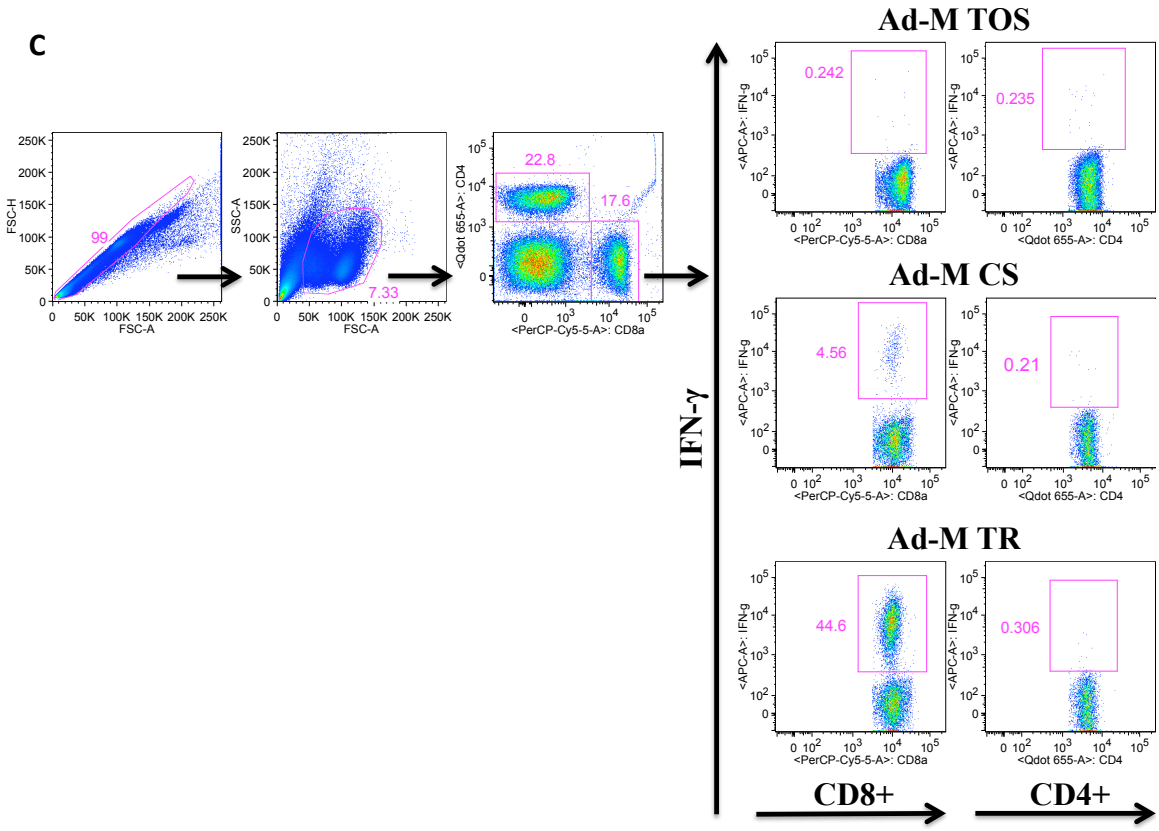


**Figure 16: Humoral and cellular post-boost immune responses following Ad-M vaccinations encoding different pre-erythrocytic stage antigens and antigen combinations.**

The C57BL/6 animals were vaccinated as previously described and outlined in table 1. Two weeks after the boost and a day before the challenge humoral and cellular immune responses were assessed using end-point ELISA and ICS, respectively. (A) The whole IgG Ab titres were measured against (i) PbCSP, (ii) PbTRAP, and (iii) PbTOS recombinant proteins. No responses were seen in this or subsequent ELISAs to serum from VC groups. Also, (B) the whole-blood PBMCs were re-stimulated with single peptide pools representing the full length of (i) PbCSP, (ii) PbTRAP, or (ii) PbTOS antigens and frequencies of either $CD8^{+}IFN\text{-}\gamma^{+}$ (left y-axis) or $CD8^{+}IFN\text{-}\gamma^{+}$ (right y-axis) T cell subsets quantified. (C) The representative FlowJo images showing the gating strategy and respective proportions of T cells. *p<0.05, **p<0.01, ****p<0.0001, ns=not significant by one-way ANOVA with Bonferroni's multiple comparison post-test.

### 4.2.3 The protective efficacy elicited by different malaria pre-erythrocytic stage vaccine candidates in ICR (CD1) outbred strain of mice

To determine whether the level of protective efficacy obtained using the pre-erythrocytic stage antigen combinations in C57BL/6 model would also apply to outbred strain of rodents, ICR (CD1) mice were immunized as outlined in table 1. Two weeks after the last vaccination animals were challenged with 2000 *P. berghei* sporozoites and monitored for blood-stage infection.

Consistent with the results obtained in C57BL/6 model, the highest degree of protection was induced by individual Ad-M CS and Ad-M TR vaccines, each conferring sterile protection in 50% of the animals (3 out of 6) (Table 6). On the other hand, Ad-M TOS sterilely protected only 17% of mice (1 out of 6). Disappointingly, none of the combination vaccines resulted in the enhanced protection when compared to individual constituent elements. Both Ad-M CS+TR and Ad-M CS+TOS combination vaccines sterilely protected 50% of the animals, whereas lower level of sterile immunity was observed following vaccination with the Ad-M TR+TOS.

The challenge results obtained with the outbred CD1 strain of mice demonstrated that consistent with C57BL/6 rodent model, the most protective regimens encoding single antigen were Ad-M CS and Ad-M TR. In contrast, Ad-M TOS vaccination did not protect mice of both strains to any considerable degree. Interestingly, the administration of TOS antigen in a heterologous Ad prime – recombinant protein in Abisco 100 boost regimen (Ad-P), which is meant to maximize Ab responses when compared to Ad-M TOS regimen, also did not elicit any protective efficacy (Figure 17). Similarly, combining any

two pre-erythrocytic stage malaria vaccine candidates did not translate into enhanced protection in C57BL/6 (Figure 17A) or CD1 (Figure 17B) strains of mice, indicating that a careful selection of antigens and perhaps even vaccination strategies is important and cannot be underestimated. These ideas are further explored in chapters 5 and 6.

| Group (n=6/group) | % Sterile protection (No. sterile/no. challenged) | Time to 1% blood-stage infection, mean (95% CI) (no. parasitaemic) | Time to 1% blood-stage infection (median) |
|---|---|---|---|
| **Ad-M TR** | 50% (3/6) | 6.514 (5.595, 7.434) (n=3) | 6.317 |
| **Ad-M CS** | 50% (3/6) | 7.869 (1.793, 13.95) (n=3) | 6.942 |
| **Ad-M TOS** | 17% (1/6) | 7.239 (5.002, 9.475) (n=5) | 6.699 |
| **Ad-M TR+CS** | 50% (3/6) | 6.891 (3.687, 10.10) (n=3) | 6.699 |
| **Ad-M TR+TOS** | 33% (2/6) | 6.901 (4.605, 9.196) (n=4) | 6.498 |
| **Ad-M TOS+CS** | 50% (3/6) | 7.052 (6.110, 7.994) (n=3) | 7.092 |
| **Ad-M VC** | 0% (0/6) | 6.632 (6.204, 7.059) (n=6) | 6.763 |

**Table 6: The screening of the pre-erythrocytic stage antigen combinations in ICR (CD1) outbred strain of mice.**

The CD1 mice (n=6/group) were vaccinated in the identical manner as outlined in table 5. Two weeks after the last vaccination animals were challenged with 2000 *P. berghei* sporozoites. The table lists all of the different vaccination groups and the protection conferred by the relevant regimen. The protection readouts include the number of sterilely protected mice and time (in days) to 1% blood-stage infection for the animals that became parasitaemic.

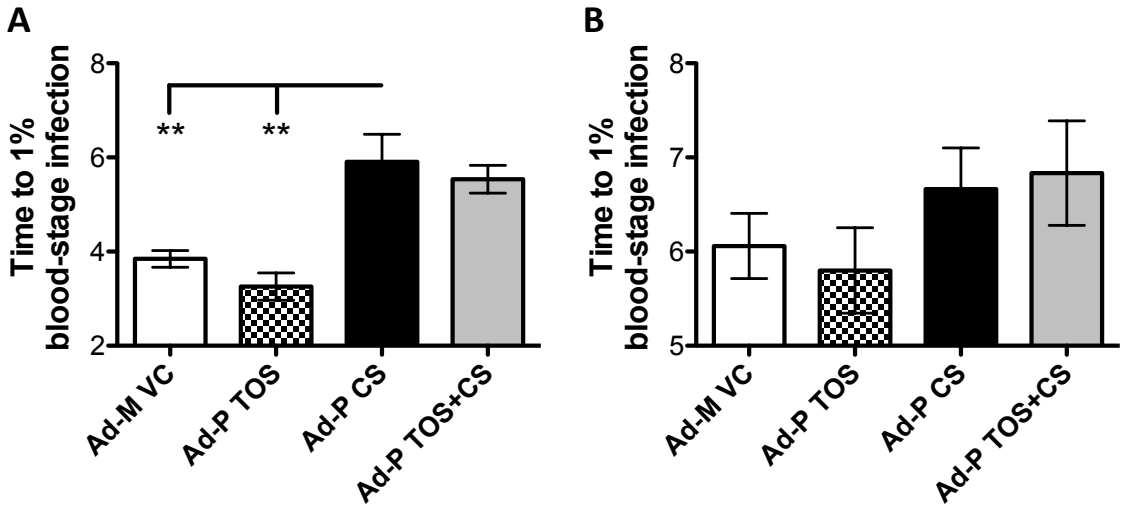


**Figure 17: The protective efficacy of Ad-P CS and Ad-P TOS combination vaccine.**

(A) C57BL/6 (n=6/group) and (B) CD1 (n=6/group) mice were vaccinated either with the individual Ad-P CS or Ad-P TOS vaccines or the combination of the two (Ad-P CS+TOS) all formulated in Abisco 100 adjuvant. The combination was administered into a separate thigh muscle. Two weeks after the boost animals were challenged with the 2000 *P. berghe*i spz injection. Blood-film analysis was performed and Tto1 (in days) predicted using linear regression modeling. **p<0.01 by one-way ANOVA with Bonferroni's multiple comparison post-test.

## 4.3 Discussion

In this chapter three leading pre-erythrocytic stage vaccine antigens, including CSP, TRAP, and TOS, and their combinations were evaluated using well-established experimental mouse malaria *P. berghei* model. The heterologous prime-boost regimen employing recombinant ChAd63 and MVA viral vectors administered 8 weeks apart was chosen, because previously it has been demonstrated that strong T cell responses and high-titer Abs against malaria Ags could be induced using this regimen in rodent (215, 254, 269), rabbit (213, 272), rhesus macaque (214), and human (209) studies. However, in the studies reported herein the concurrent induction of Ag-specific Abs and T cells following Ad-M vaccination was observed for PbCSP and PbTRAP antigens, whereas only Ag-specific Ab responses were significant following Ad-M TOS vaccination in C57BL/6 strain. Low level of T cell immunogenicity associated with PbTOS antigen, possibly, could be explained by the lack of immunodominant T cell epitopes (Hafalla *et al.* submitted), rather than the incompatible vaccine platform.

The C57BL/6 mice for performing these (and all of the other coming up) studies were chosen for a few reasons. Ad-M ME.TRAP vaccination confers 100% and 60% sterile protection in BALB/c strain of mice against 1000 and even 16,000 *P. berghei* sporozoite challenges, respectively (Chapter 3). The protection following Ad-M ME.TRAP regimen is mediated by anti-CS cytotoxic T lymphocytes (CTLs) recognizing the Pb9 immunodominant epitope presented on MHC I complexes of infected hepatocytes (264), therefore, rendering the BALB/c model inconclusive to detect a statistically significant enhancement of protective efficacy induced by combination vaccine containing PbCSP

antigen. Also, it has been demonstrated that C57BL/6 mice was significantly more susceptible to *P. berghei* infection when compared to other strains, including BALB/c, and that a dose of as few as 50 sporozoites was sufficient to infect 5 out of 5 animals (273). Furthermore, the study performed by Schmidt *et al.* suggested that significantly higher radiation-attenuated sporozoite (RAS) induced memory $CD8^+$ T cell responses were required for sterilizing protection in C57BL/6 mice as compared to inbred BALB/c or even Swiss Webster outbred strains of mice (224). The challenge results using either C57BL/6 or CD1 strains of mice were consistent with the latter study, as significantly higher levels of sterile protection was observed in the outbred rodents after immunization with the identical vaccination regimens. It remains to be determined which mouse strain(s) (if any) is more relevant to the protection observed in humans using comparable vaccination strategies, but it is evident that C57BL/6 animals require extremely potent regiments for sterilizing protection, which is desirable when working with vaccine constructs that are of clinical relevance.

The degree of protection observed with Ad-M CS+TR combination vaccine in C57BL/6 mice was substantially lower than that seen in the Schneider *et al.* study, where DNA/MVA prime-boost vaccination employing the combination of the same PbCSP and PbTRAP antigens elicited 60% and 100% sterile protection against 1000 and 200 *P. berghei* sporozoite challenges, respectively (169). However, in the latter case at the time of boosting MVA was administered intravenously, which is more protective mode of vaccination (169). Since the intravenous injection of MVA viral vectors is not permitted

in the clinical setting, intramuscular route of administration was chosen for the studies described in this and upcoming chapters.

Unexpectedly and, perhaps, in a disagreement with the previous studies a relatively low level of protective efficacy against *P. berghei* was induced by Ad-M TOS vaccine in both mice strains used. Bergmann-Leitner *et al.* reported that vaccination of CD1 mice with three doses of recombinant *P. falciparum* TOS protein formulated in Montanide ISA-720 adjuvant sterilely protected 12 out of 20 animals against subcutaneous challenge with 15.000 heterologous *P. berghei* sporozoites (88). Moreover, in a follow-up study the same authors claimed that the protection induced by PfTOS recombinant protein in Montanide ISA-720 was dependent on Ag-specific Abs as well as T cells (89). It is unlikely that the disappointingly low level of protection induced by Ad-M TOS vaccine could be attributed to the lowered dose of MVA-PbTOS used for the boost ($10^6$ versus $10^7$ plaque forming units used for the other antigens). The reduced amount of MVA would have little (if any) effect on the cellular immune responses in C57BL/6 model as only relatively insignificant $CD8^+$ and $CD4^+$ T cell responses were reported with the $10^6$ dose of MVA. On the other hand, it has been demonstrated that Ag-specific Ab titres are reduced in a dose-dependent manner when 10 times less recombinant viral vector is used at the time of the boost in a homologous Ad-Ad prime-boost regimen (274). Therefore, anti-TOS Ab titres may well be lower when $10^6$ rather than $10^7$ pfu of MVA-PbTOS was injected. Interestingly, the Ad/protein in Abisco 100 prime-boost regimen, which is thought to maximize Ag-specific Ab responses (215, 217) did not elicited improved protective efficacy in either C57BL/6 or CD1 strains of mice, whereas, the administration

of PbCSP in the identical manner resulted in the statistically significant protection in C57BL/6, but not CD1 animals (Figure 17A, B) ($p<0.01$ by one-way ANOVA with Bonferroni's post-test). It is also possible that the disappointing results obtained using Ad-M TOS or even Ad-P TOS vaccinations in C57BL/6 and CD1 strains of mice, may simply be associated with low level of anti-TOS cellular immune responses observed in these specific genetic backgrounds. Higher anti-PfTOS cellular immune responses and protection have been reported in BALB/c model, and therefore it would be interesting to explore the level of protective efficacy conferred by Ad-M or Ad-P PbTOS regiments in those animals. Finally, Doolan *et al.* demonstrated that PfTOS-specific peptides could stimulate anti-TOS IFN-γ responses in PBMCs isolated from volunteers immunized with highly protective irradiated-sporozoite vaccine, highlighting the potential immunological significance of this antigen (90).

Separate-site administration for the combination vaccines was chosen because previously it has been found that multiple malaria Ags administered that way display minimized antigenic interference as compared to the mixture single-site DNA (271) and viral vector (269) vaccinations encoding malarial antigens. Despite the separate-site vaccine administration mode, the diminished immune responses were still present within Ag combination groups. Consistent with the Forbes *et al.* data, the immune interference phenomenon was especially evident for the $CD8^+$ T cell responses against both PbCSP and PbTRAP antigens (269). The humoral immune responses, while maintaining obvious trend towards diminished Ab titres in the combination groups against all three Ags tested, seemed to be more resistant to the antigenic interference. Further, Forbes *et al.* suggested

that the immune interference may be due to enhanced killing by MVA coinfected cells expressing both CSP- and MSP-1-specific epitopes, by previously adenovirus primed cytotoxic T lymphocytes (269). It is unclear whether the same mechanism is important here, but both anti-PbCSP and anti-PbTRAP cellular immune responses contain high frequencies of Ag-specific $CD8^{+}IFN\text{-}\gamma^{+}$ T cells, which may contribute to the increased killing of MVA coinfected cells in the Ad-M CS+TR combination group. Also, it seems that the immunological interference is not specific to malarial Ags. Larke *et al.* reported that the combination of multiple single-clade HIV-1 vaccines into formulations that target multiple clades resulted in *in vivo* $CD8^{+}$ T cell immune interference (275). Moreover, humoral immune responses induced by a trivalent human papillomavirus vaccine were lower when compared to the same monovalent vaccines (276), demonstrating that immune interference is also present with antigens representing diseases other than malaria.

It is possible that the Ad-M vaccine platform may not be optimal for some of the antigens tested leading to lower than expected protection in co-administration vaccinations. For example, a higher degree of protection was obtained when PbCSP was administered in Ad-P rather than Ad-M CSP regimen. This, in part, demonstrates that one vaccine formulation, in this case heterologous Ad-M prime-boost regimen may not be optimal for all of the antigens. Therefore, careful attention must be paid to which arm of immunity – humoral or cellular – should be targeted for inducing the highest degree of protection possible for that specific antigen. All this has important ramifications for selecting the

vaccine Ags as well as the vaccine platforms for multi-antigen, multi-stage, and even multi-formulation vaccination regimens.

# Chapter 5

# Tailoring a PbCSP and PbTRAP combination vaccine

# 5 Tailoring a PbCSP and PbTRAP combination vaccine

## 5.1 Introduction

Many attempts have been made to develop an efficacious pre-erythrocytic stage vaccine against malaria. To date, the most successful subunit vaccine candidates rely on the induction of either exceptionally high antibody (Ab) titers or T cell frequencies. However, in both cases only partial immunity is achieved and, thus, there is a need to improve the protection.

Some of the most potent Ab inducing vaccines, including the most advanced pre-erythrocytic stage malaria vaccine candidate, termed RTS,S, are based on protein particles. In the case of RTS,S, part of the *P. falciparum* sporozoite surface circumsporozoite protein (CSP) is fused to the hepatitis B surface antigen (HBsAg) and, when administered together with potent adjuvants, CSP and HBsAg particle confers 30-50% sterilizing protection in malaria naïve volunteers (162). Similarly, RTS,S formulated with AS01 adjuvant system (RTS,S/AS01) elicited 34.8% efficacy against severe malaria in African children in the ongoing Phase III clinical trial (161). The correlates of protection in the RTS,S vaccinees have not been well established, however, both high anti-PfCS repeat region antibodies (Ab) and $CD4^+$ T cells have been implicated (277) (278) (279-281), although the evidence for a $CD4^+$ T cell correlate that is not secondary to the antibody correlation is very weak.

An alternative strategy to recombinant protein vaccines employs genetically modified adeno (Ad) and modified vaccinia strain Ankara viruses (M) in a heterologous prime-boost regimen (Ad-M). These recombinant viruses encoding highly conserved *P. falciparum* thrombospondin-related adhesive protein (TRAP) administered 8 weeks apart have demonstrated promising levels of protection in pre-clinical (165) and clinical (Ewer *et al*. submitted) studies. TRAP is expressed throughout the sporozoite and early-liver stages of parasite development, thus both anti-TRAP Abs and T cells could mediate the protection. In fact, it has been demonstrated that the protection in human volunteers elicited by Ad-M ME.TRAP vaccination was associated with the induction of monofunctional Ag-specific IFN-γ secreting $CD8^+$ T cells (Ewer *et al.* submitted).

A concurrent induction of optimal humoral and cellular immune responses bears an attractive option for maximizing pre-erythrocytic stage vaccine efficacy induced by RTS,S or Ad-M ME.TRAP vaccination strategies. Sporozoite-specific Abs could target the extracellular, whereas protective $CD4^+$ or $CD8^+$ T cells could target the intrahepatic stages of the parasite's development. However, efforts to accomplish simultaneous induction of potent humoral and cellular immune responses using PfCSP-based vaccine platforms have met with mixed success. A sequential immunization of humans using 3 doses of PfCSP DNA vaccine followed by two doses of RTS,S/AS02A generated not only PfCSP-specific Abs and $CD4^+$, but also $CD8^+$ T cells, all three Ag-specific factors of adaptive immunity that were not induced when the same vaccines were used individually alone (282). On the other hand, a heterologous prime-boost regimen employing 2 PfCSP DNA immunization boosted by $1/5^{th}$ human dose of RTS,S/AS02A

did not induce higher Ab responses against CSP repeats than those seen after RTS,S vaccination alone (283). Also, the combined use of recombinant MVA encoding full-length PfCSP and RTS,S/AS02A administered as a heterologous prime-boost regimen in a Phase I/IIa clinical trial neither enhanced immunogenicity nor protection above those seen with RTS,S alone (284). More recently, the co-administration of protein and viral vector combination vaccine encoding PbCSP induced significantly higher humoral and cellular immune responses and sterilely protected more mice than the same immunizations when employed alone (264). Also, use of Ad35 expressing part of PfCSP as a prime, boosted by two doses of RTS,S induced significantly higher $CD4^+$ T cells, but not Ab responses as compared to RTS,S alone group in macaques (216). Interestingly, despite the fact that consistent efficacy in clinical trials has been achieved by RTS, S and viral vectors expressing ME.TRAP used individually, the protective potential associated with the combination of the two Ags has not been well studied.

In this chapter, *P. berghei* CS and TRAP antigens are employed for the investigation of protective efficacy elicited by CS and TRAP combination vaccine. The optimal induction of T cell and Ab responses was achieved and protection in C57BL/6 mice enhanced after the use of these antigens in a viral vector plus protein-in-adjuvant combination regimen.

## 5.2 Results

### 5.2.1 Immunogenicity and protective efficacy of PbCSP and PbTRAP combination vaccine

To evaluate the protective efficacy of pre-erythrocytic stage PbCSP and PbTRAP combination vaccine, C57BL/6 mice were immunized intramuscularly with the combination of recombinant ChAd63 and MVA viral vectors each expressing either PbCSP or PbTRAP transgenes (Ad-M CS+TR) in an 8-week heterologous prime-boost regimen. The prime-boost immunizations with single PbCSP (Ad-M CS) or PbTRAP (Ad-M TR) antigens using the same viral vectors were also included. To minimize the presence of antigenic interference existing when more than one antigen is incorporated into the vaccine regimes as seen in chapter 4 and (269), viral vectors coding each transgene were administered into separate mouse thigh muscle in the Ad-M CS+TR group. Two weeks after the last immunization mice were challenged by intravenous injection of 2000 *P. berghei* sporozoites expressing a fusion of green-fluorescent and luciferase proteins (GFP/Luc). To directly assess vaccines' pre-erythrocytic stage efficacy, the bioluminescence signal (BLS), corresponding to the intrahepatic parasite burden, emitted from the infected animals was quantified using *in vivo* imaging (IVIS) of whole animals 44 hours (h) post-challenge. The results revealed that all vaccine groups had statistically significantly less BLS ($p<0.0001$ by one-way ANOVA with Bonferroni's post-test) corresponding to the pre-erythrocytic stage protection when compared to the animals that received only empty viral vector control immunizations (Ad-M VC)(Figure 18A). Also, no improvement in the efficacy was observed with the Ad-M CS+TR

combination vaccine, as Ad-M TR immunization alone conferred an almost identical level of protection at 44 h after challenge as measured by *in vivo* imaging system (IVIS).

The same animals were followed through to the secondary end-point of blood-stage parasitaemia. The level of blood-stage parasitaemia evaluated over a few consecutive days was consistent with the results obtained using IVIS (Figure 18B). All of the vaccination groups conferred statistically significantly higher degree of protection when compared to Ad-M VC immunization. However, the most potent Ad-M CS+TR and Ad-M TR regimes (Figure 18B) were not statistically significantly different, suggesting that the inclusion of Ad-M CS element into the Ad-M TR vaccination does not result in the enhanced protection, despite the fact that both Ad-M CS and Ad-M TR individually confer a statistically significant level of protective efficacy.

To delineate whether antigenic interference is playing a role in an Ad-M CS+TR group, CSP- and TRAP-specific humoral and cellular immune responses were assayed for three time-points, including two (day 14) and eight (day 56) weeks post-Ad prime, and two weeks (day 70) post-MVA boost. Measured PbCSP-specific whole IgG serum titres (Figure 19A(i)) showed a statistically significantly lower level of humoral responses in the vaccine combination group when compared to Ad-M CS alone immunization for day 14 ($p<0.001$ by unpaired t-test) and day 70 ($p<0.05$ by unpaired t-test) time-points corresponding to post-prime and post-boost responses, respectively. PbCSP-specific IFN-γ secreting lymphocyte responses as measure by *ex-vivo* IFN-γ enzyme-linked immunosorbent spot (ELISPOT) assay in the Ad-M CS+TR combination group correlated with the anti-CS Ab titres and, when compared to Ad-M CS group, were lower

for all three time points (Figure 19A(ii)). However, the statistically significant difference was recorded only for day 14 ($p<0.01$ by unpaired t-test) ELISPOT responses ($p=0.06$ for day 70).

The kinetic analysis of anti-PbTRAP humoral immune responses as measure by end-point ELISA in the Ad-M CS+TR combination group revealed that statistically significantly lower ($p<0.01$ by unpaired t-test) whole IgG titres, when compared to Ad-M TR group, were observed only for day 14 post-prime time-point (Figure 19B(i)). The comparable ELISPOT responses were recorded for both Ad-M CS+TR and Ad-M TR groups for all three time-points tested (Figure 19B(ii)).

All this data taken together demonstrated that Ad-M CS and Ad-M TR vaccines administered individually elicit substantial level of protective efficacy in C57BL/6 mice against malaria spz challenge. Unfortunately, the combination of PbCSP and PbTRAP antigens in the heterologous ChAd63-prime, MVA-boost regimen administered in the separate thigh muscles did not provide superior protection when compared to Ad-M TR alone vaccination. It is possible that, antigenic interference phenomenon, in part, could be responsible for the disappointing protection seen with Ad-M CS+TR combination vaccine. The level of both anti-PbCSP cellular and especially humoral immune pre-challenge (day 70) responses were affected when more immunogenic Ad-M TR vaccine was incorporated into the immunization regimen. This provides important implications for further CSP and TRAP combination vaccine study and design.

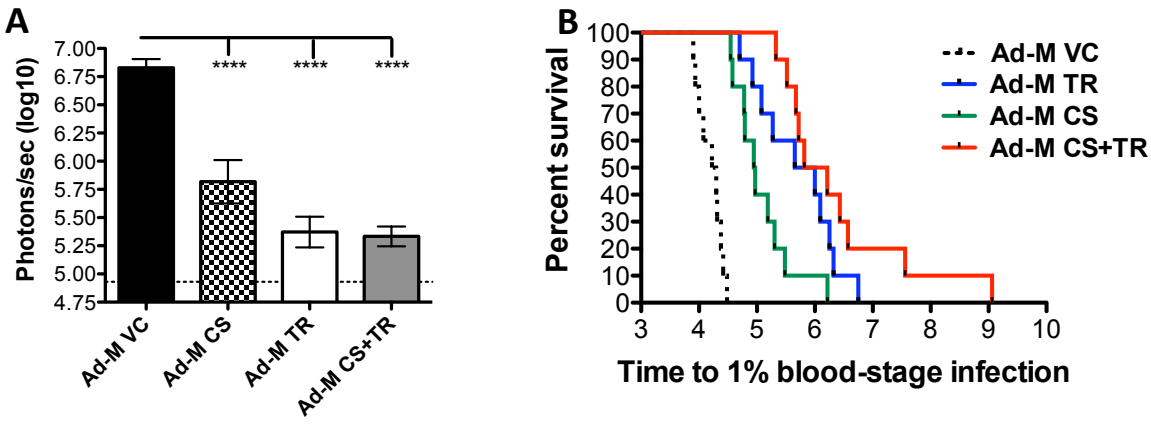


**Figure 18: Protective efficacy of PbCSP and PbTRAP combination vaccine administered in heterologous ChAd63-prime, MVA-boost regimen.**

C57BL/6 strain of mice (n=10/group) was immunized with ChAd63 (Ad) (10^8 iu) and MVA (M) (10^7 pfu) viral vectors administered 8 weeks apart in the heterologous prime-boost (Ad-M) regimen. Recombinant ChAd63 and MVA viral vectors each expressed either PbCSP or PbTRAP transgene. PbCSP or PbTRAP were injected intramuscularly either alone (Ad-M CS and Ad-M TR groups) or administered as a combination into left or right thigh muscle, respectively ((Ad-M CS)+(Ad-M TR) group). Empty ChAd63 and MVA viral vectors containing no transgene were also included as a control for viral vector immunization (Ad-M VC). 2 weeks after the boost, animals were challenged with the IV injection of 2000 *P. berghei* spz expressing GFP/Luc cassette. (A) 44 h post-challenge mice were imaged using IVIS and BLS, corresponding to liver parasite burden, quantified. Means with SEM are shown. ****$p<0.0001$ by one-way ANOVA with Bonferroni's multiple comparison post-test. The dotted line indicates the strength of the background BLS. (B) The same animals were also monitored for blood-stage infection by blood film analysis. Linear regression model predicting Tto1 (in days) was generated and the results were used to obtain Kaplan-Meier survival curves. Percent survival in this and every subsequent Kaplan-Meier survival plot indicates the proportion of animals within specified vaccination group that have not reached the level of 1% blood-stage infection, including animals that remain sterilely protected throughout the study (up to day 15 post-challenge).

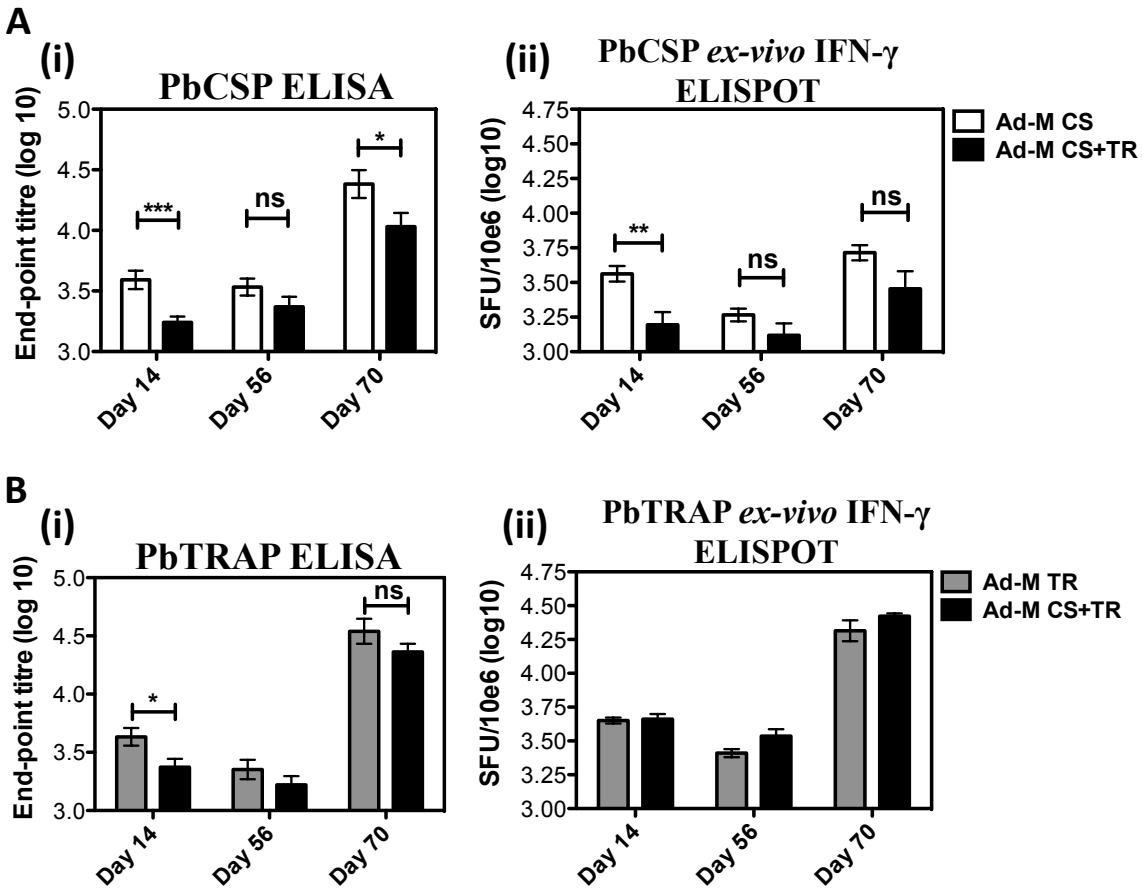


**Figure 19: Kinetic humoral and cellular immune responses.**

C57BL/6 mice (n=6-14/group) were vaccinated with Ad-M regimens expressing different transgenes as outlined above. PbCSP- and PbTRAP-specific humoral and cellular immune responses were assayed 2 (Day 14) and 8 (Day 56) weeks after prime, and 2 weeks (Day 70) after the boost. (A(i)) PbCSP end-point ELISA was employed to measure PbCSP-specific whole IgG ab titres. (ii) To measure IFN-γ secreting lymphocytes whole-blood PBMCs were stimulated with three different sub-pools of peptides collectively constituting the full-length of PbCSP in the *ex vivo* IFN-γ ELISPOT assay. Also, (B(i)) end-point ELISA and (ii) *ex vivo* IFN-γ ELISPOT (three sub-pools of PbTRAP peptides used for stimulation as well) were employed to assess PbTRAP-specific humoral and cellular immune responses, respectively. ***$p<0.001$, **$p<0.01$, *$p<0.05$, ns = not significant by unpaired t-test. Mean with SEM are shown.

### 5.2.2 Mediators of protection following Ad-M CS and Ad-M TR vaccinations

It has been demonstrated that heterologous prime-boost regimen using ChAd63 and MVA viral vectors are capable of inducing potent transgene-specific humoral and cellular immune responses (208, 209, 254). As shown above, immunizations using Ad-M CS and Ad-M TR vaccines also resulted in the induction of high numbers of transgene-specific IFN-γ secreting lymphocytes and high-titre Abs. Each of these factors could play a role in the protection against malaria sporozoite challenge.

To delineate which arm of the immune response is mediating the protection following Ad-M CS or Ad-M TR immunizations, vaccinated animals prior to challenge were depleted of either $CD4^+$ or $CD8^+$ T cells by administering GK1.5 and 2.43 depleting monoclonal antibodies (mAbs), respectively. The mAb treatment showed that neither $CD4^+$ nor $CD8^+$ T cell depletions had any effect on Ad-M CS vaccine-induced protection, as measure by IVIS 44 h post-challenge (Figure 20A(i)). Mice immunized with Ad-M CS vaccine showed a statistically significantly higher level of pre-erythrocytic stage efficacy, despite receiving either $CD4^+$ or $CD8^+$ depleting mAbs, when compared to untreated Ad-M VC vaccination controls ($p<0.05$ by one-way ANOVA with Bonferroni's post-test).

On the other hand, a statistically significant effect was observed when $CD8^+$, but not $CD4^+$ T cells were depleted from animals immunized with Ad-M TR vaccine (Figure 20A(ii)). Mice immunized with Ad-M TR and treated with $CD4^+$ T cell depleting mAb or control rat IgG1 had statistically significantly less BLS ($p<0.05$ and $p<0.001$, respectively) when compared to Ad-M VC group, whereas mice in the same vaccine group that were administered $CD8^+$ T cell depleting 2.43 mAb recorded comparable

levels of luciferase signal to the animals that received only Ad-M VC immunization, indicating that the CD8+ T cell depletion abolished the Ad-M TR vaccine-associated protection.

As expected, mice in the Ad-M CS+TR combination group maintained the vaccine-induced protection when GK1.5 or control rat IgG1 antibodies were administered, but a statistically significant loss of protective efficacy was observed when $CD8^+$ T cell depleting mAb was injected (Figure 20A(iii)). Also, a comparable level of BLS was quantified from animals immunized with only Ad-M VC vaccine versus the animals that were immunized with Ad-M CS+TR combination vaccine and additionally prior to challenge depleted of $CD8^+$ T cells, suggesting that humoral immune responses were contributing very little (if any) to the protection.

All these $CD4^+$ and $CD8^+$ T cell depletion experiments demonstrated that the protection associated with either Ad-M CS or Ad-M TR vaccines is, most likely, dependent on the induction of antigen-specific high-titre Abs or sufficient levels of $CD8^+$ T cells, respectively. The Ab-mediated protection conferred by Ad-M CS alone vaccination in C57BL/6 model is further supported by the fact that there was a very strong correlation between the anti-PbCS whole IgG Ab titres and pre-erythrocytic stage protection ($p=0.0072$ by Spearman's test) (Figure 20B(i)), whereas no relationship was observed ($p=0.813$ by Spearman's test) between the protection and the PbCSP-specific *ex-vivo* IFN-γ ELISPOT responses (Figure 20B(ii)). The protective efficacy in Ad-M CS+TR combination group was abolished with the complete depletion of $CD8^+$ (Figure 20C) and not $CD4^+$ T cells, indicating that anti-PbCSP and anti-PbTRAP Abs were only minimally

involved in protection. The fact that immunity conferred by Ad-M CS vaccine is Ab-dependent, together with the previous demonstration of antigenic interference phenomenon, resulting in the diminished anti-PbCSP specific Ab titres in the Ad-M CS+TR combination group, suggests that a PbCSP-based regime that circumvents the Ad-M TRAP-associated immune inhibition is required. Then the full potential of PbCSP and PbTRAP combination vaccine may be realized.

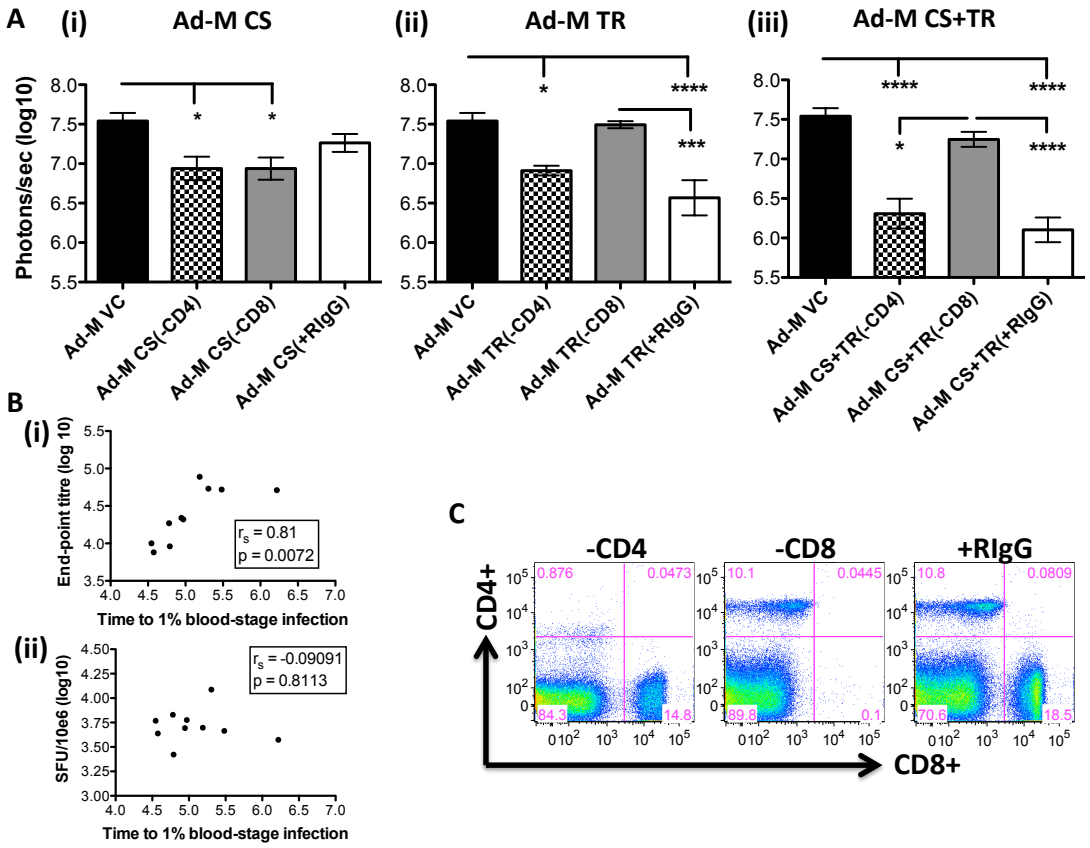


**Figure 20: Depletions of either CD4$^+$ or CD8$^+$ T cells in animals immunized with Ad-M PbCSP or Ad-M PbTRAP vaccines.**

(A) C57BL/6 mice (n=20/group) were immunized either with (i) Ad-M PbCSP or (ii) Ad-M PbTRAP vaccines administered alone or as a (iii) combination. Vector control (n=10) vaccination was also included (Ad-M VC). Two weeks after the boost part of the animals within each different vaccination group were depleted of either CD4$^+$ (n=6/group) or CD8$^+$ (n=6/group) T cells by three 200µg IP injections of rat GK1.5 or 2.43 mAbs, respectively, on days -2, -1, and 0 relative to challenge with 5000 *P. berghei* GFP/Luc spz. The control rat IgG1 (+RIgG) antibodies were used as injection control (n=8/group). 44 h post-challenge BLS emitted from infected animals was quantified. Means with SEM are shown. *p<0.05, ***p<0.001, ****p<0.0001 by one-way ANOVA with Bonferroni's multiple comparison post-test. (B) The strong correlation between Tto1 (x-axis) and (i) anti-PbCSP Ab titres (y-axis) and not (ii) *ex-vivo* IFN-γ ELISPOT responses supports the Ab-mediated protection in Ad-M CS group. (C) Representative FlowJo plots demonstrating the degree of either CD4$^+$ or CD8$^+$ T cell depletions as compared to the vaccinated animals that received control rat IgG1.

### 5.2.3 Extremely high anti-PbCSP Ab requirement for the protection against *P. berghei* challenge in C57BL/6 mice

Numerous papers exist demonstrating the anti-CSP Ab importance in the protection against malaria in both rodent and human models (159) (277) (278) (279). However, protection normally is associated with relatively high anti-CS Ab responses. Kester *et al.* reported that protected vaccinees had a geometric mean titre of 188 µg/ml of anti-CS IgG versus 73 µg/ml measured in the unprotected volunteers following RTS,S vaccination (162).

To delineate the anti-PbCSP Ab titres required to obtain up to 50% sterile protection in C57BL/6 mice against 2000 *P. berghei* spz challenge, the mouse IgG1 mAb 3D11 was employed (159). 3D11 is specific against the central repeat region of PbCSP and has been previously used in *P. berghei* spz neutralization assays both *in vitro* and *in vivo* (159).

Varying concentrations of 3D11 were injected intravenously into naïve C57BL/6 animals prior to challenge. A control mouse IgG1 was also included. The results demonstrated that 200µg dose of 3D11 for total of 3 doses resulted in sterile protection in approximately 40%, whereas the administration in total of up to 750µg of the 3D11 mAb (3 injections of 250µg on 3 consecutive days prior to challenge) was enough to obtain a sterile protection in 60% of the animals (Figure 21A). Also, none of the mice became parasitaemic in the 300, 400, and 800µg of 3D11 dose groups (for the total of 900, 1200, and 2400µgs of 3D11 per animal). The anti-PbCSP whole IgG Ab titres obtained using the serum collected immediately before the challenge from animals that had undergone 3D11 mAb treatment, revealed that on average an end-point PbCSP ELISA titre above 5,

on a log 10 transformed data, may be required in order to have 100% sterile protection. The anti-PbCSP mAb titres in 300µg group, where none of the mice developed blood-stage parasitaemia, ranged from 5.02 to 5.23 ELISA units (EU) (Figure 21B). Consistent with that observation, 3D11 mAb treatment groups whose whole IgG Ab titres were lower than the average of 5 EU, including 250, 200, and 150µg doses, did not have complete sterile protection within that group.

The mice that were sterilely protected against the first *P. berghei* challenge were re-challenged with an identical dose of *P. berghei* spz two months later (Figure 21C). As expected, all of the mice became parasitaemic, indicating that the level of protection conferred by passive immunization using 3D11 mAb waned over time. Moreover, in agreement with previous observations, the 3D11 mAb titres against PbCSP recombinant protein were well below the required average value of 5 EU in all of the groups involved in the re-challenge study (Figure 21D).

The results obtained by passive transfer vaccinations using 3D11 mAb specific against the central repeat region of PbCSP, suggested that anti-PbCSP Ab-mediated sterile protection in C57BL/6 model was possible, but required relatively high titres of Abs. The average end-point ELISA unit of 5 against the recombinant PbCSP protein was indicative of a complete sterile protection. However, the immunity associated with 3D11 mAb vaccinations, as expected, was short-lived. The direct comparison of end-point PbCSP ELISA Ab titres between the Ad-M CS and 300µg of 3D11 vaccination groups (average 4.4 EU versus 5.1 EU, respectively) indicates that Ad-M CS regimen is probably just not immunogenic enough for inducing anti-PbCSP Ab titres required for sterile protection.

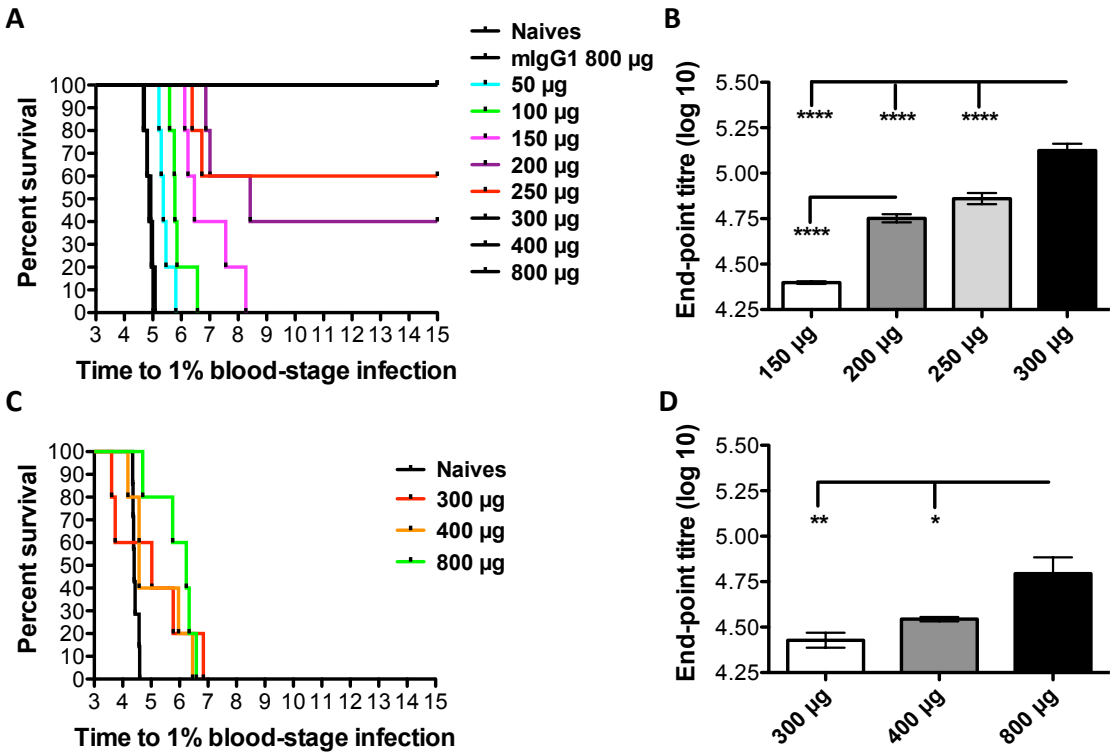


**Figure 21: High concentrations of anti-PbCSP mAb are required to protect against *P. berghei* malaria in C57BL/6 strain of mice.**

Naïve C57BL/6 mice (n=5-6/group) were treated with 3 doses injected IV of anti-PbCSP mouse mAb 3D11 on days -3, -2, and -1 relative to challenge. The animals were then challenged with 2000 *P. berghei* spz and the blood-stage parasitaemia monitored by Giemsa stained blood films. (A) A linear regression modeling was employed to predict Tto1 for all parasitaemic animals and the obtained values used for Kaplan-Meier analysis. The mice that did not develop blood-stage infection by day 9 were also sterilely protected on day 15 post-challenge. (B) Also, 3D11 mAb titres present in the serum immediately before the challenge for some of the groups (indicated on the x-axis) were measured by end-point PbCSP ELISA. Animals that were sterilely protected against the first challenge, two months later were re-challenged with the identical dose of *P. berghei* spz and (C) Kaplan-Meier survival curves were generated using prediction Tto1 values. (D) The 3D11 mAb serum titres immediately before the re-challenge were also measured. The amount of single dose of 3D11 is indicated on the graphs. *p<0.05, **p<0.01, ****p<0.0001 by one-way ANOVA with Bonferroni's multiple comparison post-test. Means with SEM are shown.

### 5.2.4 The synergistic effect of 3D11 and Ad-M TR combination vaccine

As mentioned above, the passive immunization studies using 3D11 allowed delineating the approximate amount of the mAb necessary to protect 100% and, more importantly, 40% of C57BL/6 mice. To investigate the protective potential of the combination of anti-PbCSP mAb and PbTRAP-specific T cells, prior to challenge, Ad-M TR vaccinated animals were administered 3 injections of 180μg of 3D11 mAb, the dose that was sub-optimal for a complete sterile protection. The quantification of BLS 44 h after the challenge with 2000 *P. berghei* GFP/Luc spz revealed that a statistically significantly lower intrahepatic parasite burden was present in the animals vaccinated with the Ad-M TR and 3D11 combination vaccine as compared to the animals that received only Ad-M TR immunization ($p<0.05$ by one-way ANOVA with Bonferroni's post-test) (Figures 22A, B). The protection associated with the most potent immunizations, including Ad-M TR + 3D11 or Ad-M VC + 3D11 combination vaccines were not statistically significantly different between each other as measured by IVIS.

The same animals were also monitored for blood-stage parasitaemia starting on day 5 post-challenge. 100% of the mice (6/6) in the Ad-M + 3D11 and 18% (1/6) in the Ad-M VC + 3D11 combination groups did not develop blood-stage infection ($p=0.015$ between the two by Fisher's exact test) (Figure 2C). Also, consistent with the previous experiments, none of the animals in the Ad-M TR + mIgG1 combination group were sterilely protected against the 2000 *P. berghei* spz challenge.

The fact that 18% of the animals in the Ad-M VC + 3D11 combination group did not become parasitaemic indicated that possibly the administration of even lower amount of

the 3D11 could potentially lead to the synergistic effect in the Ad-M TR + 3D11 group. To investigate this hypothesis, Ad-M TR vaccinated mice were administered decreasing amounts of 3D11 for three consecutive days prior to challenge (Figure 22D). The administration of as low as 3 doses of 120μg of 3D11 was sufficient to maintain the high level of protective efficacy (80% of mice sterilely protected in Ad-M TR + 3D11 group, versus 0% sterile protection in both Ad-M TR and 3D11 alone groups), suggesting that a range of anti-PbCSP mAb titres is sufficient to sterilely protect mice in the Ad-M TR + 3D11 combination group.

All this data taken together demonstrate the protective potential of Ad-M TR + 3D11 vaccine in C57BL/6 model. Unlike the results obtained using Ad-M CS+TR combination immunizations, the inclusion of 3D11 mAb treatment within Ad-M TR vaccinated mice resulted in a superior immunity. Also, the synergistic effect, possibly, between 3D11 mAbs and PbTRAP-specific cellular immune responses was observed. Moreover, the protective synergy was maintained over a fairly broad range of different 3D11 concentrations. This observation has important implications for the study and design of a putative CSP- and TRAP-based combination vaccine, which targets an outbred human population.

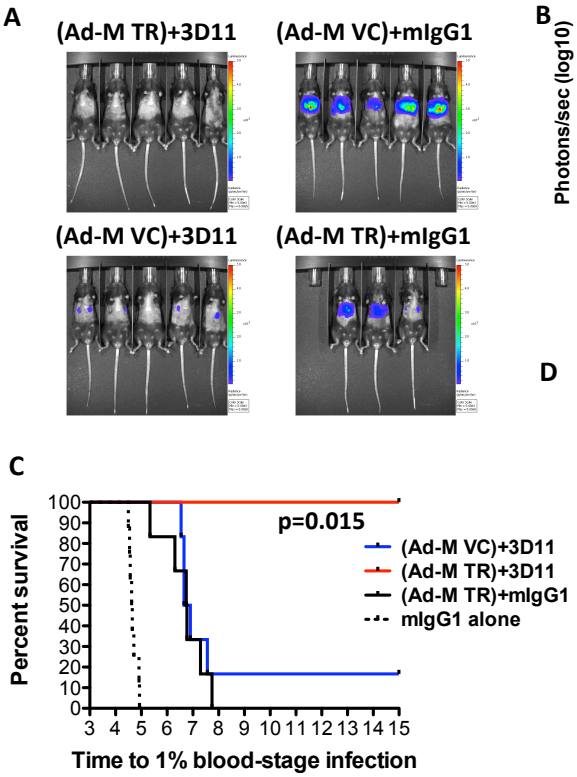


D

| Amount of 3D11 mAb (in µg) per injection | Viral vector vaccination | % Sterile protection (no.infected/ no.challenged) |
|---|---|---|
| 180 | Ad-M PbTRAP | 100 (0/6) |
| | Ad-M VC | 17 (5/6) |
| 150 | Ad-M PbTRAP | 100 (0/5) |
| | Ad-M VC | 20 (4/5) |
| 120 | Ad-M PbTRAP | 80 (1/5) |
| | Ad-M VC | 0 (5/5) |
| 90 | Ad-M PbTRAP | 0 (5/5) |
| | Ad-M VC | 0 (5/5) |
| 60 | Ad-M PbTRAP | 40 (3/5) |
| | Ad-M VC | 0 (5/5) |
| 180 of mIgG1 | Ad-M PbTRAP | 0 (6/6) |
| | Ad-M VC | 0 (6/6) |

**Figure 22: The synergistic effect of 3D11 mAb and Ad-M PbTRAP combination vaccine.**

C57BL/6 strain of mice (n=5-6/group) were vaccinated with heterologous prime-boost regimen employing ChAd63 and MVA viral vectors expressing PbTRAP. Animals vaccinated with empty vector control recombinant viruses were also included (n=6/group). Two weeks after the boost and on days -3, -2, and -1 relative to the challenge with 2000 *P. berghei* GFP/Luc parasites vaccinated animals each day were injected 180µg of 3D11 mAb. 44 h post-challenge pre-erythrocytic stage vaccination efficacy was evaluated using IVIS. (A) The images used for the quantification of BLS, which corresponds to intrahepatic parasite burden (the treatment group indicated above the image) and (B) BLS measurements. The dotted line indicates the background BLS. *p<0.05, ****p<0.0001 by one-way ANOVA with Bonferroni's multiple comparison post-test. Mean with SEM are shown. The same animals were monitored for blood-stage parasitaemia and linear regression model (LR) predicting Tto1 was generated. (C) Kaplan-Meier survival curves using the LR results were generated. The p value was obtained comparing the most protective (Ad-M TR)+3D11 versus the second most protective (Ad-M VC)+3D11 regimens by Fisher's exact test. (D) Animals were immunized with either Ad-M PbTRAP or Ad-M VC vaccines and treated with decreasing amounts of 3D11 mAb (indicated by the first column) in the identical manner as described above.

### 5.2.5 The synergistic effect of Ad-P CS and Ad-M TR combination vaccine

The studies performed using either 3D11 alone or in combination with Ad-M TR immunized animals, provided some insights into the required anti-PbCSP Ab level necessary for sterile protection. To mimic the degree of protective efficacy observed with Ad-M TR + 3D11 regimen, the PbCSP and PbTRAP combination vaccine administered as a clinically relevant regimen first would have to induce higher levels of anti-PbCSP Abs than those seen after Ad-M CS alone vaccination. Also, the immune responses generated by PbCSP-based vaccine, if possible, should be impervious to the antigenic interference exerted by the immunodominant Ad-M TR vaccination.

To attempt addressing all of these requirements, the C57BL/6 mice were immunized as described in table 7. As previously, PbTRAP antigen was administered in the heterologous Ad-M regimen. On the other hand, the heterologous prime-boost regimen using ChAd63 as a prime, and recombinant protein-in-adjuvant as a boost for the administration of PbCSP (Ad-P CS) antigen was chosen. The induction of potent cellular and, most importantly, humoral immune responses have been reported using adeno and recombinant protein in Abisco 100 in an 8-week prime-boost regimen (217). Similarly to the Ad-M CS+TR vaccination, in (Ad-P CS)+(Ad-M TR) combination vaccine each antigen was administered into the separate hamstring muscle (PbCSP left leg, and PbTRAP right leg). The control vaccinations were also incorporated using empty ChAd63 and MVA viral vectors for an Ad-M and AdHu5 encoding ovalbumin (OVA) and recombinant OVA formulated in Abisco 100 for an Ad-P regimens (Ad-P OVA)+(Ad-M VC).

In parallel, another experiment was performed where (Ad-P CS)+(Ad-M TR) combination vaccine at the prime and boost was administered as a mixture in a single injection (Ad-P CS)+(Ad-M TR)(Mix) (Table 8). To accomplish that, a mixture of two ChAd63 viral vectors each encoding PbCSP or PbTRAP was used for priming, and another mixture containing MVA-PbTRAP and PbCSP recombinant protein all formulated in Abisco 100 adjuvant was employed at the time of boosting. The (Ad-P CS)+(Ad-M TR)(Mix) regimen is more relevant for the clinical development as the vaccinees would be receiving in total of two injections, rather than four (2 at the prime and another 2 at the boost), which would be the case if (Ad-P CS)+(Ad-M TR) combination vaccine was used.

Two weeks after the last vaccination animals were challenged with 2000 *P. berghei* spz expressing GFP/Luc gene. As previously, 44 h post-challenge luciferase signal, corresponding to the parasite liver burden, was quantified using IVIS (Figure 23A). All of the groups that received different pre-erythrocytic stage malaria vaccine formulations, when compared to the control groups, recorded statistically significantly weaker BLS ($p<0.001$ by one-way ANOVA with Bonferroni's post-test), corresponding to pre-erythrocytic stage vaccination efficacy. The strength of luciferase signal observed within the most protective (Ad-P CS)+(Ad-M TR) group was indistinguishable from the background, suggesting that some, or all, of the animals in the group may be sterilely protected. Also, the direct comparison of the BLS emitted by the animals within the two most protective regimens, including (Ad-P CS)+(Ad-M TR) and Ad-P CS indicated that they were not statistically significantly different, despite the fact that the visual

examination of the images showed that most of the animals in Ad-P CS group emitted some level of BLS, whereas no BLS was observed in (Ad-P CS)+(Ad-M TR) group (Figure 23B). The strength of luciferase radiated from Ad-M TR or Ad-M CS alone, or from animals immunized with Ad-M CS+TR combination vaccine was consistent with the previous experiments, where Ad-M CS was the least protective regime, followed by the more protective Ad-M TR and Ad-M CS+TR regimens.

The same animals were followed through to the secondary end-point, which was blood-stage infection. The blood film analysis showed that 0/8 animals in the (Ad-P CS)+(Ad-M TR) combination and 5/8 in Ad-P CS group developed blood-stage parasitaemia (p=0.026 by Fisher's exact test comparing groups against each other) (Figure 23C). As expected, none of the animals were sterilely protected in the other vaccination groups. Moreover, the re-challenge of the initially immune mice two months after the first challenge with the same dose of *P. berghei* spz showed that 50% of the animals (4 out of 8) did not develop blood-stage parasitaemia in (Ad-P CS)+(Ad-M TR) combination vaccine, whereas all of the remaining animals in the Ad-P CS group came down with the potent blood-stage infection.

Slightly more disappointing challenge results were obtained using (Ad-M CS)+(Ad-M TR)(Mix) vaccinations. Only 3 out of 8 animals were sterilely protection in the mixture combination group (p=ns by Fisher's exact test comparing the relevant vaccine group with the naïve mice), whereas all of the animals in the other vaccine groups developed potent blood-stage infections (Figure 23D). Nonetheless, the less stringent, but still adequate statistical analysis of protection based on the Tto1 values, generated using the

linear regression modeling, indicated that a statistically significant difference in protection between the two most protective regimens, including (Ad-M CS)+(Ad-M TR)(Mix) and Ad-P CS was maintained ($p<0.01$ by Kruskal-Wallis with Dunn's multiple comparison post-test), despite the lower overall number of sterilely protected animals, when compared to (Ad-M CS)+(Ad-M TR) combination vaccine.

This set of experiments showed that similar levels of long-lasting sterile protection can be obtained by complementing 3D11 mAb injections with the clinically relevant Ad-P CS regimen in the (Ad-M CS)+(Ad-M TR) combination vaccine. Also, the protective synergistic effect when Ad-P CS and Ad-M TR vaccines were combined was observed, suggesting that the synergy phenomenon, previously seen with the 3D11 mAb administrations, was not limited to the passive transfer vaccinations, and can also be induced within the setting of active immunization. Both, (Ad-M CS)+(Ad-M TR) administered in a separate thigh muscles or (Ad-M CS)+(Ad-M TR)(Mix) injected as a mixture, combination vaccines demonstrate that superior protection is obtained when PbCSP and PbTRAP antigens are combined. However, a lower overall level of sterile protection was seen when (Ad-M CS)+(Ad-M TR) combination vaccine was administered as a mixture. It demonstrated that a careful selection of the vaccine platform as well as the regimen and route associated with the administration of each antigen is important, if the full benefits of the CSP and TRAP combination vaccine are to be reaped.

| Group | Antigen | Priming agent | Boosting agent | Protection (1st challenge) | | Protection (2nd challenge) |
|---|---|---|---|---|---|---|
| | | | | % Sterile (no.infected/ no.challenged) | Days to 1% parasitaemia (median) | % Sterile (no.infected/ no.challenged) |
| **Naïve** | GFP | ChAd63 (1e10^8 iu IM) | MVA (1e10^7 pfu IM) | **0 (8/8)** | 5.85 | **N/A** |
| **(Ad-P OVA) + (Ad-M VC)** | Ovalbumin | AdHu5 (1e10^8 iu IM) | 15 µg of OVA + Abisco 100 | **0 (8/8)** | 4.64 | **N/A** |
| | GFP | ChAd63 (1e10^8 iu IM) | MVA (1e10^7 pfu IM) | | | |
| **Ad-M TR** | *Pb*TRAP | ChAd63 (1e10^8 iu IM) | MVA (1e10^7 pfu IM) | **0 (8/8)** | 6.76 | **N/A** |
| **Ad-M CS** | *Pb*CSP | ChAd63 (1e10^8 iu IM) | MVA (1e10^7 pfu IM) | **0 (8/8)** | 5.58 | **N/A** |
| **Ad-P CS** | *Pb*CSP | ChAd63 (1e10^8 iu IM) | 15 µg of *Pb*CSP + Abisco 100 | **38 (5/8)** | 6.26 | **0 (3/3)** |
| **Ad-M CS+TR** | *Pb*CSP (l.l.) | ChAd63 (1e10^8 iu IM) | MVA (1e10^7 pfu IM) | **0 (8/8)** | 6.44 | **N/A** |
| | *Pb*TRAP (r.l.) | ChAd63 (1e10^8 iu IM) | MVA (1e10^7 pfu IM) | | | |
| **(Ad-P CS) + (Ad-M TR)** | *Pb*CSP (l.l.) | ChAd63 (1e10^8 iu IM) | 15 µg of *Pb*CSP + Abisco 100 | **100 (0/8)*** | N/A | **50 (4/8)** |
| | *Pb*TRAP (r.l.) | ChAd63 (1e10^8 iu IM) | MVA (1e10^7 pfu IM) | | | |

**Table 7: Ad-M TR and Ad-P vaccination groups (Experiment 1).**

The table outlining different vaccination groups in C57BL/6 strain of mice. The name of the immunization regime, the transgene employed and the modality used for priming and boosting 8 weeks apart are shown. Also, the protection against 2000 *P. berghei* spz challenge is indicated for each group. The first challenge was performed two weeks after the last vaccination (indicated by the column representing 1st challenge). The animals that were sterilely protected during the initial challenge, were re-challenged 2 months later (2nd challenge). Both, no. of animals that did not develop blood stage infection (% sterile) and Tto1 for the parasitaemic animals, vaccine efficacy readouts are included. *$p<0.05$ by Fisher's exact test comparing the most protective (Ad-P CS)+(Ad-M TR) versus the second best Ad-P CS groups. l.l. and r.l. indicate left and right thigh muscles, respectively. Iu and pfu are the measures for the viral vector titres and stands for infectious units and plaque forming units, respectively. IM is the abbreviation for the vaccines' administration route and stands for intramuscular.

| Group | Antigen | Priming agent | Boosting agent | Protection | |
|---|---|---|---|---|---|
| | | | | % Sterile (no.infected/ no.challenged) | Days to 1% parasitaemia (median) |
| **Naïve** | GFP | ChAd63 (1e10^8 iu IM) | MVA (1e10^7 pfu IM) | **0 (0/6)** | 3.8 |
| **Ad-M TR** | *Pb*TRAP | ChAd63 (1e10^8 iu IM) | MVA (1e10^7 pfu IM) | **0 (0/8)** | 4.46 |
| **Ad-M TR (Ab100)** | *Pb*TRAP | ChAd63 (1e10^8 iu IM) | MVA (1e10^7 pfu IM) + Abisco 100 | **0 (0/8)** | 5.29 |
| **Ad-P CS** | *Pb*CSP | ChAd63 (1e10^8 iu IM) | 15 µg of *Pb*CSP + Abisco 100 | **0 (0/6)** | 5.94 |
| **(Ad-P CS)+(Ad-M TR)(Mix)** | *Pb*CSP + *Pb*TRAP (Mix) | ChAd63 (1e10^8 iu IM) | 15 µg of *Pb*CSP + Abisco 100 | **38 (5/8)$^{ns}$** | 6.14$^{**}$ |
| | | ChAd63 (1e10^8 iu IM) | MVA (1e10^7 pfu IM) | | |

**Table 8: Ad-M TR and Ad-P CS vaccination groups (Experiment 2).**

The table outlining different vaccination groups in C57BL/6 strain of mice in the second experiment is presented. The name of the immunization regime, the transgene employed and the modality used for priming and boosting 8 weeks apart are showed. Also, the protection against 2000 *P. berghei* spz challenge is indicated for each group. The challenge was performed two weeks after the last vaccination. Two vaccine efficacy readouts, including no. of animals that did not develop blood stage infection (% sterile) and Tto1 for the parasitaemic animals are shown. ns = not significant by Fisher's exact test comparing the most protective (Ad-P CS)+(Ad-M TR)(Mix) versus the Naïve groups. **p<0.01 by Kruskal-Wallis test with Dunn's multiple comparison post-test comparing (Ad-P CS)+(Ad-M TR)(Mix) and Ad-M TR groups. For the explanation of other abbreviations, please, refer to table 8.

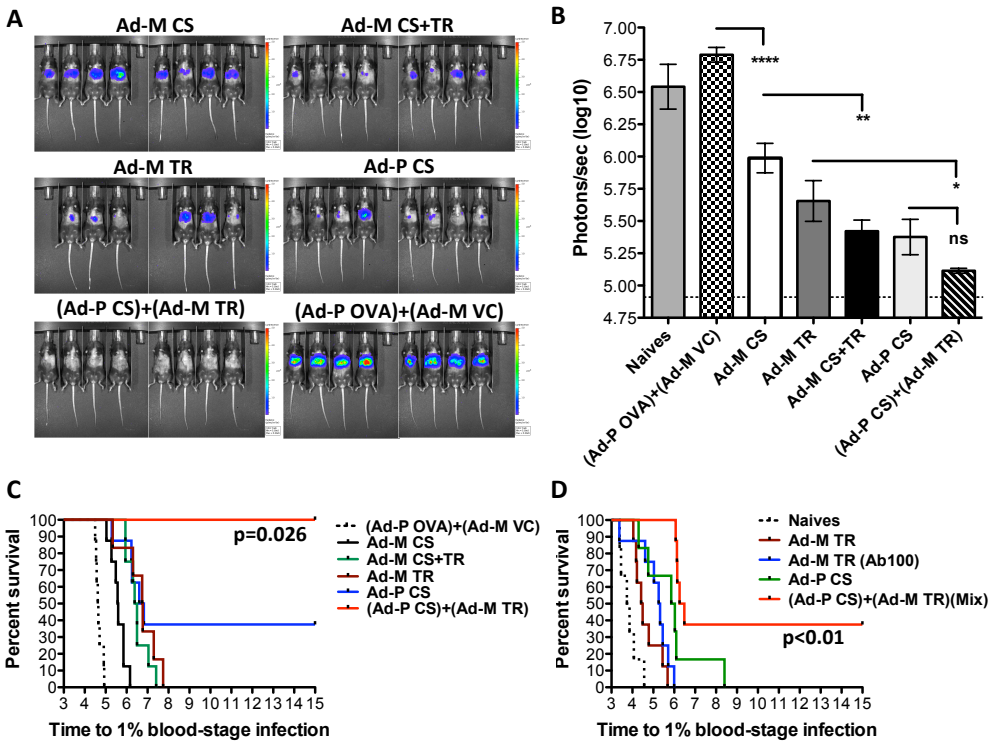


**Figure 23: The synergistic effect of PbCSP and PbTRAP combination vaccine administered as heterologous prime-boost regimen employing viral vector and protein modalities.**

C57BL/6 strain of mice (n=6-8/group) were vaccinated with different regimens as outlined in table 1. Two weeks after the last vaccination mice were challenged with an IV injection of 2000 *P. berghei* spz expressing GFP/Luc gene. 44 h post-challenge vaccines' pre-erythrocytic stage efficacy was measured using IVIS. (A) The visual evaluation of acquired images generated by IVIS imaging system (vaccination regime indicated above the image) and (B) the quantification of BLS emitted by the infected animals and corresponding to parasite burden revealed a statistically significantly less luciferase signal in the vaccinated animals. The dotted line indicates the strength of the background BLS. Means with SEM are shown. *p<0.05, **p<0.01, ****p<0.0001 by one-way ANOVA with Bonferroni's multiple comparison post-test. The same animals were also monitored for blood-stage parasitaemia and Tto1 calculated using linear regression modeling. (C) Kaplan-Meier survival curves representing the obtained prediction values were generated. The p value was acquired by comparing the most protective versus the second most protective regimes by Fisher's exact test. The second experiment, as outlined in the table, 2 was performed. (D) Kaplan-Meier survival curves were generated using Tto1 values. The indicated p value was obtained by Kruskal-Wallis test with Dunn's multiple comparison post-test comparing (Ad-P CS)+(Ad-M TR)(Mix) and Ad-M TR groups.

### 5.2.6 Pre-challenge cellular and humoral immune responses in different PbCSP and/or PbTRAP antigen-based vaccine formulations

The level of cellular and humoral immune responses in C57BL/6 mice vaccinated with different regimens as outlined in tables 1 and 2 was measured using intracellular cytokine staining (ICS) and end-point ELISA techniques. The ICS analysis indicated that in the Ad-M TR group high percentage of PbTRAP-specific $CD8^+$ T cells had the effector cytokine IFN-γ (median % response in Ad-M TR group was 30) upon re-stimulation of whole-blood PBMCs with a single pool of peptides constituting the full length of PbTRAP (Figure 24A). Also, comparable levels of IFN-γ positive $CD8^+$ T cells were observed in all of the other PbTRAP antigen-based vaccine groups ($p<0.0001$ by one-way ANOVA with Bonferroni's post-test when comparing the relevant group against the (Ad-P OVA)+(Ad-M VC)). Interestingly, the direct comparison of (Ad-P CS)+(Ad-M TR) versus the (Ad-P CS)+(Ad-M TR)(Mix) combination groups indicated that there was a statistically significant difference in the percentage of $CD8^+IFN\text{-}\gamma^+$ T cells between the two ($p=0.0042$ by unpaired t-test), with the mixture group showing a lower response.

The percentages of PbCSP-specific $CD8^+IFN\text{-}\gamma^+$ T cells were very hierarchical and depended on the vaccination regimen. The highest percentage of $CD8^+IFN\text{-}\gamma^+$ lymphocytes was observed within the Ad-M CS group (median response approximately 4%) followed by Ad-P CS, and the different PbCSP and PbTRAP combination regimens (Figure 24A). Consistent with the *ex-vivo* IFN-γ ELISPOT results, there was a statistically significant difference in the percentage of $CD8^+IFN\text{-}\gamma^+$ T cells between Ad-M CS and Ad-M CS+TR ($p<0.05$ by one-way ANOVA with Bonferroni's post-test). Also, a

statistically significant reduction was observed when the percentage of $CD8^{+}IFN\text{-}\gamma^{+}$ T cells in the Ad-P CS group was compared to the responses seen in the (Ad-P CS)+(Ad-M TR)(Mix) combination group ($p<0.01$ by one-way ANOVA with Bonferroni's post-test).

Relatively low proportions of PbCSP- and PbTRAP-specific $CD4^{+}IFN\text{-}\gamma^{+}$ T cells were quantified for all of the groups (Figure 24B). There was no statistically significant difference between any of the vaccination groups when compared to the control animals against each of PbCSP or PbTRAP peptide pools, suggesting that vaccines were fairly un-immunogenic for the $CD4^{+}$ T cell subpopulation.

As expected, the assessment of anti-PbTRAP whole IgG Ab titres using end-point ELISA revealed that comparable level of humoral responses was quantified in all of the PbTRAP antigen containing groups (Figure 24C). On the other hand, the anti-PbCSP Ab titres differed substantially between the groups that employed MVA-PbCSP (M-PbCSP) versus recombinant PbCSP protein formulated in Abisco 100 (rP-PbCSP) at the time of boost. Close to a log improvement was seen in the anti-PbCSP whole IgG Ab titres in the groups that received Ad-P CS vaccination administered either alone or in combination with the Ad-M TR (Figure 24D). Also, unlike the observations made when viral vectors only were employed to deliver PbCSP antigen and statistically significantly lower anti-PbCSP Ab titres were recorded in the Ad-M CS+TR combination versus the Ad-M CS alone group, no antigenic interference in the anti-PbCSP Ab responses was observed in the (Ad-P CS)+(Ad-M TR) group as measured by ELISA. An almost identical Ab titre was quantified for both Ad-P CS and (Ad-P CS)+(Ad-M TR) vaccine groups. However, statistically significantly lower anti-PbCSP Ab titres were observed in (Ad-P CS)+(Ad-M

TR)(Mix) versus (Ad-P CS)+(Ad-M TR) combination groups, suggesting that mixing Ad-P CS and Ad-M TR vaccines results in the diminished anti-PbCSP Ab titres.

The assessment of pre-challenge (day 70) cellular and humoral immune responses revealed that statistically significantly higher percentages of PbTRAP-specific $CD8^+IFN\text{-}\gamma^+$ T cells were quantified in all of the vaccination when compared to the control (Ad-P OVA)+(Ad-M VC) groups. Also, a clear hierarchy in the proportion of PbCSP-specific $CD8^+IFN\text{-}\gamma^+$ T cells was observed. Regarding the humoral arm of the immune system, comparable anti-PbTRAP Ab titres were measured in all of the PbTRAP antigen containing vaccine groups, whereas a statistically significant improvement in the anti-PbCSP Ab titres was recorded when the PbCSP antigen was injected as a part of the Ad-P CS regimen. Moreover, the whole IgG Ab titres against PbCSP in the Ad-P CS group were the same as in the more protective (Ad-P CS)+(Ad-M TR) combination group, suggesting that Ad-P CS and Ad-M TR regimens can be combined without negative consequences in the form of antigenic interference. However, the statistically significant reduction in the proportion of PbTRAP-specific $CD8^+IFN\text{-}\gamma^+$ T cells and the anti-PbCSP Ab titres in the (Ad-P CS)+(Ad-M TR)(Mix) combination group highlighted the importance of the separate-site administration.

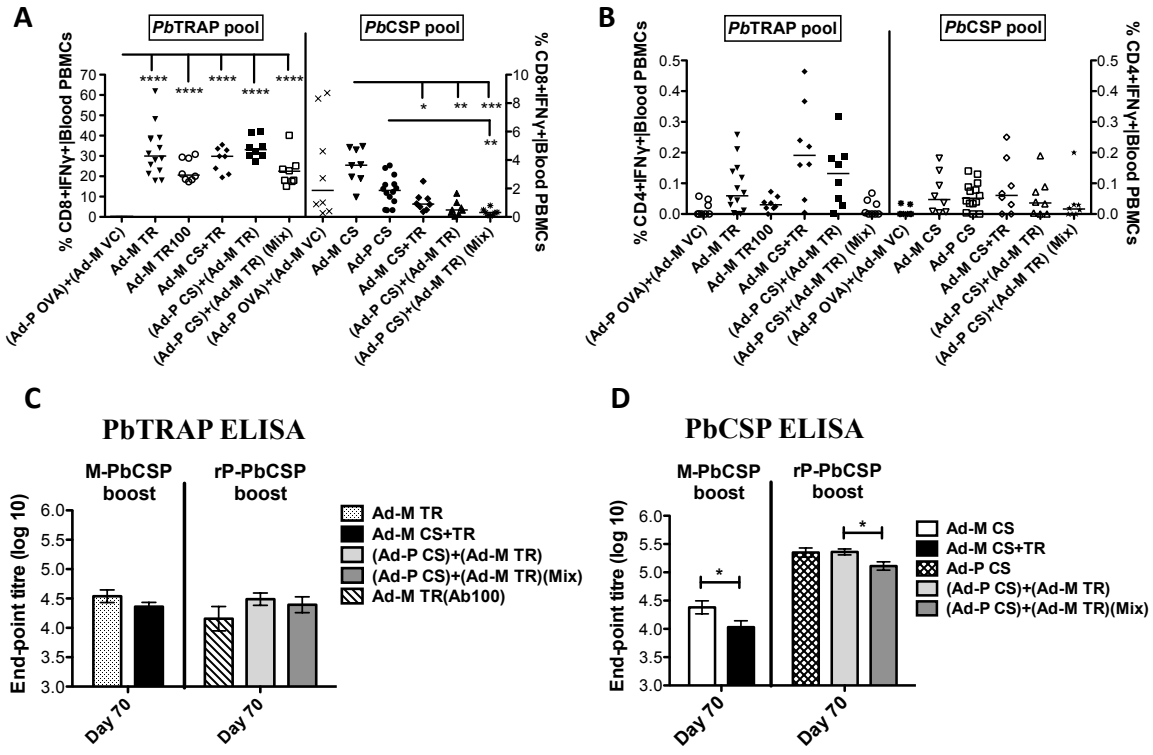


**Figure 24: The post-boost ICS and humoral responses.**

C57BL/6 mice (n=6-14/group) were vaccinated with different regimens as outlined in tables 1 and 2. Two weeks after the last immunization whole-blood PBMCs were stimulated with a single peptide pool representing full length of either PbCSP or PbTRAP antigen. Percentages of (A) $CD8^+IFN\text{-}\gamma^+$ and (B) $CD4^+IFN\text{-}\gamma^+$ T cells were quantified using BD LSRII flow-cytometry instrument and FlowJo analysis software. The PbTRAP-specific responses for either $CD8^+$ or $CD4^+$ T cells were plotted on the right y-axis, whereas left y-axis was used to plot PbCSP responses. *p<0.05, **p<0.01, ***p<0.001, ****p<0.001 by one-way ANOVA with Bonferroni's multiple comparison post-test. Median with individual data points are shown. Also, (C) PbTRAP- and (D) PbCSP-specific whole IgG serum Ab titres were measured two weeks after the boost by end-point ELISA. *p<0.05 by unpaired t-test. Means with SEM are shown. M=MVA, and rP=recombinant protein.

### 5.2.7 Depletion of Natural killer, but not Kupffer cells abolishes the protection in Ad-M TR + 3D11 combination vaccine

As mentioned above, anti-PbCSP Abs and PbTRAP-specific $CD8^+$ T cells are important contributors to the 100% sterile protection induced by Ad-M TR + 3D11 or (Ad-P CS)+(Ad-M TR) combination vaccines. Additionally, the direct PbTRAP-specific T cell-mediated killing of *P. berghei* intrahepatic stages has been demonstrated *in vitro* (Longley *et al.* in preparation). However, the exact mechanism whereby cytotoxic $CD8^+$ T cells (CTLs) targeting TRAP or any other liver-stage antigen are able to protect against malaria is unknown. One of the hypothetical mechanisms proposes that CTLs can act through the secretion of IFN-γ, which in turn stimulates the production of inducible nitric oxide synthase (iNOS) within the infected hepatocyte that leads to the induction of NO and subsequent destruction of infected cell by apoptosis (150). Also, some evidence suggests that CTL effector functions seem to be dependent on mice strain and vaccination regimen (150).

Even less is known about the effector functions of spz-specific Abs in the pre-erythrocytic stage defense against malaria. It has been suggested that opsonizing CSP-specific Abs from RTS,S-immunized subjects demonstrated significantly higher endocytic activity in the protected subjects (285). Moreover, Seguin *et al.* showed that *in vitro* liver-resident macrophages, called Kupffer cells, did not readily internalize *P. berghei* spz, unless the parasites were first coated with sporozoite-specific Abs (286). Phagocytosis by Kupffer cells or other macrophages of opsonized malaria spz is the process that heavily relies on the Fc region of spz-specific Abs.

To investigate whether the anti-PbCSP Ab-mediated effector functions in the highly protective Ad-M TR + 3D11 vaccination regimen are Fc-dependent, a spz neutralization assay (SNA) was employed. *In vivo* fragmented IgG is cleared at a much faster rate than intact IgG (287). Therefore, prior to challenge, *P. berghei* spz were incubated *in vitro* with equal concentrations of either intact or the Fab regions of 3D11 mAb. After a 30-min incubation at room temperature 5000 spz opsonized with a different amount of either whole or Fab fragments of 3D11 were injected into Ad-M TR vaccinated animals. The results demonstrated that comparable level of sterile protection was obtained regardless of the status of 3D11, indicating that the 3D11 mAb-mediated effector functions were independent of the Fc region (Figure 25A).

The results obtained using 3D11 Fab fragments suggested that Fc region did not perform any significant effector functions necessary for the protection in Ad-M TR + 3D11 regimen. However, the 3D11 mAb fragmentation experiments did not answer whether liver-resident phagocytic cells, such as Kupffer cells capable of internalizing pathogens independently of FcR, or even liver-homing natural killer (NK) cells were involved in the synergistic effect observed with Ad-M TR + 3D11 vaccination. Moreover, the importance of Kupffer (288, 289) (290) and/or NK (291) cells in the malaria liver-stage development has been documented.

To investigate the contribution of liver-resident Kupffer and NK cells to the pre-erythrocytic stage protection against *P. berghei* malaria elicited by Ad-M TR + 3D11 regimen, these cells were removed from mice by the IV administration of either clodronate formulated liposomes or anti-Asialo GM1 rabbit polyclonal Abs, respectively.

The use of anti-Asialo GM1 polyclonal was chosen over anti-NK1.1 mAb, because unlike depletion with anti-NK1.1, this procedure removes NK cells without affecting CD1d-restricted NKT cells. Also, for performing macrophage and NK cell depletions, the Ad-M TR + 3D11 regimen was selected over the more clinically relevant (Ad-P CS)+(Ad-M TR), because the protection induced by the latter was far above the threshold needed for the sterile protection, as 50% of the animals in that group remained immune even 2 months after the first challenge. On the other hand, the dose of 120μg of 3D11 administered 3 times to the Ad-M TR vaccinated mice prior to challenge resulted in 80% sterile protection indicating that this specific regime is minimally above the threshold necessary for either complete or partial sterile protection (Figure 22D). For the scope of this thesis, it would have been impractical (and perhaps impossible) to optimize the (Ad-P CS)+(Ad-M TR) regimen in the same way.

The results obtained after depleting macrophages, and more importantly, Kupffer cells showed that the administration of clodronate liposomes had no effect on the protection induced by Ad-M TR + 3D11 vaccination (Figure 25B), suggesting that these phagocytic cells are playing a minimal role in the protective efficacy of Ad-M TR + 3D11 vaccine. However, the depletion of NK cells resulted in only 33%, as compared to 83% level of sterile protection observed in Ad-M TR + 3D11 combination group that received rabbit IgG as a control ($p=0.015$ by Fisher's exact test). Interestingly, the level of sterile protection in the Ad-M TR + 3D11 (-NK) group was identical to the Ad-M VC + 3D11 vaccination.

The results obtained using 3D11 Fab fragments and the macrophage and NK cell depletions indicated that mechanistically anti-PbCSP Abs, most likely, neutralize a large portion of the sporozoites by the mechanism that is independent of functional Fc, or phagocytic cells, such as macrophages or Kupffer cells. The small amount of sporozoites, however, that do manage to escape the initial anti-PbCSP Ab attack and are successful in establishing an intrahepatic infection are then destroyed by the collective effort of $CD8^{+}IFN\text{-}\gamma^{+}$ T and NK cells, and possibly other factors. Therefore, the Ad-M TR vaccination alone should be able to confer a sterile protection against a much smaller dose of sporozoite challenge.

To test this hypothesis, C57BL/6 mice, as previously, were vaccinated with the Ad-M TR regimen. Two weeks after the last vaccination mice were challenged with 200 *P. berghei* sporozoites administered IV. The blood-film analysis demonstrated that 33% of the animals in the Ad-M TR vaccination group were sterilely protected whereas all of the mice developed blood-stage parasitaemia in the Ad-M VC group ($p=0.013$ by Mann-Whitney comparing Ad-M TR versus Ad-M VC), suggesting that Ad-M TR vaccination alone is capable of inducing sterile protection against a relatively low dose of sporozoite challenge (Figure 25C).

All these mechanistic experiments suggested that the protection afforded by the dual 3D11 and Ad-M TR vaccination was independent of the Fc-mediated effector functions or the presence of Kupffer cells. On the other hand, the removal of NK cells significantly diminished the level of sterile protection obtained by Ad-M TR + 3D11 combination vaccine. Moreover, the protective efficacy that remained after NK cell depletion was

comparable to that observed in the Ad-M VC + 3D11 group, suggesting that, perhaps, NK cell cytolytic action is more associated with cellular rather than humoral factors of protection induced by Ad-M TR + 3D11 vaccination.

A

| µg/ml | Ad-M *Pb*TRAP | |
|---|---|---|
| | 3D11 | 3D11 Fab |
| 12 | 0% (4/4) | 0% (4/4) |
| 48 | 25% (3/4) | 50% (2/4) |
| 192 | 50% (2/4) | 100% (0/4) |
| | mIgG1 | mIgG1 Fab |
| 192 | 0% (4/4) | 0% (4/4) |

B

| Vaccination | Depletion treatment | % Protection (no.protected/ no.challenged) |
|---|---|---|
| Ad-M *Pb*TRAP + 3D11 | PBS | 100% (6/6)* |
| | -Kf | 100% (6/6)* |
| | Control Kf | 50% (3/6)ns |
| | -NK | 33% (2/6)ns |
| | control NK | 83% (5/6)* |
| Ad-M VC + 3D11 | PBS | 33% (2/6)ns |
| Ad-M PbTRAP + mIgG1 | PBS | 0% (0/6) |
| Naives | -Kf | 0% (0/6) |
| Naives | -NK | 0% (0/6) |
| Naives | PBS | 0% (0/6) |

C

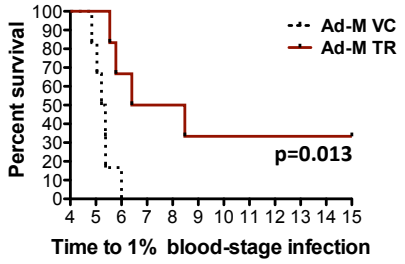


**Figure 25: Immunological mechanisms of 3D11 and Ad-M PbTRAP combination vaccine.**

C57BL/6 strain of mice (n=6/group) were vaccinated with heterologous prime-boost regimen employing ChAd63 and MVA viral vectors expressing PbTRAP. Animals vaccinated with empty vector control recombinant viruses were also included (n=6/group). (A) The influence of the Fc region of 3D11 in the protection was investigated by employing sporozoite neutralization assay (SNA). 50.000 *P. berghei* spz were incubated with either intact or the Fab fragments of 3D11 at the designated concentrations (indicated in the first column). 5000 of either 3D11 or 3D11 Fab opsonized spz were subsequently injected IV into Ad-M PbTRAP vaccinated animals. Percent (%) of sterilely protected animals is shown. (B) Two weeks after the boost and on days -3, -2, and -1 relative to challenge with 2000 *P. berghei* spz vaccinated animals each day were injected 120µg of 3D11 mAb as indicated in the first column. Control mIgG1 was also administered in the identical manner. Additionally, either NK (-NK) or Kupffer (-Kf) cells in the vaccinated animals were depleted, by multiple IV injections of either anti-Asialo GM1 or clodronate liposomes, respectively, prior to challenge. The NK and Kf cell depletion controls were also included. The sterile protection readout was used to quantify the effect of different treatments on the vaccine-induced protection. *$p<0.05$, ns=not significant by Fisher's exact test comparing the indicated group to (Ad-M PbTRAP)+mIgG1 group. (C) C57BL/6 mice were immunized with Ad-M PbTRAP or Ad-M VC vaccines (n=6/group). Two weeks after the boost animals in both groups were challenged with 200 *P. berghei* spz. Kaplan-Meier survival curves were generated on Tto1 readout. The p value was obtained by comparing treatment groups against each other by Mann-Whitney test.

### 5.2.8 The increased activation of NK and $CD8^+$ T cells in the ChAd63-PbTRAP vaccinated animals as a response to *P. berghei* spz challenge

To further investigate the NK cell role in the protection against malaria, C57BL/6 mice were immunized with the single injection of ChAd63-PbTRAP vaccine. Two weeks later vaccinated animals were challenged with 2000 *P. berghei* spz. 24 h post-challenge mice livers were extracted and lymphocytes purified. The ICS analysis of $CD8^+CD3^+$, $NK1.1^+CD3^-$, and $CD1d^+CD3^+$ lymphocyte populations, corresponding to $CD8^+$ T cells, NK, and invariant NK T cells, respectively, was performed (Figure 26A).

As expected, a statistically significantly higher total number of $CD8^+$ T cells were quantified per liver in the animals that received the ChAd63-PbTRAP vaccination (Ad) as compared to the total $CD8^+$ T cell numbers within the naïve (N) livers (Figure 26B top panel). Also, statistically significantly higher ($p<0.05$ by two-way ANOVA) percentages and the total number (Figure 26B middle and bottom panels, respectively) of $CD8^+IFN\text{-}\gamma^+$ T cells per liver were observed in Ad vaccinated and challenged versus vaccinated unchallenged animals, suggesting that the sporozoite challenge did stimulate $CD8^+$ T cells.

Unlike with the $CD8^+$ T cell population, the total numbers of iNKT cells were not different between Ad and N mice (Figure 26C top). Also, no difference was observed in the percentages or total number of $iNKT^+IFN\text{-}\gamma^+$ cells between Ad versus N or challenged versus un-challenged treatment groups (Figure 26C middle and bottom, respectively), indicating that minimal (if any) activation of iNKT cells took place following ChAd63-PbTRAP vaccination as a result of spz challenge.

Similarly, comparable number of NK cells was observed regardless of the vaccination or challenge (Figure 26D top). However, a statistically significantly higher percentage and the total number of $NK^+IFN\text{-}\gamma^+$ cells per liver was seen in the Ad vaccinated and challenged as compared to vaccinated and unchallenged animals ($p<0.05$ by two-way ANOVA) (Figure 26D middle & bottom, respectively). Furthermore, there was a very strong correlation between the $NK^+IFN\text{-}\gamma^+$ and $CD8^+IFN\text{-}\gamma^+$ T cell responses ($p=0.017$) only in the Ad vaccinated and challenged group (Figure 26E).

The examination of $CD69^+$ activation marker revealed that a statistically significantly higher percentage and total number of $NK^+CD69^+$ cells per liver in the Ad vaccinated versus N animals ($p<0.05$ by two-way ANOVA) was measured, suggesting that it is possible that ChAd63-PbTRAP vaccination activates liver-resident NK cells (Figure 26F top and bottom panels, respectively).

The ICS analysis of lymphocytes obtained from livers of Ad vaccinated or N mice that had also either undergone spz or mock challenges indicated that significantly higher number of $CD8^+$ T cells were quantified within the livers of vaccinated animals and that significantly higher number of these $CD8^+$ T cells were activated as compared to N mice. Furthermore, the spz challenge induced higher percentages and overall total number of $CD8^+IFN\text{-}\gamma^+$ T cells and $NK^+IFN\text{-}\gamma^+$ cell per liver in the ChAd63-PbTRAP vaccinated mice. Moreover, the proportions of these lymphocytes correlated strongly with each other only in the vaccinated and challenged mice.

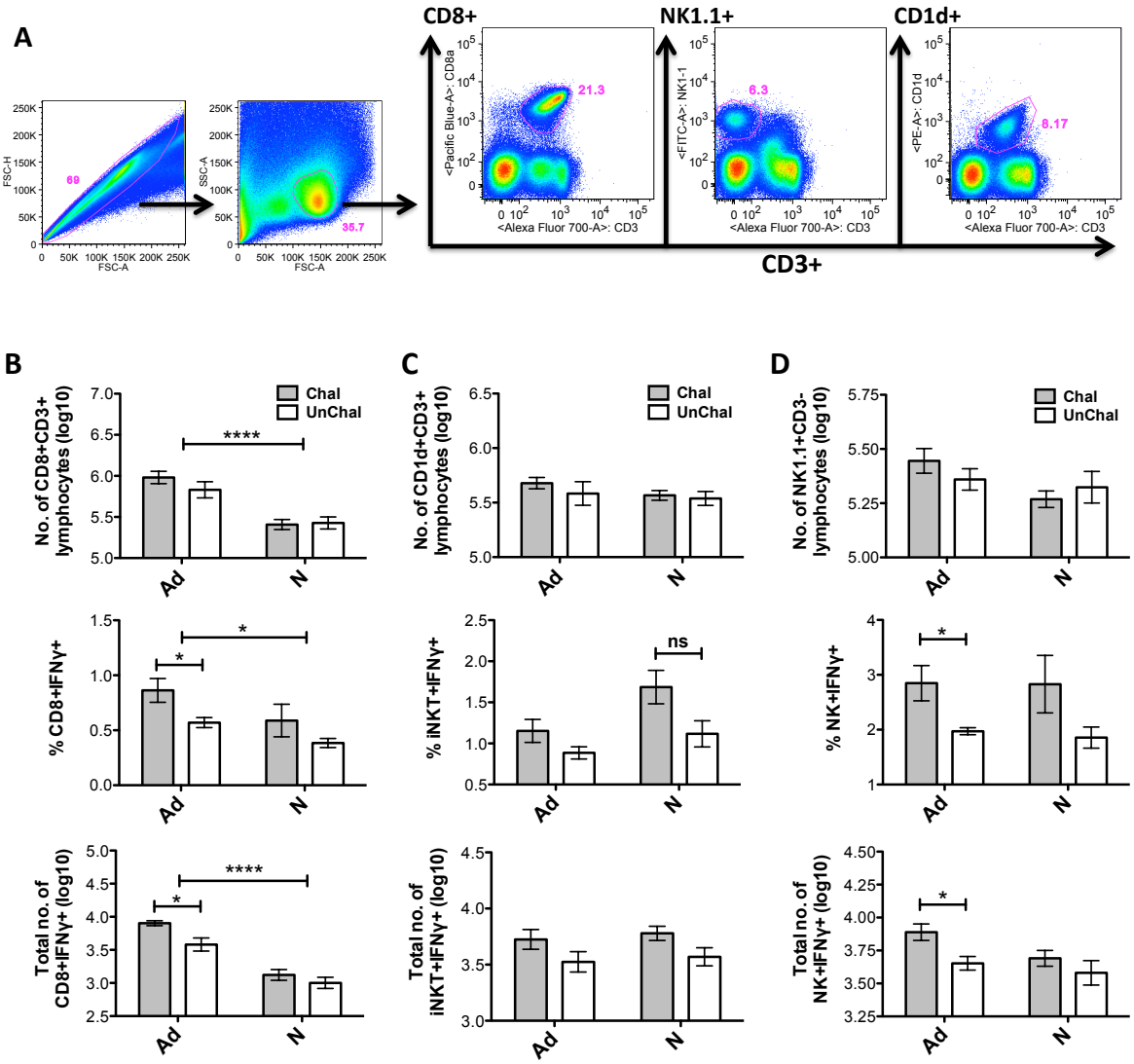
A
CD8+
NK1.1+
CD1d+
CD3+
FSC-H
FSC-A
SSC-A
<Pacific Blue-A>: CD8a
<FITC-A>: NK1-1
<PE-A>: CD1d
<Alexa Fluor 700-A>: CD3
69
35.7
21.3
6.3
8.17
B
C
D
Chal
UnChal
No. of CD8+CD3+ lymphocytes (log10)
No. of CD1d+CD3+ lymphocytes (log10)
No. of NK1.1+CD3- lymphocytes (log10)
% CD8+IFNγ+
% iNKT+IFNγ+
% NK+IFNγ+
Total no. of CD8+IFNγ+ (log10)
Total no. of iNKT+IFNγ+ (log10)
Total no. of NK+IFNγ+ (log10)
Ad
N
****
*
ns

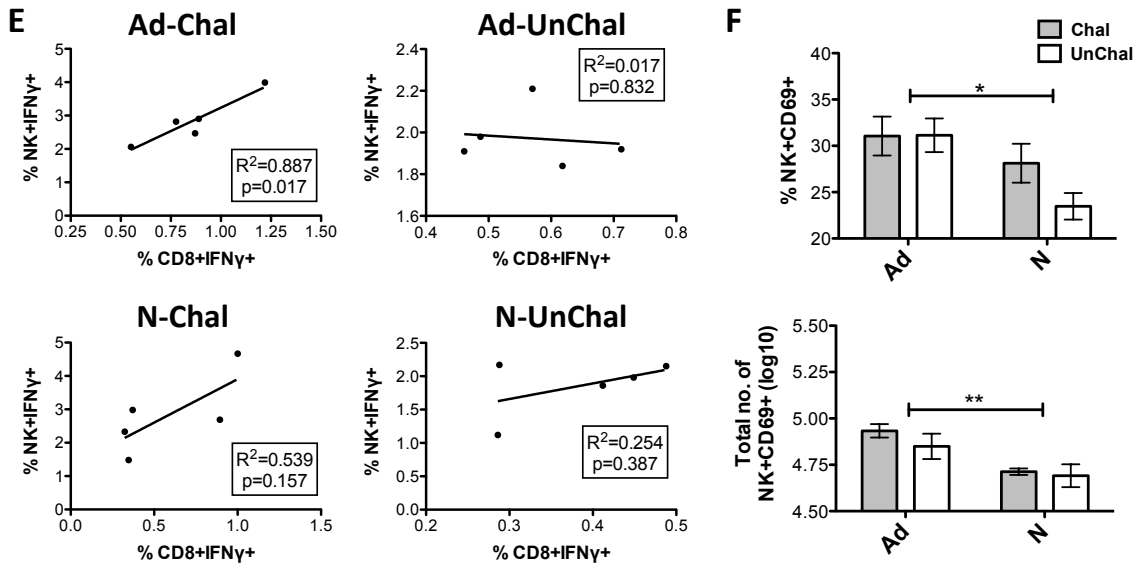


**Figure 26: The ICS analysis of liver-resident lymphocytes.**

C57BL/6 mice (n=5/group) were immunized with a single ChAd63-PbTRAP vaccine (Ad) and two weeks later challenged with 3000 *P. berghei* spz. 24 h post challenge livers from vaccinated challenged (Ad-Chal) and un-challenged (Ad-UnChal) animals were extracted, lymphocytes purified and quantified. Livers from naïve challenged (N-Chal) and un-challenged (N-UnChal) animals were also included. ICS was performed and samples acquired using BD LSRII flow-cytometry instrument. (A) FlowJo plots showing the gating strategy for $CD8^+$ T cell (CD8+CD3+), NK (NK1.1+CD3-), and invariant NK T (CD1d-tet+CD3+) cell subsets. Total number per mouse liver of (B) $CD8^+$ T, (C) iNKT, and (D) NK cells was quantified (top panel) as well as percent (middle panel) and total number (bottom panel) of IFN-γ positive cells within each subset for all treatment groups were measured. (E) A strong correlation between the proportions of $CD8^+$IFN-$\gamma^+$ and $NK^+$IFN-$\gamma^+$ cells for Ad-UnChal group, and not the other groups was obtained. (F) The percentage of $NK^+CD69^+$ (top panel) and the total number of $NK^+CD69^+$ (bottom panel) cell for each treatment group per liver are shown. ****p<0.0001, **p<0.01, *p<0.05, ns=not significant by two-way ANOVA. Means with SEM are shown.

## 5.3 Discussion

In this chapter, initially, the effect of combining PbCSP and PbTRAP expressed individually in the recombinant viruses ChAd63 and MVA was investigated and the mechanisms that were associated with protection analyzed. The Ad-M prime-boost regimen was chosen for its ability to induce potent humoral and cellular immune responses simultaneously (254) (208, 209).

The depletion of either $CD4^+$ or $CD8^+$ T cells in C57BL/6 mice indicated that protection elicited by the PbCSP Ag relied on Abs while PbTRAP protected through the action of $CD8^+$ T cells. Furthermore, the administration of small amount of anti-CS monoclonal antibodies substantially enhanced the sub-optimal protection conferred by PbTRAP. These results provided some insights into the required optimization of PbCSP and PbTRAP combination vaccine to enhance protection by maximizing the induction of anti-CS antibodies and anti-TRAP $CD8^+$ T cell responses. Therefore, a bifurcated way to maximize both, anti-CS antibodies by Ad-P prime-boost vaccination and anti-TRAP T cell responses using Ad-M was explored.

Combination of Ad-P PbCSP and Ad-M PbTRAP vaccination strategies induced optimal humoral and cellular immune responses that elicited sterile protection in C57BL/6 rodent model, which is highly susceptible to *P. berghei* infection (273). The superior pre-erythrocytic stage protection associated with the concurrent induction of humoral and cellular immune responses in BALB/c model has been documented previously (264). The vaccination approaches there relied on antibody and $CD8^+$ T cell responses targeting

single CSP antigen. However, similar strategy based on anti-CS responses proved disappointing in human clinical trials. A phase I/IIa clinical trial of MVA-CSP prime with RTS,S/AS02A boost did not improve immunogenicity or protective efficacy beyond that achieved by RTS,S alone (284). More recently, the use of adenovirus vectored-CSP prime and RTS,S boost resulted in the significantly enhanced $CD4^+$ T cell immunogenicity when compared to those vaccines alone, but did not increase anti-CS antibodies above those seen with RTS, S alone (216).

The Ad-P regimen for the administration of PbCSP was chosen for a couple of reasons. It has been shown that heterologous adenovirus prime and protein boost induces superior Ab responses than those that are obtained if each of these vaccination strategies are employed individually (214) (215). Furthermore, these Abs are dominated by IgG2a, which mainly function through Fc receptors and are involved in Ab-dependent cellular inhibition as well as phagocytosis (215) (217). Also, the significantly differential immunogenicity of adjuvants usually seen in the recombinant protein-based vaccinations can be overcome by priming the Ab responses with an adenovirus vector that encodes the same antigen, suggesting that through the use of Ad-P regimen comparable humoral responses can be stimulated irrespective of the adjuvant used (217).

Interestingly, administration of Ad-P CS and Ad-M TR combination vaccine as a mixture elicited lower level of sterile protection compared to the individual elements of the same combination vaccine administered into the separate sites. One of the plausible explanations for decreased protection observed within (Ad-M CS)+(Ad-M TR)(Mix) and especially within Ad-P CS alone groups in the second experiment could be the fact that

the challenge inoculum was more infectious (in experiment 1 Naïve group's median Tto1 was 5.85 days as compared to median of 3.8 days Tto1 obtained for Naïves in experiment 2). Another possible explanation could be that PbTRAP-specific $CD8^+$ T cells and anti-PbCSP Ab responses in the mixture group were lower when compared to the separate site immunizations, suggesting that mixture vaccination strategy is more susceptible to antigenic interference.

The passive immunization experiments using anti-PbCSP mAb 3D11 indicated that whole IgG ELISA titres on average above 5 EU against PbCSP protein were indicative of complete sterile protection. Surprisingly, the majority of the mice were not sterilely protected following Ad-P CS immunization despite higher than 5 EU anti-PbCSP Ab titres. The discrepancy possibly has occurred because only protective anti-repeat region responses were measured in the case of 3D11 passive transfer immunization, whereas the active immunization using the full-length PbCSP could in theory induce Ab responses against all three regions of PbCSP, including amino and carboxy terminal domains, and the central repeat region. It has been suggested that because of an unusual conformation the N-terminal domain shields the C-terminus of PbCS protein from protective Ab attack as the sporozoites journey from mosquito salivary glands to the vertebrate liver (76). Therefore, the induction of anti-carboxy terminal antibodies functionally would have little effect for sporozoite neutralization *in vivo*, however, they most likely would be measured in an end-point ELISA assay *in vitro*.

The anti-CSP Ab levels induced by RTS,S vaccine varies quite substantially from individual to individual (292). The high degree of biological variability in the anti-CSP

Ab responses following immunization with RTS,S suggests that single antigen vaccine modality may not be able to protect most of heterogeneous population of people, as low responders are likely to succumb to infection (162). Thus, the presence of another protective antigen can work as a buffer and provide the protection to those individuals whose Ab responses were inadequate. The protective effect of anti-PbCSP 3D11 and Ad-M TR combination vaccine was maintained over a broad range of different amounts of 3D11. It demonstrated that despite relatively low levels of anti-CSP Abs, it is still possible that the protection associated with Ad-M TR component would be able to cope with the intrahepatic infection leading to the sterile protection.

The analyses of the effector functions of antibodies indicated that the efficacy of Ad-M TR + 3D11, and most likely (Ad-P CS)+(Ad-M TR), vaccines relied on a two-stage attack against the parasite, whereby anti-CS antibodies diminish the number of sporozoites reaching the liver, thus reducing the number of infected hepatocytes that are eliminated by the collective effort of PbTRAP-specific $CD8^+$ T cells and NK cells. The anti-CSP Ab-mediated sporozoite neutralization in theory can be accomplished by a few mechanisms, including complement-dependent lysis, receptor-mediated phagocytosis and/or perhaps inhibition of sporozoite binding to the liver (293). Touray *et al*. demonstrated that *in vitro* 93-95% of *P. gallinaceum* sporozoites were lysed in the presence of anti-sporozoite Abs and mammalian serum, as compared to only 11-15% lysis observed using non-immune serum in the identical assay (294). Also, the serum samples from RTS,S-immunized volunteers contained opsonizing abs and these antibodies significantly enhanced *in vitro* endocytic activity of the FcR (+) THP-1 human

monocyte line in protected volunteers compared to those susceptible to sporozoite infection (285). The complement fixation and endocytosis of opsonized sporozoites, in part, relies on the functional Fc region of the Ab. However, the investigation of whether the Fc-region is playing a role in the protection elicited by Ad-M TR + 3D11 vaccination, did not lead to the demonstration of any of the aforementioned Ab-effector mechanisms. In fact, the Fc-independent neutralization of *P. berghei* spz was in agreement with previous observation whereby comparable level of neutralization was achieved upon opsonization of *P. berghei* spz with either intact or Fab fragments of 3D11 (159). However, it remains unclear whether Fc-independent phagocytosis was occurring and, if so, what was its contribution to the protection inducing by Ad-M TR + 3D11 combination vaccine.

The decreased level of protection obtained after the removal of NK cells is consistent with the studies performed by Doolan *et al.*, where the protective immunity in irradiated *P. yoelii* spz or plasmid DNA vaccinated mice was mediated by effector $CD8^+$ T cells and NK cells and depended on IL-12, IFN-γ, and NO (295). Moreover, in the follow up study the same authors established that perforin, granzyme B, and Fas L (Fas ligand) were not required for the protection induced by irradiated *P. yoelii* spz (150). In the proposed mechanism the authors stipulated that the protective response is initiated by antigen specific $CD8^+$ T cells that upon the recognition of specific peptide-MHC complexes secrete IFN-γ, which, in turn, induces IL-12 secretion from innate immune cells, such as macrophages, dendritic cells, or monocytes. The IL-12 subsequently stimulates the NK cells, which then may directly kill infected hepatocytes or induce anti-

parasitic activity through the secretion of IFN-γ. Although, the contribution of IL-12 to the protection elicited by Ad-M TR + 3D11 combination vaccine was not assessed, the fact that depletion of NK cells significantly abrogated the protection, in part supports the above signaling cascade model. It remains unclear whether the NK cell involvement in the protection is by direct killing of infected hepatocytes or via the bystander effect, where NK cell-secreted IFN-γ mediates the effector functions. However, the results obtained using anti-Asialo GM1 depleting polyclonal Abs should be interpreted cautiously, as the specificity of these abs have been questioned (296) (297), and these antibodies may also reduce $CD8^+$ T cell numbers, leading to diminished efficacy.

Natural killer T (NKT) cells are a relatively recently described subset of innate immune cells that express markers of both T cells and NK cells. In naïve mice they constitute up to 30% of liver lymphocytes and bridge the innate and adaptive immune responses. A significant amount of NK T cells recognize antigens present in the context of CD1d molecule, a nonpolymorphic protein expressed on dendritic, B, and T cells, macrophages and hepatocytes. Schofield *et al.* made the first demonstration of NK T cell contribution to the pre-erythrocytic stage protection against malaria by showing that CD1d-deficient mice immunized twice with *P. berghei* spz had significantly lower anti-CSP humoral responses when compared to the wild-type mice that had undergone the same vaccination (298). A conflicting study performed by Romero *et al.* indicated that following *P. berghei* spz immunizations no difference in the level of humoral responses or protection was observed between CD1d-deficient and wild-type mice, indicating that NK T cells have a dispensable role in the anti-malarial pre-erythrocytic stage protection (299). Consistent

with the Romero *et al*. observations, the ICS analysis of lymphocytes extracted from ChAd63-PbTRAP vaccinated mice that have also undergone spz challenge showed that neither IFN-$\gamma^+$ nor $CD69^+$ markers were up-regulated in liver-resident NK T cells when compared to vaccinated unchallenged or even naïve challenged or unchallenged animals. Taken together, these data indicate that NK T cells may not have a clear immunological role in the protection against malaria induced by ChAd63-PbTRAP vaccine in C57BL/6 model. Interestingly, the administration of CD1d-restricted alpha-GalCer ligand, 2 days before the challenge induced significant level of sterile protection that is mediated by IFN-γ secreted from NK T cells and is independent of Fas-ligand, TNF-a, or perforin (300), nevertheless demonstrating the anti-plasmodia potential of NK T cells.

The quantification of total lymphocyte numbers purified from vaccinated and naive mice livers confirmed that vaccination with adenovirus viral vectors deploys T cells to the liver (301). Significantly higher number of $CD8^+$ T cells was measured in the livers of mice that were immunized with ChAd63-PbTRAP as compared to naïve animals. Also, the enhanced activation of $CD8^+$ T cells as a response to the challenge was consistent with the fact that potent cellular immune responses were measured 2 weeks after the ChAd63-PbTRAP prime by *ex-vivo* IFN-γ ELISPOT. Interestingly, a strong correlation between $CD8^+$IFN-$\gamma^+$ and $NK^+$IFN-$\gamma^+$ lymphocyte subsets was also observed. Further studies are needed to assess whether this correlation in Ad-PbTRAP vaccinated mice was mediated by another variable, or there is truly a direct causative relationship between the two. However, a few publications point at the NK-specific IFN-γ responses being tightly

associated with the T cell responses at the pre-erythrocytic (302) as well as blood stages (303) of infection.

Also, it remains to be determined whether the protection seen with Ad-M TR + 3D11 or (Ad-P CS)+(Ad-M TR) combination vaccines in C57BL/6 mice would also extend to other mice strains. The studies performed using C57BL/6 model merely underline the importance and protective potential of the concurrent induction of potent PbTRAP-specific $CD8^+$ T cells and anti-PbCSP Abs. It is likely that in other strains of mice the same antigens are less immunogenic, and thus the vaccination efficacy would be much reduced. However, the sub-optimal protection associated with the two currently leading pre-erythrocytic stage malaria vaccine candidates including PfCSP-based RTS,S and an Ad/MVA prime-boost regimen administered ME.TRAP relies on the induction of high-titre Abs and $CD8^+$ T cells, respectively . Therefore, the use of PbCSP and PbTRAP in C57BL/6 model closely simulates the situation observed with human clinical trials, providing a useful tool for the evaluation of future vaccine formulations based on the CS and TRAP antigens.

Furthermore, it may not be feasible to deploy a vaccine based on three different viral vectors and a recombinant protein, as this could be too expensive for malaria afflicted countries (see chapter 7 for further comments of how it would be possible to make CS and TRAP combination vaccine cheaper than the one used in these experiments). Nonetheless, the studies in this chapter provide an invaluable insight into the potential that lies within the CS and TRAP combination vaccine.

# Chapter 6

# *Plasmodium vivax* vaccines

# 6 *Plasmodium vivax* vaccines

## 6.1 *P. vivax* TRAP vaccine

### 6.1.1 Introduction

Vaccines against two of the most prevalent causative agents of human malaria, *Plasmodium falciparum* and *Plasmodium vivax* remain elusive despite great efforts towards their development. *P. vivax* is the most geographically widespread human parasite and it is considered to be the most prevalent form in some regions of Latin America, Central and South-East Asia, accounting for 132-391 million clinical infections every year and an estimated 2.6 billion people being at risk of *P. vivax* infection (5, 304). Therefore, a highly effective vaccine against this protozoan parasite would have a major global impact on disease burden (305).

Development of a vaccine against *P. vivax* has been difficult due to, amongst others, the lack of a robust and long-term *in vitro* red-blood cell (RBC) culture, thus complicating the conduct of clinical trials and increasing the costs of studies assessing the vaccine's efficacy in humans. In addition, the current difficulty in culturing the parasites has impaired the development of a widely available primate challenge model, albeit significant progress has been recently achieved in the development of infrastructure to reliably challenge *Aotus* monkeys and humans (306-308). Nevertheless, such studies are still limited to endemic regions where the parasites can be collected from infected patients. In a recent elegant approach, the rodent malaria model *P. berghei* has been used to generate transgenic (tg) parasites expressing the ookinete protein P25 to assess a *P.*

*vivax* transmission-blocking vaccine candidate (243), opening the possibility for similar approaches aimed at assessing *P. vivax* antigens (Ags) from other stages, such as the pre-erythrocytic CSP and TRAP.

An effective *P. vivax* pre-erythrocytic vaccine should ideally induce high antibody (Ab) titres to target sporozoites (spz) and high frequencies of T cells capable of eliminating infected hepatocytes to arrest the parasite's cycle during its development in the parasitophorous vacuole or to target the hypnozoites, which is the dormant form of *P. vivax* liver development. Modified Vaccinia Ankara (MVA) and the chimpanzee adenovirus 63 (ChAd63) have been used as recombinant vectored vaccines to induce strong and protective antibody and T cell responses against the encoded *P. falciparum* TRAP (PfTRAP) both in pre-clinical studies and clinical trials (165, 199, 309, 310).

In this study, heterologous prime-boost vaccinations utilizing these clinically relevant recombinant ChAd63 and MVA (Ad-M) viral vectors expressing the *P. vivax* TRAP transgene were assessed in various mouse strains. Furthermore, the vaccine efficacy was measured using a novel 'marker-free' tg *P. berghei* parasite expressing *P. vivax* TRAP (PvTRAP) generated by allelic replacement.

### 6.1.2 Results

#### 6.1.2.1 Generation of maker-free *P. berghei* expressing *P. vivax* TRAP

One of the major obstacles in using rodents to develop human malaria vaccines is the fact that neither *P. falciparum* nor *P. vivax* parasites are capable of infecting mice. Therefore, malaria vaccine candidates often have to be evaluated using mouse malaria homologs at the initial pre-clinical stage although they do not necessarily predict the outcome with the human malaria parasite. To overcome these problems tg *P. berghei* parasites were generated by substituting the endogenous PbTRAP gene with the TRAP homolog from the *P. vivax* parasite (PvTRAP). A pJAZZ vector containing *P. berghei* gDNA encoding the TRAP loci was merged with a Geneart-synthesized *P. vivax* TRAP fragment by recombineering techniques as described in materials and methods section 2.4.1. The resulting pJAZZ clone containing the PvTRAP gene flanked by 2.9kb and 0.5kb of UTR PbTRAP at 5' and 3' ends, respectively, was then digested at NotI sites and the resulting integration cassette was subsequently electroporated into schizont stage *P. berghei* wild-type (wt) parasites using long UTR sequences as homology arms for double cross-over integration (Figure 27A(i)). The parasites were then cloned by limited dilution techniques to yield a homogeneous population composed only of mutants with the integrated cassette. This novel cloning scheme permitted the excision of a bicistronic positive-negative selection marker downstream of the PvTRAP gene. The administration of 5-FC prodrug recycled the *hDHFR-yFCU* cassette leaving the 3'UTR downstream of PvTRAP unaltered (Figure 27A(ii)&(iii)). Integration of PvTRAP and excision of the selection marker were both confirmed by diagnostic PCR (Figure 27B). Removal of the selection

marker was an essential part of the cloning scheme as it has been demonstrated previously that the selection marker downstream of a pre-erythrocytic stage gene may negatively affect the parasite's ability to infect vertebrate hosts (236).

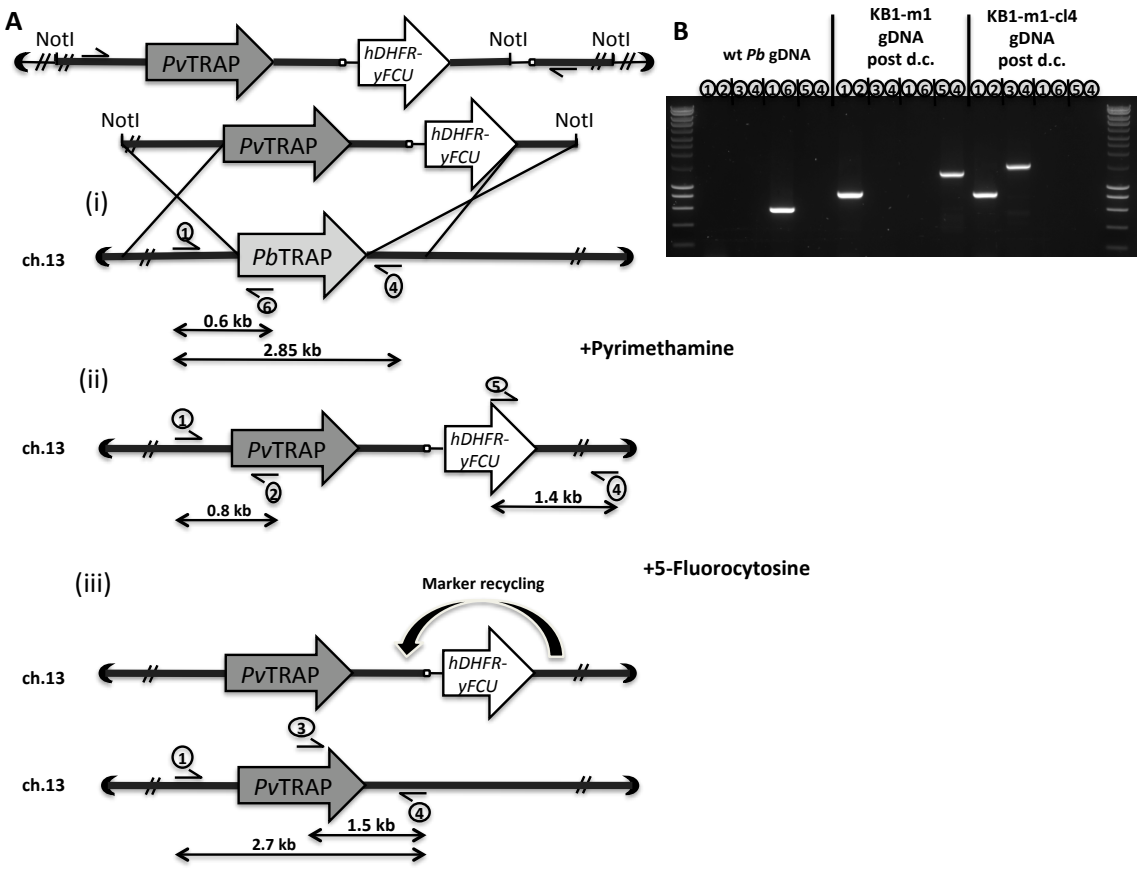


**Figure 27: Generation of marker-free tg *P. berghei* parasites expressing *P. vivax* TRAP.**

(A) Cloning scheme demonstrating the steps involved in the construction of tg *P. berghei* mutant: (i) modified pJAZZ vector allowing propagation of AT-rich fragments of genomic *P. berghei* DNA containing PvTRAP gene and the relevant selection marker (*hDHFR-yFCU*) was digested at the NotI sites before being electroporated into wt *P. berghei* schizonts. (ii) After the selection with pyrimethamine and subsequent cloning of mutants by limited dilution techniques, parasites were subject to another round of drug selection. (iii) The 5-FC prodrug was used to induce the recombination event whereby the bicistronic selection cassette was excised generating a 'marker-free' mutants with an unaltered 3'UTR PbTRAP. (B) Genotyping image confirming the integration of PvTRAP cassette (KB1-m1) and the excision of selection marker (KB1-m1-cl4) as compared to wt genome (WT Pb). The PCR analysis was performed on gDNA isolated from blood-stage parasite clones after dilutional cloning using indicated primers (the sequence of primers used in the study is listed in table 4).

### 6.1.2.2 Assessment of the tg parasite's biological fitness

An allelic substitution of the endogenous *P. berghei* TRAP with the homologous gene from other malaria species could affect the parasite's ability to develop within the mosquito and the vertebrate hosts (232). Therefore, we assessed the tg parasite's fitness by direct feeds of mosquitoes on mice infected with either tg or wt *P. berghei* parasites. Similar numbers of oocysts per mosquito were found indicating a comparable sexual development of tg and wt parasites (Figure 28A). A subsequent analysis of mosquito salivary glands showed a reduction in tg sporozoite numbers when compared to wt parasites. However, the difference was not statistically significant ($p=0.2$ by Student's t-test), indicating that salivary gland infection is comparable between tg and wt parasites (Figure 28A).

To delineate whether exogenous PvTRAP is localized within the same anatomical regions of the *P. berghei* spz, an immunofluorescence assay (IFA) was performed on spz from salivary glands as outlined in materials and methods section 2.6.4. Polyclonal Abs against both PbTRAP and PvTRAP were raised in mice and used for the staining. A control 3D11 mAb against the repeat-region of PbCSP was also included. IFA results confirmed expression of PvTRAP and indicated a localization on the same regions on the surface of spz as in the wt parasite (Figure 28B).

Next, the vertebrate liver stage infection was assessed by intravenous administration of either 1000 tg or wt spz into C57BL/6 mice. Mice in both groups developed blood-stage parasitaemia indicating that both tg and wt parasites are capable of establishing an exoerythrocytic stage and fully developing to infect red-blood cells. Furthermore, linear

regression analysis based on the percentage of blood-stage infection over three consecutive days revealed a slight delay to 1% blood-stage infection (Tto1) with tg parasites when compared to wt infection (Figures 28C, D). However, this difference was not statistically significant ($p=0.15$ by Student's t-test). Taken together, these data show that the allelic substitution of PbTRAP with a codon-optimized PvTRAP gene did not diminish the parasite's ability to develop within *A. stephensi* mosquitoes or the vertebrate host, thus offering a robust model for PvTRAP based human vaccine assessment in rodents.

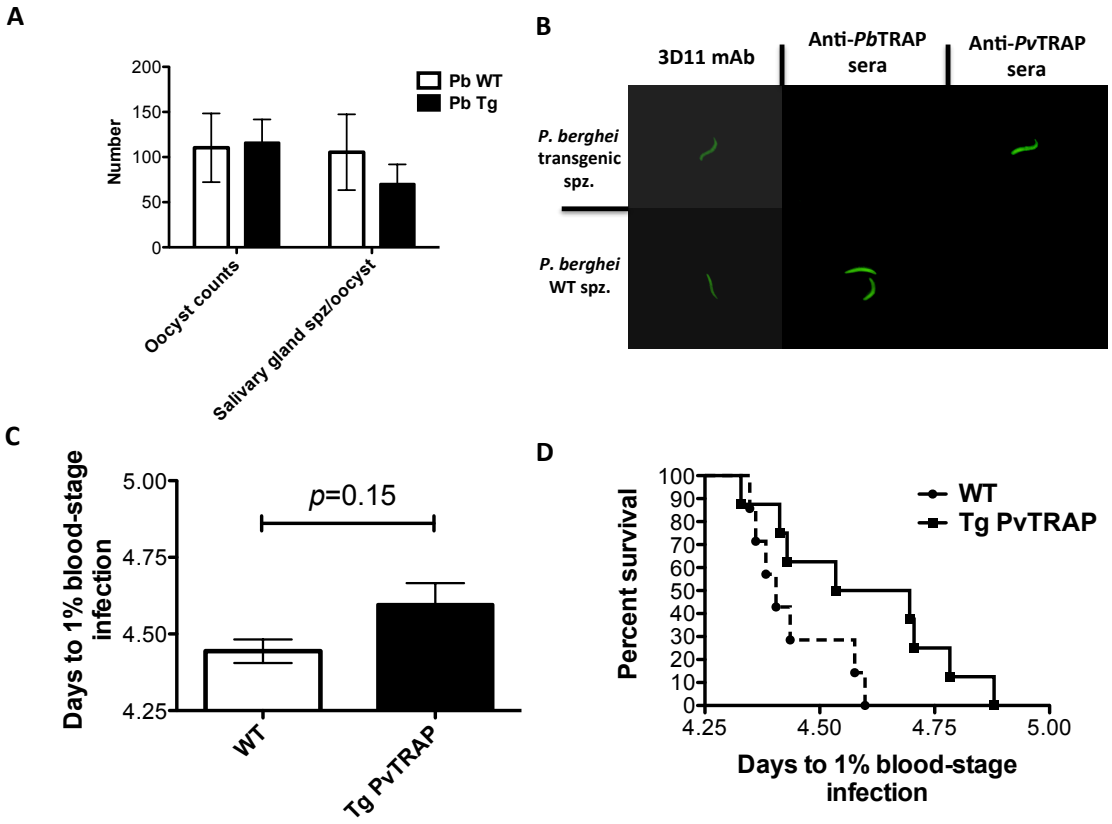


**Figure 28: The assessment of tg parasite's development in *A. stephensi* mosquitoes, IFAT analysis, and the infectivity of vertebrate host.**

*A. stephensi* mosquitoes were fed on mice infected with either tg or wt *P. berghei* parasites. (A) 10 and 21 days post-feed mosquitoes were dissected for oocysts and salivary gland spz, respectively. The results are the summary of 2 experiments with 40-50 mosquitoes each. (B) Tg and wt salivary gland sporozoites were stained with one of the following Abs at 1:100 dilution: either PbCSP specific mAb 3D11, or polyclonal sera specific against either PbTRAP or PvTRAP proteins. (C) C57BL/6 animals (n=8 for each group) were injected with 1000 of either tg or wt salivary gland sporozoites. Blood-stage parasitaemias were monitored for three consecutive days starting at day 5 after sporozoite injection. Linear regression model was generated to predict Tto1. (D) The Kaplan-Meier survival analysis using Tto1 data demonstrates a minimal difference in vertebrate liver infection between wt and tg *P. berghei*. Means with SEM are plotted and student's t-test was used where relevant.

#### 6.1.2.3 Immunogenicity of ChAd63-PvTRAP prime – MVA-PvTRAP boost regime

In parallel, a clinically relevant *P. vivax* vaccine using the chimpanzee adenovirus ChAd63 and MVA, two viral vectors that have been tested in malaria clinical trials (199), was developed and assessed using novel *P. vivax* tg parasite as a challenge. Inbred (BALB/c, C57BL/6) and outbred (CD1) mice were immunized with the replication deficient ChAd63 and MVA expressing PvTRAP using regimens that have demonstrated efficacy in pre-clinical models when used in an Adenovirus-prime, MVA-boost (Ad-M) regime with an 8 week immunization interval (165, 309).

High frequencies of T cell responses and antibody titers were observed 14 days after immunization with ChAd63-PvTRAP. Responses were further boosted by MVA-PvTRAP (Figures 29A, B). Intracellular Cytokine Staining (ICS) by flow cytometry revealed a predominant $CD8^+$ response that was particularly strong in the C57BL/6 strain, while $CD4^+$ T cells were only marginally increased (Figures 29C, D). High levels of $CD8^+$ T cell functionality were found in both inbred mouse strains, especially in C57BL/6, while the outbred CD1 expressed only CD107a on stimulated cells (Figure 30A-C).

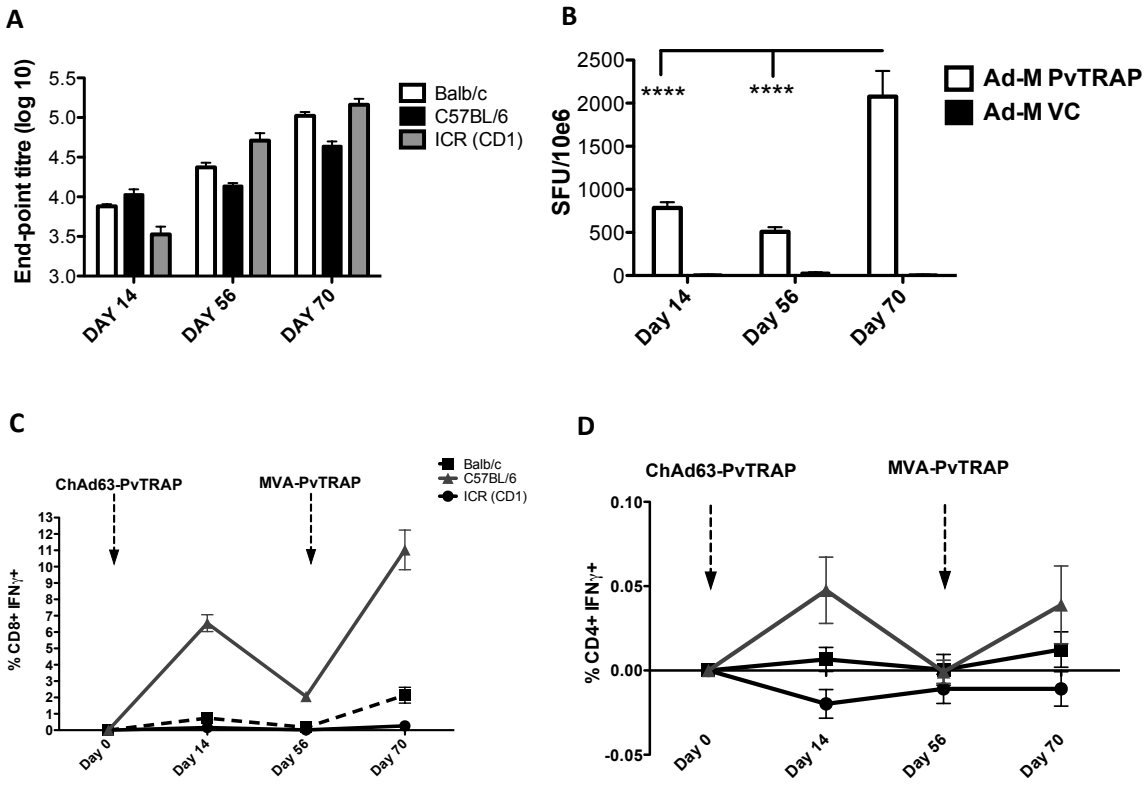


**Figure 29: The kinetics of the humoral and cellular immune responses following Ad-M PvTRAP vaccination.**

Three different strains of mice, including BALB/c, C57BL/6, and CD1 (n=6/strain) were vaccinated with heterologous Ad-M PvTRAP regime and humoral and cellular immune responses were assayed two (Day 14) and eight weeks (Day 56) post-prime and two weeks (Day 70) post boost. (A) The Ag-specific Ab titres for all three mice strains used were determined by end-point ELISA. The plates were coated with recombinant PvTRAP and the serum diluted at 1:100 for earlier time points, and 1:500 for the post-MVA responses. (B) The kinetics of IFN-γ secreting lymphocyte responses in BALB/c strain of mice were measured by *ex-vivo* IFN-γ ELISPOT assay. Whole-blood PBMCs were re-stimulated with three sub-pools of peptides overlapping the whole length of PvTRAP protein in the presence of naïve lymphocytes. The unstimulated wells were subtracted from the stimulated to obtain spot forming units (SFU), which are represented per 1 million of whole-blood PBMCs. (C) ICS analysis revealed that strong IFN-γ producing $CD8^+$ T cell responses were being induced by the vaccination regime upon re-stimulation with PvTRAP peptide pool, whereas (D) relatively low responses were recorded for $CD4^+IFN\text{-}\gamma^+$ T cells. Mean data with SEM are plotted.

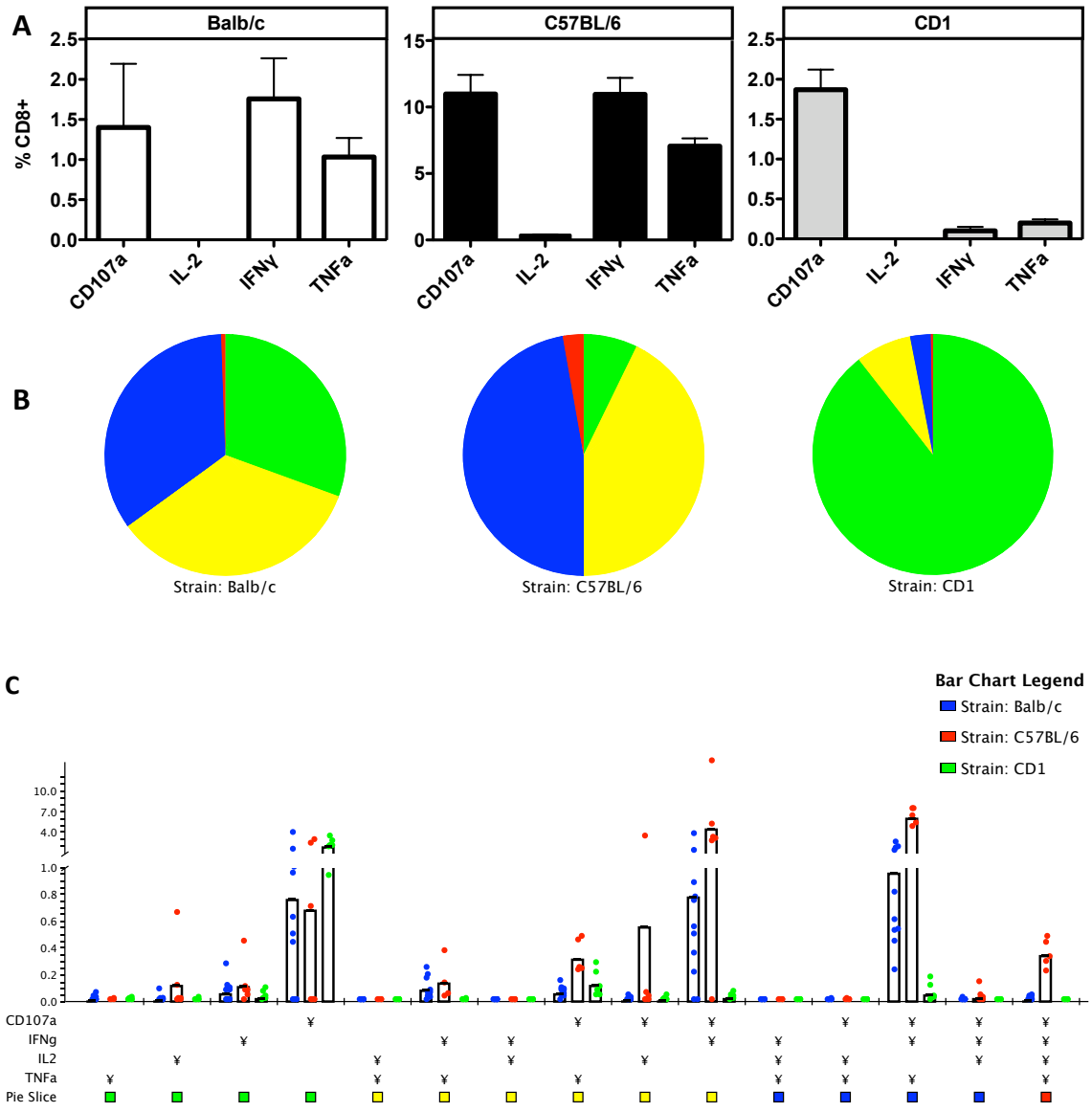


**Figure 30: Polychromatic CD8$^+$ T cell responses.**

Mice (n=6/strain) were vaccinated with Ad-M PvTRAP regime. Two weeks after MVA boost blood PBMCs were re-stimulated with overlapping peptide pool representing the whole length of PvTRAP protein. (A) Polyfunctional CD8$^+$ T cells in all three strains of mice were induced following the vaccination regimen. (B) Graphic and (C) tabular representation of CD8$^+$ T cell response hierarchy.

#### 6.1.2.4 Mapping the immunodominant T cell epitopes in mice

Vaccination with recombinant ChAd63 and MVA viral vectors expressing the PvTRAP antigen induced high frequencies of Ag-specific T cells, which belonged mainly to the $CD8^+$ compartment. This permitted further mapping of the immunodominant peptides that are recognized by T cells. Using an *ex vivo* IFN-γ ELISPOT assay with individual 20-mer peptides, the responses were focused to mainly focus on one peptide in BALB/c and CD1 mouse strains, while C57BL/6 responded to two peptides (Figure 31A). All immunodominant peptides were located within von Willebrand factor type A-domain within the ectodomain of the protein (Figure 31B). As expected, all immunodominant peptides stimulated predominantly $CD8^+$ T cells (Figure 32A).

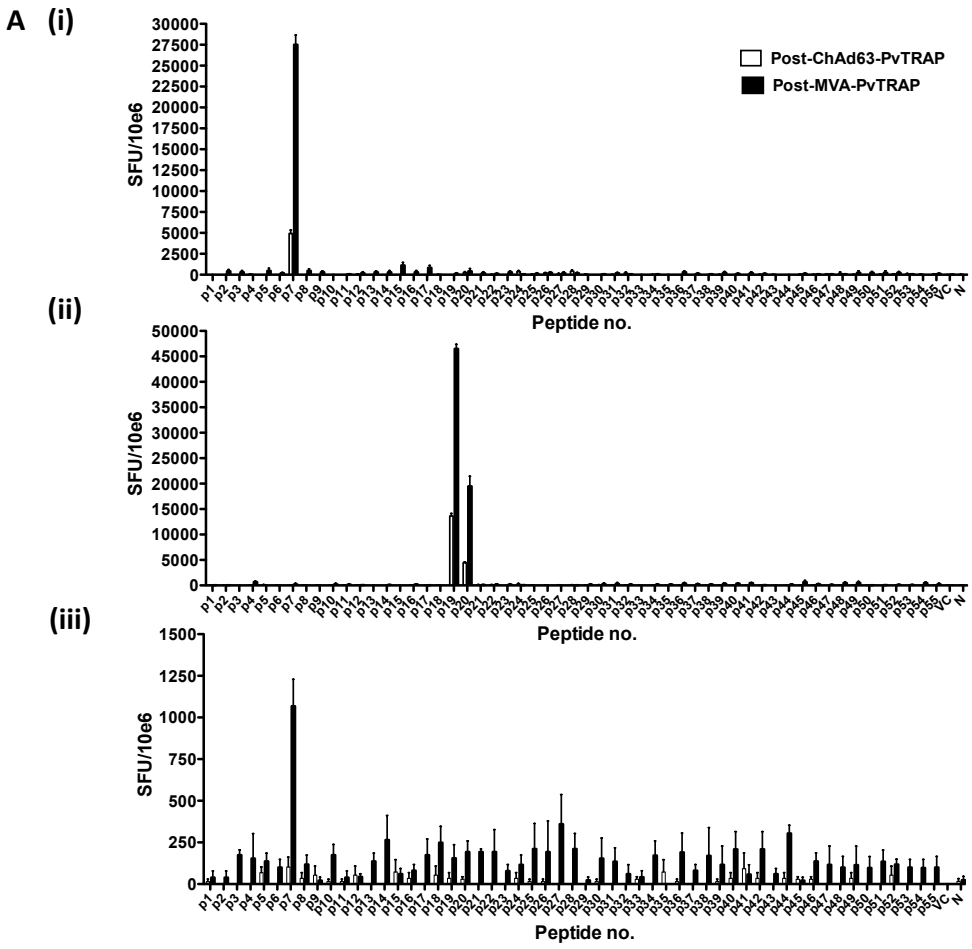


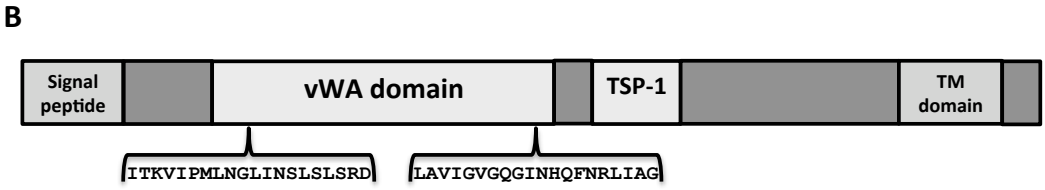


**Figure 31: Immunodominant peptide mapping.**

Mice (n=6/strain) were vaccinated with Ad-M PvTRAP regime. Either two weeks post-Ad or post-MVA immunization blood PBMCs were isolated and combined into one sample within the same strain of mice. Combined PBMCs were then incubated in triplicates with the mixture of individual peptides containing naïve splenocytes. (A) *Ex-vivo* IFN-γ ELISPOT responses to individual peptides were plotted for two time points for (i) BALB/c, (ii) C57BL/6, or (iii) CD1 genetic backgrounds. (B) The schematic representation of PvTRAP protein including main functional domains and the location of immunodominant peptides. vWA = von Willebrand factor A domain, TSP-1 = thrombospondin-like 1 domain, TM = transmembrane domain.

A

| Strain of mice | Peptide | Sequence | T cell subtype | % of parent (mean) (95% CI) |
|---|---|---|---|---|
| Balb/c | Peptide 7 | ITKVIPMLNGLINSLSLSRD | CD8+ | 0.5940 (0.1954, 0.9925) |
| | | | CD4+ | 0.007 (-0.0006, 0.015) |
| C57BL/6 | Peptide 19 | LAVIGVGQGINHQFNRLIAG | CD8+ | 6.826 (3.400, 10.25) |
| | | | CD4+ | -0.0068 (-0.0209, 0.0072) |
| | Peptide 20 | NHQFNRLIAGCRPREPNCKF | CD8+ | 0.5163 (-0.3955, 1.428) |
| | | | CD4+ | 0.0280 (0.0126, 0.0433) |
| ICR (CD1) | Peptide 7 | ITKVIPMLNGLINSLSLSRD | CD8+ | 0.0620 (-0.1304, 0.2544) |
| | | | CD4+ | -0.0261 (-0.1021, 0.0499) |

B

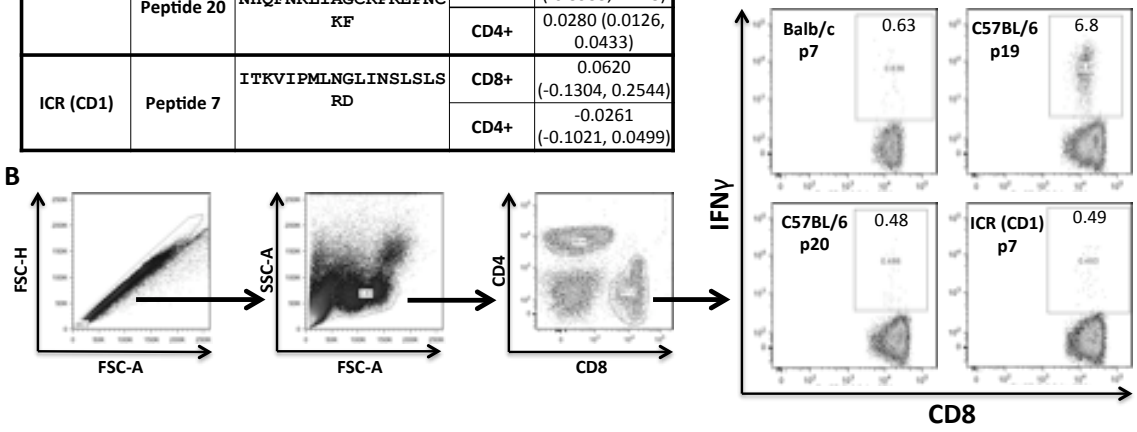


**Figure 32: The phenotype of the immunodominant epitopes.**

Two weeks post-ChAd63 immunization blood PBMCs were isolated and combined into one sample within the same strain of mice. (A) ICS analysis performed using PvTRAP-specific individual immunodominant peptides as indicated, revealed that predominantly $CD8^{+}$IFN-$\gamma^{+}$ T cells were induced. (B) The gating strategy for the $CD8^{+}$ T cells is shown.

### 6.1.2.5 ChAd63-MVA expressing PvTRAP protects against Tg *P. berghei* sporozoite challenge

Next the protective efficacy of ChAd63-MVA PvTRAP regimen was assessed against an intravenous challenge with 1000 tg spz. The same three strains of mice were used. The protective mechanisms against malaria at a pre-erythrocytic stage vary in all three strains, suggesting that different aspects of immune system can provide sufficient response to protect against spz challenge (150). All three strains of mice demonstrated varying levels of protective efficacy suggesting that PvTRAP is a promising pre-erythrocytic stage *P. vivax* vaccine candidate. Protection against infection was highest in BALB/c and CD1 strains of mice, which varied between 45 and 55% of sterile protection, respectively (Figure 33A, B). Such protective levels despite low Ag-specific $CD8^+$ responses were surprising considering the fact that historically TRAP has been thought to be mainly a T cell target (Ewer *et al.* submitted). Protection in the C57BL/6 strain of mice was modest as there were no sterilely protected animals following the vaccination, despite having the highest $CD8^+$ T cell responses (Figure 33C).

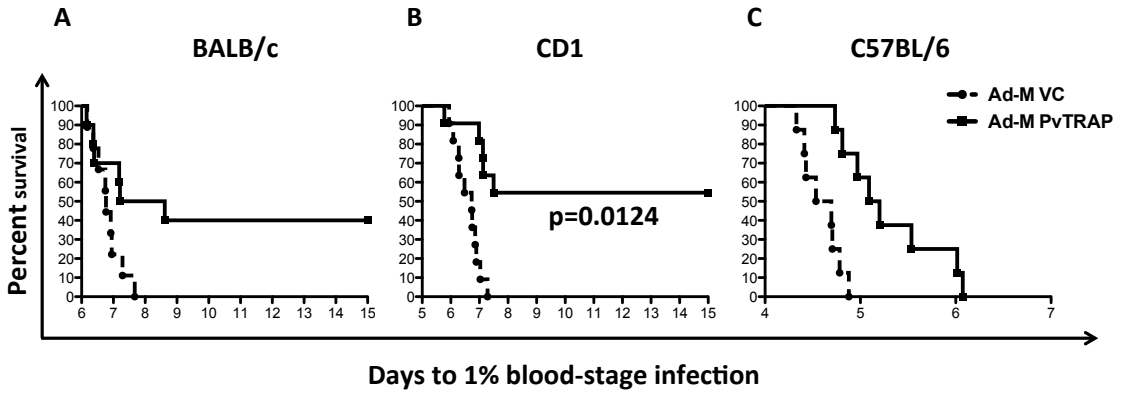


**Figure 33: The protective efficacy conferred by Ad-M PvTRAP vaccination against tg *P.berghei* parasite.**

(A) BALB/c, (B) CD1, and (C) C57BL/6 were vaccinated with heterologous prime-boost regime using ChAd63-MVA viral vectors expressing PvTRAP. Two weeks after the boost mice were challenged with 1000 tg *P. berghei* sporozoites by IV injection. The blood-stage infection was monitored for 3 consecutive days starting at day 5 post-challenge and linear model predicting Tto1 was generated. The absence of blood-stage parasites in the animals that remained sterilely protected by day 8 was confirmed on day 15 post-challenge. The Kaplan-Meier survival curves are shown. P value was generated using Fisher's exact test.

### 6.1.2.6 Both Ab and T cells are important for the protection against Tg challenge

Further attempts to delineate the immune mechanisms associated with protection were made since both, T cells and Abs can target TRAP. $CD4^+$ or $CD8^+$ T cells were depleted by administration of either GK1.5 or 2.43 mAb, respectively. The 99% level of depletion was confirmed by surface staining of whole-blood PBMCs obtained immediately before the challenge. As expected, $CD4^+$ T cell depletion did not affect protection against a challenge with tg parasites in any of the three mouse strains (Figure 34A). However, depletion of $CD8^+$ cells with the 2.43 mAb completely abrogated protection in the BALB/c and CD1 mouse strains while results in C57BL/6 mice remained unaltered (2 sterilely protected mice within the $CD8^+$ T cell depletion group probably were chance variation). However other factors could play a role in protection as 17% of the CD1 mice were sterilely protected even in the absence of Ag-specific $CD8^+$ T cells (Figure 34B).

The role of PvTRAP-specific antibodies in protection was also investigated. Total IgG was purified from ChAd63-MVA PvTRAP CD1 immunized mice and approximately 2 mg of IgG was transferred to individual naïve CD1 mice that were subsequently challenged with tg spz. Upon IgG transfer, 50% of the CD1 were sterilely protected ($p=0.04$ by Fisher's exact) while all the control (receiving vector control IgG) and naïve mice succumbed to infection (Figure 34C). This result indicated that anti-PvTRAP antibodies could mediate protection in addition to the Ag-specific $CD8^+$ T cells.

A

| Strain of mice | Vaccination | Depleting mAb | % Sterile protection | No.infected/ no.challenged (*p* value) |
|---|---|---|---|---|
| Balb/c | Ad-M *Pv*TRAP | N/A | 40% | 3/5 (0.1) |
| | | RIgG | 50% | 3/6 (0.04) |
| | | GK1.5 | 20% | 4/5 (0.35) |
| | | 2.43 | 0% | 6/6 (N/A) |
| | Vector control | N/A | 0% | 9/9 |
| C57BL/6 | Ad-M *Pv*TRAP | N/A | 0% | 5/5 (N/A) |
| | | RIgG | 0% | 6/6 (N/A) |
| | | GK1.5 | 17% | 5/6 (0.35) |
| | | 2.43 | 33% | 4/6 (0.1) |
| | Vector control | N/A | 0% | 11/11 |
| ICR (CD1) | Ad-M *Pv*TRAP | N/A | 60% | 2/5 (0.02) |
| | | RIgG | 50% | 3/6 (0.035) |
| | | GK1.5 | 66% | 2/6 (0.008) |
| | | 2.43 | 17% | 5/6 (0.37) |
| | Vector control | N/A | 0% | 10/10 |

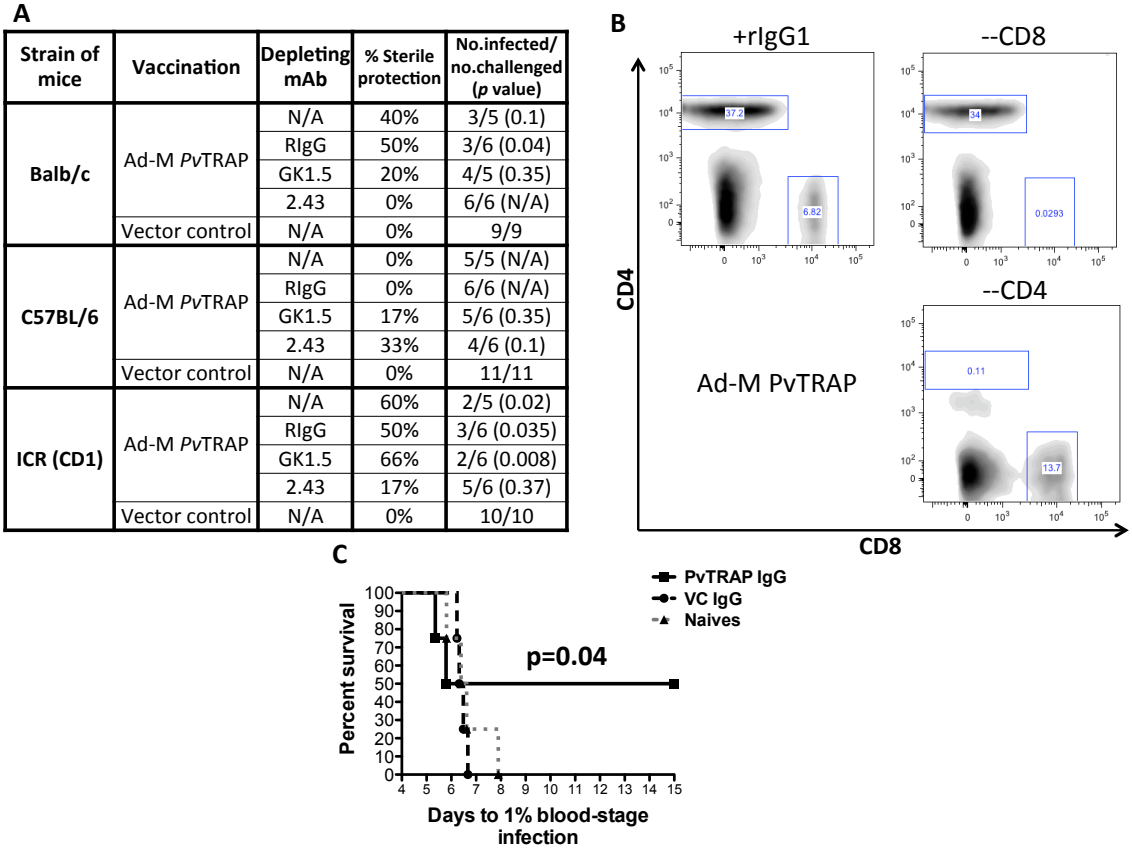


**Figure 34: Both PvTRAP-specific T cells and Abs mediate protection against tg *P. berghei* challenge.**

Mice were vaccinated with heterologous prime-boost ChAd63-MVA regime expressing PvTRAP. (A) Two weeks after the boost mice were administered depleting Abs as indicated on days -2, -1, and 0 relative to challenge. The p value in parentheses was generated by using Fisher's exact test. (B) The FlowJo graphs confirming 99% depletion of either $CD4^+$ or $CD8^+$ T cells. (C) CD1 animals were vaccinated with Ad-M PvTRAP regimen. Two weeks after the last vaccination whole IgG from serum was purified and 2 mg of it passively injected into naïve CD1 mice (PvTRAP IgG). Whole IgG raised against empty viral vectors was also included (VC IgG). The p value was generated by Fisher's exact test comparing the control animals versus animals that received anti-PvTRAP IgG.

### 6.1.3 Discussion

In this study a pre-erythrocytic stage vaccine candidate against human malaria caused by *P. vivax* was assessed. The clinically relevant recombinant viruses MVA and ChAd63 were used to develop vectored vaccines expressing TRAP from *P. vivax* malaria, which were administered as a ChAd63-MVA prime-boost regime. This regime has been shown to be safe and highly immunogenic in a recent set of Phase I clinical trials targeting malaria (199, 209). The immunization regimen induced high Ab titers in all mouse strains tested and high frequencies of multifunctional T cells and the results indicated that, depending on mice strain, both factors played a role in protecting mice against sporozoite challenge.

To enable the assessment of vaccine efficacy in pre-clinical models, a tg *P. berghei* expressing PvTRAP was generated. The complete substitution of *P. berghei* TRAP gene without leaving a selectable marker in the adjacent downstream region of the gene was performed. This step was important in maintaining the parasite's fitness, in particular the ability to infect the vertebrate host as it has been shown that the presence of the *hDHFR* selectable marker cassette in the CS locus can decrease the infective inoculum by approximately 90%, thus requiring larger numbers of spz to successfully infect 100% of the challenged mice (236). The cloning and selection strategy permitted the development of a markerless tg *P. berghei* that did not have any significant decrease in the parasite's ability to form oocysts, infect mosquito salivary glands, or invade vertebrate hepatocytes, thus becoming a robust system for *P. vivax* pre-erythrocytic vaccine candidate evaluation. In the absence of a continuous culture of *P. vivax* parasites, new world monkeys and

infected humans in an endemic region are the only available sources to study the biology, pathology and immunology of *P. vivax* malaria (311). Thus, new small animal models are much in need to develop novel vaccine candidates. Mouse models are easily accessible and constitute an inexpensive option compared to new world monkeys at the same time raising less ethical issues. Moreover, the lack of a good correlate of protection for pre-erythrocytic malaria emphasizes the need of a challenge model to assess the protective efficacy of a vaccine (165). Whilst this new tg parasite would require further comparison with a *P. vivax* challenge in new world primates, if proven useful it could become a standard first line assessment of vaccine candidates and could be helpful in defining new correlates of protection to permit validation of new vaccines without further need of large animal challenges.

The protective efficacy observed in three strains of mice was somewhat surprising as the C57BL/6 strain demonstrated the lowest level of protection despite having the highest frequencies of Ag-specific $CD8^+$ T cells. $CD8^+$ cells producing IFN-γ have been implicated in protection against pre-erythrocytic stage malaria in both pre-clinical and clinical models (150)(Ewer *et al.* submitted). BALB/c and CD1 animals demonstrated the highest level of sterile protection. This is in agreement with previous reports describing the protection in these three mouse strains (224). Providing that all mice strains had an immunodominant peptide, perhaps there is something different and unique about the $CD8^+$ T cell immunodominance, conferring a much greater level of protection in BALB/c and CD1 strains, when compared to the C57BL/6 model. Also, the mapping of immunodominant peptides revealed that the immunodominant PvTRAP epitopes from all

three strains of mice were located within the von Willebrand factor type A-domain (vWA) (Figure 31). The limited amount of research investigating PvTRAP polymorphism identifies vWA domain as one of the most polymorphic structures of the gene (312) (313).

Mechanistic experiments revealed that while depletion of T cells substantially reduced the levels of protection in BALB/c and CD1 models, it appeared to have little, if any, effect in C57BL/6 mice. In fact, in the latter model some sterilely protected animals were observed in the groups where either $CD4^+$ or $CD8^+$ T cells were depleted. All these data taken together indicated that Abs might have been playing an important role in protection in our system. Indeed, a few studies exist showing that Abs against TRAP do correlate with protection in the endemic regions and that there are TRAP specific Abs in the blood of patients who live in the malaria endemic regions (314). Also, Charoenvit *et al.* demonstrated that PyTRAP-specific monoclonal and polyclonal antibodies raised in mice after immunization with multiple antigen peptides comprising PfSSP2/TRAP, partially inhibited *P. falciparum* liver-stage parasite development and sporozoite invasion of human hepatoma cells respectively (315). In contrast, Gantt *et al.* did not observe an inhibitory effect of TRAP-specific antibodies on *P. yoelii* sporozoite infectivity of mice hepatocytes *in vivo* (85). Nonetheless, in our system PvTRAP-specific whole IgG passive transfer into naïve mice also transferred some level of protection. It is unlikely that the moderate level of Ab-mediated protection was due to the possible overexpression of exogenous PvTRAP gene, as the transgene was placed under the control of endogenous PbTRAP promoter. Provided that TRAP is translocated from micronemes onto the

surface of sporozoites and plays a crucial role in parasites gliding motility and infectivity (316), it is not surprising that high Ab titres against the antigen can protect and the vaccination regimens tested here using ChAd63 prime – MVA boost could induce both, high Abs and T cells as has previously been shown (254) (208, 209). PvTRAP-specific Abs can target and neutralize spz before they establish an exoerythrocytic infection in the liver while the remainder of the parasites that manage to escape the initial Ab attack resulting in liver infection can become a target for T cells. It remains to be explored whether the same factors would be able to protect vaccinees against wt *P. vivax* challenge. Also, it is not known whether the dormant hepatic forms of *P. vivax,* known as hypnozoites, can be targeted by Ag-specific T cells. However, hypnozoites are established shortly after hepatocyte invasion, and transcriptomics data indicate that the TRAP transcripts are numerous during early stages of hepatocyte development (317). Therefore, there is a possibility that developing *P. vivax* parasites in the human hepatocytes could be killed even before they establish hypnozoites, especially considering that adenovirus vectors are very efficient at deploying protective $CD8^+$ T cells to the liver (165).

The results in this section of the chapter describe a highly immunogenic *P. vivax* candidate vaccine that can induce protection in mice against a tg parasite expressing the PvTRAP transgene. As both, ChAd63 and MVA have shown good immunogenicity and protective efficacy using *P. falciparum* TRAP in mouse models (309) which have been useful to predict the good immunogenicity in rhesus macaques and humans (199, 309),

the ChAd63/MVA prime-boost regimen expressing PvTRAP warrants further assessment in *Aotus lemurinus griseimembra* monkeys (307, 308) and humans.

## 6.2 *P. vivax* CSP-based vaccines and vaccine combinations

### 6.2.1 Introduction

As mentioned in previous chapters, PfCSP-based RTS,S/AS01 vaccine is currently the leading malaria vaccine candidate (161). The CS sequence used in RTS,S is strain-specific, thus vaccinated individuals do not develop specific immune responses directed against other malaria species. In some regions of the world *P. vivax* is the most prevalent form of this protozoan parasite, causing a considerable degree of morbidity and mortality (318). There is minimal chance that RTS,S/AS01 would be effective in those locations, therefore, a vaccine against *P. vivax* malaria based on CS protein will have to incorporate PvCSP as the immunogen.

Thus far, the efforts to develop PvCSP-based vaccine have been complicated by the fact that the gene coding the CS protein is quite heterogeneous. Two variants of PvCSP exist, termed VK210 and VK247, that differ mostly at the amino acid (aa) sequence of the central repeat region of the gene (Figure 35) (319, 320). In addition, some level of heterogeneity is also present in another three non-repetitive locations, one in each of N- and C- terminal regions of the gene and the third in the region between the central repeat and the C- terminal domain (321). The amino acid sequence of PvCSP central repeat region has been divided into two kinds of repeating aa sequences: a tetrapeptide (GDRA in VK210 and ANGA in VK247) followed by a pentapeptide (AGQPA or DGQPA in VK210 and GNQPG or GDQPG in VK247). These alternating repeats account for 82% to 98% of all central repeat regions (321). Both VK210 and VK247 variants are distributed globally (322). Moreover, both types of alleles were found in localities from

Colombia, South America (323) and even in samples from a single locality in Mae Sod in Thailand (324). Also, a significant level of mixed infections with both VK210 and VK247 types of parasites were identified in Myanmar (325), suggesting that both variants of PvCS gene can co-exist and a protective vaccine against one type would most likely result in the worldwide selection for heterologous form of the gene.

There are studies demonstrating that individuals exposed to natural *P. vivax* infection contain Abs directed against the central repeat region of PvCSP (326) (327). Interestingly, Abs against a non-repeat portion of PvCS protein have also been reported (328), which is in contrast with the situation observed with PfCSP-specific humoral responses, where Abs predominantly target the NANP motif of the repeat region (329). In addition to humoral immune responses, the cellular immunity against PvCSP in some individuals living in *P. vivax* endemic regions have also been observed (330) and $CD4^+$ (331) as well as $CD8^+$ (332) restricted T-cell epitopes identified. Thus, it is possible that PvCSP-based vaccine could induce potent Ab and T cell responses.

Attempts have been made to develop a PvCSP-based vaccine using the VK210 sequence of the parasite. Arevalo-Herrera *et al.* reported the development of PvCSP VK210-based vaccine consisting of three long synthetic peptides (LSP) each corresponding to amino-terminal, central repeat, and carboxy-terminal regions of the CS protein (307). Using these PvCSP-based LSPs formulated in Montanide ISA-720 or Montanide ISA-51 adjuvants high Abs titres were induced in rodent and primate models (307). The safety, tolerability, and immunogenicity of a mixture of these three LSPs derived from PvCS

protein formulated in Montanide ISA-720 or Montanide ISA-51 has also been assessed in a Phase I clinical trial (306).

Another approach has been to develop a single vaccine targeting both variants of PvCS gene. A clinical grade chimeric recombinant PvCS protein, named VMP001, containing a hybrid repeat region constituting both VK210 and VK247 variants has been synthesized in the *E. coli* system (333). Abs raised in the CD1 strain of mice following the vaccination with VMP001 recognized *P. vivax* sporozoites of both VK210 and VK247 types by IFAT (334), and even conferred a considerable degree of cross-species protection against *P. berghei* spz challenge (335). Phase I and II clinical trials (clinical trials registration number NCT00866619) using VMP001 recombinant protein formulated with AS01B adjuvant system will provide more evidence concerning the degree of protection that the vaccination with this PvCSP-based hybrid recombinant protein will confer to malaria-naïve individuals.

In this part of the chapter, immunogenicity and protective efficacy of heterologous prime-boost regimens employing ChAd63 viral vectors and recombinant proteins of different PvCSP-based constructs is assessed.

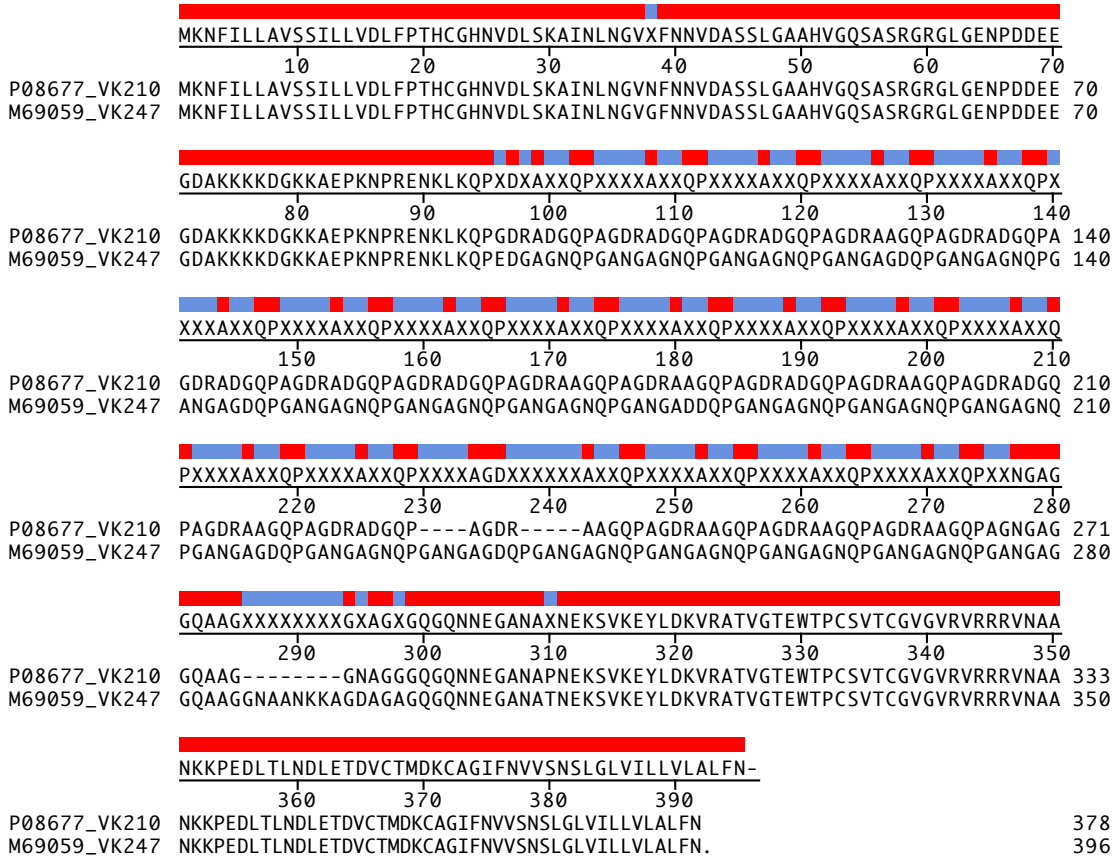


**Figure 35: Alignment of PvCSP variants VK210 and VK247.**

The alignment at the polypeptide level of two major PvCSP variants was performed using Belem I (Accession no.: P08677) and Papua New Guinea (PNG) (Accession no.: M69059) amino acid sequences representing VK210 and VK247 variants, respectively. The sequences were aligned using Lasergene's MegAlign software and ClustalW multiple alignment algorithm. The highly conserved or variable regions are indicated by red or blue, respectively.

### 6.2.2 Results

#### 6.2.2.1 The immunogenicity of recombinant ChAd63-PvCSP VK210 viral vector

Four different strains of mice, including three inbred: BALB/c, C57BL/6, and C3H, and one outbred: ICR (CD1) were immunized with recombinant ChAd63 viral vector expressing PvCSP VK210 variant. Two weeks after the vaccination cellular and humoral immune responses in all four strains of mice were measured by *ex-vivo* IFN-γ ELISPOT and ELISA assays, respectively. A clear hierarchy in IFN-γ secreting lymphocyte responses was observed upon re-stimulation of whole-blood PBMCs with peptide pools representing the full length of VK210 protein (Figure 36A). Substantially higher cellular immune responses were recorded for C3H and outbred strains of mice, followed by C57BL/6 and BALB/c animals.

Whole IgG Ab titres measured by end-point ELISA showed that outbred and inbred C57BL/6 strains of mice were highly susceptible to PvCSP VK210-specific Ab induction, generating the highest humoral responses. Lower IgG Ab titres were observed in BALB/c and C3H mice strains (Figure 36B).

Interestingly, a considerable degree of cross-reactivity was recorded when ELISA plates were coated with recombinant protein representing the heterologous PvCSP strain, namely the VK247 variant (Figure 36B). Also, the level of cross-reactivity seemed to correlate with the overall PvCSP-specific Ab responses, because the animals that had higher VK210-specific Ab titres, also recorded higher VK247-specific Ab titres.

The data showed that ChAd63-PvCSP VK210 vaccine was immunogenic for both cellular and humoral immune responses in the four mouse strains tested. Also, a considerable degree of cross-reactivity against VK247 variant was observed suggesting that perhaps VK210-based vaccine alone could recognize both homologous and heterologous forms of the PvCS gene *in vivo*.

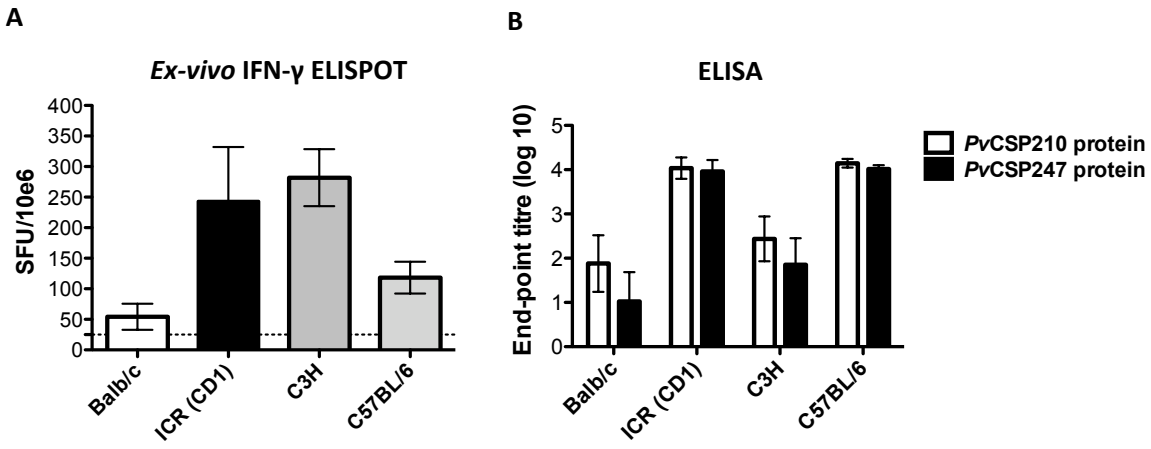


**Figure 36: Interstrain comparison of ChAd63-PvCSP VK210 vaccine immunogenicity.**

Four different strains of mice (n=6/strain) were vaccinated with a single dose of recombinant ChAd63 viral vector expressing PvCSP VK210 variant. Two weeks after the vaccination IFN-γ secreting lymphocytes were enumerated by (A) *ex-vivo* IFN-γ ELISPOT assay upon re-stimulation of whole blood PBMCs with three sub-pools of peptides representing the whole length of PvCSP VK210 variant. The results are represented as spot forming units (SFU) per million (10e6) of PBMCs. (B) At the same time point Ag-specific whole IgG Ab titres were measured by end-point ELISA. Plates were coated with either PvCSP VK210 (open bars) or VK247 (solid bars) recombinant protein. Means with SEM are showed. The dotted line indicates the mean background responses.

#### 6.2.2.2 Immunogenicity of PvCSP-based vaccine constructs in heterologous prime-boost regimen

It has been demonstrated that PvCSP-specific abs directed against non-repeat regions of the protein, including N- and C-terminal domains, have inhibitory potential against *P. vivax* spz (336). Also, it has been suggested that N-terminal portion of the CS protein contains an immunologically cryptic epitope, which plays a crucial role in liver cell recognition and induces inhibitory abs only when administered as a separate polypeptide independent of the rest of the protein (143). To test whether N- and C- terminal domains of CS protein could induce measurable Ab responses, recombinant ChAd63 viral vector expressing just highly conserved amino and carboxy terminal regions of PvCSP gene was generated (termed NC). Recombinant protein corresponding to the same construct was also synthesized. Additionally, another two recombinant ChAd63 viral vectors each expressing either VK247 or a chimeric version of PvCS protein containing repeat sequences of both VK210 and VK247 types were made and two recombinant proteins each representing VK210 or VK247 alleles of PvCS gene synthesized (for further details on recombinant viral vector and protein generation, refer to the materials and methods sections 2.2.7 and 2.5.3, respectively). CD1 mice were immunized with the heterologous prime-boost regimen employing ChAd63 viral vectors at the prime and recombinant proteins in Abisco 100 adjuvant at the boost as outlined in table 9.

Two weeks after the booster vaccination, humoral and cellular immune responses were assayed by end-point ELISA and *ex-vivo* IFN-γ ELISPOT, respectively. Uniformly high whole IgG ab titres were recorded for all vaccination groups against both variants of

PvCSP gene (Figure 37A, B). Also, relatively low IFN-γ secreting lymphocyte responses were observed in all vaccination groups against both VK210 and VK247 peptide pools following an adeno prime – protein-in-adjuvant boost vaccination (Figure 37C).

This set of experiments demonstrated that PvCSP-based constructs in heterologous Ad-P regime in CD1 mice were highly immunogenic for Abs, but induced relatively low numbers of IFN-γ secreting lymphocytes. Also, amino and carboxy domains of PvCSP alone were potent inducers of humoral response, despite the absence of the immunodominant central repeat region, which in the case of *P. falciparum* CSP is the major target of Ab response (329). Moreover, abs induced by Ad-P vaccination in all immunization groups were cross-reactive against both alleles of PvCS protein, and the cross-reactivity profile was consistent with the one seen just after ChAd63-PvCSP VK210 vaccinations.

| Group | Antigen | Priming agent | Boosting agent |
|---|---|---|---|
| **Control** | Ovalbumin | AdHu5 (1e10^8 iu IM) | 15 µg of OVA + Abisco 100 |
| **NC** | *Pv*CSP N- and C-terminus | ChAd63 (1e10^8 iu IM) | 15 µg of *Pv*CSP NC + Abisco 100 |
| **210** | *Pv*CSP VK210 | ChAd63 (1e10^8 iu IM) | 15 µg of *Pv*CSP VK210 + Abisco 100 |
| **247** | *Pv*CSP VK247 | ChAd63 (1e10^8 iu IM) | 15 µg of *Pv*CSP VK247 + Abisco 100 |
| **210\|247** | *Pv*CSP VK210\|247 | ChAd63 (1e10^8 iu IM) | 15 µg of *Pv*CSP VK210 + 15 µg of *Pv*CSP VK247 + Abisco 100 (mixture) |

**Table 9: The table listing the different Ad-P PvCSP variant vaccinations.**

CD1 mice (n=6/group) were vaccinated with heterologous prime-boost employing ChAd63 viral vectors and recombinant proteins in Abisco 100 adjuvant administered 8 weeks apart. The name of the group, PvCSP antigen variant, and prime – boost agents and vaccine doses are indicated.

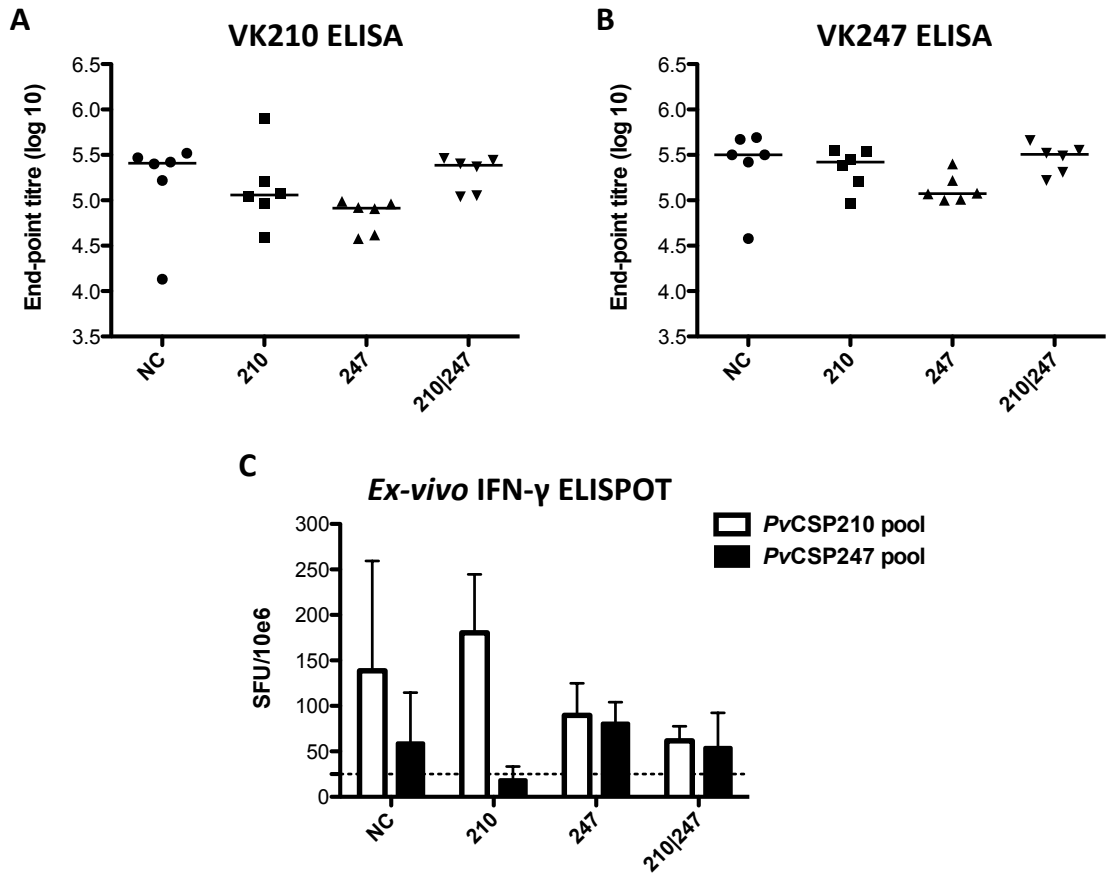


**Figure 37: Immunogenicity of PvCSP-based vaccines.**

CD1 strain of mice (n=6/group) were vaccinated as outlined in table 9. Viral vectors expressing either PvCSP VK210 (abbreviated as 210), PvCSP VK247 (247) or the combination of both alleles of PvCSP VK210|247 (210|247) were used as priming agents. Recombinant ChAd63 expressing just N- and C-terminus of PvCSP gene (abbreviated as NC) were also included. Recombinant proteins for NC, 210, and 247 forms of PvCSP were synthesized and used as boosting agents. ChAd63-PvCSP VK210|247 responses were boosted with the mixture of equal amounts of 210 and 247 recombinant proteins. The control animals received HAdV-5-OVA and recombinant OVA in Abisco 100 at the time of priming and boosting, respectively. Two weeks after the boost whole IgG Ab titres specific for either (A) PvCSP VK210 or (B) PvCSP VK247 alleles were measured for all animals by end-point ELISA and individual dot points plotted with line indicating median. (C) *Ex-vivo* IFN-γ ELISPOT responses were also quantified by re-stimulation of whole blood PBMCs in the presence of naïve splenocytes with three sub-pools of peptides representing either PvCSP VK210 allele (empty bars) or PvCSP VK247 allele (solid bars). Means with SEM are shown.

### 6.2.2.3 Generation of tg *P. berghei* expressing either VK210 or VK247 variants of PvCSP and the assessment of their phenotype

Yadava *et al.* in their study employed *P. berghei* spz to test the protective efficacy of recombinant VMP001 vaccine, as rodent models are not amenable to human *P. vivax* parasite infection (335). Indeed, *P. berghei* challenge model can serve as a tool for the evaluation of human malaria vaccines, provided that the responses induced by the vaccination are cross-reactive. However, in the absence of sufficient cross-reactivity or when the level of protection associated with different variants of the same gene, such as PvCSP, needs to be investigated, the *P. berghei* challenge model fails to generate conclusive results. To circumvent this problem two tg *P. berghei* parasites were generated, each expressing either VK210 or VK247 variant of PvCSP.

Initially, to produce the *P. berghei* parasite line receptive for the insertion of VK210 or VK247 variant without the need for a separate selection marker, the *hDHFR-yFCU* selection cassette was introduced by double cross-over homologous recombination knocking-out the endogenous PbCS gene (Figure 38A(i)) (refer to the materials and methods section 2.4.2 for the details on how the insertion constructs were generated). The mutants lacking a PbCS gene were selected by treating mice with pyrimethamine and southern blot analysis of pulse-field gel (PFG) electrophoresis-separated chromosomes probed with the 3′untranslated region (UTR) of the *dhfr/ts* gene of *P. berghei* was performed to verify the correct location of *hDHFR-yFCU* incorporation. Once the successful knockout of PbCS was confirmed (mutants 2150 and 2151 chromosome 4) (Figure 38A(ii)), mutant 2151 was cloned by limited dilution technique. Three

homogenous populations of cloned 2151 parasite emerged (2151 cl1-3) and all of their identities were confirmed once again by southern blot analysis of PFG-separated chromosomes hybridized with the same *dhfr/ts* probe (Figure 38A(iii)).

The 2151 cl1 tg parasite was then used for another round of electroporation, resulting in the introduction of either VK210 or VK247 allele (Figure 38B(i)) after treating mice with 5-fluorocytosine (5-FC) pro-drug. The successful introduction of either variant of PvCS was once again confirmed by southern blot using a mix of probes specific for chromosome 5 and the *hDHFR-yFCU* selection cassette on chromosome 4 (2196, 2197 are VK210, and 2198, 2199 are VK247 mutants) (Figure 38B(ii)). The absence of a band within chromosome 4 observed in the 2196 cl1-5 and 2199 cl1-2 parasite clones indicated the effective exchange of the selection cassette with one of the PvCS alleles (Figure 38B(iii)). Clones 2196 cl1 and 2199cl1 corresponding to VK210 and VK247 variants of PvCS gene, respectively, were selected for further testing.

Next the tg parasites' sexual-stage development and infectivity in *A. stephensi* mosquitoes was evaluated. The oocyst numbers for 2196 cl1 and 2199 cl mutants were compared against GFP/Luc control parasites 10 days after the female mosquitoes were fed on infected mice. Similar number of developing midgut oocysts (oocyst counts) was observed for all three lines of mutants (Figure 38C). Moreover, a comparable numbers of salivary gland spz per oocyst (SG spz./Oocyst) were also recorded for all three tg *P. berghei* mutants after dissecting infectious mosquitoes 21 days post-feed (Figure 38D).

The construction of two tg markerless *P. berghei* parasite lines containing either one of two PvCS alleles resulted in mutants that had normal phenotype for sexual-stage

development and invertebrate host infectivity. These tgs provide a useful tool to assess PvCSP-specific functional abs *in vivo* and facilitate the further design and optimization of PvCSP-based malaria vaccines.

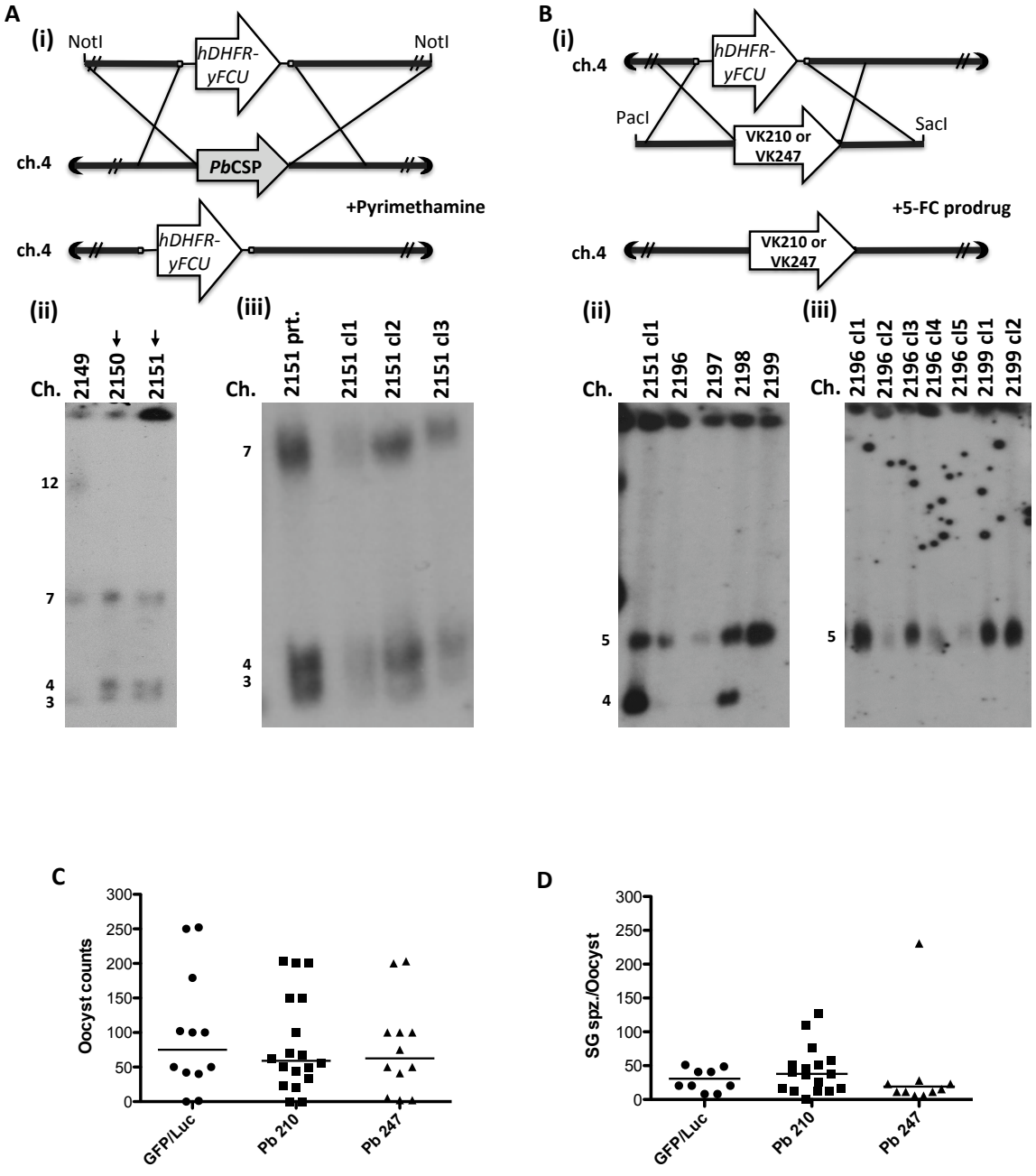
A
(i)
NotI
hDHFR-yFCU
NotI
ch.4
PbCSP
+Pyrimethamine
ch.4
hDHFR-yFCU
(ii)
Ch.
2149
2150
2151
12
7
4
3
(iii)
Ch.
2151 prt.
2151 cl1
2151 cl2
2151 cl3
7
4
3
B
(i)
ch.4
hDHFR-yFCU
PacI
VK210 or VK247
SacI
+5-FC prodrug
ch.4
VK210 or VK247
(ii)
Ch.
2151 cl1
2196
2197
2198
2199
5
4
(iii)
Ch.
2196 cl1
2196 cl2
2196 cl3
2196 cl4
2196 cl5
2199 cl1
2199 cl2
5
C
Oocyst counts
300
250
200
150
100
50
0
GFP/Luc
Pb 210
Pb 247
D
SG spz./Oocyst
300
250
200
150
100
50
0
GFP/Luc
Pb 210
Pb 247

**Figure 38: The making of tg *P. berghei* expressing either VK210 or VK247 variants of PvCSP.**

(A(i)) Cloning scheme representing the creation of *P. berghei* parent line receptive for the introduction of either VK210 or VK247 gene. For Southern analysis, PFG-separated chromosome were hybridized using a 3′UTR *pbdhfr/ts* probe that recognizes the reporter GFP/Luc gene integrated into *P. berghei 230p* locus on chromosome 3 and the endogenous locus of *dhfr/ts* on chromosome 7. The successful knockout of PbCSP gene by insertion of *hDHFR/yfcu* cassette was confirmed on chromosome 4 (ii) before and (iii) after cloning of mutant lines by limiting dilution techniques.

(B) *P. berghei* mutant 2151 cl1 was chosen for further modification. (i) Cloning scheme corresponding to the generation of either VK210 or VK247 *P. berghei*. Geneart plasmids containing codon-optimized versions of either VK210 or VK247 were linearized at the PacI and SacI sites and electroporated into the schizont-stage 2151 cl1 parent line parasites. (ii) Mixed probe recognizing chromosome 5 and the *hDHFR* selectable marker in chromosome 4 was used to confirm the correct integration of PvCSP constructs into 2151 cl1 parent line (resulting in 2196, 2197 and 2198, 2199 mutants corresponding to VK210 and VK247 alleles, respectively). Mutants 2196 and 2199 were then taken forward and the (iii) homogeneity of parasite population was confirmed after the dilutional cloning step. The absence of signal in chromosome 4 for all clones indicate a successfull cloning of mutant lines. 2196 cl1 and 2199 cl1 represent Pb 210 and Pb 247, respectively.

*A. stephensi* mosquitoes were fed on mice infected with either GFP/Luc, Pb 210, or Pb 247 *P. berghei* mutant lines. (B) 10 days post-feed oocyst numbers in individual mosquitoes were quantified and plotted with median. (C) 21 days post-feed salivary gland spz were extracted from all three different mutant lines and enumerated. The data is represented as number of salivary gland spz per oocyst with the line indicating the median value.

### 6.2.2.4 Protective efficacy of PvCSP-based vaccine constructs against tg *P. berghei* challenge

The CD1 strain of mice was vaccinated with heterologous prime-boost regime employing ChAd63 viral vectors and recombinant proteins formulated in Abisco 100 adjuvant as described before and outlined in table 9. Two weeks post-boost animals were challenged with intravenous injection of 2000 tg *P. berghei* spz expressing VK210 variant of PvCSP (Pb210) and monitored for blood-stage infection. A statistically significantly ($p<0.05$ by Kruskal-Wallis test with Dunn's multiple comparison post-test) higher degree of protection was afforded to the animals immunized with the homologous type of the vaccine as measured by Tto1 (median Tto1 6.9) (Figure 39A, B). Interestingly, comparable levels of protection were observed in the vaccinated group that received either VK210 or a hybrid constructs, indicating that the inclusion of VK247 repeat motifs did not inhibit the level or biological activity of VK210-specific abs. Surprisingly, no protection was detected in the NC or VK247 alone vaccination groups upon the challenge with VK210-expressing *P. berghei*, suggesting that Abs directed against the repeat region are protective, but the protection is strain-specific.

To further confirm strain-specific effect CD1 mice were vaccinated with the same Ad-P regime encoding VK210 variant and challenged with 2000 tg *P. berghei* spz expressing heterotypic VK247 allele of PvCSP (Pb 247). As anticipated, no protective efficacy was detected (Figure 39C).

This set of efficacy experiments using two tg *P. berghei* expressing either VK210 or VK247 variants unequivocally demonstrated that heterologous ChAd63 – prime and

protein formulated in Abisco 100 – boost immunizations administered 8 weeks apart induce immune responses capable of protecting against malaria sporozoite challenge in rodent model. Moreover, the immune responses induced by the PvCSP-based constructs confer protection only against homologous strain of parasites, even though the IgG Ab titres against each variant of PvCS were identical. This observation has important implications for further PvCSP Ag-based pre-erythrocytic *P. vivax* malaria vaccine study and design.

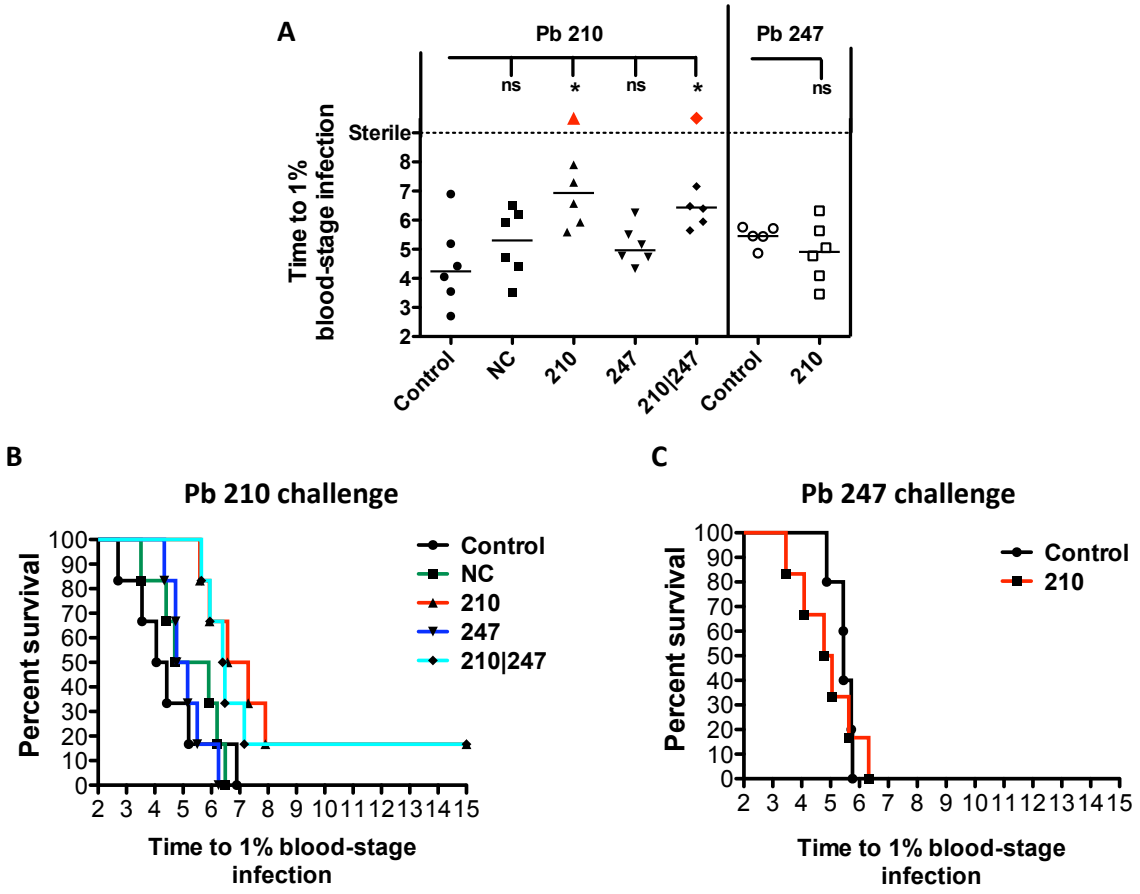


**Figure 39: Protective efficacy of PvCSP-based vaccines against tg *P. berghei* sporozoite challenge.**

Outbred ICR (CD1) strain of mice (n=6/group) were vaccinated with heterologous prime-boost regimen employing recombinant ChAd63 viral vectors and proteins formulated in Abisco 100 adjuvant as outlined in table 9. Two weeks post-boost animals were challenged by IV injection of 2000 tg *P. berghei* spz expressing either VK210 (Pb 210) or VK247 (Pb 247) alleles of PvCSP gene. Blood stage infection was monitored for three consecutive days by microscopic analysis of blood films starting at day 4 post-challenge. (A) Linear regression model predicting Tto1 for each animal was generated and individual values plotted with median. Red points corresponding to animals that did not develop blood-stage parasitaemia by day 15 post-challenge are plotted above the dotted line. The same values were also used to generate Kaplan-Meier survival curves separately for groups challenged by either (B) Pb 210 or (C) Pb 247 tg parasites. *p<0.05, Kruskal-Wallis test with Dunn's multiple comparison post-test.

### 6.2.2.5 Immunogenicity of PvCSP and PvTRAP combination vaccine administered in heterologous prime-boost regimen

In chapter 5 complete sterile protection was achieved against 2000 *P. berghei* spz challenge following the immunization with Ad-P PbCSP and Ad-M PbTRAP combination vaccine. To investigate whether the same effect could be observed with PvCSP and PvTRAP combination vaccine, BALB/c mice were immunized with the combination of recombinant ChAd63 and MVA viral vectors and PvCSP-based recombinant proteins in the heterologous prime-boost regimes as outlined in table 10. Two weeks after the boost cellular and humoral immune responses in all vaccinated animals were measured by *ex-vivo* IFN-γ ELISPOT and end-point ELISA, respectively. In line with previous observations, strong IFN-γ responses were observed in animals that received Ad-M PvTRAP alone or in combination with Ad-P PvCSP vaccines (mean SFU of 6000 per million of PBMCs) (Figure 40A(i)). On the other hand, relatively low IFN-γ secreting lymphocyte numbers were recorded for the animals that were immunized with PvCSP-based vaccines administered either alone or in combination with Ad-M PvTRAP upon re-stimulation of whole-blood PBMCs with peptide pools representing either VK210 or VK247 variants (Figure 40A(ii) and (iii), respectively). Consistent with the previous observations using PbCSP and PbTRAP combination vaccine administered in the identical heterologous prime-boost manner no antigenic interference at the lymphocyte level was observed when the second antigen was incorporated into the vaccination regime.

End-point ELISA revealed that similarly to the previous experiments high PvTRAP-specific whole IgG Ab titres were induced in vaccinated animals (median EU ~5.25) (Figure 40B(i)). Disappointingly, relatively low PvCSP-specific whole IgG responses were observed against both VK210 (Figure 40B(ii) and VK247 (Figure 40B(iii)) variants in all animals that received PvCSP-based vaccine administered either alone or in combination with Ad-M PvTRAP (median EU ~4). Consistent with the findings on IFN-γ secreting lymphocyte responses no antigenic competition phenomenon was observed for whole IgG Ab titres against both PvTRAP and PvCSP-based Ags.

This set of data showed that PvCSP and PvTRAP combination vaccine administered as heterologous prime-boost regimen employing genetically engineered ChAd63 and MVA viral vectors and recombinant proteins induce potent cellular and humoral immune responses. Moreover, consistent with the previous observations using PbCSP and PbTRAP combination immunizations administered in the identical manner, no antigenic competition was seen for both Ab and IFN-γ secreting whole-blood PBMC responses. The absence of antigenic interference affords hope that a clinically relevant PvCSP and PvTRAP combination vaccine will be more protective against malaria sporozoite challenge than the protection obtained if individual vaccine elements were administered alone.

| Group | Antigen | Priming agent | Boosting agent |
|---|---|---|---|
| **Control** | Ovalbumin (l.l.) | AdHu5 (1e10^8 iu IM) | 15 µg of OVA + Abisco 100 |
| | GFP (r.l.) | ChAd63 (1e10^8 iu IM) | MVA (1e10^7 pfu IM) |
| **PvTRAP** | *Pv*TRAP | ChAd63 (1e10^8 iu IM) | MVA (1e10^7 pfu IM) |
| **210** | *Pv*CSP VK210 | ChAd63 (1e10^8 iu IM) | 15 µg of *Pv*CSP VK210 + Abisco 100 |
| **247** | *Pv*CSP VK247 | ChAd63 (1e10^8 iu IM) | 15 µg of *Pv*CSP VK247 + Abisco 100 |
| **210+PvTRAP** | *Pv*CSP VK210 (l.l.) | ChAd63 (1e10^8 iu IM) | 15 µg of *Pv*CSP VK210 + Abisco 100 |
| | *Pv*TRAP (r.l.) | ChAd63 (1e10^8 iu IM) | MVA (1e10^7 pfu IM) |
| **247+PvTRAP** | *Pv*CSP VK247 (l.l.) | ChAd63 (1e10^8 iu IM) | 15 µg of *Pv*CSP VK247 + Abisco 100 |
| | *Pv*TRAP (r.l.) | ChAd63 (1e10^8 iu IM) | MVA (1e10^7 pfu IM) |

**Table 10: The table listing the immunization groups for PvCSP and PvTRAP combination vaccine.**

BALB/c mice (n=8/group) were vaccinated as outlined in the table. The vaccination group, antigen together with vaccine injection location (l.l. = left leg, r.l. = right leg), and prime - boost agents and their doses are included.

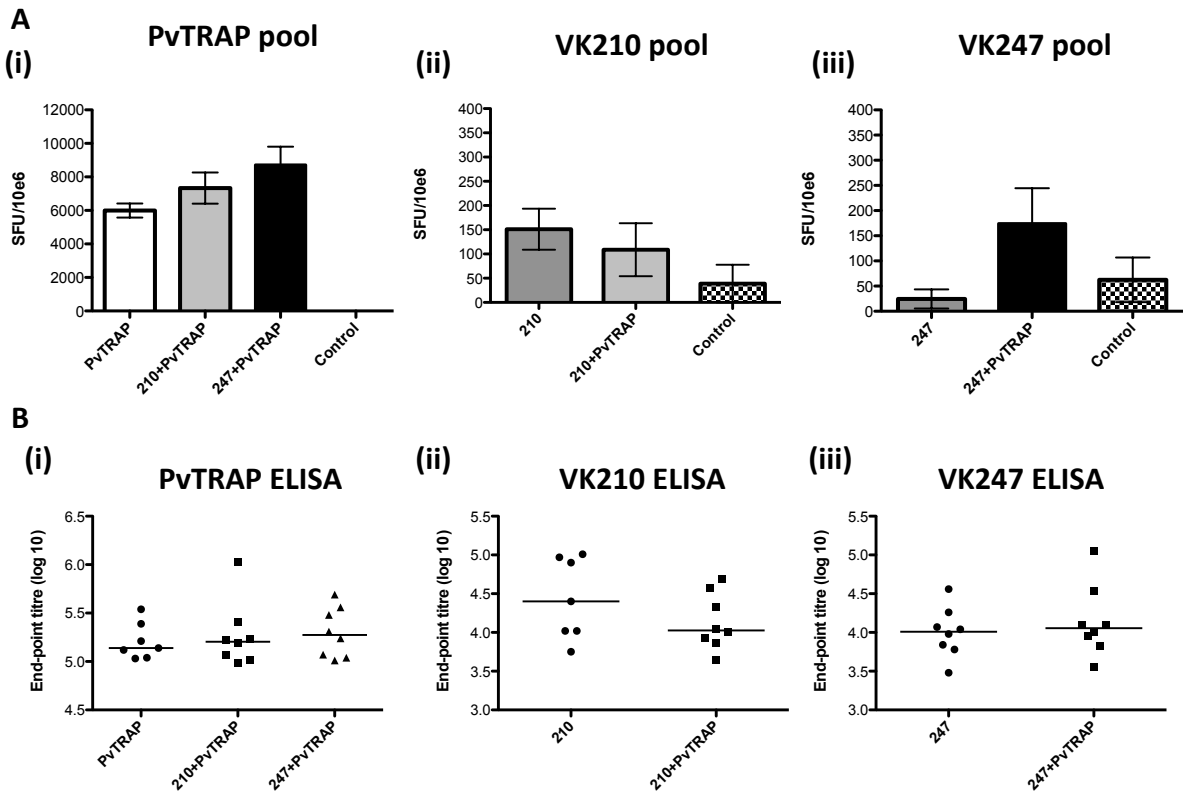


**Figure 40: Immunogenicity of PvCSP and PvTRAP combination vaccine.**

Inbred female BALB/c strain of mice (n=7-8/group) was vaccinated with heterologous prime-boost regimen expressing either different variants of PvCSP or PvTRAP alone or the combination of the two as outlined in Table 10. Two weeks after the boost (A) *ex-vivo* IFN-γ ELISPOT responses were measured upon re-stimulation of whole blood PBMCs with three sub-pools of peptides representing either the full length of (i) PvTRAP, (ii) PvCSP VK210, or (iii) PvCSP VK247 genes. Presented are the means with SEM. (B) To quantify Ag-specific whole IgG Ab titres end-point ELISA was employed coating plates with 1 µg/ml of recombinant protein corresponding to either (i) PvTRAP, (ii) PvCSP VK210, or (iii) PvCSP VK247 sequences. Individual values are plotted with lines indicating median responses.

### 6.2.2.6 Generation and assessment of tg *P. berghei* expressing both PvCSP VK210 and PvTRAP genes

To evaluate the protective potential of PvCSP and PvTRAP combination vaccine, a tg *P. berghei* encoding both transgenes was generated. A *P. berghei* mutant expressing VK210 variant of PvCS gene (termed Pb 210) whose generation is described above was used as the template. Linearized pJAZZ construct encoding PvTRAP gene and *hDHFR-yfcu* selection cassette (the generation of the construct is described in the materials and methods section 2.4.1) was electroporated into the schizont stage of Pb 210 parasites. The construct containing PvTRAP gene was integrated by double crossover homologous recombination event as a substitute for the endogenous PbTRAP gene. The location of PvTRAP cassette's integration within chromosome 13 was confirmed by southern blotting of PFG-separated chromosomes hybridized using a 3′UTR *pbdhfr/ts* probe (Figure 41A(i)). The probe also recognized reporter GFP/Luc cassette on chromosome 3, and endogenous *dhfr/ts* gene on chromosome 7. After the successful introduction of PvTRAP within Pb 210 genome mutants were cloned by limited dilution technique with the aim of obtaining homogenous population of parasites consisting only of double-tg *P. berghei*. Southern analysis was performed once more to confirm successful dilutional cloning hybridizing the chromosomes with the same 3′UTR *pbdhfr/ts* probe (Figure 41A(ii)). A strong signal in chromosome 13 was observed that corresponded with the modified PbTRAP locus in the recovered clones (2207 cl1-4) and 2207 cl1 clone was selected for further evaluation.

We next assessed the double transgenic parasite's sexual development and invertebrate host infectivity. Similar level of gametogenesis was observed when 2207 cl1 mutants were compared to GFP/Luc control parasites by visual examination of Giemsa stained blood films. This suggested that the few rounds of electroporations that mutant parasites encountered, in addition to the processes of negative and positive selection visually, did not impair gamete formation. Also, comparable numbers of oocysts and salivary gland spz were observed between the control and 2207 cl1 parasites (Figure 41B), indicating that the allelic substitution of both PbCSP and PbTRAP with the Pv homologous genes, did not affect oocyst and spz development, a process that heavily relies on the functional CS and TRAP transcripts. Finally, to evaluate double-tg *P. berghei* parasite's ability to infect vertebrate host BALB/c mice were injected with varying numbers of 2207 cl1 spz. Surprisingly, even mice receiving the lowest dose of double-tg spz became parasitaemic on day 5 post-challenge (Figure 41C), further confirming that the combined exchange of PbCS and PbTRAP genes with those of PvCS and PvTRAP did not have any detrimental consequences to the *P. berghei* parasite's vertebrate infectivity phenotype. To our knowledge, this is the first double-tg (triple if the GFP/Luc cassette is considered) *P. berghei* parasite generated for the vaccine purposes. The fact that the allelic substitution of two essential genes, involved in parasite's motility and host cell infectivity, with the homologous genes from other malaria species did not alter the parasite's infectivity phenotype has important implications for the study of parasite biology and vaccine development.

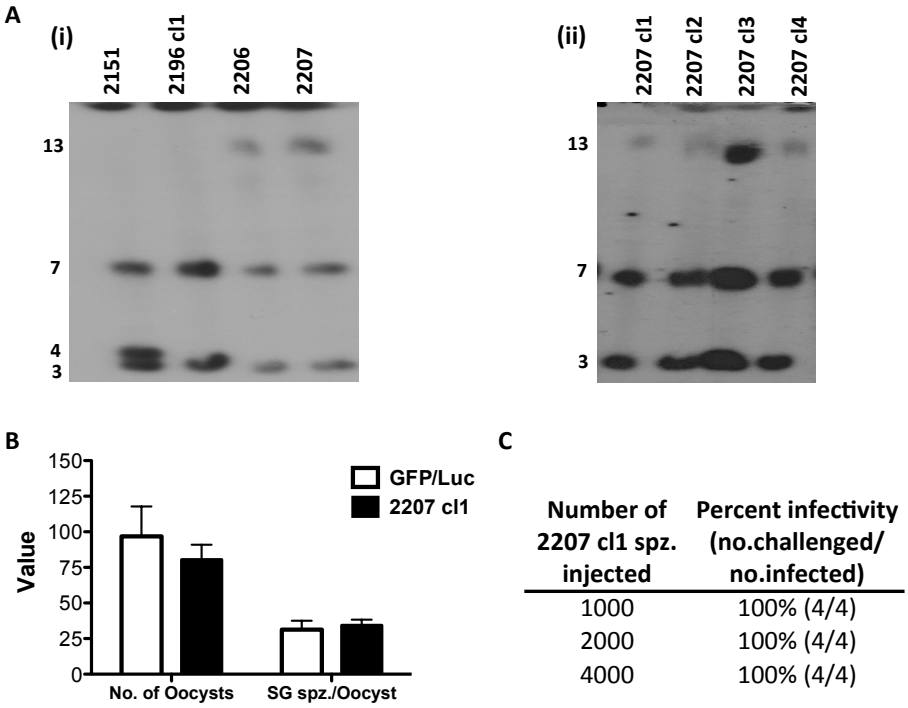


**Figure 41: Genotyping analysis and assessment of infectivity phenotype of tg *P. berghei* expressing both PvCSP VK210 and PvTRAP genes.**

(A) Southern analysis of PFG-separated chromosomes was carried out (i) before and (ii) after cloning of mutants by a limited dilution technique to confirm correct integration of the linearized PvTRAP construct (corresponds to 2206 and 2207) within the genome of 2196 cl1 (Pb 210) parasites. The exchange of wt PbTRAP gene with PvTRAP was accomplished by a double crossover homologous recombination event. PFG-separated chromosomes were hybridized using 3′UTR *pbdhfr/ts* probe, which recognizes the reporter GFP/Luc cassette on chromosome 3, the positive-negative selection marker on chromosome 4, the endogenous *dhfr/ts* gene on chromosome 7, and the modified TRAP locus on chromosome 13. Mutant 2207 cl1 corresponding to double-tg *P. berghei* expressing both PvCSP VK210 and PvTRAP genes was chosen to be used in subsequent challenge experiments. (B) The double-tg parasite's ability to develop in the invertebrate host was evaluated. 10 days post-feed on infected mice, mosquito midguts were obtained and developing oocysts enumerated for both GFP/Luc and 2207 cl1 parasites. Also, 21 days post-feed salivary gland spz were extracted and quantified. The spz quantities were adjusted to represent the number of spz per single oocyst. Data is shown as means with SEM. (C) Mutant's 2207 cl1 ability to infect vertebrate host was also evaluated by injecting varying numbers of salivary gland spz into naive BALB/c mice and monitoring for blood-stage infection.

#### 6.2.2.7 Protection conferred by the PvCSP and PvTRAP combination vaccine against a double-tg *P. berghei* spz challenge

BALB/c mice were vaccinated as described above and outlined in table 10. Two weeks after the boost, animals were challenged by IV injection of 2000 luciferase-expressing double-tg *P. berghei* spz. Pre-erythrocytic stage vaccine efficacy was assessed 44 h post-challenge employing *in vivo* imaging of whole animals (IVIS). The images obtained using live animals showed that considerably more bioluminescence (BLS), corresponding to parasite density, was emitted by animals that received vaccines either encoding single antigen or the combination of heterologous VK247 and PvTRAP (Figure 42A). As expected, the least amount of BLS was observed in the animals that were immunized with the homotypic VK210 and PvTRAP combination vaccine. The actual quantification of BLS using specialized software confirmed the conclusions generated by visual evaluation of the images. The total amount of luciferase signal (measured in total flux of photons over one second of imaging time) was highest in the control animals followed (in decreasing order) by VK247, VK210 single antigen and VK247 and PvTRAP combination vaccinations. Both PvTRAP alone and VK210 and PvTRAP combination vaccine groups were statistically significantly better protected when compared to control animals ($p<0.01$ by Kruskal-Wallis with Dunn's multiple comparison post-test) (Figure 42B). Moreover, the direct comparison of PvTRAP alone versus VK210 and PvTRAP combination groups suggested that statistically significantly better protection (ns by Kruskal-Wallis with Dunn's multiple comparison post-test, but $p = 0.04$ by Mann-Whitney test) is achieved when both PvCSP and PvTRAP antigens are incorporated into the vaccine formulation.

Blood-film analysis started on day 5 post-challenge revealed that none of the animals was sterilely protected against blood-stage infection (Figure 42C). Nonetheless, quantification of blood-stage parasitaemias over 3 consecutive days correlated strongly with the results seen after IVIS. The highest level of blood-stage prepatency delay, measured as Tto1, was recorded for the VK210 and PvTRAP combination group (Figure 42D). Moreover, the protection seen by VK210 and PvTRAP combination vaccine was yet again statistically significantly better than the protection observed with the second best regime corresponding to PvTRAP alone immunization (ns by Kruskal-Wallis with Dunn's multiple comparison post-test, but p=0.01 by Mann-Whitney test). Interestingly, the VK247 and PvTRAP combination vaccine was substantially worse than the combined VK210 and PvTRAP immunization in protecting against double-tg *P. berghei* encoding VK210 variant of the CS gene. It further strengthened the evidence suggesting that the protection induced by PvCSP VK210-based vaccine is strain-specific.

These challenge studies further confirmed that when co-administered in separate legs CSP- and TRAP-based antigen vaccinations induce superior protection to what is obtained if these antigens are employed alone. Also, this set of data demonstrates the importance of including the homologous allele of PvCSP to that present in the challenge parasites if the full potential of the PvCSP and PvTRAP combination vaccine is to be fulfilled.

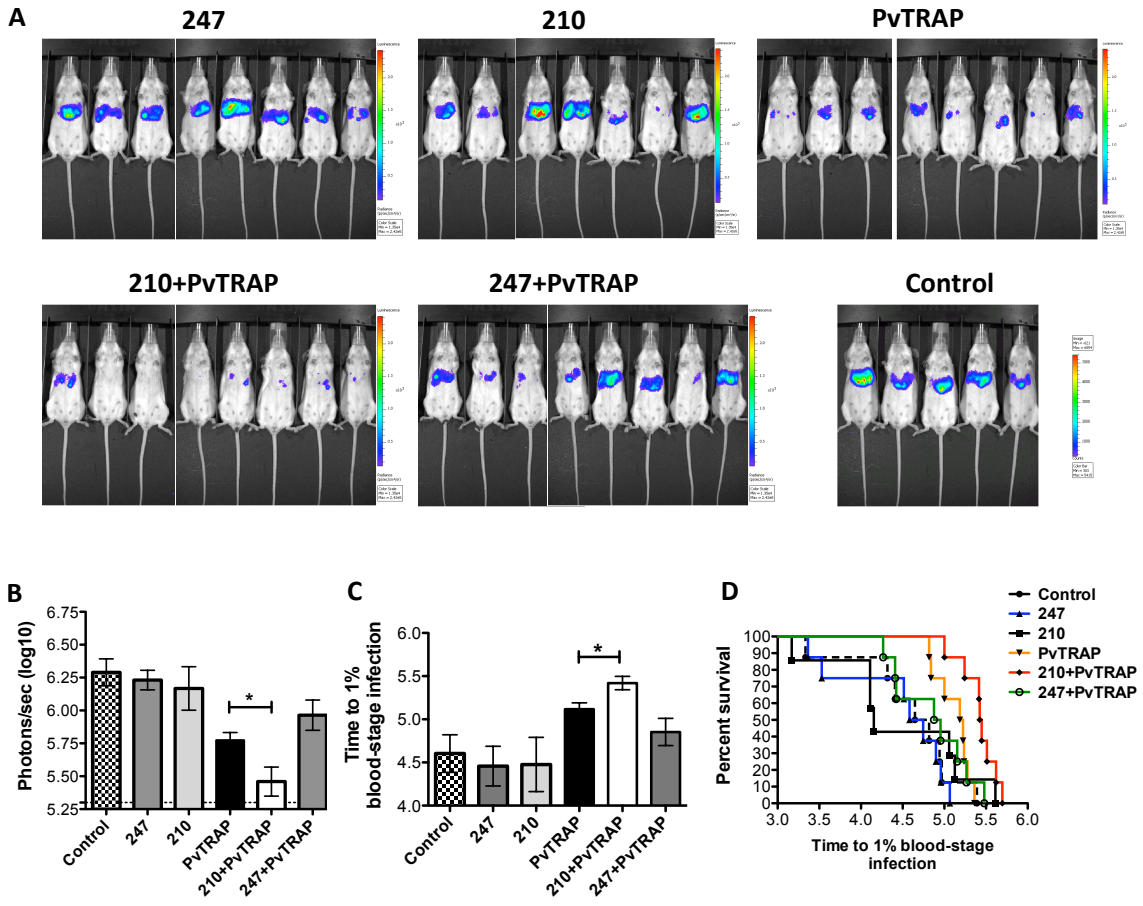


**Figure 42: Pre-erythrocytic stage efficacy of PvCSP and PvTRAP combination vaccine.**

Female BALB/c strain of mice (n=7-8/group) was vaccinated with a heterologous prime-boost regime as outlined in table 10. Two weeks after the last vaccination animals were challenged by IV injection of 2000 double-tg *P. berghei* spz (2207 cl1) expressing GFP/Luc cassette. (A) At 44 h post-challenge *in vivo* imaging of whole animals was performed using IVIS. The name of the vaccination group is indicated above the image. (B) Also, the BLS corresponding to liver stage parasite load was quantified using Living Image 4.3 analysis software. (C) Blood-stage infection over three consecutive days starting at day 5 post-challenge was recorded and linear regression model predicting Tto1 for individual animals generated. (D) Prediction values were subsequently used in Kaplan-Meier survival analysis showing a substantial delay in the group that received PvCSP VK210 and PvTRAP combination vaccine as compared to the other treatment groups. Means with SEM are represented. *p<0.05, Mann-Whitney test comparing two groups.

### 6.2.3 Discussion

A recombinant chimpanzee adenovirus-based viral vector ChAd63 vaccine expressing PvCSP VK210 variant was immunogenic in four different mice strains tested, including BALB/c, C57BL/6, C3H, and CD1. To my knowledge, this was the first attempt to immunize rodents with ChAd63 encoding CS antigen from *P. vivax* malaria.

A considerable degree of antibody cross-reactivity against the heterologous variant of the gene observed two weeks after ChAd63 PvCSP VK210 immunization was anticipated. N- and C- terminal ends of the protein are relatively conserved between the two different variants of PvCSP (Figure 35). Moreover, antibody responses against those non-repetitive parts of the protein have been documented in individuals exposed to *P. vivax* infection (328). Indeed, it is possible that some level of antibody cross-reactivity could also occur against a heterologous central repeat region.

For further analysis of PvCSP-based constructs, heterologous prime-boost regimens employing ChAd63 and recombinant proteins adjuvanted with Abisco 100 (abbreviated Ad-P) was used. De Cassan *et al.* demonstrated the Ad-P regime's potency in inducing high-titre abs, also resulted in improved efficacy against a *P. yoelii* blood-stage challenge (217).

To assess the protective efficacy of Ad-P regimes containing different PvCSP constructs, two tg *P. berghei* parasites expressing either VK210 or VK247 were generated. The previous attempts to construct tg *P. berghei* mutants containing full-length CS genes from other malaria species resulted in parasites with highly reduced ability to both infect mosquito salivary glands and mammalian host (67, 337). Moreover, recently it was

shown that a mere inclusion of a selection cassette downstream of endogenous PbCS gene alters the wt *P. berghei*'s infectivity phenotype (236). To circumvent that problem, the 'gene insertion/marker out' (GIMO) technology was employed allowing the generation of marker-free tg *P. berghei* (251). To further take advantage of the GIMO technology PvCS constructs were codon-optimized for expression in *P. berghei*, although it was not tested whether that had any effect on PvCS transcript levels.

Using newly generated *P. berghei* mutants expressing either the VK210 or VK247 allele, it was confirmed that the vaccine-induced protection was strain-specific, an observation that was consistent with some other existing evidence. Biswas *et al.* demonstrated that AdHu5-MVA prime-boost vaccination in mice and rabbits using these vectors encoding the 3D7 allele of PfAMA1 induced high cellular and humoral immune responses that showed growth inhibitory activity (GIA) against the homologous but not heterologous parasite strains (213). Interestingly, no protection was observed when Ad-P NC vaccination group was challenged with Pb 210 tg parasites, despite having the highest PbCSP-specific whole IgG antibody titres measured by end-point ELISA. It is possible, that inhibitory Abs simply were not induced as further improvements to the NC construct design may be necessary (refer to future directions within thesis discussion section for more detail). Another explanation for low level protection observed in the NC group could be that hepatocyte invasion inhibitory epitopes present on N- or C-terminal domains are shielded from Ab attack by the protein's conformational changes that take place during spz's travel from mosquito salivary glands to the site of infection within host liver (76). Nonetheless, the use of tg *P. berghei* parasites expressing different PvCSP

alleles allows a further study and optimization of PvCSP-based vaccines, including constructs targeting either just N- and C- terminal domains or those incorporating repeat region sequences constituting both VK210 and VK247 alleles of PvCS gene.

PfCSP-based RTS,S/AS01 vaccine efficacy was 34.8% against severe malaria in the combined age categories during an average follow-up of 11 months in the ongoing Phase III clinical trial (161). It is difficult to imagine that the PvCSP-based vaccine by itself in the Ad-P regime could confer the sufficient level of protection required to interrupt the transmission of *P. vivax* malaria. Therefore, the potential of combining Ad-P PvCSP and Ad-M PvTRAP vaccines was investigated.

The observed humoral and cellular immune responses after administering PvCSP and PvTRAP combination vaccine in heterologous prime-boost regime employing genetically engineered replication-incompetent ChAd63 and MVA viral vectors and PvCSP-based recombinant proteins formulated in Abisco 100 were consistent with previous experiments. High numbers of PvTRAP-specific IFN-γ secreting lymphocytes were recorded in all PvTRAP construct containing vaccination groups. On the other hand, relatively low numbers of whole-blood PBMCs obtained from groups immunized with PvCS-based vaccines alone or in combination with Ad-M PvTRAP were secreting IFN-γ. Considering the vaccination and challenge studies performed employing Ad-M PvTRAP regime in BALB/c model (the first part of this chapter), it is safe to assumed that most of the IFN-γ response was generated by PvTRAP-specific $CD8^+$ T cells. The absence of antigenic competition between Ad-M PvTRAP alone and combination groups was

consistent with previous observations made using PbCSP and PbTRAP combination vaccines in C57BL/6 mice (chapter 3).

Unfortunately, relatively low levels of PvCSP-specific whole IgG Ab levels were measured against both VK210 and VK247 constructs in BALB/c strain of mice. In light of the results obtained using identical immunizations with CD1 strain of mice, where high-titre PvCSP-specific Abs were induced, it is difficult to explain the low levels of abs and further dose-escalation studies may be necessary to delineate the required concentration of recombinant protein for optimal induction of Ab responses. Also, it is possible that BALB/c is less amenable to Ag-specific Ab induction than CD1 strain of mice when Abisco 100 adjuvant is employed, therefore it may also be useful to test the Ad-P PvCSP regimen using different adjuvant formulations.

The generation of phenotypically 'fit' double-tg *P. berghei* expressing both PvCSP and PvTRAP genes in addition to a GFP/Luc cassette is an important milestone not only for the tg *P. berghei* technology, but also for the investigation of questions pertaining to parasite biology. For the field of vaccinology, the construction of double-tg *P. berghei* provides an elegant way of evaluating *in vivo* protective efficacy associated with different human malaria antigen combinations.

Both protection readouts, including IVIS and analysis of blood films, supported the hypothesis that a PvCSP and PvTRAP combination vaccine would induce superior protection when compared to the same antigens administered alone. Disappointingly, unlike the outcome observed with the PbCSP and PbTRAP co-administration immunizations using C57BL/6 strain of mice, no synergy in protection was seen in the

PvCSP and PvTRAP combination group, as all of the animals developed potent blood-stage infection. The PbCSP and PbTRAP combination vaccine results in synergistic effect, because PbCSP element is able to neutralize the vast majority of *P. berghei* spz. The remainder of the spz that manage to escape the initial attack of PbCSP-specific antibodies and are successful in establishing exo-erythrocytic forms within infected hepatocytes are subsequently destroyed by PbTRAP-specific cytotoxic $CD8^+$ T cells. In the case of PvCSP and PvTRAP combination vaccine, the lack of synergistic effect could be attributed to the fact that not enough double-tg *P. berghei* sporozoites are neutralized by Ad-P PvCSP arm of the vaccine, and, thus, the inclusion of Ad-M PvTRAP immunization in the combination groups does not afford sterile protection. A lower challenge dose and/or the development of more protective PvCSP-based vaccine construct could potentially tip the balance towards more protective efficacy elicited by the PvCSP and PvTRAP combination vaccine.

In conclusion, this chapter describes the development of novel human malaria *P. vivax* pre-erythrocytic stage vaccines based on CSP and TRAP antigens. The heterologous Ad-M prime-boost regimen encoding PvTRAP was immunogenic in three different strains of mice and elicited high levels of sterile protection against the tg *P. berghei* spz challenge. Similarly, Ad-P PvCSP vaccination strategy induced high-titre Abs in CD1 mice that were able to protect against homologous strain of tg *P. berghei* mutant. Finally, the protective potential of PvCSP and PvTRAP combination vaccine was also evaluated and the results suggested that superior protective efficacy is possible to achieve when both antigens are co-administered rather than used individually.

# Chapter 7

# Discussion and Future Directions

# 7 Discussion and Future Directions

## 7.1 Overview

The first part of this thesis employed the *P. berghei* mouse malaria model to identify the most protective pre-erythrocytic stage antigens (Ag) and Ag combination using heterologous chimpanzee adenovirus 63 (Ad) and modified vaccinia strain Ankara (MVA) prime-boost strategy (Ad-M). The Ad-M regimen has been demonstrated to induce strong humoral and cellular immune responses in mice (165, 254), rabbits (213), rhesus macaques (214), and humans, showing an excellent safety profile in the latter (208, 209) using different malarial antigens. Three pre-erythrocytic stage antigens chosen for the initial *P. berghei* challenge studies included circumsporozoite (CS) and thrombospondin-related adhesive proteins (TRAP), and cell-traversal protein for ookinetes and sporozoites (TOS). Both CSP and TRAP individually have been extensively explored in the vaccine setting in pre-clinical (264) (Hafalla *et al.* submitted) and clinical studies (220)(Ewer *at al.* submitted) employing various vaccine platforms. Part of the *P. falciparum* CS protein has been shown to be the most protective malaria vaccine to date, a protein particle termed RTS,S which is undergoing Phase III clinical trials (161). Similarly, *P. falciparum* TRAP is the major antigen in the highly efficacious Ad-M prime-boost vaccine encoding the ME.TRAP transgene (Ewer *et al.* submitted). Unlike CSP and TRAP, a TOS-based vaccine has not been evaluated in the experimental *P. falciparum* spz challenge model in humans. However, existing pre-clinical studies in mice have demonstrated that when administered as protein-in-adjuvant vaccine based recombinant PfTOS conferred a relatively high degree of protection against a

heterologous *P. berghei* challenge (88). This indicates that immune responses induced using this antigen could sterilely protect against malaria. Thus, the need to evaluate these three antigens against each other within the same vaccine platform in order to find out their protective potential was addressed. Also, the protective potential of combining these pre-erythrocytic stage vaccine candidates was explored.

The head-to-head comparison of CSP, TRAP, and TOS antigens using heterologous Ad-M prime-boost strategy revealed that in the highly susceptible to *P. berghei* malaria C57BL/6 strain of mice the statistically significant level of protection was observed only using PbTRAP- and PbCSP-based viral vector vaccines. The immunity conferred by PbCelTOS antigen was not statistically significantly different from the control mice despite inducing high-titre antibody (Ab) responses. Interestingly, similar observations were made when the more genetically diverse outbred CD1 strain of mice was used.

None of the antigen combination vaccines tried in C57BL/6 and CD1 strains of mice induced statistically significantly superior immunity when compared to the most protective single Ag immunization. However, a trend towards increased immunity was observed when PbTRAP and PbCSP antigens were co-administered into separate sites, suggesting that this particular combination could offer a high degree of protective efficacy if it was carefully tailored for the concurrent induction of higher Ab and T cell responses. Therefore, the remainder of the thesis focused on improving the protective efficacy associated with *P. berghei* and *P. vivax* TRAP- and CSP-based vaccine constructs administered individually or in combination.

The monoclonal Ab (mAb) 3D11 specific against the central repeat region of PbCSP Ag was used to delineate anti-PbCSP Ab requirements necessary for sterile protection in C57BL/6 animal model. As expected, a clear dose-dependence effect was observed whereby with increasing amounts of 3D11 there also was an increase in number of animals sterilely protected against *P. berghei* challenge (159). Also, consistent with other reports, extremely high concentration of anti-CS 3D11 was required for complete sterile protection. Interestingly, substantially lower amounts of 3D11 were sufficient for sterile protection if the mAb vaccinations were performed on previously Ad-M PbTRAP immunized animals. Moreover, an interaction between 3D11 and anti-PbTRAP immune responses resulted in synergistic protection, suggesting that it may be possible to induce superior immunity using CS and TRAP combination in an active vaccination setting if higher anti-CS Ab responses than those observed after Ad-M PbCSP immunization were induced. Thus, the heterologous Ad prime – protein-in-adjuvant boost (Ad-P) regimen for the administration of PbCSP antigen was explored, since a few reports have previously suggested that Ad-P regimen induces significantly higher Ab responses when compared to these regimens administered individually (214, 215, 217).

The immunization of C57BL/6 mice using the Ad-P PbCSP and Ad-M PbTRAP combination vaccine conferred an exceptionally high level of sterile protection when each antigen was administered into separate sites. Interestingly, Ad-P PbCSP and Ad-M PbTRAP combination vaccine administered as a mixture into a single site at the time of prime and boost, despite demonstrating significantly higher levels of protection when compared to individual antigen immunizations, were less protective than separate-site

vaccination strategy. The mixing of vaccines prior to single-site administration seemed to increase antigenic interference between PbTRAP and PbCSP immunogens, resulting in the diminished immune responses against individual antigens, which, in part, could explain the lower level of protective efficacy.

The observations generated using *P. berghei* challenge model were then applied to the development of a human malaria *P. vivax* CS- and TRAP-based combination vaccine. Since *P. vivax* does not infect rodents, transgenic (tg) *P. berghei* parasites each expressing the relevant *P. vivax* antigen were generated and used for the challenge studies. The Ad-M PvTRAP vaccination not only induced high-titre Abs and powerful T cell responses, but also conferred a statistically significant level of sterile protection in BALB/c, C57BL/6, and CD1 strains of mice. Also, Ad-P vaccine encoding different PvCSP alleles induced relatively high titres of Abs against the antigen and protection was observed against the homologous strain of tg *P. berghei*. Interestingly, consistent with the results obtained using PbTRAP and PbCSP Ags in C57BL/6 mice, Ad-M PvTRAP and Ad-P PvCSP combination vaccine administered into the separate sites into BALB/c animals elicited superior levels of protection when compared to those vaccines administered individually. The similar results obtained immunizing mice with *P. berghei* vaccines against the *P. berghei* challenge, and *P. vivax* vaccines against the tg *P. berghei* challenge in different mouse strains indicated that one overriding protection mechanism might be at play.

## 7.2 Conclusions and future directions

### 7.2.1 Comparative assessment of pre-erythrocytic stage antigens

Inbred C57BL/6 and outbred CD1 strains of mice were used for the comparative screen of three pre-erythrocytic stage antigens, including PbTRAP, PbCSP, and PbTOS. These antigens were all administered as individual Ad-M prime-boost vaccines. In C57BL/6 model the Ag-specific $CD8^+$ T cell and Ab responses were associated with protection following Ad-M vaccinations encoding either PbTRAP or PbCSP transgenes, respectively, whereas no protective efficacy was observed after immunizing with Ad-M PbTOS construct. The vaccination of mice with Ad-P PbTOS regimen, which is meant to enhance Ab responses when compared to Ad-M regimen, also did not elicit significant level of protection. Consequently, PbTRAP and PbCSP antigens were taken forward for further development. However, overall conclusions drawn from these initial comparative studies using particular mice strains have to be treated carefully for couple of reasons.

For a T-cell inducing vaccine, as in the case of Ad-M immunization, to be able to protect against a malaria challenge two factors are crucial. First, it is important that the target antigen is immunogenic towards T cell induction. The stimulation of T cell immunity following Ad-M regimen is largely dependent on the presence of immunodominant epitopes within the antigen of interest. PbTRAP, unlike PbCSP and PbTOS antigens, has a protective H-2K(b)-restricted immunodominant $CD8^+$ T cell epitope (Hafalla *et al.* submitted) and thus the induction of high number of these cells was observed following Ad-M PbTRAP vaccination. However, while stimulation of powerful T cells is required for protection following Ad-M vaccination, high level of T cell immunogenicity alone

may not be sufficient to guarantee the protection. $CD8^+$ T cells exert their cytotoxic effector functions through recognition of MHCI-epitope complexes loaded onto the surface of the infected hepatocytes. Since the parasite's intrahepatic development is confined within the parasitophorous vacuole, which forms a physical barrier between the host cell cytoplasm and the exo-erythrocytic forms of parasite, it seems that the export of parasite proteins outside the parasitophorous vacuole is tightly regulated (338, 339) and only crucial proteins necessary for parasite's liver stage development may be granted access to the hepatocyte cytosol (75). Therefore, for a T cell vaccine to be able to afford protection not only the target antigen needs to be immunogenic, but also it has to be present within hepatocyte's cytoplasm. From there the target antigen can be processed and loaded onto the MHCI molecules, the process that has been shown to use the transporters associated with antigen processing (TAP) to access the endoplasmic reticulum (340).

Therefore, the lack of protective efficacy associated with PbTOS cannot be generalized to other homologous genes or mice strains. The protection in C57BL/6 model depended on the presence of protective T cell epitopes or high Ab titres. It could simply be that this particular mouse strain lacked the PbTOS-associated protective epitope(s), therefore the T cell inducing PbTOS vaccine could not be properly evaluated. Therefore, it would be interesting to see whether other strains of mice with different genetic background, including BALB/c and C3H would contain an immunodominant epitope, which then would permit the more conclusive evaluation of Ad-M PbTOS vaccine. However, even then different strains of mice are not equally susceptible to malaria infection (273),

therefore the direct evaluation of 'antigenicity' associated with these three or other pre-erythrocytic stage antigens becomes complicated if multiple strains of mice are employed. Therefore, if one wishes to comparatively assess the potential of T cell-inducing vaccine for different pre-erythrocytic stage malaria antigens, more elegant way than 'raw' immunizations may be necessary. Through the use of tg *P. berghei* technology, it would be possible to generate mutant parasite lines that have model $CD8^+$ T cell epitopes engineered within each pre-erythrocytic stage antigen of interest. The H-2K(b) epitope SIINFEKL is highly immunogenic in C57BL/6 strain of mice and it has been demonstrated that the injection of high numbers of epitope-specific $CD8^+$ T cells protected mice against tg *P. berghei* expressing mutant CS containing this immunodominant epitope (340). Similarly, tg *P. berghei* expressing mutant TRAP and TOS genes containing SIINFEKL could be generated and used to directly compare the 'antigenicity' associated with these antigens in the same strain of mice vaccinated with Ad-M regimen encoding the immunodominant epitope. This way the 'antigenicity' and the protective efficacy associated with these tg mutants could be evaluated and used to draw valid conclusions about which Ag(s) would have the highest chance of protecting against experimental sporozoite challenge when used in T cell-inducing Ad-M vaccine regimen.

### 7.2.2 Killing intrahepatic forms of malaria parasite

The mechanistic cell depletion experiments performed on Ad-M PbTRAP and 3D11 mAb immunized mice have demonstrated that the protection induced by this combination vaccine was mediated by anti-PbCSP Abs that are capable of neutralizing a large

proportion of spz, whereas PbTRAP-specific $CD8^+$ T cells and liver-resident NK cells were important during the second line of defense against the remainder of parasites that managed to establish intrahepatic infection. The protection mediated by highly protective irradiated spz vaccination, through the use of depletion and adoptive as well as passive transfer studies, has also been shown to be dependent on cellular and humoral immune responses against various spz stage antigens (341). However, the precise mechanism of $CD8^+$ T cell mediated killing of intracellular parasites in C57BL/6 or other mice models remains to be determined. The extensive literature on the subject suggests that the type of protective $CD8^+$ T cell effector functions utilized against the intrahepatic parasites depend not only on the mice strain used, but also vaccination strategy (150). While perforin, Fas ligand (FasL), and IFN-γ are well-documented mediators of $CD8^+$ T cell effector functions, the protective $CD8^+$ T cell responses can be generated in perforin (342), FasL (342), and IFN-γ (343) knockout mice models. Also, some reports suggest that the direct contact of $CD8^+$ cytotoxic T lymphocytes (CTLs) with the infected hepatocyte is crucial (344) in order for the CTLs to exercise their effector functions. Interestingly, it is known that CTLs can secrete relatively large amounts of IFN-γ and this cytokine is able to kill developing intracellular parasites through the induction of nitric oxide (NO) molecule (258, 345). Since IFN-γ has many pleiotropic effects it is possible that the release of this cytokine by CTLs may also interfere with parasite development inside hepatocytes located in the periphery. Rhea Longley (a graduate student in the Hill group) *et al*. has developed an *in vitro* T cell killing assay, whereby Ag-specific T cells can be introduced onto parasite infected hepatocyte lines and the level of hepatocyte infection can be quantified using flow cytometry techniques. Through the use of this

assay a consistent killing of infected hepatocytes by PbTRAP-specific $CD8^+$ T cells was observed (unpublished data/in preparation). Moreover, by employing this assay it would be interesting to further dissect the molecular basis behind the $CD8^+$ T cell effector functions.

### 7.2.3 Tg *P. berghei* technology

Tg *P. berghei* technology has revolutionized the malaria field. Various knockout tg *P. berghei* clones have been instrumental in deciphering parasite protein functions (232), mechanisms of severe malaria pathology (346), or basic parasite biology (347). Less commonly tg *P. berghei* models have also been used in the vaccine studies where they offer an *in vitro* or *in vivo* assessment of functional immunogenicity.

In this thesis four novel tg *P. berghei* parasites were generated and utilized to assess *P. vivax* malaria vaccine efficacy in mouse models. Surprisingly, the infectivity phenotype of tg parasites generated in this thesis was comparable to the wild-type (wt) *P. berghei* parasites. In part, this could possibly be explained by the decision to codon-optimize the *P. vivax* transgenes, which naturally are GC-rich (348), for the expression within the AT-rich *P. berghei* genome. Additionally, the novel cloning strategy permitting the removal of the resistance cassette could have possibly contributed to the excellent tg *P. berghei* infectivity profile, particularly for mutants carrying PvCSP genes. It has been shown that merely inserting *hDHFR* resistance marker downstream of otherwise unaltered PbCSP gene negatively affected the transgenic parasite's ability to infect mosquito and vertebrate hosts (236), suggesting that preserving the wt 3'UTR PbCSP region may be crucial for successful transcription termination.

Also, the recycling of selection marker allowed the insertion of the second *P. vivax* pre-erythrocytic stage antigen into tg *P. berghei* already carrying PvCSP VK210 allele. Moreover, the double-tg parasite's infectivity of mice was comparable to the wt parasites. The successful making of double-tg *P. berghei* is not only curious from the tg parasite technology point of view, but also may provide some insights related to the basic biology of malaria pre-erythrocytic stage. It would be interesting to see how many (if any) more genes from *P. vivax* could be inserted into the *P. berghei* genome without jeopardizing parasite's infectivity. Also, it is known that both CSP and TRAP proteins are essential for the attachment and initiation of liver stage infection (67, 78, 79). Therefore, it would be interesting to attempt infecting normally non-permissible to wt *P. berghei* infection human hepatocytes *in vitro* using these double-tg *P. berghei* parasites or any other tg where as many as possible *P. berghei* genes were substituted with *P. vivax* homologs. Also, then perhaps through the use of these multi-antigen tg *P. berghei* parasites it would be possible to determine the relative contribution and importance of different human malaria genes for the hepatocyte infection and that way the key determinants of infectivity could be targeted by the vaccine. Finally, provided that multi-antigen tg *P. berghei* could establish an intrahepatic infection in humans, it would be interesting to see whether these *P. berghei* mutants could be employed for the whole-parasite vaccination strategies.

In conclusion, the generation of tg *P. berghei* expressing different pre-erythrocytic stage *P. vivax* antigens provide useful tools for the malaria vaccine community. The use of these tg models should expedite the development and optimization of *P. vivax* CSP- or

TRAP-based vaccines. Also, the most advanced vaccines that are based on the same antigens from other labs around the world could be assessed head-to-head in mice rather than humans immensely reducing the cost associated with human clinical trials.

### 7.2.4 Evaluation of *P. vivax* vaccines

This thesis evaluated novel *P. vivax* vaccines based on leading pre-erythrocytic stage antigens, including PvCSP and PvTRAP. PvCSP antigen, coded by two alleles named VK210 and VK247, was assessed in Ad-P regimen. The vaccination of CD1 strain of mice induced high-titre Ab responses whereas relatively low numbers of T cells were stimulated following this vaccine approach. The challenge results revealed that the protection was PvCSP allele-specific. Therefore, a successful PvCSP vaccine would require the incorporation of antigenic determinants from both VK210 and VK247 variants in order to be globally efficacious.

The Ad-P vaccination using chimeric PvCSP constructs expressing repeat regions from both VK210 and VK247 variants induced comparable immunogenicity to mono-allelic PvCSP constructs. Also, similar levels of protective efficacy against VK210 transgenic parasites was observed. These results add to previous studies demonstrating that soluble chimeric PvCSP protein vaccine termed VMP001 administered with Montanide ISA-720 adjuvant was capable of inducing Ab responses that recognized both VK210 and VK247 wt *P. vivax* parasites (335). It would be interesting to assess VMP001 vaccine in the challenge study employing tg *P. berghei* parasites expressing PvCSP alleles in various mice models. Also, using the tg parasite model, it would be curious to see if homologous prime-boost strategy employing the same soluble protein formulated in different

adjuvants would elicit higher level of protective efficacy than that seen after Ad-P regimen, although the current evidence suggests that two-shot protein immunizations result in lower immunogenicity than Ad-P immunization (217).

Further optimization of PvCSP construct itself may also enhance the protection against tg *P. berghei* parasites observed in this thesis. *P. falciparum* CSP comprising the highly efficacious RTS,S vaccine is administered fused to hepatitis B surface antigen forming a highly stable protein particle. The *P. berghei* tg expressing *P. falciparum* CSP, which would allow the evaluation of RTS,S in mice has long been sought, however, the published attempts to generate the tg have indicated that the parasites were suboptimal in infecting vertebrate livers (67). Therefore, it would be interesting to try synthesizing RTS,S-like protein particle based on PvCSP antigen and use with the most optimal vaccination regimen in the challenge studies.

Interestingly, the Ad-P vaccinations with highly conserved N- and C-terminal domains (NC) of PvCSP did not elicit any protection despite inducing relatively high Ab responses further strengthening the observations that immunity elicited by CSP-based vaccines is mostly based on Abs against central repeat region (329). It suggests that it may not be necessary to have full-length PvCSP protein, which has been difficult to synthesize, in order to obtain optimal protection. Therefore, a stable, easily synthesized and cheap protein or protein particle could possibly be employed with equal or higher protective efficacy.

The protective potential of PvTRAP antigen was also evaluated using the Ad-M prime-boost vaccine strategy. Administration of this virally vectored vaccine induced PvTRAP-

specific high-titre Abs and strong T cell responses in multiple strains of mice. Further T cell depletion experiments coupled with Ag-specific whole IgG passive transfer vaccinations of naïve mice suggested that both cellular and humoral factors were important for the protective immunity. Schneider *et al.* has demonstrated that higher level of immunogenicity could be achieved by intravenous administration of MVA viral vectors. Therefore, further improvements to sub-optimal protection observed after intramuscular administration of MVA PvTRAP could be made by administering the vaccine agent intravenously. However, currently it is not routinely possible to inject MVA IV into human volunteers, therefore, the results obtained after using this route may have little clinical relevance.

Alternatively, higher T cell immune responses against *Mycobacterium tuberculosis* antigen 85A have been achieved by fusing IMX313 oligomerization domain to the C-terminal end of the immunogen (222). Therefore, it would be interesting to explore whether it would be possible to increase PvTRAP-specific T cell responses by incorporating IMX313 into the vaccine design, and if so, would those higher cellular immune responses transfer to the enhanced protective efficacy.

The most protective regimen incorporating Ad-M PvTRAP and Ad-P PvCSP vaccines required manufacturing of two different recombinant Ad and single MVA viral vectors, and synthesis of PvCSP soluble protein. Currently such regimen, if proven successful in further pre-clinical and clinical studies, could be too expensive to deploy for wide-scale vaccinations. Therefore, cheaper formulations may be necessary. One way to make Ad-M PvTRAP and Ad-P PvCSP combination vaccine more affordable could be to incorporate

both PvCSP and PvTRAP antigens within the genome of one Ad viral vector for the use as a single injection at the prime. The Glycine-Proline (GGGPGGG) linker has been employed successfully to fuse two different AMA-1 alleles in tandem and place the construct within the backbone of single recombinant Ad virus (213). Moreover, these bi-allelic AMA-1 constructs induced comparable immunogenicity to mono-allelic vaccines, suggesting that antigenic interference contributed little (if any) to the induction of immune responses. Alternatively, viral 2A sequences that mediate self-cleavage reaction have been used to reliably co-express two proteins within a single lentiviral vector (349). If employed, 2A sequence could be inserted between PvCSP and PvTRAP antigens in a single open reading frame (ORF), which would yield two discrete proteins at the end of polypeptide translation, leading to the need of only one recombinant Ad rather than two as it is the case with current mode of vaccination.

## 7.3 Final Remarks

Currently the most protective pre-erythrocytic stage malaria vaccine candidates in human clinical trials – RTS,S and Ad-M ME.TRAP – rely on the induction of high Ab titres and powerful T cell responses, against CS and TRAP proteins, respectively. However, individually both vaccine agents elicit only sub-optimal protection against experimental malaria sporozoite challenge.

This thesis described the development of novel *P. vivax* CS- and TRAP-based vaccines and evaluated their potential in protecting against the tg *P. berghei* parasites. Ad-M administration of PvTRAP antigen stimulated Ag-specific humoral and cellular immune responses and conferred protection against tg *P. berghei* challenge in multiple mice

strains. Similarly, a substantial degree of protection was achieved following Ad-P PvCSP VK210 vaccination against the homotypic strain of tg *P. berghei* expressing PvCSP. Furthermore, concurrent induction of high-titre Abs and potent T cell responses was accomplished by a Ad-M PvTRAP and Ad-P PvCSP combination regimen, which also resulted in the superior protection. Further optimization of Ad-M PvTRAP and Ad-P PvCSP combination vaccine is underway to make the regime more protective and feasible for large-scale vaccinations. The most promising vaccine approach will then be taken into an *Aotus* monkey *P. vivax* challenge study to further assess the clinical utility of this combination vaccine in the fight against *P. vivax* malaria.

**References:**


1. Escalante AA, Ayala FJ. 1994. Phylogeny of the malarial genus Plasmodium, derived from rRNA gene sequences. *Proc Natl Acad Sci U S A* 91: 11373-7
2. Knowles R DGB. 1932. A study of monkey-malaria and its experimental transmission to man. *Indian Medical Gazette* 67: 301-20
3. Gething PW, Elyazar IR, Moyes CL, Smith DL, Battle KE, Guerra CA, Patil AP, Tatem AJ, Howes RE, Myers MF, George DB, Horby P, Wertheim HF, Price RN, Mueller I, Baird JK, Hay SI. 2012. A Long Neglected World Malaria Map: Plasmodium vivax Endemicity in 2010. *PLoS Negl Trop Dis* 6: e1814
4. WHO. 2011. The World Health Report. 278
5. Guerra CA, Howes RE, Patil AP, Gething PW, Van Boeckel TP, Temperley WH, Kabaria CW, Tatem AJ, Manh BH, Elyazar IR, Baird JK, Snow RW, Hay SI. 2010. The international limits and population at risk of Plasmodium vivax transmission in 2009. *PLoS Negl Trop Dis* 4: e774
6. Greenwood BM, Bojang K, Whitty CJ, Targett GA. 2005. Malaria. *Lancet* 365: 1487-98
7. Sachs J, Malaney P. 2002. The economic and social burden of malaria. *Nature* 415: 680-5
8. Murray CJ, Rosenfeld LC, Lim SS, Andrews KG, Foreman KJ, Haring D, Fullman N, Naghavi M, Lozano R, Lopez AD. 2012. Global malaria mortality between 1980 and 2010: a systematic analysis. *Lancet* 379: 413-31
9. Penny MA, Maire N, Studer A, Schapira A, Smith TA. 2008. What should vaccine developers ask? Simulation of the effectiveness of malaria vaccines. *PLoS One* 3: e3193
10. Maire N, Tediosi F, Ross A, Smith T. 2006. Predictions of the epidemiologic impact of introducing a pre-erythrocytic vaccine into the expanded program on immunization in sub-Saharan Africa. *Am J Trop Med Hyg* 75: 111-8
11. Baer K, Klotz C, Kappe SH, Schnieder T, Frevert U. 2007. Release of hepatic Plasmodium yoelii merozoites into the pulmonary microvasculature. *PLoS Pathog* 3: e171
12. Krotoski WA, Collins WE, Bray RS, Garnham PC, Cogswell FB, Gwadz RW, Killick-Kendrick R, Wolf R, Sinden R, Koontz LC, Stanfill PS. 1982. Demonstration of hypnozoites in sporozoite-transmitted Plasmodium vivax infection. *Am J Trop Med Hyg* 31: 1291-3
13. Sturm A, Amino R, van de Sand C, Regen T, Retzlaff S, Rennenberg A, Krueger A, Pollok JM, Menard R, Heussler VT. 2006. Manipulation of host hepatocytes by the malaria parasite for delivery into liver sinusoids. *Science* 313: 1287-90
14. Graewe S, Rankin KE, Lehmann C, Deschermeier C, Hecht L, Froehlke U, Stanway RR, Heussler V. 2011. Hostile takeover by Plasmodium: reorganization of parasite and host cell membranes during liver stage egress. *PLoS Pathog* 7: e1002224

15. Leech JH, Barnwell JW, Miller LH, Howard RJ. 1984. Identification of a strain-specific malarial antigen exposed on the surface of Plasmodium falciparum-infected erythrocytes. *J Exp Med* 159: 1567-75
16. Jensen AT, Magistrado P, Sharp S, Joergensen L, Lavstsen T, Chiucchiuini A, Salanti A, Vestergaard LS, Lusingu JP, Hermsen R, Sauerwein R, Christensen J, Nielsen MA, Hviid L, Sutherland C, Staalsoe T, Theander TG. 2004. Plasmodium falciparum associated with severe childhood malaria preferentially expresses PfEMP1 encoded by group A var genes. *J Exp Med* 199: 1179-90
17. Lavstsen T, Turner L, Saguti F, Magistrado P, Rask TS, Jespersen JS, Wang CW, Berger SS, Baraka V, Marquard AM, Seguin-Orlando A, Willerslev E, Gilbert MT, Lusingu J, Theander TG. 2012. Plasmodium falciparum erythrocyte membrane protein 1 domain cassettes 8 and 13 are associated with severe malaria in children. *Proc Natl Acad Sci U S A* 109: E1791-800
18. Claessens A, Adams Y, Ghumra A, Lindergard G, Buchan CC, Andisi C, Bull PC, Mok S, Gupta AP, Wang CW, Turner L, Arman M, Raza A, Bozdech Z, Rowe JA. 2012. A subset of group A-like var genes encodes the malaria parasite ligands for binding to human brain endothelial cells. *Proc Natl Acad Sci U S A* 109: E1772-81
19. Ndungu FM, Sanni L, Urban B, Stephens R, Newbold CI, Marsh K, Langhorne J. 2006. CD4 T cells from malaria-nonexposed individuals respond to the CD36-Binding Domain of Plasmodium falciparum erythrocyte membrane protein-1 via an MHC class II-TCR-independent pathway. *J Immunol* 176: 5504-12
20. Urban BC, Ferguson DJ, Pain A, Willcox N, Plebanski M, Austyn JM, Roberts DJ. 1999. Plasmodium falciparum-infected erythrocytes modulate the maturation of dendritic cells. *Nature* 400: 73-7
21. Vigan-Womas I, Guillotte M, Le Scanf C, Igonet S, Petres S, Juillerat A, Badaut C, Nato F, Schneider A, Lavergne A, Contamin H, Tall A, Baril L, Bentley GA, Mercereau-Puijalon O. 2008. An in vivo and in vitro model of Plasmodium falciparum rosetting and autoagglutination mediated by varO, a group A var gene encoding a frequent serotype. *Infect Immun* 76: 5565-80
22. Vigan-Womas I, Guillotte M, Juillerat A, Vallieres C, Lewit-Bentley A, Tall A, Baril L, Bentley GA, Mercereau-Puijalon O. 2011. Allelic diversity of the Plasmodium falciparum erythrocyte membrane protein 1 entails variant-specific red cell surface epitopes. *PLoS One* 6: e16544
23. Ghumra A, Khunrae P, Ataide R, Raza A, Rogerson SJ, Higgins MK, Rowe JA. 2011. Immunisation with recombinant PfEMP1 domains elicits functional rosette-inhibiting and phagocytosis-inducing antibodies to Plasmodium falciparum. *PLoS One* 6: e16414
24. Rowe JA, Moulds JM, Newbold CI, Miller LH. 1997. P. falciparum rosetting mediated by a parasite-variant erythrocyte membrane protein and complement-receptor 1. *Nature* 388: 292-5
25. Salanti A, Dahlback M, Turner L, Nielsen MA, Barfod L, Magistrado P, Jensen AT, Lavstsen T, Ofori MF, Marsh K, Hviid L, Theander TG. 2004. Evidence for the involvement of VAR2CSA in pregnancy-associated malaria. *J Exp Med* 200: 1197-203

26. Turner GD, Morrison H, Jones M, Davis TM, Looareesuwan S, Buley ID, Gatter KC, Newbold CI, Pukritayakamee S, Nagachinta B, et al. 1994. An immunohistochemical study of the pathology of fatal malaria. Evidence for widespread endothelial activation and a potential role for intercellular adhesion molecule-1 in cerebral sequestration. *Am J Pathol* 145: 1057-69
27. Newbold C, Warn P, Black G, Berendt A, Craig A, Snow B, Msobo M, Peshu N, Marsh K. 1997. Receptor-specific adhesion and clinical disease in Plasmodium falciparum. *Am J Trop Med Hyg* 57: 389-98
28. Clark IA. 1978. Does endotoxin cause both the disease and parasite death in acute malaria and babesiosis? *Lancet* 2: 75-7
29. Krishnegowda G, Hajjar AM, Zhu J, Douglass EJ, Uematsu S, Akira S, Woods AS, Gowda DC. 2005. Induction of proinflammatory responses in macrophages by the glycosylphosphatidylinositols of Plasmodium falciparum: cell signaling receptors, glycosylphosphatidylinositol (GPI) structural requirement, and regulation of GPI activity. *J Biol Chem* 280: 8606-16
30. Coban C, Ishii KJ, Kawai T, Hemmi H, Sato S, Uematsu S, Yamamoto M, Takeuchi O, Itagaki S, Kumar N, Horii T, Akira S. 2005. Toll-like receptor 9 mediates innate immune activation by the malaria pigment hemozoin. *J Exp Med* 201: 19-25
31. Parroche P, Lauw FN, Goutagny N, Latz E, Monks BG, Visintin A, Halmen KA, Lamphier M, Olivier M, Bartholomeu DC, Gazzinelli RT, Golenbock DT. 2007. Malaria hemozoin is immunologically inert but radically enhances innate responses by presenting malaria DNA to Toll-like receptor 9. *Proc Natl Acad Sci U S A* 104: 1919-24
32. Togbe D, Schofield L, Grau GE, Schnyder B, Boissay V, Charron S, Rose S, Beutler B, Quesniaux VF, Ryffel B. 2007. Murine cerebral malaria development is independent of toll-like receptor signaling. *Am J Pathol* 170: 1640-8
33. Kwiatkowski D. 1990. Tumour necrosis factor, fever and fatality in falciparum malaria. *Immunol Lett* 25: 213-6
34. Gimenez F, Barraud de Lagerie S, Fernandez C, Pino P, Mazier D. 2003. Tumor necrosis factor alpha in the pathogenesis of cerebral malaria. *Cell Mol Life Sci* 60: 1623-35
35. Kurtzhals JA, Adabayeri V, Goka BQ, Akanmori BD, Oliver-Commey JO, Nkrumah FK, Behr C, Hviid L. 1998. Low plasma concentrations of interleukin 10 in severe malarial anaemia compared with cerebral and uncomplicated malaria. *Lancet* 351: 1768-72
36. Awandare GA, Goka B, Boeuf P, Tetteh JK, Kurtzhals JA, Behr C, Akanmori BD. 2006. Increased levels of inflammatory mediators in children with severe Plasmodium falciparum malaria with respiratory distress. *J Infect Dis* 194: 1438-46
37. Taverne J, Sheikh N, de Souza JB, Playfair JH, Probert L, Kollias G. 1994. Anaemia and resistance to malaria in transgenic mice expressing human tumour necrosis factor. *Immunology* 82: 397-403

38. Clark IA, Chaudhri G. 1988. Tumour necrosis factor may contribute to the anaemia of malaria by causing dyserythropoiesis and erythrophagocytosis. *Br J Haematol* 70: 99-103
39. Baird JK. 1998. Age-dependent characteristics of protection v. susceptibility to Plasmodium falciparum. *Ann Trop Med Parasitol* 92: 367-90
40. Gupta S, Snow RW, Donnelly CA, Marsh K, Newbold C. 1999. Immunity to non-cerebral severe malaria is acquired after one or two infections. *Nat Med* 5: 340-3
41. Owusu-Agyei S, Koram KA, Baird JK, Utz GC, Binka FN, Nkrumah FK, Fryauff DJ, Hoffman SL. 2001. Incidence of symptomatic and asymptomatic Plasmodium falciparum infection following curative therapy in adult residents of northern Ghana. *Am J Trop Med Hyg* 65: 197-203
42. Bruce-Chwatt LJ. 1963. A LONGITUDINAL SURVEY OF NATURAL MALARIA INFECTION IN A GROUP OF WEST AFRICAN ADULTS. *West Afr Med J* 12: 199-217
43. Riley EM, Allen SJ, Wheeler JG, Blackman MJ, Bennett S, Takacs B, Schonfeld HJ, Holder AA, Greenwood BM. 1992. Naturally acquired cellular and humoral immune responses to the major merozoite surface antigen (PfMSP1) of Plasmodium falciparum are associated with reduced malaria morbidity. *Parasite Immunol* 14: 321-37
44. al-Yaman F, Genton B, Kramer KJ, Taraika J, Chang SP, Hui GS, Alpers MP. 1995. Acquired antibody levels to Plasmodium falciparum merozoite surface antigen 1 in residents of a highly endemic area of Papua New Guinea. *Trans R Soc Trop Med Hyg* 89: 555-9
45. Jakobsen PH, Kurtzhals JA, Riley EM, Hviid L, Theander TG, Morris-Jones S, Jensen JB, Bayoumi RA, Ridley RG, Greenwood BM. 1997. Antibody responses to Rhoptry-Associated Protein-1 (RAP-1) of Plasmodium falciparum parasites in humans from areas of different malaria endemicity. *Parasite Immunol* 19: 387-93
46. Polley SD, Mwangi T, Kocken CH, Thomas AW, Dutta S, Lanar DE, Remarque E, Ross A, Williams TN, Mwambingu G, Lowe B, Conway DJ, Marsh K. 2004. Human antibodies to recombinant protein constructs of Plasmodium falciparum Apical Membrane Antigen 1 (AMA1) and their associations with protection from malaria. *Vaccine* 23: 718-28
47. Bouharoun-Tayoun H, Druilhe P. 1992. Plasmodium falciparum malaria: evidence for an isotype imbalance which may be responsible for delayed acquisition of protective immunity. *Infect Immun* 60: 1473-81
48. Stanisic DI, Richards JS, McCallum FJ, Michon P, King CL, Schoepflin S, Gilson PR, Murphy VJ, Anders RF, Mueller I, Beeson JG. 2009. Immunoglobulin G subclass-specific responses against Plasmodium falciparum merozoite antigens are associated with control of parasitemia and protection from symptomatic illness. *Infect Immun* 77: 1165-74
49. Aucan C, Traore Y, Tall F, Nacro B, Traore-Leroux T, Fumoux F, Rihet P. 2000. High immunoglobulin G2 (IgG2) and low IgG4 levels are associated with human resistance to Plasmodium falciparum malaria. *Infect Immun* 68: 1252-8
50. Fernandez V, Hommel M, Chen Q, Hagblom P, Wahlgren M. 1999. Small, clonally variant antigens expressed on the surface of the Plasmodium falciparum-

infected erythrocyte are encoded by the rif gene family and are the target of human immune responses. *J Exp Med* 190: 1393-404
51. Kaviratne M, Khan SM, Jarra W, Preiser PR. 2002. Small variant STEVOR antigen is uniquely located within Maurer's clefts in Plasmodium falciparum-infected red blood cells. *Eukaryot Cell* 1: 926-35
52. Winter G, Kawai S, Haeggstrom M, Kaneko O, von Euler A, Kawazu S, Palm D, Fernandez V, Wahlgren M. 2005. SURFIN is a polymorphic antigen expressed on Plasmodium falciparum merozoites and infected erythrocytes. *J Exp Med* 201: 1853-63
53. Marsh K, Howard RJ. 1986. Antigens induced on erythrocytes by P. falciparum: expression of diverse and conserved determinants. *Science* 231: 150-3
54. Biggs BA, Gooze L, Wycherley K, Wollish W, Southwell B, Leech JH, Brown GV. 1991. Antigenic variation in Plasmodium falciparum. *Proc Natl Acad Sci U S A* 88: 9171-4
55. Chan JA, Howell KB, Reiling L, Ataide R, Mackintosh CL, Fowkes FJ, Petter M, Chesson JM, Langer C, Warimwe GM, Duffy MF, Rogerson SJ, Bull PC, Cowman AF, Marsh K, Beeson JG. 2012. Targets of antibodies against Plasmodium falciparum-infected erythrocytes in malaria immunity. *J Clin Invest*
56. Mo M, Lee HC, Kotaka M, Niang M, Gao X, Iyer JK, Lescar J, Preiser P. 2008. The C-terminal segment of the cysteine-rich interdomain of Plasmodium falciparum erythrocyte membrane protein 1 determines CD36 binding and elicits antibodies that inhibit adhesion of parasite-infected erythrocytes. *Infect Immun* 76: 1837-47
57. Makobongo MO, Keegan B, Long CA, Miller LH. 2006. Immunization of Aotus monkeys with recombinant cysteine-rich interdomain region 1 alpha protects against severe disease during Plasmodium falciparum reinfection. *J Infect Dis* 193: 731-40
58. Taylor-Robinson AW, Phillips RS, Severn A, Moncada S, Liew FY. 1993. The role of TH1 and TH2 cells in a rodent malaria infection. *Science* 260: 1931-4
59. Amante FH, Good MF. 1997. Prolonged Th1-like response generated by a Plasmodium yoelii-specific T cell clone allows complete clearance of infection in reconstituted mice. *Parasite Immunol* 19: 111-26
60. Lau LS, Fernandez Ruiz D, Davey GM, de Koning-Ward TF, Papenfuss AT, Carbone FR, Brooks AG, Crabb BS, Heath WR. 2011. Blood-stage Plasmodium berghei infection generates a potent, specific CD8+ T-cell response despite residence largely in cells lacking MHC I processing machinery. *J Infect Dis* 204: 1989-96
61. Fell AH, Currier J, Good MF. 1994. Inhibition of Plasmodium falciparum growth in vitro by CD4+ and CD8+ T cells from non-exposed donors. *Parasite Immunol* 16: 579-86
62. Carvalho LH, Fontes CJ, Krettli AU. 1999. Cellular responses to Plasmodium falciparum major surface antigens and their relationship to human activities associated with malaria transmission. *Am J Trop Med Hyg* 60: 674-9
63. Pombo DJ, Lawrence G, Hirunpetcharat C, Rzepczyk C, Bryden M, Cloonan N, Anderson K, Mahakunkijcharoen Y, Martin LB, Wilson D, Elliott S, Eisen DP,

Weinberg JB, Saul A, Good MF. 2002. Immunity to malaria after administration of ultra-low doses of red cells infected with Plasmodium falciparum. *Lancet* 360: 610-7

64. Teirlinck AC, McCall MB, Roestenberg M, Scholzen A, Woestenenk R, de Mast Q, van der Ven AJ, Hermsen CC, Luty AJ, Sauerwein RW. 2011. Longevity and composition of cellular immune responses following experimental Plasmodium falciparum malaria infection in humans. *PLoS Pathog* 7: e1002389
65. Nussenzweig V, Nussenzweig RS. 1985. Circumsporozoite proteins of malaria parasites. *Cell* 42: 401-3
66. Wang Q, Fujioka H, Nussenzweig V. 2005. Mutational analysis of the GPI-anchor addition sequence from the circumsporozoite protein of Plasmodium. *Cell Microbiol* 7: 1616-26
67. Tewari R, Spaccapelo R, Bistoni F, Holder AA, Crisanti A. 2002. Function of region I and II adhesive motifs of Plasmodium falciparum circumsporozoite protein in sporozoite motility and infectivity. *J Biol Chem* 277: 47613-8
68. Wang Q, Fujioka H, Nussenzweig V. 2005. Exit of Plasmodium sporozoites from oocysts is an active process that involves the circumsporozoite protein. *PLoS Pathog* 1: e9
69. Sidjanski SP, Vanderberg JP, Sinnis P. 1997. Anopheles stephensi salivary glands bear receptors for region I of the circumsporozoite protein of Plasmodium falciparum. *Mol Biochem Parasitol* 90: 33-41
70. Myung JM, Marshall P, Sinnis P. 2004. The Plasmodium circumsporozoite protein is involved in mosquito salivary gland invasion by sporozoites. *Mol Biochem Parasitol* 133: 53-9
71. Frevert U, Sinnis P, Cerami C, Shreffler W, Takacs B, Nussenzweig V. 1993. Malaria circumsporozoite protein binds to heparan sulfate proteoglycans associated with the surface membrane of hepatocytes. *J Exp Med* 177: 1287-98
72. Doud MB, Koksal AC, Mi LZ, Song G, Lu C, Springer TA. 2012. Unexpected fold in the circumsporozoite protein target of malaria vaccines. *Proc Natl Acad Sci U S A* 109: 7817-22
73. Sinnis P, Clavijo P, Fenyo D, Chait BT, Cerami C, Nussenzweig V. 1994. Structural and functional properties of region II-plus of the malaria circumsporozoite protein. *J Exp Med* 180: 297-306
74. Ding Y, Huang X, Liu T, Fu Y, Tan Z, Zheng H, Zhou T, Dai J, Xu W. 2012. The Plasmodium Circumsporozoite Protein, a Novel NF-kappaB Inhibitor, Suppresses the Growth of SW480. *Pathol Oncol Res*
75. Singh AP, Buscaglia CA, Wang Q, Levay A, Nussenzweig DR, Walker JR, Winzeler EA, Fujii H, Fontoura BM, Nussenzweig V. 2007. Plasmodium circumsporozoite protein promotes the development of the liver stages of the parasite. *Cell* 131: 492-504
76. Coppi A, Natarajan R, Pradel G, Bennett BL, James ER, Roggero MA, Corradin G, Persson C, Tewari R, Sinnis P. 2011. The malaria circumsporozoite protein has two functional domains, each with distinct roles as sporozoites journey from mosquito to mammalian host. *J Exp Med* 208: 341-56

77. Ghosh AK, Devenport M, Jethwaney D, Kalume DE, Pandey A, Anderson VE, Sultan AA, Kumar N, Jacobs-Lorena M. 2009. Malaria parasite invasion of the mosquito salivary gland requires interaction between the Plasmodium TRAP and the Anopheles saglin proteins. *PLoS Pathog* 5: e1000265
78. Matuschewski K, Nunes AC, Nussenzweig V, Menard R. 2002. Plasmodium sporozoite invasion into insect and mammalian cells is directed by the same dual binding system. *EMBO J* 21: 1597-606
79. Sultan AA, Thathy V, Frevert U, Robson KJ, Crisanti A, Nussenzweig V, Nussenzweig RS, Menard R. 1997. TRAP is necessary for gliding motility and infectivity of plasmodium sporozoites. *Cell* 90: 511-22
80. Kappe S, Bruderer T, Gantt S, Fujioka H, Nussenzweig V, Menard R. 1999. Conservation of a gliding motility and cell invasion machinery in Apicomplexan parasites. *J Cell Biol* 147: 937-44
81. Bosch J, Buscaglia CA, Krumm B, Ingason BP, Lucas R, Roach C, Cardozo T, Nussenzweig V, Hol WG. 2007. Aldolase provides an unusual binding site for thrombospondin-related anonymous protein in the invasion machinery of the malaria parasite. *Proc Natl Acad Sci U S A* 104: 7015-20
82. Akhouri RR, Bhattacharyya A, Pattnaik P, Malhotra P, Sharma A. 2004. Structural and functional dissection of the adhesive domains of Plasmodium falciparum thrombospondin-related anonymous protein (TRAP). *Biochem J* 379: 815-22
83. Todryk SM, Bejon P, Mwangi T, Plebanski M, Urban B, Marsh K, Hill AV, Flanagan KL. 2008. Correlation of memory T cell responses against TRAP with protection from clinical malaria, and CD4 CD25 high T cells with susceptibility in Kenyans. *PLoS One* 3: e2027
84. John CC, Tande AJ, Moormann AM, Sumba PO, Lanar DE, Min XM, Kazura JW. 2008. Antibodies to pre-erythrocytic Plasmodium falciparum antigens and risk of clinical malaria in Kenyan children. *J Infect Dis* 197: 519-26
85. Gantt S, Persson C, Rose K, Birkett AJ, Abagyan R, Nussenzweig V. 2000. Antibodies against thrombospondin-related anonymous protein do not inhibit Plasmodium sporozoite infectivity in vivo. *Infect Immun* 68: 3667-73
86. Offeddu V, Thathy V, Marsh K, Matuschewski K. 2012. Naturally acquired immune responses against Plasmodium falciparum sporozoites and liver infection. *Int J Parasitol* 42: 535-48
87. Kariu T, Ishino T, Yano K, Chinzei Y, Yuda M. 2006. CelTOS, a novel malarial protein that mediates transmission to mosquito and vertebrate hosts. *Mol Microbiol* 59: 1369-79
88. Bergmann-Leitner ES, Mease RM, De La Vega P, Savranskaya T, Polhemus M, Ockenhouse C, Angov E. 2010. Immunization with pre-erythrocytic antigen CelTOS from Plasmodium falciparum elicits cross-species protection against heterologous challenge with Plasmodium berghei. *PLoS One* 5: e12294
89. Bergmann-Leitner ES, Legler PM, Savranskaya T, Ockenhouse CF, Angov E. 2011. Cellular and humoral immune effector mechanisms required for sterile protection against sporozoite challenge induced with the novel malaria vaccine candidate CelTOS. *Vaccine* 29: 5940-9

90. Doolan DL, Southwood S, Freilich DA, Sidney J, Graber NL, Shatney L, Bebris L, Florens L, Dobano C, Witney AA, Appella E, Hoffman SL, Yates JR, 3rd, Carucci DJ, Sette A. 2003. Identification of Plasmodium falciparum antigens by antigenic analysis of genomic and proteomic data. *Proc Natl Acad Sci U S A* 100: 9952-7
91. Good MF. 2001. Towards a blood-stage vaccine for malaria: are we following all the leads? *Nat Rev Immunol* 1: 117-25
92. Bull PC, Lowe BS, Kortok M, Molyneux CS, Newbold CI, Marsh K. 1998. Parasite antigens on the infected red cell surface are targets for naturally acquired immunity to malaria. *Nat Med* 4: 358-60
93. Osier FH, Fegan G, Polley SD, Murungi L, Verra F, Tetteh KK, Lowe B, Mwangi T, Bull PC, Thomas AW, Cavanagh DR, McBride JS, Lanar DE, Mackinnon MJ, Conway DJ, Marsh K. 2008. Breadth and magnitude of antibody responses to multiple Plasmodium falciparum merozoite antigens are associated with protection from clinical malaria. *Infect Immun* 76: 2240-8
94. Roestenberg M, McCall M, Hopman J, Wiersma J, Luty AJ, van Gemert GJ, van de Vegte-Bolmer M, van Schaijk B, Teelen K, Arens T, Spaarman L, de Mast Q, Roeffen W, Snounou G, Renia L, van der Ven A, Hermsen CC, Sauerwein R. 2009. Protection against a malaria challenge by sporozoite inoculation. *N Engl J Med* 361: 468-77
95. Blackman MJ, Scott-Finnigan TJ, Shai S, Holder AA. 1994. Antibodies inhibit the protease-mediated processing of a malaria merozoite surface protein. *J Exp Med* 180: 389-93
96. Gilson PR, O'Donnell RA, Nebl T, Sanders PR, Wickham ME, McElwain TF, de Koning-Ward TF, Crabb BS. 2008. MSP1(19) miniproteins can serve as targets for invasion inhibitory antibodies in Plasmodium falciparum provided they contain the correct domains for cell surface trafficking. *Mol Microbiol* 68: 124-38
97. Bergmann-Leitner ES, Duncan EH, Angov E. 2009. MSP-1p42-specific antibodies affect growth and development of intra-erythrocytic parasites of Plasmodium falciparum. *Malar J* 8: 183
98. Moss DK, Remarque EJ, Faber BW, Cavanagh DR, Arnot DE, Thomas AW, Holder AA. 2012. Plasmodium falciparum 19-kilodalton merozoite surface protein 1 (MSP1)-specific antibodies that interfere with parasite growth in vitro can inhibit MSP1 processing, merozoite invasion, and intracellular parasite development. *Infect Immun* 80: 1280-7
99. Holder AA. 2009. The carboxy-terminus of merozoite surface protein 1: structure, specific antibodies and immunity to malaria. *Parasitology* 136: 1445-56
100. Combe A, Giovannini D, Carvalho TG, Spath S, Boisson B, Loussert C, Thiberge S, Lacroix C, Gueirard P, Menard R. 2009. Clonal conditional mutagenesis in malaria parasites. *Cell Host Microbe* 5: 386-96
101. O'Donnell RA, Saul A, Cowman AF, Crabb BS. 2000. Functional conservation of the malaria vaccine antigen MSP-119across distantly related Plasmodium species. *Nat Med* 6: 91-5
102. Gerold P, Schofield L, Blackman MJ, Holder AA, Schwarz RT. 1996. Structural analysis of the glycosyl-phosphatidylinositol membrane anchor of the merozoite

surface proteins-1 and -2 of Plasmodium falciparum. *Mol Biochem Parasitol* 75: 131-43
103. Yeoh S, O'Donnell RA, Koussis K, Dluzewski AR, Ansell KH, Osborne SA, Hackett F, Withers-Martinez C, Mitchell GH, Bannister LH, Bryans JS, Kettleborough CA, Blackman MJ. 2007. Subcellular discharge of a serine protease mediates release of invasive malaria parasites from host erythrocytes. *Cell* 131: 1072-83
104. Koussis K, Withers-Martinez C, Yeoh S, Child M, Hackett F, Knuepfer E, Juliano L, Woehlbier U, Bujard H, Blackman MJ. 2009. A multifunctional serine protease primes the malaria parasite for red blood cell invasion. *EMBO J* 28: 725-35
105. Blackman MJ, Holder AA. 1992. Secondary processing of the Plasmodium falciparum merozoite surface protein-1 (MSP1) by a calcium-dependent membrane-bound serine protease: shedding of MSP133 as a noncovalently associated complex with other fragments of the MSP1. *Mol Biochem Parasitol* 50: 307-15
106. Harris PK, Yeoh S, Dluzewski AR, O'Donnell RA, Withers-Martinez C, Hackett F, Bannister LH, Mitchell GH, Blackman MJ. 2005. Molecular identification of a malaria merozoite surface sheddase. *PLoS Pathog* 1: 241-51
107. Child MA, Epp C, Bujard H, Blackman MJ. 2010. Regulated maturation of malaria merozoite surface protein-1 is essential for parasite growth. *Mol Microbiol* 78: 187-202
108. Shi YP, Sayed U, Qari SH, Roberts JM, Udhayakumar V, Oloo AJ, Hawley WA, Kaslow DC, Nahlen BL, Lal AA. 1996. Natural immune response to the C-terminal 19-kilodalton domain of Plasmodium falciparum merozoite surface protein 1. *Infect Immun* 64: 2716-23
109. al-Yaman F, Genton B, Kramer KJ, Chang SP, Hui GS, Baisor M, Alpers MP. 1996. Assessment of the role of naturally acquired antibody levels to Plasmodium falciparum merozoite surface protein-1 in protecting Papua New Guinean children from malaria morbidity. *Am J Trop Med Hyg* 54: 443-8
110. Hirunpetcharat C, Tian JH, Kaslow DC, van Rooijen N, Kumar S, Berzofsky JA, Miller LH, Good MF. 1997. Complete protective immunity induced in mice by immunization with the 19-kilodalton carboxyl-terminal fragment of the merozoite surface protein-1 (MSP1[19]) of Plasmodium yoelii expressed in Saccharomyces cerevisiae: correlation of protection with antigen-specific antibody titer, but not with effector CD4+ T cells. *J Immunol* 159: 3400-11
111. Kumar S, Yadava A, Keister DB, Tian JH, Ohl M, Perdue-Greenfield KA, Miller LH, Kaslow DC. 1995. Immunogenicity and in vivo efficacy of recombinant Plasmodium falciparum merozoite surface protein-1 in Aotus monkeys. *Mol Med* 1: 325-32
112. Lyon JA, Angov E, Fay MP, Sullivan JS, Girourd AS, Robinson SJ, Bergmann-Leitner ES, Duncan EH, Darko CA, Collins WE, Long CA, Barnwell JW. 2008. Protection induced by Plasmodium falciparum MSP1(42) is strain-specific, antigen and adjuvant dependent, and correlates with antibody responses. *PLoS One* 3: e2830

113. Ogutu BR, Apollo OJ, McKinney D, Okoth W, Siangla J, Dubovsky F, Tucker K, Waitumbi JN, Diggs C, Wittes J, Malkin E, Leach A, Soisson LA, Milman JB, Otieno L, Holland CA, Polhemus M, Remich SA, Ockenhouse CF, Cohen J, Ballou WR, Martin SK, Angov E, Stewart VA, Lyon JA, Heppner DG, Withers MR. 2009. Blood stage malaria vaccine eliciting high antigen-specific antibody concentrations confers no protection to young children in Western Kenya. *PLoS One* 4: e4708
114. Silvie O, Franetich JF, Charrin S, Mueller MS, Siau A, Bodescot M, Rubinstein E, Hannoun L, Charoenvit Y, Kocken CH, Thomas AW, Van Gemert GJ, Sauerwein RW, Blackman MJ, Anders RF, Pluschke G, Mazier D. 2004. A role for apical membrane antigen 1 during invasion of hepatocytes by Plasmodium falciparum sporozoites. *J Biol Chem* 279: 9490-6
115. Thomas AW, Deans JA, Mitchell GH, Alderson T, Cohen S. 1984. The Fab fragments of monoclonal IgG to a merozoite surface antigen inhibit Plasmodium knowlesi invasion of erythrocytes. *Mol Biochem Parasitol* 13: 187-99
116. Narum DL, Thomas AW. 1994. Differential localization of full-length and processed forms of PF83/AMA-1 an apical membrane antigen of Plasmodium falciparum merozoites. *Mol Biochem Parasitol* 67: 59-68
117. Howell SA, Well I, Fleck SL, Kettleborough C, Collins CR, Blackman MJ. 2003. A single malaria merozoite serine protease mediates shedding of multiple surface proteins by juxtamembrane cleavage. *J Biol Chem* 278: 23890-8
118. Dutta S, Sullivan JS, Grady KK, Haynes JD, Komisar J, Batchelor AH, Soisson L, Diggs CL, Heppner DG, Lanar DE, Collins WE, Barnwell JW. 2009. High antibody titer against apical membrane antigen-1 is required to protect against malaria in the Aotus model. *PLoS One* 4: e8138
119. Thera MA, Doumbo OK, Coulibaly D, Laurens MB, Ouattara A, Kone AK, Guindo AB, Traore K, Traore I, Kouriba B, Diallo DA, Diarra I, Daou M, Dolo A, Tolo Y, Sissoko MS, Niangaly A, Sissoko M, Takala-Harrison S, Lyke KE, Wu Y, Blackwelder WC, Godeaux O, Vekemans J, Dubois MC, Ballou WR, Cohen J, Thompson D, Dube T, Soisson L, Diggs CL, House B, Lanar DE, Dutta S, Heppner DG, Jr., Plowe CV. 2011. A field trial to assess a blood-stage malaria vaccine. *N Engl J Med* 365: 1004-13
120. Douglas AD, Williams AR, Illingworth JJ, Kamuyu G, Biswas S, Goodman AL, Wyllie DH, Crosnier C, Miura K, Wright GJ, Long CA, Osier FH, Marsh K, Turner AV, Hill AV, Draper SJ. 2011. The blood-stage malaria antigen PfRH5 is susceptible to vaccine-inducible cross-strain neutralizing antibody. *Nat Commun* 2: 601
121. Takala SL, Smith DL, Thera MA, Coulibaly D, Doumbo OK, Plowe CV. 2007. Short report: rare Plasmodium falciparum merozoite surface protein 1 19-kda (msp-1(19)) haplotypes identified in Mali using high-throughput genotyping methods. *Am J Trop Med Hyg* 76: 855-9
122. Kappe SH, Noe AR, Fraser TS, Blair PL, Adams JH. 1998. A family of chimeric erythrocyte binding proteins of malaria parasites. *Proc Natl Acad Sci U S A* 95: 1230-5

123. Baum J, Maier AG, Good RT, Simpson KM, Cowman AF. 2005. Invasion by P. falciparum merozoites suggests a hierarchy of molecular interactions. *PLoS Pathog* 1: e37
124. Dolan SA, Miller LH, Wellems TE. 1990. Evidence for a switching mechanism in the invasion of erythrocytes by Plasmodium falciparum. *J Clin Invest* 86: 618-24
125. Rayner JC, Vargas-Serrato E, Huber CS, Galinski MR, Barnwell JW. 2001. A Plasmodium falciparum homologue of Plasmodium vivax reticulocyte binding protein (PvRBP1) defines a trypsin-resistant erythrocyte invasion pathway. *J Exp Med* 194: 1571-81
126. Miller LH, Haynes JD, McAuliffe FM, Shiroishi T, Durocher JR, McGinniss MH. 1977. Evidence for differences in erythrocyte surface receptors for the malarial parasites, Plasmodium falciparum and Plasmodium knowlesi. *J Exp Med* 146: 277-81
127. Miller LH, Mason SJ, Clyde DF, McGinniss MH. 1976. The resistance factor to Plasmodium vivax in blacks. The Duffy-blood-group genotype, FyFy. *N Engl J Med* 295: 302-4
128. Wertheimer SP, Barnwell JW. 1989. Plasmodium vivax interaction with the human Duffy blood group glycoprotein: identification of a parasite receptor-like protein. *Exp Parasitol* 69: 340-50
129. Adams JH, Hudson DE, Torii M, Ward GE, Wellems TE, Aikawa M, Miller LH. 1990. The Duffy receptor family of Plasmodium knowlesi is located within the micronemes of invasive malaria merozoites. *Cell* 63: 141-53
130. Fang XD, Kaslow DC, Adams JH, Miller LH. 1991. Cloning of the Plasmodium vivax Duffy receptor. *Mol Biochem Parasitol* 44: 125-32
131. Chaudhuri A, Polyakova J, Zbrzezna V, Williams K, Gulati S, Pogo AO. 1993. Cloning of glycoprotein D cDNA, which encodes the major subunit of the Duffy blood group system and the receptor for the Plasmodium vivax malaria parasite. *Proc Natl Acad Sci U S A* 90: 10793-7
132. Haynes JD, Dalton JP, Klotz FW, McGinniss MH, Hadley TJ, Hudson DE, Miller LH. 1988. Receptor-like specificity of a Plasmodium knowlesi malarial protein that binds to Duffy antigen ligands on erythrocytes. *J Exp Med* 167: 1873-81
133. Singh AP, Puri SK, Chitnis CE. 2002. Antibodies raised against receptor-binding domain of Plasmodium knowlesi Duffy binding protein inhibit erythrocyte invasion. *Mol Biochem Parasitol* 121: 21-31
134. Grimberg BT, Udomsangpetch R, Xainli J, McHenry A, Panichakul T, Sattabongkot J, Cui L, Bockarie M, Chitnis C, Adams J, Zimmerman PA, King CL. 2007. Plasmodium vivax invasion of human erythrocytes inhibited by antibodies directed against the Duffy binding protein. *PLoS medicine* 4: e337
135. Wu Y, Ellis RD, Shaffer D, Fontes E, Malkin EM, Mahanty S, Fay MP, Narum D, Rausch K, Miles AP, Aebig J, Orcutt A, Muratova O, Song G, Lambert L, Zhu D, Miura K, Long C, Saul A, Miller LH, Durbin AP. 2008. Phase 1 trial of malaria transmission blocking vaccine candidates Pfs25 and Pvs25 formulated with montanide ISA 51. *PLoS One* 3: e2636
136. Williamson KC, Keister DB, Muratova O, Kaslow DC. 1995. Recombinant Pfs230, a Plasmodium falciparum gametocyte protein, induces antisera that

reduce the infectivity of Plasmodium falciparum to mosquitoes. *Mol Biochem Parasitol* 75: 33-42
137. Farrance CE, Rhee A, Jones RM, Musiychuk K, Shamloul M, Sharma S, Mett V, Chichester JA, Streatfield SJ, Roeffen W, van de Vegte-Bolmer M, Sauerwein RW, Tsuboi T, Muratova OV, Wu Y, Yusibov V. 2011. A plant-produced Pfs230 vaccine candidate blocks transmission of Plasmodium falciparum. *Clin Vaccine Immunol* 18: 1351-7
138. Chowdhury DR, Angov E, Kariuki T, Kumar N. 2009. A potent malaria transmission blocking vaccine based on codon harmonized full length Pfs48/45 expressed in Escherichia coli. *PLoS One* 4: e6352
139. Laveran CL. 1982. Classics in infectious diseases: A newly discovered parasite in the blood of patients suffering from malaria. Parasitic etiology of attacks of malaria: Charles Louis Alphonse Laveran (1845-1922). *Rev Infect Dis* 4: 908-11
140. Ross R. 2002. The role of the mosquito in the evolution of the malarial parasite: the recent researches of Surgeon-Major Ronald Ross, I.M.S. 1898. *Yale J Biol Med* 75: 103-5
141. Gardner MJ, Hall N, Fung E, White O, Berriman M, Hyman RW, Carlton JM, Pain A, Nelson KE, Bowman S, Paulsen IT, James K, Eisen JA, Rutherford K, Salzberg SL, Craig A, Kyes S, Chan MS, Nene V, Shallom SJ, Suh B, Peterson J, Angiuoli S, Pertea M, Allen J, Selengut J, Haft D, Mather MW, Vaidya AB, Martin DM, Fairlamb AH, Fraunholz MJ, Roos DS, Ralph SA, McFadden GI, Cummings LM, Subramanian GM, Mungall C, Venter JC, Carucci DJ, Hoffman SL, Newbold C, Davis RW, Fraser CM, Barrell B. 2002. Genome sequence of the human malaria parasite Plasmodium falciparum. *Nature* 419: 498-511
142. Bharadwaj A, Sharma P, Joshi SK, Singh B, Chauhan VS. 1998. Induction of protective immune responses by immunization with linear multiepitope peptides based on conserved sequences from Plasmodium falciparum antigens. *Infect Immun* 66: 3232-41
143. Rathore D, Nagarkatti R, Jani D, Chattopadhyay R, de la Vega P, Kumar S, McCutchan TF. 2005. An immunologically cryptic epitope of Plasmodium falciparum circumsporozoite protein facilitates liver cell recognition and induces protective antibodies that block liver cell invasion. *J Biol Chem* 280: 20524-9
144. Egan A, Waterfall M, Pinder M, Holder A, Riley E. 1997. Characterization of human T- and B-cell epitopes in the C terminus of Plasmodium falciparum merozoite surface protein 1: evidence for poor T-cell recognition of polypeptides with numerous disulfide bonds. *Infect Immun* 65: 3024-31
145. Clyde DF. 1975. Immunization of man against falciparum and vivax malaria by use of attenuated sporozoites. *Am J Trop Med Hyg* 24: 397-401
146. Hoffman SL, Goh LM, Luke TC, Schneider I, Le TP, Doolan DL, Sacci J, de la Vega P, Dowler M, Paul C, Gordon DM, Stoute JA, Church LW, Sedegah M, Heppner DG, Ballou WR, Richie TL. 2002. Protection of humans against malaria by immunization with radiation-attenuated Plasmodium falciparum sporozoites. *J Infect Dis* 185: 1155-64
147. Silvie O, Semblat JP, Franetich JF, Hannoun L, Eling W, Mazier D. 2002. Effects of irradiation on Plasmodium falciparum sporozoite hepatic development:

implications for the design of pre-erythrocytic malaria vaccines. *Parasite Immunol* 24: 221-3
148. Hafalla JC, Cockburn IA, Zavala F. 2006. Protective and pathogenic roles of CD8+ T cells during malaria infection. *Parasite Immunol* 28: 15-24
149. Krzych U, Schwenk J. 2005. The dissection of CD8 T cells during liver-stage infection. *Curr Top Microbiol Immunol* 297: 1-24
150. Doolan DL, Hoffman SL. 2000. The complexity of protective immunity against liver-stage malaria. *J Immunol* 165: 1453-62
151. Mueller AK, Labaied M, Kappe SH, Matuschewski K. 2005. Genetically modified Plasmodium parasites as a protective experimental malaria vaccine. *Nature* 433: 164-7
152. van Dijk MR, Douradinha B, Franke-Fayard B, Heussler V, van Dooren MW, van Schaijk B, van Gemert GJ, Sauerwein RW, Mota MM, Waters AP, Janse CJ. 2005. Genetically attenuated, P36p-deficient malarial sporozoites induce protective immunity and apoptosis of infected liver cells. *Proc Natl Acad Sci U S A* 102: 12194-9
153. Aly AS, Mikolajczak SA, Rivera HS, Camargo N, Jacobs-Lorena V, Labaied M, Coppens I, Kappe SH. 2008. Targeted deletion of SAP1 abolishes the expression of infectivity factors necessary for successful malaria parasite liver infection. *Mol Microbiol* 69: 152-63
154. Vaughan AM, O'Neill MT, Tarun AS, Camargo N, Phuong TM, Aly AS, Cowman AF, Kappe SH. 2009. Type II fatty acid synthesis is essential only for malaria parasite late liver stage development. *Cell Microbiol* 11: 506-20
155. Butler NS, Schmidt NW, Vaughan AM, Aly AS, Kappe SH, Harty JT. 2011. Superior antimalarial immunity after vaccination with late liver stage-arresting genetically attenuated parasites. *Cell Host Microbe* 9: 451-62
156. Belnoue E, Costa FT, Frankenberg T, Vigario AM, Voza T, Leroy N, Rodrigues MM, Landau I, Snounou G, Renia L. 2004. Protective T cell immunity against malaria liver stage after vaccination with live sporozoites under chloroquine treatment. *J Immunol* 172: 2487-95
157. Gwadz RW, Cochrane AH, Nussenzweig V, Nussenzweig RS. 1979. Preliminary studies on vaccination of rhesus monkeys with irradiated sporozoites of Plasmodium knowlesi and characterization of surface antigens of these parasites. *Bull World Health Organ* 57 Suppl 1: 165-73
158. Nardin EH, Nussenzweig V, Nussenzweig RS, Collins WE, Harinasuta KT, Tapchaisri P, Chomcharn Y. 1982. Circumsporozoite proteins of human malaria parasites Plasmodium falciparum and Plasmodium vivax. *J Exp Med* 156: 20-30
159. Potocnjak P, Yoshida N, Nussenzweig RS, Nussenzweig V. 1980. Monovalent fragments (Fab) of monoclonal antibodies to a sporozoite surface antigen (Pb44) protect mice against malarial infection. *J Exp Med* 151: 1504-13
160. Gordon DM, McGovern TW, Krzych U, Cohen JC, Schneider I, LaChance R, Heppner DG, Yuan G, Hollingdale M, Slaoui M, et al. 1995. Safety, immunogenicity, and efficacy of a recombinantly produced Plasmodium falciparum circumsporozoite protein-hepatitis B surface antigen subunit vaccine. *J Infect Dis* 171: 1576-85

161. Agnandji ST, Lell B, Soulanoudjingar SS, Fernandes JF, Abossolo BP, et al. 2011. First results of phase 3 trial of RTS,S/AS01 malaria vaccine in African children. *N Engl J Med* 365: 1863-75
162. Kester KE, Cummings JF, Ofori-Anyinam O, Ockenhouse CF, Krzych U, Moris P, Schwenk R, Nielsen RA, Debebe Z, Pinelis E, Juompan L, Williams J, Dowler M, Stewart VA, Wirtz RA, Dubois MC, Lievens M, Cohen J, Ballou WR, Heppner DG, Jr. 2009. Randomized, double-blind, phase 2a trial of falciparum malaria vaccines RTS,S/AS01B and RTS,S/AS02A in malaria-naive adults: safety, efficacy, and immunologic associates of protection. *J Infect Dis* 200: 337-46
163. Weiss WR, Sedegah M, Beaudoin RL, Miller LH, Good MF. 1988. CD8+ T cells (cytotoxic/suppressors) are required for protection in mice immunized with malaria sporozoites. *Proc Natl Acad Sci U S A* 85: 573-6
164. Overstreet MG, Cockburn IA, Chen YC, Zavala F. 2008. Protective CD8 T cells against Plasmodium liver stages: immunobiology of an 'unnatural' immune response. *Immunol Rev* 225: 272-83
165. Reyes-Sandoval A, Wyllie DH, Bauza K, Milicic A, Forbes EK, Rollier CS, Hill AV. 2011. CD8+ T effector memory cells protect against liver-stage malaria. *J Immunol* 187: 1347-57
166. Jenner E. 1798. *An inquiry into the causes and effects of the variolae vaccinae, a disease discovered in some of the western counties of England, particularly Gloucestershire, and known by the name of the cow pox*. London,: Printed, for the author, by Sampson Low. [1], iv, 75, [1] p. pp.
167. Global Commission for the Certification of Smallpox Eradication., World Health Organization. 1980. *The global eradication of smallpox : final report of the Global Commission for the Certification of Smallpox, Geneva, December 1979*. Geneva: World Health Organization. 122 pp.
168. Slifka MK. 2005. The Future of Smallpox Vaccination: is MVA the key? *Med Immunol* 4: 2
169. Schneider J, Gilbert SC, Blanchard TJ, Hanke T, Robson KJ, Hannan CM, Becker M, Sinden R, Smith GL, Hill AV. 1998. Enhanced immunogenicity for CD8+ T cell induction and complete protective efficacy of malaria DNA vaccination by boosting with modified vaccinia virus Ankara. *Nat Med* 4: 397-402
170. McConkey SJ, Reece WH, Moorthy VS, Webster D, Dunachie S, Butcher G, Vuola JM, Blanchard TJ, Gothard P, Watkins K, Hannan CM, Everaere S, Brown K, Kester KE, Cummings J, Williams J, Heppner DG, Pathan A, Flanagan K, Arulanantham N, Roberts MT, Roy M, Smith GL, Schneider J, Peto T, Sinden RE, Gilbert SC, Hill AV. 2003. Enhanced T-cell immunogenicity of plasmid DNA vaccines boosted by recombinant modified vaccinia virus Ankara in humans. *Nat Med* 9: 729-35
171. Im EJ, Hanke T. 2004. MVA as a vector for vaccines against HIV-1. *Expert Rev Vaccines* 3: S89-97
172. Nicol MP, Grobler LA. 2010. MVA-85A, a novel candidate booster vaccine for the prevention of tuberculosis in children and adults. *Curr Opin Mol Ther* 12: 124-34

173. Song GY, Gibson G, Haq W, Huang EC, Srivasta T, Hollstein M, Daftarian P, Wang Z, Diamond D, Ellenhorn JD. 2007. An MVA vaccine overcomes tolerance to human p53 in mice and humans. *Cancer Immunol Immunother* 56: 1193-205
174. Larocca C, Schlom J. 2011. Viral vector-based therapeutic cancer vaccines. *Cancer J* 17: 359-71
175. Goonetilleke NP, McShane H, Hannan CM, Anderson RJ, Brookes RH, Hill AV. 2003. Enhanced immunogenicity and protective efficacy against Mycobacterium tuberculosis of bacille Calmette-Guerin vaccine using mucosal administration and boosting with a recombinant modified vaccinia virus Ankara. *J Immunol* 171: 1602-9
176. McShane H, Brookes R, Gilbert SC, Hill AV. 2001. Enhanced immunogenicity of CD4(+) t-cell responses and protective efficacy of a DNA-modified vaccinia virus Ankara prime-boost vaccination regimen for murine tuberculosis. *Infect Immun* 69: 681-6
177. Williams A, Goonetilleke NP, McShane H, Clark SO, Hatch G, Gilbert SC, Hill AV. 2005. Boosting with poxviruses enhances Mycobacterium bovis BCG efficacy against tuberculosis in guinea pigs. *Infect Immun* 73: 3814-6
178. Vordermeier HM, Villarreal-Ramos B, Cockle PJ, McAulay M, Rhodes SG, Thacker T, Gilbert SC, McShane H, Hill AV, Xing Z, Hewinson RG. 2009. Viral booster vaccines improve Mycobacterium bovis BCG-induced protection against bovine tuberculosis. *Infect Immun* 77: 3364-73
179. McShane H, Pathan AA, Sander CR, Keating SM, Gilbert SC, Huygen K, Fletcher HA, Hill AV. 2004. Recombinant modified vaccinia virus Ankara expressing antigen 85A boosts BCG-primed and naturally acquired antimycobacterial immunity in humans. *Nat Med* 10: 1240-4
180. Brookes RH, Hill PC, Owiafe PK, Ibanga HB, Jeffries DJ, Donkor SA, Fletcher HA, Hammond AS, Lienhardt C, Adegbola RA, McShane H, Hill AV. 2008. Safety and immunogenicity of the candidate tuberculosis vaccine MVA85A in West Africa. *PLoS One* 3: e2921
181. Hawkridge T, Scriba TJ, Gelderbloem S, Smit E, Tameris M, Moyo S, Lang T, Veldsman A, Hatherill M, Merwe L, Fletcher HA, Mahomed H, Hill AV, Hanekom WA, Hussey GD, McShane H. 2008. Safety and immunogenicity of a new tuberculosis vaccine, MVA85A, in healthy adults in South Africa. *J Infect Dis* 198: 544-52
182. Dunachie SJ, Walther M, Epstein JE, Keating S, Berthoud T, Andrews L, Andersen RF, Bejon P, Goonetilleke N, Poulton I, Webster DP, Butcher G, Watkins K, Sinden RE, Levine GL, Richie TL, Schneider J, Kaslow D, Gilbert SC, Carucci DJ, Hill AV. 2006. A DNA prime-modified vaccinia virus ankara boost vaccine encoding thrombospondin-related adhesion protein but not circumsporozoite protein partially protects healthy malaria-naive adults against Plasmodium falciparum sporozoite challenge. *Infect Immun* 74: 5933-42
183. Tine JA, Lanar DE, Smith DM, Wellde BT, Schultheiss P, Ware LA, Kauffman EB, Wirtz RA, De Taisne C, Hui GS, Chang SP, Church P, Hollingdale MR, Kaslow DC, Hoffman S, Guito KP, Ballou WR, Sadoff JC, Paoletti E. 1996.

NYVAC-Pf7: a poxvirus-vectored, multiantigen, multistage vaccine candidate for Plasmodium falciparum malaria. *Infect Immun* 64: 3833-44
184. Ockenhouse CF, Sun PF, Lanar DE, Wellde BT, Hall BT, Kester K, Stoute JA, Magill A, Krzych U, Farley L, Wirtz RA, Sadoff JC, Kaslow DC, Kumar S, Church LW, Crutcher JM, Wizel B, Hoffman S, Lalvani A, Hill AV, Tine JA, Guito KP, de Taisne C, Anders R, Ballou WR, et al. 1998. Phase I/IIa safety, immunogenicity, and efficacy trial of NYVAC-Pf7, a pox-vectored, multiantigen, multistage vaccine candidate for Plasmodium falciparum malaria. *J Infect Dis* 177: 1664-73
185. Berthoud TK, Hamill M, Lillie PJ, Hwenda L, Collins KA, Ewer KJ, Milicic A, Poyntz HC, Lambe T, Fletcher HA, Hill AV, Gilbert SC. 2011. Potent CD8+ T-cell immunogenicity in humans of a novel heterosubtypic influenza A vaccine, MVA-NP+M1. *Clin Infect Dis* 52: 1-7
186. Wilson JM. 1996. Adenoviruses as gene-delivery vehicles. *N Engl J Med* 334: 1185-7
187. Tatsis N, Ertl HC. 2004. Adenoviruses as vaccine vectors. *Mol Ther* 10: 616-29
188. Saito I, Oya Y, Yamamoto K, Yuasa T, Shimojo H. 1985. Construction of nondefective adenovirus type 5 bearing a 2.8-kilobase hepatitis B virus DNA near the right end of its genome. *J Virol* 54: 711-9
189. Sedegah M, Tamminga C, McGrath S, House B, Ganeshan H, Lejano J, Abot E, Banania GJ, Sayo R, Farooq F, Belmonte M, Manohar N, Richie NO, Wood C, Long CA, Regis D, Williams FT, Shi M, Chuang I, Spring M, Epstein JE, Mendoza-Silveiras J, Limbach K, Patterson NB, Bruder JT, Doolan DL, King CR, Soisson L, Diggs C, Carucci D, Dutta S, Hollingdale MR, Ockenhouse CF, Richie TL. 2011. Adenovirus 5-vectored P. falciparum vaccine expressing CSP and AMA1. Part A: safety and immunogenicity in seronegative adults. *PLoS One* 6: e24586
190. Tamminga C, Sedegah M, Regis D, Chuang I, Epstein JE, Spring M, Mendoza-Silveiras J, McGrath S, Maiolatesi S, Reyes S, Steinbeiss V, Fedders C, Smith K, House B, Ganeshan H, Lejano J, Abot E, Banania GJ, Sayo R, Farooq F, Belmonte M, Murphy J, Komisar J, Williams J, Shi M, Brambilla D, Manohar N, Richie NO, Wood C, Limbach K, Patterson NB, Bruder JT, Doolan DL, King CR, Diggs C, Soisson L, Carucci D, Levine G, Dutta S, Hollingdale MR, Ockenhouse CF, Richie TL. 2011. Adenovirus-5-vectored P. falciparum vaccine expressing CSP and AMA1. Part B: safety, immunogenicity and protective efficacy of the CSP component. *PLoS One* 6: e25868
191. Draper SJ, Heeney JL. 2010. Viruses as vaccine vectors for infectious diseases and cancer. *Nat Rev Microbiol* 8: 62-73
192. Casimiro DR, Tang A, Chen L, Fu TM, Evans RK, Davies ME, Freed DC, Hurni W, Aste-Amezaga JM, Guan L, Long R, Huang L, Harris V, Nawrocki DK, Mach H, Troutman RD, Isopi LA, Murthy KK, Rice K, Wilson KA, Volkin DB, Emini EA, Shiver JW. 2003. Vaccine-induced immunity in baboons by using DNA and replication-incompetent adenovirus type 5 vectors expressing a human immunodeficiency virus type 1 gag gene. *J Virol* 77: 7663-8

193. Shiver JW, Fu TM, Chen L, Casimiro DR, Davies ME, Evans RK, Zhang ZQ, Simon AJ, Trigona WL, Dubey SA, Huang L, Harris VA, Long RS, Liang X, Handt L, Schleif WA, Zhu L, Freed DC, Persaud NV, Guan L, Punt KS, Tang A, Chen M, Wilson KA, Collins KB, Heidecker GJ, Fernandez VR, Perry HC, Joyce JG, Grimm KM, Cook JC, Keller PM, Kresock DS, Mach H, Troutman RD, Isopi LA, Williams DM, Xu Z, Bohannon KE, Volkin DB, Montefiori DC, Miura A, Krivulka GR, Lifton MA, Kuroda MJ, Schmitz JE, Letvin NL, Caulfield MJ, Bett AJ, Youil R, Kaslow DC, Emini EA. 2002. Replication-incompetent adenoviral vaccine vector elicits effective anti-immunodeficiency-virus immunity. *Nature* 415: 331-5
194. Jaiswal S, Khanna N, Swaminathan S. 2003. Replication-defective adenoviral vaccine vector for the induction of immune responses to dengue virus type 2. *J Virol* 77: 12907-13
195. Casimiro DR, Chen L, Fu TM, Evans RK, Caulfield MJ, Davies ME, Tang A, Chen M, Huang L, Harris V, Freed DC, Wilson KA, Dubey S, Zhu DM, Nawrocki D, Mach H, Troutman R, Isopi L, Williams D, Hurni W, Xu Z, Smith JG, Wang S, Liu X, Guan L, Long R, Trigona W, Heidecker GJ, Perry HC, Persaud N, Toner TJ, Su Q, Liang X, Youil R, Chastain M, Bett AJ, Volkin DB, Emini EA, Shiver JW. 2003. Comparative immunogenicity in rhesus monkeys of DNA plasmid, recombinant vaccinia virus, and replication-defective adenovirus vectors expressing a human immunodeficiency virus type 1 gag gene. *J Virol* 77: 6305-13
196. Rodrigues EG, Zavala F, Eichinger D, Wilson JM, Tsuji M. 1997. Single immunizing dose of recombinant adenovirus efficiently induces CD8+ T cell-mediated protective immunity against malaria. *J Immunol* 158: 1268-74
197. Tatsis N, Tesema L, Robinson ER, Giles-Davis W, McCoy K, Gao GP, Wilson JM, Ertl HC. 2006. Chimpanzee-origin adenovirus vectors as vaccine carriers. *Gene Ther* 13: 421-9
198. Colloca S, Barnes E, Folgori A, Ammendola V, Capone S, Cirillo A, Siani L, Naddeo M, Grazioli F, Esposito ML, Ambrosio M, Sparacino A, Bartiromo M, Meola A, Smith K, Kurioka A, O'Hara GA, Ewer KJ, Anagnostou N, Bliss C, Hill AV, Traboni C, Klenerman P, Cortese R, Nicosia A. 2012. Vaccine vectors derived from a large collection of simian adenoviruses induce potent cellular immunity across multiple species. *Sci Transl Med* 4: 115ra2
199. O'Hara GA, Duncan CJ, Ewer KJ, Collins KA, Elias SC, Halstead FD, Goodman AL, Edwards NJ, Reyes-Sandoval A, Bird P, Rowland R, Sheehy SH, Poulton ID, Hutchings C, Todryk S, Andrews L, Folgori A, Berrie E, Moyle S, Nicosia A, Colloca S, Cortese R, Siani L, Lawrie AM, Gilbert SC, Hill AV. 2012. Clinical assessment of a recombinant simian adenovirus ChAd63: a potent new vaccine vector. *J Infect Dis* 205: 772-81
200. Dicks MD, Spencer AJ, Edwards NJ, Wadell G, Bojang K, Gilbert SC, Hill AV, Cottingham MG. 2012. A novel chimpanzee adenovirus vector with low human seroprevalence: improved systems for vector derivation and comparative immunogenicity. *PLoS One* 7: e40385

201. Allsopp CE, Plebanski M, Gilbert S, Sinden RE, Harris S, Frankel G, Dougan G, Hioe C, Nixon D, Paoletti E, Layton G, Hill AV. 1996. Comparison of numerous delivery systems for the induction of cytotoxic T lymphocytes by immunization. *Eur J Immunol* 26: 1951-9
202. Harari A, Bart PA, Stohr W, Tapia G, Garcia M, Medjitna-Rais E, Burnet S, Cellerai C, Erlwein O, Barber T, Moog C, Liljestrom P, Wagner R, Wolf H, Kraehenbuhl JP, Esteban M, Heeney J, Frachette MJ, Tartaglia J, McCormack S, Babiker A, Weber J, Pantaleo G. 2008. An HIV-1 clade C DNA prime, NYVAC boost vaccine regimen induces reliable, polyfunctional, and long-lasting T cell responses. *J Exp Med* 205: 63-77
203. Allen TM, Vogel TU, Fuller DH, Mothe BR, Steffen S, Boyson JE, Shipley T, Fuller J, Hanke T, Sette A, Altman JD, Moss B, McMichael AJ, Watkins DI. 2000. Induction of AIDS virus-specific CTL activity in fresh, unstimulated peripheral blood lymphocytes from rhesus macaques vaccinated with a DNA prime/modified vaccinia virus Ankara boost regimen. *J Immunol* 164: 4968-78
204. Anderson RJ, Hannan CM, Gilbert SC, Laidlaw SM, Sheu EG, Korten S, Sinden R, Butcher GA, Skinner MA, Hill AV. 2004. Enhanced CD8+ T cell immune responses and protection elicited against Plasmodium berghei malaria by prime boost immunization regimens using a novel attenuated fowlpox virus. *J Immunol* 172: 3094-100
205. Gherardi MM, Najera JL, Perez-Jimenez E, Guerra S, Garcia-Sastre A, Esteban M. 2003. Prime-boost immunization schedules based on influenza virus and vaccinia virus vectors potentiate cellular immune responses against human immunodeficiency virus Env protein systemically and in the genitorectal draining lymph nodes. *J Virol* 77: 7048-57
206. Liu J, O'Brien KL, Lynch DM, Simmons NL, La Porte A, Riggs AM, Abbink P, Coffey RT, Grandpre LE, Seaman MS, Landucci G, Forthal DN, Montefiori DC, Carville A, Mansfield KG, Havenga MJ, Pau MG, Goudsmit J, Barouch DH. 2009. Immune control of an SIV challenge by a T-cell-based vaccine in rhesus monkeys. *Nature* 457: 87-91
207. Masalova OV, Lesnova EI, Pichugin AV, Melnikova TM, Grabovetsky VV, Petrakova NV, Smirnova OA, Ivanov AV, Zaberezhny AD, Ataullakhanov RI, Isaguliants MG, Kushch AA. 2010. The successful immune response against hepatitis C nonstructural protein 5A (NS5A) requires heterologous DNA/protein immunization. *Vaccine* 28: 1987-96
208. Sheehy SH, Duncan CJ, Elias SC, Biswas S, Collins KA, O'Hara GA, Halstead FD, Ewer KJ, Mahungu T, Spencer AJ, Miura K, Poulton ID, Dicks MD, Edwards NJ, Berrie E, Moyle S, Colloca S, Cortese R, Gantlett K, Long CA, Lawrie AM, Gilbert SC, Doherty T, Nicosia A, Hill AV, Draper SJ. 2012. Phase Ia clinical evaluation of the safety and immunogenicity of the Plasmodium falciparum blood-stage antigen AMA1 in ChAd63 and MVA vaccine vectors. *PLoS One* 7: e31208
209. Sheehy SH, Duncan CJ, Elias SC, Collins KA, Ewer KJ, Spencer AJ, Williams AR, Halstead FD, Moretz SE, Miura K, Epp C, Dicks MD, Poulton ID, Lawrie AM, Berrie E, Moyle S, Long CA, Colloca S, Cortese R, Gilbert SC, Nicosia A,

Hill AV, Draper SJ. 2011. Phase Ia clinical evaluation of the Plasmodium falciparum blood-stage antigen MSP1 in ChAd63 and MVA vaccine vectors. *Mol Ther* 19: 2269-76

210. Odunsi K, Matsuzaki J, Karbach J, Neumann A, Mhawech-Fauceglia P, Miller A, Beck A, Morrison CD, Ritter G, Godoy H, Lele S, duPont N, Edwards R, Shrikant P, Old LJ, Gnjatic S, Jager E. 2012. Efficacy of vaccination with recombinant vaccinia and fowlpox vectors expressing NY-ESO-1 antigen in ovarian cancer and melanoma patients. *Proc Natl Acad Sci U S A* 109: 5797-802
211. Bruna-Romero O, Gonzalez-Aseguinolaza G, Hafalla JC, Tsuji M, Nussenzweig RS. 2001. Complete, long-lasting protection against malaria of mice primed and boosted with two distinct viral vectors expressing the same plasmodial antigen. *Proc Natl Acad Sci U S A* 98: 11491-6
212. Draper SJ, Moore AC, Goodman AL, Long CA, Holder AA, Gilbert SC, Hill F, Hill AV. 2008. Effective induction of high-titer antibodies by viral vector vaccines. *Nat Med* 14: 819-21
213. Biswas S, Dicks MD, Long CA, Remarque EJ, Siani L, Colloca S, Cottingham MG, Holder AA, Gilbert SC, Hill AV, Draper SJ. 2011. Transgene optimization, immunogenicity and in vitro efficacy of viral vectored vaccines expressing two alleles of Plasmodium falciparum AMA1. *PLoS One* 6: e20977
214. Draper SJ, Biswas S, Spencer AJ, Remarque EJ, Capone S, Naddeo M, Dicks MD, Faber BW, de Cassan SC, Folgori A, Nicosia A, Gilbert SC, Hill AV. 2010. Enhancing blood-stage malaria subunit vaccine immunogenicity in rhesus macaques by combining adenovirus, poxvirus, and protein-in-adjuvant vaccines. *J Immunol* 185: 7583-95
215. Douglas AD, de Cassan SC, Dicks MD, Gilbert SC, Hill AV, Draper SJ. 2010. Tailoring subunit vaccine immunogenicity: maximizing antibody and T cell responses by using combinations of adenovirus, poxvirus and protein-adjuvant vaccines against Plasmodium falciparum MSP1. *Vaccine* 28: 7167-78
216. Stewart VA, McGrath SM, Dubois PM, Pau MG, Mettens P, Shott J, Cobb M, Burge JR, Larson D, Ware LA, Demoitie MA, Weverling GJ, Bayat B, Custers JH, Dubois MC, Cohen J, Goudsmit J, Heppner DG, Jr. 2007. Priming with an adenovirus 35-circumsporozoite protein (CS) vaccine followed by RTS,S/AS01B boosting significantly improves immunogenicity to Plasmodium falciparum CS compared to that with either malaria vaccine alone. *Infect Immun* 75: 2283-90
217. de Cassan SC, Forbes EK, Douglas AD, Milicic A, Singh B, Gupta P, Chauhan VS, Chitnis CE, Gilbert SC, Hill AV, Draper SJ. 2011. The requirement for potent adjuvants to enhance the immunogenicity and protective efficacy of protein vaccines can be overcome by prior immunization with a recombinant adenovirus. *J Immunol* 187: 2602-16
218. Brewer JM, Conacher M, Satoskar A, Bluethmann H, Alexander J. 1996. In interleukin-4-deficient mice, alum not only generates T helper 1 responses equivalent to freund's complete adjuvant, but continues to induce T helper 2 cytokine production. *Eur J Immunol* 26: 2062-6
219. Kool M, Petrilli V, De Smedt T, Rolaz A, Hammad H, van Nimwegen M, Bergen IM, Castillo R, Lambrecht BN, Tschopp J. 2008. Cutting edge: alum adjuvant

stimulates inflammatory dendritic cells through activation of the NALP3 inflammasome. *J Immunol* 181: 3755-9

220. Bejon P, Lusingu J, Olotu A, Leach A, Lievens M, Vekemans J, Mshamu S, Lang T, Gould J, Dubois MC, Demoitie MA, Stallaert JF, Vansadia P, Carter T, Njuguna P, Awuondo KO, Malabeja A, Abdul O, Gesase S, Mturi N, Drakeley CJ, Savarese B, Villafana T, Ballou WR, Cohen J, Riley EM, Lemnge MM, Marsh K, von Seidlein L. 2008. Efficacy of RTS,S/AS01E vaccine against malaria in children 5 to 17 months of age. *N Engl J Med* 359: 2521-32
221. Engel J, Kammerer RA. 2000. What are oligomerization domains good for? *Matrix Biol* 19: 283-8
222. Spencer AJ, Hill F, Honeycutt JD, Cottingham MG, Bregu M, Rollier CS, Furze J, Draper SJ, Sogaard KC, Gilbert SC, Wyllie DH, Hill AV. 2012. Fusion of the Mycobacterium tuberculosis antigen 85A to an oligomerization domain enhances its immunogenicity in both mice and non-human primates. *PLoS One* 7: e33555
223. Butler NS, Schmidt NW, Harty JT. 2010. Differential effector pathways regulate memory CD8 T cell immunity against Plasmodium berghei versus P. yoelii sporozoites. *J Immunol* 184: 2528-38
224. Schmidt NW, Butler NS, Badovinac VP, Harty JT. 2010. Extreme CD8 T cell requirements for anti-malarial liver-stage immunity following immunization with radiation attenuated sporozoites. *PLoS Pathog* 6: e1000998
225. Tarun AS, Baer K, Dumpit RF, Gray S, Lejarcegui N, Frevert U, Kappe SH. 2006. Quantitative isolation and in vivo imaging of malaria parasite liver stages. *Int J Parasitol* 36: 1283-93
226. van Dijk MR, Waters AP, Janse CJ. 1995. Stable transfection of malaria parasite blood stages. *Science* 268: 1358-62
227. van Dijk MR, Janse CJ, Waters AP. 1996. Expression of a Plasmodium gene introduced into subtelomeric regions of Plasmodium berghei chromosomes. *Science* 271: 662-5
228. Vlachou D, Zimmermann T, Cantera R, Janse CJ, Waters AP, Kafatos FC. 2004. Real-time, in vivo analysis of malaria ookinete locomotion and mosquito midgut invasion. *Cell Microbiol* 6: 671-85
229. Franke-Fayard B, Waters AP, Janse CJ. 2006. Real-time in vivo imaging of transgenic bioluminescent blood stages of rodent malaria parasites in mice. *Nat Protoc* 1: 476-85
230. Ploemen IH, Prudencio M, Douradinha BG, Ramesar J, Fonager J, van Gemert GJ, Luty AJ, Hermsen CC, Sauerwein RW, Baptista FG, Mota MM, Waters AP, Que I, Lowik CW, Khan SM, Janse CJ, Franke-Fayard BM. 2009. Visualisation and quantitative analysis of the rodent malaria liver stage by real time imaging. *PLoS One* 4: e7881
231. Mlambo G, Kumar N. 2008. Transgenic rodent Plasmodium berghei parasites as tools for assessment of functional immunogenicity and optimization of human malaria vaccines. *Eukaryot Cell* 7: 1875-9
232. Wengelnik K, Spaccapelo R, Naitza S, Robson KJ, Janse CJ, Bistoni F, Waters AP, Crisanti A. 1999. The A-domain and the thrombospondin-related motif of

Plasmodium falciparum TRAP are implicated in the invasion process of mosquito salivary glands. *EMBO J* 18: 5195-204

233. Jacobs-Lorena VY, Mikolajczak SA, Labaied M, Vaughan AM, Kappe SH. 2010. A dispensable Plasmodium locus for stable transgene expression. *Mol Biochem Parasitol* 171: 40-4
234. Kocken CH, van der Wel AM, Dubbeld MA, Narum DL, van de Rijke FM, van Gemert GJ, van der Linde X, Bannister LH, Janse C, Waters AP, Thomas AW. 1998. Precise timing of expression of a Plasmodium falciparum-derived transgene in Plasmodium berghei is a critical determinant of subsequent subcellular localization. *J Biol Chem* 273: 15119-24
235. Persson C, Oliveira GA, Sultan AA, Bhanot P, Nussenzweig V, Nardin E. 2002. Cutting edge: a new tool to evaluate human pre-erythrocytic malaria vaccines: rodent parasites bearing a hybrid Plasmodium falciparum circumsporozoite protein. *J Immunol* 169: 6681-5
236. Aldrich C, Magini A, Emiliani C, Dottorini T, Bistoni F, Crisanti A, Spaccapelo R. 2012. Roles of the amino terminal region and repeat region of the Plasmodium berghei circumsporozoite protein in parasite infectivity. *PLoS One* 7: e32524
237. Kumar KA, Oliveira GA, Edelman R, Nardin E, Nussenzweig V. 2004. Quantitative Plasmodium sporozoite neutralization assay (TSNA). *J Immunol Methods* 292: 157-64
238. Blackman MJ, Heidrich HG, Donachie S, McBride JS, Holder AA. 1990. A single fragment of a malaria merozoite surface protein remains on the parasite during red cell invasion and is the target of invasion-inhibiting antibodies. *J Exp Med* 172: 379-82
239. Egan AF, Burghaus P, Druilhe P, Holder AA, Riley EM. 1999. Human antibodies to the 19kDa C-terminal fragment of Plasmodium falciparum merozoite surface protein 1 inhibit parasite growth in vitro. *Parasite Immunol* 21: 133-9
240. O'Donnell RA, de Koning-Ward TF, Burt RA, Bockarie M, Reeder JC, Cowman AF, Crabb BS. 2001. Antibodies against merozoite surface protein (MSP)-1(19) are a major component of the invasion-inhibitory response in individuals immune to malaria. *J Exp Med* 193: 1403-12
241. de Koning-Ward TF, O'Donnell RA, Drew DR, Thomson R, Speed TP, Crabb BS. 2003. A new rodent model to assess blood stage immunity to the Plasmodium falciparum antigen merozoite surface protein 119 reveals a protective role for invasion inhibitory antibodies. *J Exp Med* 198: 869-75
242. Mlambo G, Maciel J, Kumar N. 2008. Murine model for assessment of Plasmodium falciparum transmission-blocking vaccine using transgenic Plasmodium berghei parasites expressing the target antigen Pfs25. *Infect Immun* 76: 2018-24
243. Ramjanee S, Robertson JS, Franke-Fayard B, Sinha R, Waters AP, Janse CJ, Wu Y, Blagborough AM, Saul A, Sinden RE. 2007. The use of transgenic Plasmodium berghei expressing the Plasmodium vivax antigen P25 to determine the transmission-blocking activity of sera from malaria vaccine trials. *Vaccine* 25: 886-94

244. Ashok MS, Rangarajan PN. 2002. Protective efficacy of a plasmid DNA encoding Japanese encephalitis virus envelope protein fused to tissue plasminogen activator signal sequences: studies in a murine intracerebral virus challenge model. *Vaccine* 20: 1563-70
245. Aricescu AR, Lu W, Jones EY. 2006. A time- and cost-efficient system for high-level protein production in mammalian cells. *Acta Crystallogr D Biol Crystallogr* 62: 1243-50
246. Pfander C, Anar B, Schwach F, Otto TD, Brochet M, Volkmann K, Quail MA, Pain A, Rosen B, Skarnes W, Rayner JC, Billker O. 2011. A scalable pipeline for highly effective genetic modification of a malaria parasite. *Nat Methods* 8: 1078-82
247. Wang J, Sarov M, Rientjes J, Fu J, Hollak H, Kranz H, Xie W, Stewart AF, Zhang Y. 2006. An improved recombineering approach by adding RecA to lambda Red recombination. *Mol Biotechnol* 32: 43-53
248. Skarnes WC, Rosen B, West AP, Koutsourakis M, Bushell W, Iyer V, Mujica AO, Thomas M, Harrow J, Cox T, Jackson D, Severin J, Biggs P, Fu J, Nefedov M, de Jong PJ, Stewart AF, Bradley A. 2011. A conditional knockout resource for the genome-wide study of mouse gene function. *Nature* 474: 337-42
249. Braks JA, Franke-Fayard B, Kroeze H, Janse CJ, Waters AP. 2006. Development and application of a positive-negative selectable marker system for use in reverse genetics in Plasmodium. *Nucleic Acids Res* 34: e39
250. Godiska R, Mead D, Dhodda V, Wu C, Hochstein R, Karsi A, Usdin K, Entezam A, Ravin N. 2010. Linear plasmid vector for cloning of repetitive or unstable sequences in Escherichia coli. *Nucleic Acids Res* 38: e88
251. Lin JW, Annoura T, Sajid M, Chevalley-Maurel S, Ramesar J, Klop O, Franke-Fayard BM, Janse CJ, Khan SM. 2011. A novel 'gene insertion/marker out' (GIMO) method for transgene expression and gene complementation in rodent malaria parasites. *PLoS One* 6: e29289
252. Janse CJ, Ramesar J, Waters AP. 2006. High-efficiency transfection and drug selection of genetically transformed blood stages of the rodent malaria parasite Plasmodium berghei. *Nat Protoc* 1: 346-56
253. Moore AC, Gallimore A, Draper SJ, Watkins KR, Gilbert SC, Hill AV. 2005. Anti-CD25 antibody enhancement of vaccine-induced immunogenicity: increased durable cellular immunity with reduced immunodominance. *J Immunol* 175: 7264-73
254. Draper SJ, Goodman AL, Biswas S, Forbes EK, Moore AC, Gilbert SC, Hill AV. 2009. Recombinant viral vaccines expressing merozoite surface protein-1 induce antibody- and T cell-mediated multistage protection against malaria. *Cell Host Microbe* 5: 95-105
255. Van Rooijen N, Sanders A. 1996. Kupffer cell depletion by liposome-delivered drugs: comparative activity of intracellular clodronate, propamidine, and ethylenediaminetetraacetic acid. *Hepatology* 23: 1239-43
256. Bejon P, Andrews L, Andersen RF, Dunachie S, Webster D, Walther M, Gilbert SC, Peto T, Hill AV. 2005. Calculation of liver-to-blood inocula, parasite growth rates, and preerythrocytic vaccine efficacy, from serial quantitative polymerase

chain reaction studies of volunteers challenged with malaria sporozoites. *J Infect Dis* 191: 619-26
257. Limbach K, Aguiar J, Gowda K, Patterson N, Abot E, Sedegah M, Sacci J, Richie T. 2011. Identification of two new protective pre-erythrocytic malaria vaccine antigen candidates. *Malar J* 10: 65
258. Doolan DL, Sedegah M, Hedstrom RC, Hobart P, Charoenvit Y, Hoffman SL. 1996. Circumventing genetic restriction of protection against malaria with multigene DNA immunization: CD8+ cell-, interferon gamma-, and nitric oxide-dependent immunity. *J Exp Med* 183: 1739-46
259. Weiss WR, Kumar A, Jiang G, Williams J, Bostick A, Conteh S, Fryauff D, Aguiar J, Singh M, O'Hagan DT, Ulmer JB, Richie TL. 2007. Protection of rhesus monkeys by a DNA prime/poxvirus boost malaria vaccine depends on optimal DNA priming and inclusion of blood stage antigens. *PLoS One* 2: e1063
260. Bottius E, Guanzirolli A, Trape JF, Rogier C, Konate L, Druilhe P. 1996. Malaria: even more chronic in nature than previously thought; evidence for subpatent parasitaemia detectable by the polymerase chain reaction. *Trans R Soc Trop Med Hyg* 90: 15-9
261. Bruna-Romero O, Hafalla JC, Gonzalez-Aseguinolaza G, Sano G, Tsuji M, Zavala F. 2001. Detection of malaria liver-stages in mice infected through the bite of a single Anopheles mosquito using a highly sensitive real-time PCR. *Int J Parasitol* 31: 1499-502
262. Witney AA, Doolan DL, Anthony RM, Weiss WR, Hoffman SL, Carucci DJ. 2001. Determining liver stage parasite burden by real time quantitative PCR as a method for evaluating pre-erythrocytic malaria vaccine efficacy. *Mol Biochem Parasitol* 118: 233-45
263. Ploemen I, Behet M, Nganou-Makamdop K, van Gemert GJ, Bijker E, Hermsen C, Sauerwein R. 2011. Evaluation of immunity against malaria using luciferase-expressing Plasmodium berghei parasites. *Malar J* 10: 350
264. Hutchings CL, Birkett AJ, Moore AC, Hill AV. 2007. Combination of protein and viral vaccines induces potent cellular and humoral immune responses and enhanced protection from murine malaria challenge. *Infect Immun* 75: 5819-26
265. Vanderberg JP, Frevert U. 2004. Intravital microscopy demonstrating antibody-mediated immobilisation of Plasmodium berghei sporozoites injected into skin by mosquitoes. *Int J Parasitol* 34: 991-6
266. Gueirard P, Tavares J, Thiberge S, Bernex F, Ishino T, Milon G, Franke-Fayard B, Janse CJ, Menard R, Amino R. 2010. Development of the malaria parasite in the skin of the mammalian host. *Proc Natl Acad Sci U S A* 107: 18640-5
267. Favre N, Da Laperousaz C, Ryffel B, Weiss NA, Imhof BA, Rudin W, Lucas R, Piguet PF. 1999. Role of ICAM-1 (CD54) in the development of murine cerebral malaria. *Microbes Infect* 1: 961-8
268. Epstein JE, Tewari K, Lyke KE, Sim BK, Billingsley PF, Laurens MB, Gunasekera A, Chakravarty S, James ER, Sedegah M, Richman A, Velmurugan S, Reyes S, Li M, Tucker K, Ahumada A, Ruben AJ, Li T, Stafford R, Eappen AG, Tamminga C, Bennett JW, Ockenhouse CF, Murphy JR, Komisar J, Thomas N, Loyevsky M, Birkett A, Plowe CV, Loucq C, Edelman R, Richie TL, Seder RA,

Hoffman SL. 2011. Live attenuated malaria vaccine designed to protect through hepatic CD8(+) T cell immunity. *Science* 334: 475-80
269. Forbes EK, Biswas S, Collins KA, Gilbert SC, Hill AV, Draper SJ. 2011. Combining liver- and blood-stage malaria viral-vectored vaccines: investigating mechanisms of CD8+ T cell interference. *J Immunol* 187: 3738-50
270. Pichyangkul S, Tongtawe P, Kum-Arb U, Yongvanitchit K, Gettayacamin M, Hollingdale MR, Limsalakpetch A, Stewart VA, Lanar DE, Dutta S, Angov E, Ware LA, Bergmann-Leitner ES, House B, Voss G, Dubois MC, Cohen JD, Fukuda MM, Heppner DG, Miller RS. 2009. Evaluation of the safety and immunogenicity of Plasmodium falciparum apical membrane antigen 1, merozoite surface protein 1 or RTS,S vaccines with adjuvant system AS02A administered alone or concurrently in rhesus monkeys. *Vaccine* 28: 452-62
271. Sedegah M, Charoenvit Y, Minh L, Belmonte M, Majam VF, Abot S, Ganeshan H, Kumar S, Bacon DJ, Stowers A, Narum DL, Carucci DJ, Rogers WO. 2004. Reduced immunogenicity of DNA vaccine plasmids in mixtures. *Gene Ther* 11: 448-56
272. Goodman AL, Epp C, Moss D, Holder AA, Wilson JM, Gao GP, Long CA, Remarque EJ, Thomas AW, Ammendola V, Colloca S, Dicks MD, Biswas S, Seibel D, van Duivenvoorde LM, Gilbert SC, Hill AV, Draper SJ. 2010. New candidate vaccines against blood-stage Plasmodium falciparum malaria: prime-boost immunization regimens incorporating human and simian adenoviral vectors and poxviral vectors expressing an optimized antigen based on merozoite surface protein 1. *Infect Immun* 78: 4601-12
273. Scheller LF, Wirtz RA, Azad AF. 1994. Susceptibility of different strains of mice to hepatic infection with Plasmodium berghei. *Infect Immun* 62: 4844-7
274. Ophorst OJ, Radosevic K, Klap JM, Sijtsma J, Gillissen G, Mintardjo R, van Ooij MJ, Holterman L, Companjen A, Goudsmit J, Havenga MJ. 2007. Increased immunogenicity of recombinant Ad35-based malaria vaccine through formulation with aluminium phosphate adjuvant. *Vaccine* 25: 6501-10
275. Larke N, Im EJ, Wagner R, Williamson C, Williamson AL, McMichael AJ, Hanke T. 2007. Combined single-clade candidate HIV-1 vaccines induce T cell responses limited by multiple forms of in vivo immune interference. *Eur J Immunol* 37: 566-77
276. Zhang T, Xu Y, Qiao L, Wang Y, Wu X, Fan D, Peng Q, Xu X. 2010. Trivalent Human Papillomavirus (HPV) VLP vaccine covering HPV type 58 can elicit high level of humoral immunity but also induce immune interference among component types. *Vaccine* 28: 3479-87
277. Bojang KA, Milligan PJ, Pinder M, Vigneron L, Alloueche A, Kester KE, Ballou WR, Conway DJ, Reece WH, Gothard P, Yamuah L, Delchambre M, Voss G, Greenwood BM, Hill A, McAdam KP, Tornieporth N, Cohen JD, Doherty T. 2001. Efficacy of RTS,S/AS02 malaria vaccine against Plasmodium falciparum infection in semi-immune adult men in The Gambia: a randomised trial. *Lancet* 358: 1927-34
278. Aponte JJ, Aide P, Renom M, Mandomando I, Bassat Q, Sacarlal J, Manaca MN, Lafuente S, Barbosa A, Leach A, Lievens M, Vekemans J, Sigauque B, Dubois

MC, Demoitie MA, Sillman M, Savarese B, McNeil JG, Macete E, Ballou WR, Cohen J, Alonso PL. 2007. Safety of the RTS,S/AS02D candidate malaria vaccine in infants living in a highly endemic area of Mozambique: a double blind randomised controlled phase I/IIb trial. *Lancet* 370: 1543-51

279. Abdulla S, Oberholzer R, Juma O, Kubhoja S, Machera F, Membi C, Omari S, Urassa A, Mshinda H, Jumanne A, Salim N, Shomari M, Aebi T, Schellenberg DM, Carter T, Villafana T, Demoitie MA, Dubois MC, Leach A, Lievens M, Vekemans J, Cohen J, Ballou WR, Tanner M. 2008. Safety and immunogenicity of RTS,S/AS02D malaria vaccine in infants. *N Engl J Med* 359: 2533-44
280. Greenwood B. 2011. Immunological correlates of protection for the RTS,S candidate malaria vaccine. *Lancet Infect Dis* 11: 75-6
281. Lumsden JM, Schwenk RJ, Rein LE, Moris P, Janssens M, Ofori-Anyinam O, Cohen J, Kester KE, Heppner DG, Krzych U. 2011. Protective immunity induced with the RTS,S/AS vaccine is associated with IL-2 and TNF-alpha producing effector and central memory CD4 T cells. *PLoS One* 6: e20775
282. Wang R, Epstein J, Charoenvit Y, Baraceros FM, Rahardjo N, Gay T, Banania JG, Chattopadhyay R, de la Vega P, Richie TL, Tornieporth N, Doolan DL, Kester KE, Heppner DG, Norman J, Carucci DJ, Cohen JD, Hoffman SL. 2004. Induction in humans of CD8+ and CD4+ T cell and antibody responses by sequential immunization with malaria DNA and recombinant protein. *J Immunol* 172: 5561-9
283. Walsh DS, Gettayacamin M, Leitner WW, Lyon JA, Stewart VA, Marit G, Pichyangkul S, Gosi P, Tongtawe P, Kester KE, Holland CA, Kolodny N, Cohen J, Voss G, Ballou WR, Heppner DG, Jr. 2006. Heterologous prime-boost immunization in rhesus macaques by two, optimally spaced particle-mediated epidermal deliveries of Plasmodium falciparum circumsporozoite protein-encoding DNA, followed by intramuscular RTS,S/AS02A. *Vaccine* 24: 4167-78
284. Dunachie SJ, Walther M, Vuola JM, Webster DP, Keating SM, Berthoud T, Andrews L, Bejon P, Poulton I, Butcher G, Watkins K, Sinden RE, Leach A, Moris P, Tornieporth N, Schneider J, Dubovsky F, Tierney E, Williams J, Heppner DG, Jr., Gilbert SC, Cohen J, Hill AV. 2006. A clinical trial of prime-boost immunisation with the candidate malaria vaccines RTS,S/AS02A and MVA-CS. *Vaccine* 24: 2850-9
285. Schwenk R, Asher LV, Chalom I, Lanar D, Sun P, White K, Keil D, Kester KE, Stoute J, Heppner DG, Krzych U. 2003. Opsonization by antigen-specific antibodies as a mechanism of protective immunity induced by Plasmodium falciparum circumsporozoite protein-based vaccine. *Parasite Immunol* 25: 17-25
286. Seguin MC, Ballou WR, Nacy CA. 1989. Interactions of Plasmodium berghei sporozoites and murine Kupffer cells in vitro. *J Immunol* 143: 1716-22
287. Spiegelberg HL, Weigle WO. 1965. THE CATABOLISM OF HOMOLOGOUS AND HETEROLOGOUS 7S GAMMA GLOBULIN FRAGMENTS. *J Exp Med* 121: 323-38
288. Vreden SG, Sauerwein RW, Verhave JP, Van Rooijen N, Meuwissen JH, Van Den Broek MF. 1993. Kupffer cell elimination enhances development of liver schizonts of Plasmodium berghei in rats. *Infect Immun* 61: 1936-9

289. Usynin I, Klotz C, Frevert U. 2007. Malaria circumsporozoite protein inhibits the respiratory burst in Kupffer cells. *Cell Microbiol* 9: 2610-28
290. Pradel G, Frevert U. 2001. Malaria sporozoites actively enter and pass through rat Kupffer cells prior to hepatocyte invasion. *Hepatology* 33: 1154-65
291. Roland J, Soulard V, Sellier C, Drapier AM, Di Santo JP, Cazenave PA, Pied S. 2006. NK cell responses to Plasmodium infection and control of intrahepatic parasite development. *J Immunol* 177: 1229-39
292. Casares S, Brumeanu TD, Richie TL. 2010. The RTS,S malaria vaccine. *Vaccine* 28: 4880-94
293. Cerami C, Frevert U, Sinnis P, Takacs B, Clavijo P, Santos MJ, Nussenzweig V. 1992. The basolateral domain of the hepatocyte plasma membrane bears receptors for the circumsporozoite protein of Plasmodium falciparum sporozoites. *Cell* 70: 1021-33
294. Touray MG, Seeley DC, Jr., Miller LH. 1994. Plasmodium gallinaceum: differential lysis of two developmental stages of malaria sporozoites by the alternative pathway of complement. *Exp Parasitol* 78: 294-301
295. Doolan DL, Hoffman SL. 1999. IL-12 and NK cells are required for antigen-specific adaptive immunity against malaria initiated by CD8+ T cells in the Plasmodium yoelii model. *J Immunol* 163: 884-92
296. Slifka MK, Pagarigan RR, Whitton JL. 2000. NK markers are expressed on a high percentage of virus-specific CD8+ and CD4+ T cells. *J Immunol* 164: 2009-15
297. Nishikado H, Mukai K, Kawano Y, Minegishi Y, Karasuyama H. 2011. NK cell-depleting anti-asialo GM1 antibody exhibits a lethal off-target effect on basophils in vivo. *J Immunol* 186: 5766-71
298. Schofield L, McConville MJ, Hansen D, Campbell AS, Fraser-Reid B, Grusby MJ, Tachado SD. 1999. CD1d-restricted immunoglobulin G formation to GPI-anchored antigens mediated by NKT cells. *Science* 283: 225-9
299. Romero JF, Eberl G, MacDonald HR, Corradin G. 2001. CD1d-restricted NK T cells are dispensable for specific antibody responses and protective immunity against liver stage malaria infection in mice. *Parasite Immunol* 23: 267-9
300. Gonzalez-Aseguinolaza G, de Oliveira C, Tomaska M, Hong S, Bruna-Romero O, Nakayama T, Taniguchi M, Bendelac A, Van Kaer L, Koezuka Y, Tsuji M. 2000. alpha -galactosylceramide-activated Valpha 14 natural killer T cells mediate protection against murine malaria. *Proc Natl Acad Sci U S A* 97: 8461-6
301. Reyes-Sandoval A, Berthoud T, Alder N, Siani L, Gilbert SC, Nicosia A, Colloca S, Cortese R, Hill AV. 2010. Prime-boost immunization with adenoviral and modified vaccinia virus Ankara vectors enhances the durability and polyfunctionality of protective malaria CD8+ T-cell responses. *Infect Immun* 78: 145-53
302. Horowitz A, Hafalla JC, King E, Lusingu J, Dekker D, Leach A, Moris P, Cohen J, Vekemans J, Villafana T, Corran PH, Bejon P, Drakeley CJ, von Seidlein L, Riley EM. 2012. Antigen-specific IL-2 secretion correlates with NK cell responses after immunization of Tanzanian children with the RTS,S/AS01 malaria vaccine. *J Immunol* 188: 5054-62

303. McCall MB, Roestenberg M, Ploemen I, Teirlinck A, Hopman J, de Mast Q, Dolo A, Doumbo OK, Luty A, van der Ven AJ, Hermsen CC, Sauerwein RW. 2010. Memory-like IFN-gamma response by NK cells following malaria infection reveals the crucial role of T cells in NK cell activation by P. falciparum. *Eur J Immunol* 40: 3472-7
304. Price RN, Tjitra E, Guerra CA, Yeung S, White NJ, Anstey NM. 2007. Vivax malaria: neglected and not benign. *Am J Trop Med Hyg* 77: 79-87
305. Hay SI, Guerra CA, Tatem AJ, Noor AM, Snow RW. 2004. The global distribution and population at risk of malaria: past, present, and future. *Lancet Infect Dis* 4: 327-36
306. Herrera S, Fernandez OL, Vera O, Cardenas W, Ramirez O, Palacios R, Chen-Mok M, Corradin G, Arevalo-Herrera M. 2011. Phase I safety and immunogenicity trial of Plasmodium vivax CS derived long synthetic peptides adjuvanted with montanide ISA 720 or montanide ISA 51. *Am J Trop Med Hyg* 84: 12-20
307. Arevalo-Herrera M, Vera O, Castellanos A, Cespedes N, Soto L, Corradin G, Herrera S. 2011. Preclinical vaccine study of Plasmodium vivax circumsporozoite protein derived-synthetic polypeptides formulated in montanide ISA 720 and montanide ISA 51 adjuvants. *Am J Trop Med Hyg* 84: 21-7
308. Jordan-Villegas A, Zapata JC, Perdomo AB, Quintero GE, Solarte Y, Arevalo-Herrera M, Herrera S. 2005. Aotus lemurinus griseimembra monkeys: a suitable model for Plasmodium vivax sporozoite infection. *Am J Trop Med Hyg* 73: 10-5
309. Capone S, Reyes-Sandoval A, Naddeo M, Siani L, Ammendola V, Rollier CS, Nicosia A, Colloca S, Cortese R, Folgori A, Hill AV. 2010. Immune responses against a liver-stage malaria antigen induced by simian adenoviral vector AdCh63 and MVA prime-boost immunisation in non-human primates. *Vaccine* 29: 256-65
310. Reyes-Sandoval A, Sridhar S, Berthoud T, Moore AC, Harty JT, Gilbert SC, Gao G, Ertl HC, Wilson JC, Hill AV. 2008. Single-dose immunogenicity and protective efficacy of simian adenoviral vectors against Plasmodium berghei. *Eur J Immunol* 38: 732-41
311. Galinski MR, Barnwell JW. 2008. Plasmodium vivax: who cares? *Malar J* 7 Suppl 1: S9
312. Putaporntip C, Jongwutiwes S, Tia T, Ferreira MU, Kanbara H, Tanabe K. 2001. Diversity in the thrombospondin-related adhesive protein gene (TRAP) of Plasmodium vivax. *Gene* 268: 97-104
313. Chenet SM, Tapia LL, Escalante AA, Durand S, Lucas C, Bacon DJ. 2012. Genetic diversity and population structure of genes encoding vaccine candidate antigens of Plasmodium vivax. *Malar J* 11: 68
314. Dodoo D, Hollingdale MR, Anum D, Koram KA, Gyan B, Akanmori BD, Ocran J, Adu-Amankwah S, Geneshan H, Abot E, Legano J, Banania G, Sayo R, Brambilla D, Kumar S, Doolan DL, Rogers WO, Epstein J, Richie TL, Sedegah M. 2011. Measuring naturally acquired immune responses to candidate malaria vaccine antigens in Ghanaian adults. *Malar J* 10: 168
315. Charoenvit Y, Fallarme V, Rogers WO, Sacci JB, Jr., Kaur M, Aguiar JC, Yuan LF, Corradin G, Andersen E, Wizel B, Houghten RA, Oloo A, De la Vega P,

Hoffman SL. 1997. Development of two monoclonal antibodies against Plasmodium falciparum sporozoite surface protein 2 and mapping of B-cell epitopes. *Infect Immun* 65: 3430-7
316. Kappe SH, Buscaglia CA, Nussenzweig V. 2004. Plasmodium sporozoite molecular cell biology. *Annu Rev Cell Dev Biol* 20: 29-59
317. Bodescot M, Silvie O, Siau A, Refour P, Pino P, Franetich JF, Hannoun L, Sauerwein R, Mazier D. 2004. Transcription status of vaccine candidate genes of Plasmodium falciparum during the hepatic phase of its life cycle. *Parasitol Res* 92: 449-52
318. Mendis K, Sina BJ, Marchesini P, Carter R. 2001. The neglected burden of Plasmodium vivax malaria. *Am J Trop Med Hyg* 64: 97-106
319. Rosenberg R, Wirtz RA, Lanar DE, Sattabongkot J, Hall T, Waters AP, Prasittisuk C. 1989. Circumsporozoite protein heterogeneity in the human malaria parasite Plasmodium vivax. *Science* 245: 973-6
320. Qari SH, Goldman IF, Povoa MM, Oliveira S, Alpers MP, Lal AA. 1991. Wide distribution of the variant form of the human malaria parasite Plasmodium vivax. *J Biol Chem* 266: 16297-300
321. Lim CS, Tazi L, Ayala FJ. 2005. Plasmodium vivax: recent world expansion and genetic identity to Plasmodium simium. *Proc Natl Acad Sci U S A* 102: 15523-8
322. Kain KC, Brown AE, Webster HK, Wirtz RA, Keystone JS, Rodriguez MH, Kinahan J, Rowland M, Lanar DE. 1992. Circumsporozoite genotyping of global isolates of Plasmodium vivax from dried blood specimens. *J Clin Microbiol* 30: 1863-6
323. Gonzalez JM, Hurtado S, Arevalo-Herrera M, Herrera S. 2001. Variants of the Plasmodium vivax circumsporozoite protein (VK210 and VK247) in Colombian isolates. *Mem Inst Oswaldo Cruz* 96: 709-12
324. Cui L, Mascorro CN, Fan Q, Rzomp KA, Khuntirat B, Zhou G, Chen H, Yan G, Sattabongkot J. 2003. Genetic diversity and multiple infections of Plasmodium vivax malaria in Western Thailand. *Am J Trop Med Hyg* 68: 613-9
325. Moon SU, Lee HW, Kim JY, Na BK, Cho SH, Lin K, Sohn WM, Kim TS. 2009. High frequency of genetic diversity of Plasmodium vivax field isolates in Myanmar. *Acta Trop* 109: 30-6
326. Franke ED, Lucas CM, Chauca G, Wirtz RA, Hinostroza S. 1992. Antibody response to the circumsporozoite protein of Plasmodium vivax in naturally infected humans. *Am J Trop Med Hyg* 46: 320-6
327. Park CG, Chwae YJ, Kim JI, Lee JH, Hur GM, Jeon BH, Koh JS, Han JH, Lee SJ, Park JW, Kaslow DC, Strickman D, Roh CS. 2000. Serologic responses of Korean soldiers serving in malaria-endemic areas during a recent outbreak of Plasmodium vivax. *Am J Trop Med Hyg* 62: 720-5
328. Franke ED, Lucas CM, San Roman E. 1991. Antibody response of humans to the circumsporozoite protein of Plasmodium vivax. *Infect Immun* 59: 2836-8
329. Zavala F, Cochrane AH, Nardin EH, Nussenzweig RS, Nussenzweig V. 1983. Circumsporozoite proteins of malaria parasites contain a single immunodominant region with two or more identical epitopes. *J Exp Med* 157: 1947-57

330. Migot F, Millet P, Chougnet C, Lepers JP, Deloron P. 1993. Humoral and cellular immune responses to the circumsporozoite protein of Plasmodium vivax in Madagascar. *Am J Trop Med Hyg* 48: 524-9
331. Bilsborough J, Carlisle M, Good MF. 1993. Identification of Caucasian CD4 T cell epitopes on the circumsporozoite protein of Plasmodium vivax. T cell memory. *J Immunol* 151: 890-9
332. Arevalo-Herrera M, Valencia AZ, Vergara J, Bonelo A, Fleischhauer K, Gonzalez JM, Restrepo JC, Lopez JA, Valmori D, Corradin G, Herrera S. 2002. Identification of HLA-A2 restricted CD8(+) T-lymphocyte responses to Plasmodium vivax circumsporozoite protein in individuals naturally exposed to malaria. *Parasite Immunol* 24: 161-9
333. Bell BA, Wood JF, Bansal R, Ragab H, Cargo J, 3rd, Washington MA, Wood CL, Ware LA, Ockenhouse CF, Yadava A. 2009. Process development for the production of an E. coli produced clinical grade recombinant malaria vaccine for Plasmodium vivax. *Vaccine* 27: 1448-53
334. Yadava A, Sattabongkot J, Washington MA, Ware LA, Majam V, Zheng H, Kumar S, Ockenhouse CF. 2007. A novel chimeric Plasmodium vivax circumsporozoite protein induces biologically functional antibodies that recognize both VK210 and VK247 sporozoites. *Infection and immunity* 75: 1177-85
335. Yadava A, Nurmukhambetova S, Pichugin AV, Lumsden JM. 2012. Cross-species immunity following immunization with a circumsporozoite protein-based vaccine for malaria. *J Infect Dis* 205: 1456-63
336. Millet P, Chizzolini C, Wirtz RA, Bathurst I, Broderson JR, Campbell GH, Collins WE. 1992. Inhibitory activity against sporozoites induced by antibodies directed against nonrepetitive regions of the circumsporozoite protein of Plasmodium vivax. *Eur J Immunol* 22: 519-24
337. Tewari R, Rathore D, Crisanti A. 2005. Motility and infectivity of Plasmodium berghei sporozoites expressing avian Plasmodium gallinaceum circumsporozoite protein. *Cell Microbiol* 7: 699-707
338. Hiller NL, Bhattacharjee S, van Ooij C, Liolios K, Harrison T, Lopez-Estrano C, Haldar K. 2004. A host-targeting signal in virulence proteins reveals a secretome in malarial infection. *Science* 306: 1934-7
339. Marti M, Good RT, Rug M, Knuepfer E, Cowman AF. 2004. Targeting malaria virulence and remodeling proteins to the host erythrocyte. *Science* 306: 1930-3
340. Cockburn IA, Tse SW, Radtke AJ, Srinivasan P, Chen YC, Sinnis P, Zavala F. 2011. Dendritic cells and hepatocytes use distinct pathways to process protective antigen from plasmodium in vivo. *PLoS Pathog* 7: e1001318
341. Doolan DL, Martinez-Alier N. 2006. Immune response to pre-erythrocytic stages of malaria parasites. *Curr Mol Med* 6: 169-85
342. Renggli J, Hahne M, Matile H, Betschart B, Tschopp J, Corradin G. 1997. Elimination of P. berghei liver stages is independent of Fas (CD95/Apo-I) or perforin-mediated cytotoxicity. *Parasite Immunol* 19: 145-8
343. Chakravarty S, Baldeviano GC, Overstreet MG, Zavala F. 2008. Effector CD8+ T lymphocytes against liver stages of Plasmodium yoelii do not require gamma interferon for antiparasite activity. *Infect Immun* 76: 3628-31

344. Trimnell A, Takagi A, Gupta M, Richie TL, Kappe SH, Wang R. 2009. Genetically attenuated parasite vaccines induce contact-dependent CD8+ T cell killing of Plasmodium yoelii liver stage-infected hepatocytes. *J Immunol* 183: 5870-8
345. Klotz FW, Scheller LF, Seguin MC, Kumar N, Marletta MA, Green SJ, Azad AF. 1995. Co-localization of inducible-nitric oxide synthase and Plasmodium berghei in hepatocytes from rats immunized with irradiated sporozoites. *J Immunol* 154: 3391-5
346. Fonager J, Pasini EM, Braks JA, Klop O, Ramesar J, Remarque EJ, Vroegrijk IO, van Duinen SG, Thomas AW, Khan SM, Mann M, Kocken CH, Janse CJ, Franke-Fayard BM. 2012. Reduced CD36-dependent tissue sequestration of Plasmodium-infected erythrocytes is detrimental to malaria parasite growth in vivo. *J Exp Med* 209: 93-107
347. Portugal S, Carret C, Recker M, Armitage AE, Goncalves LA, Epiphanio S, Sullivan D, Roy C, Newbold CI, Drakesmith H, Mota MM. 2011. Host-mediated regulation of superinfection in malaria. *Nat Med* 17: 732-7
348. Carlton JM, Adams JH, Silva JC, Bidwell SL, Lorenzi H, Caler E, Crabtree J, Angiuoli SV, Merino EF, Amedeo P, Cheng Q, Coulson RM, Crabb BS, Del Portillo HA, Essien K, Feldblyum TV, Fernandez-Becerra C, Gilson PR, Gueye AH, Guo X, Kang'a S, Kooij TW, Korsinczky M, Meyer EV, Nene V, Paulsen I, White O, Ralph SA, Ren Q, Sargeant TJ, Salzberg SL, Stoeckert CJ, Sullivan SA, Yamamoto MM, Hoffman SL, Wortman JR, Gardner MJ, Galinski MR, Barnwell JW, Fraser-Liggett CM. 2008. Comparative genomics of the neglected human malaria parasite Plasmodium vivax. *Nature* 455: 757-63
349. Verrier JD, Madorsky I, Coggin WE, Geesey M, Hochman M, Walling E, Daroszewski D, Eccles KS, Ludlow R, Semple-Rowland SL. 2011. Bicistronic lentiviruses containing a viral 2A cleavage sequence reliably co-express two proteins and restore vision to an animal model of LCA1. *PLoS One* 6: e20553

**Appendix one:**

Jenner protocols: J119, J004a, J004b, J005, J006, J259, J017, J013, J176, J131, J016, J018, J019, J079, J111.